*Author:*
**Salter, Tia**

*Title:*
**The bacterial Sec-machinery as an antibiotic target**

# The bacterial Sec-machinery as an antibiotic target

**Tia Salter**


A dissertation submitted to the University of Bristol in accordance with the requirements for award of the degree of Doctor of Philosophy in the Faculty of Life Sciences

School of Biochemistry

Faculty of Life Sciences

University of Bristol

United Kingdom

December 2022

Word count: 45,261

# Abstract

Despite the rising threat of antibiotic resistance, recent decades have seen a decline in antibiotic development. Discovery and development of compounds that inhibit the growth of Gram-negative bacteria is especially important. Target-based antibiotic drug discovery describes the identification of appropriate targets and establishment of bespoke assays for inhibitors of those targets. The bacterial Sec-machinery, a major system of protein translocation across and into the cytoplasmic membrane, is essential across bacteria, differs from the human counterpart and contributes to the virulence and antibiotic resistance of many pathogens, namely export of most β-lactamases. It therefore represents a promising target for development of antibiotic drugs, both as a standalone target and in terms of potentiating β-lactam antibiotics. This work describes the design of a whole-cell split-luciferase-based assay to monitor inhibition of the Sec-machinery. After validation with a model Sec substrate and known inhibitors of the machinery, the assay was scaled up for use in a local screen of 5000 diverse synthetic compounds, giving an average Z'-factor (robustness measure) of 0.71 and primary hit rate of 0.22%. Compared to a commercially available Sec inhibitor, hits have greater inhibitory activity against protein translocation in the Gram-negative bacterium *Escherichia coli* but negligeable effects on bacterial growth. A secondary assay strategy to complement the screen system and characterise hits is proposed. The split-luciferase-based assay was also adapted for analysing the role of Sec in export of metallo-β-lactamases IMP-1 and NDM-1, yielding data consistent with traditional assays for β-lactamase activity. Both enzymes are dependent on signal recognition particle for efficient translocation, in contrast to predictions based on signal sequence. Overall, this work further establishes the bacterial Sec-machinery as an antibiotic target, demonstrates how to design a successful strategy for Sec inhibitor discovery and provides insights into the types of Sec inhibitor most likely to be useful antibiotic leads.

## Acknowledgements

The past four (and a bit) years have gone so fast. I owe a massive thank you to Prof Ian Collinson for giving me the opportunity to work on this project. Thanks for your mentorship, expertise, and for being a calm presence throughout my PhD. I'm also incredibly grateful to Dr. William Allen and Dr. Dan Watkins for being an immense help in the lab and for being so encouraging about my work. I've loved every minute of my time on M floor and will really miss working with the whole team (even though I have to clean up your messes sometimes!) Thanks to all M floor members, past, present, and honorary, especially Sophie Williams and Beth Dean for being a major source of support during my last year in Bristol. Can't wait to see you both nail your projects and graduate! Thanks to Faye Watson for hosting my PIPS internship and for sparking my interest in science communication and public engagement. Thank you also to my progress panel Prof Paul Race and Prof Mark Dillingham for their helpful advice and support. Thanks to Prof Matthew Avison and all of D60/ 57 for welcoming me into the world of antibiotic resistance research.

I've reserved my last and biggest thank you for my family, especially my mum, Dona, my dad, Craig, and my incredible partner, Jack Williams. For your unwavering support, pride, and interest in my work, thank you so much.

## Declaration

I declare that the work in this dissertation was carried out in accordance with the requirements of the University's *Regulations and Code of Practice for Research Degree Programmes* and that it has not been submitted for any other academic award. Except where indicated by specific reference in the text, the work is the candidate's own work. Work done in collaboration with, or with the assistance of, others, is indicated as such. Any views expressed in the dissertation are those of the author.

SIGNED: Tia Salter

DATE: 20/12/2022

# Table of Contents

# List of Figures

# List of Tables

# List of Abbreviations

**ANOVA**, Analysis of variance

**ATP**, Adenosine triphosphate

**CCCP**, Carbonyl cyanide m-chlorophenyl hydrazone

**CI**, Confidence interval

**DBO**, Diazabicyclooctane

**DDM**, n-Dodecyl β-D-maltoside

**DNA**, Deoxyribonucleic acid

**DSB**, Disulfide bond formation

**DTT**, Dithiothreitol

**EB**, Erythrosin B

**$EC_{50}$**, Half maximal effective concentration

**EDTA**, Ethylenediaminetetraacetic acid

**ESBL**, Extended-spectrum β-lactamase

**EV**, Empty plasmid vector

**FRET**, Fluorescence resonance energy transfer

**GFP**, Green fluorescent protein

**GST**, Glutathione-S-transferase

**GTP**, Guanosine triphosphate

**HiBiT**, High-affinity Small BiT

**HPLC**, High-performance liquid chromatography

**HTL**, Holotranslocon

**HTS**, High throughput screen

**$IC_{50}$**, Half inhibitory concentration

**IMV**, Inner membrane vesicle

**IPTG**, Isopropyl β- d-1-thiogalactopyranoside

**LB**, Lysogeny broth

**LDS**, Lithium dodecyl sulfate

**LgBiT**, Large BiT

**MBC**, Minimum bactericidal concentration

**MBL**, Metallo-β-lactamase

**MCS**, Multiple cloning site

**MIC**, Minimum inhibitory concentration

**MRSA**, Methicillin-resistant *Staphylococcus aureus*

**$NaN_3$**, Sodium azide

**NanoBiT**, NanoLuc Binary Technology

**ND**, Not determined

**$OD_{600}$**, Optical density at 600 nm

**OMV**, Outer membrane vesicle

**PBP**, Penicillin-binding protein

**PCR**, Polymerase chain reaction

**PL**, Proteoliposome

**PMF**, Proton-motive-force

**RB**, Rose Bengal

**RLU**, Relative luminescence units

**RNA**, Ribonucleic acid

**SaFT**, *S. aureus* fitness testing

**SARS**, Structure-activity relationship studies

**SBL**, Serine-β-lactamase

**SD**, Standard deviation

**SDS-PAGE**, Sodium dodecyl-sulfate polyacrylamide gel electrophoresis

**SEM**, Standard error of the mean

**SRP**, Signal recognition particle

**SS**, Signal sequence

**TMH**, Transmembrane helix

**WT**, Wildtype

# Chapter 1 General Introduction

## 1.1 The challenges of antibiotic innovation

Antibiotics – drugs that kill or inhibit growth of bacteria and are used to treat bacterial infections – are the cornerstone of modern medicine. They save lives through effective treatment of common infectious diseases and prevention of infection during routine procedures such as surgeries. Long before their exploitation by humans, antibiotics have commonly been adopted by microorganisms to inhibit other species competing for resources in their environment. These antibiotic-producing bacteria are also the source of determinants allowing them to grow in the presence of these antibiotics, a phenomenon known as antibiotic resistance (Benveniste & Davies, 1973; Marshall *et al.*, 1998).

Growing use of antibiotics in medicine has provided a selective pressure for the occurrence and spread of antibiotic resistance in human pathogens, which has become a serious threat to global health. Antibiotic resistant infections were directly responsible for 1.27 million deaths worldwide in 2019 (Murray *et al.*, 2022). While dependence on antibiotics has increased in recent decades, discovery of novel antibiotics has declined (Payne *et al.*, 2007; Kinch *et al.*, 2014). If this trend continues, it is estimated that resistant infections could kill 10 million people per year by 2050 (Review on Antimicrobial Resistance, 2014).

The economic model for pharmaceutical research and development is said to discourage antibiotic innovation (Payne *et al.*, 2007). Two major reasons for this are the typical acute nature of bacterial infections, requiring only short treatment durations compared to more long-term diseases, and antibiotic stewardship measures in which novel antibiotics are filed away as last-resort treatments to preserve efficacy (Butler *et al.*, 2022). These complex financial challenges and development incentives to help overcome them have been discussed in depth (Morel & Mossialos, 2010; Simpkin *et al.*, 2017; World Health Organization, 2020). However, for these incentives to succeed, it is necessary to understand current gaps in the antibiotic arsenal. These shape the priorities for future antibiotic development.

### 1.1.1 Priority pathogens

In 2017, the World Health Organisation (WHO) created a priority list for antibiotic research and development based on a ranking of different bacterial species with different patterns of resistance. Criteria used to rank priority include mortality rate, healthcare burden, incidence of resistance, transmissibility, preventability, treatability and the current development pipeline (Tacconelli *et al.*, 2018). The priority list, separated into three tiers based on ranking, is shown in Figure 1.1. A major finding from the WHO analysis is that the critical priority tier is occupied solely by Gram-negative bacteria. In Gram-negative (diderm) bacteria, the cell envelope comprises two membranes: the cytoplasmic membrane, which is a phospholipid bilayer; and the outer membrane, of which the

outer leaflet comprises lipopolysaccharide. Between the membranes is the soluble periplasmic compartment, which contains the peptidoglycan cell wall (Figure 1.2a). Gram-positive (monoderm) bacteria lack an outer membrane but have a substantially thicker cell wall (Figure 1.2b).

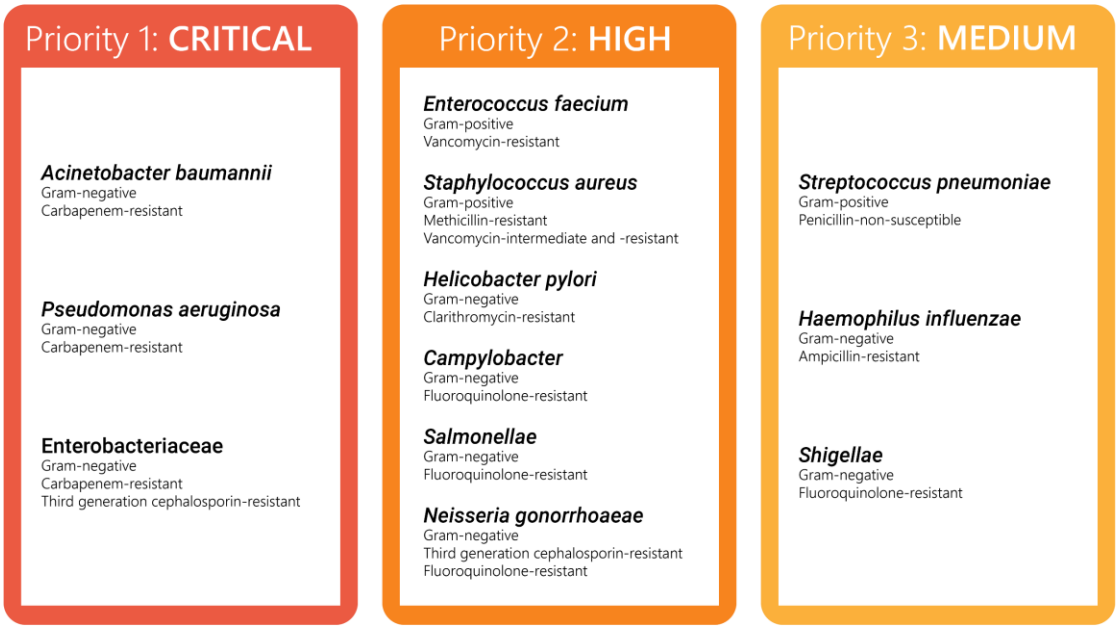


**Figure 1.1 The WHO list of priority pathogens for research and development of antibiotics**
In bold, bacterial species are ranked in order of priority (1 being highest) as determined by WHO (Tacconelli *et al.*, 2018). Enterobacteriaceae includes *Escherichia coli*, *Klebsiella* species and *Enterobacter* species. Within each species, different patterns of resistance are also ranked.

Membranes act as a barrier between the different compartments of a cell and the extracellular environment. The lipopolysaccharide-coated outer membrane provides an additional barrier for entry of antibiotic compounds into Gram-negative bacteria (Figure 1.2a). Therefore, Gram-negative bacteria are more difficult to treat with antibiotics than Gram-positives; only a subset of the existing classes of antibiotics have anti-Gram-negative activity. While small, hydrophobic compounds can diffuse directly across the outer membrane, entry of large, hydrophobic compounds is limited (Nikaido, 1976). Sufficiently small hydrophilic compounds can enter through protein pores (porins) studded throughout the outer membrane (Yoshimura & Nikaido, 1985). Additionally, the diderm structure supports a greater array of efflux systems, capable of actively expelling toxic molecules like antibiotics out of the cell. These innate properties of a bacterial cell that contribute to antibiotic resistance are examples of intrinsic resistance. They tend to be encoded in the bacterial chromosome, universal to that species of bacteria and independent of previous antibiotic treatment. Bacteria can also acquire resistance by horizontal gene transfer or mutation of existing genes. Mechanisms of antibiotic resistance can be intrinsic or acquired and include reduced uptake, active efflux, antibiotic target modification and antibiotic inactivation (for reviews see Davies & Davies, 2010; Fair & Tor, 2014; King, Sobhanifar & Strynadka, 2016; Reygaert, 2018). Chapter 5 discusses examples of the latter two mechanisms.

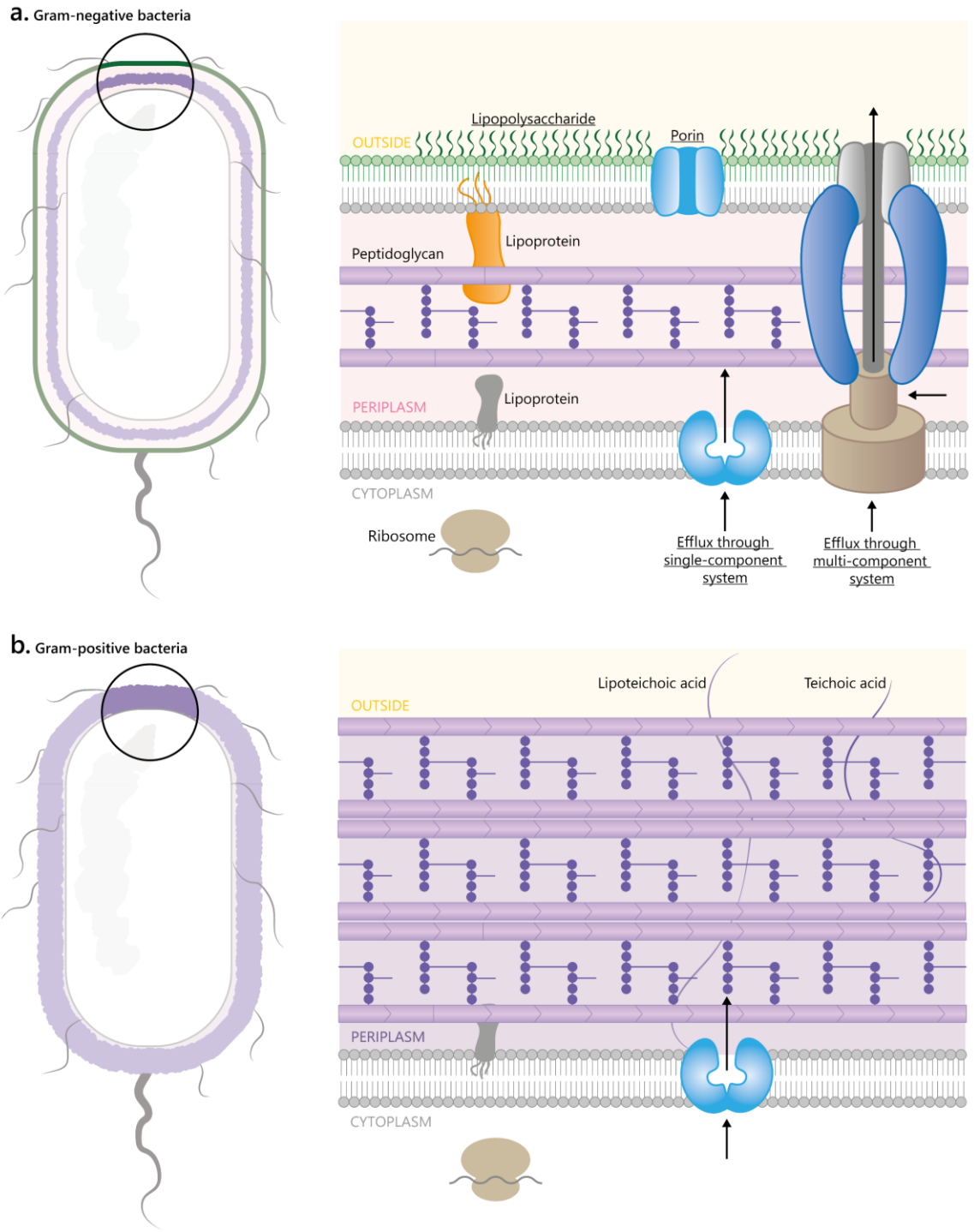


**Figure 1.2 Cell envelope structure and resistance mechanisms of Gram-negative and -positive bacteria**
The structure of the bacterial envelope (right) is given in the context of a whole cell (left). Cytoplasmic and outer membranes are shown as bilayers, with phospholipids in grey and lipopolysaccharide shown in green. Proteins may be integrated into, or peripherally associated with, either membrane, or present in the soluble cytoplasmic or periplasmic compartments. Envelope features and proteins that contribute to antibiotic resistance are labelled with underlined text. Black arrows indicate the direction of active drug efflux through single- and multi-component systems (**a**) or single-component systems only (**b**).

In Gram-negative bacteria, porins act as molecular sieves, allowing bacteria to control uptake of compounds dependent on porin characteristics such as diameter (Figure 1.2a). Mutations that alter the number or type of porins present, or that alter their selectivity, can limit drug entry and therefore

susceptibility (Nikaido & Rosenberg, 1981; Goldstein *et al.*, 1983). Efflux pumps are another bacterial feature that impact a range of drugs; indeed, collectively they have been found to limit periplasmic and/or cytoplasmic accumulation of nearly all antibiotic classes (Li & Nikaido, 2004). Efflux systems are classified into five families based on structure and energy source. The majority of these comprise a single cytoplasmic membrane component. Most often associated with the multi-drug resistant phenotype is the resistance-nodulation-cell division superfamily of efflux pumps. This is the only efflux system family to possess three key components: a cytoplasmic membrane pump, an outer membrane channel and a periplasmic adaptor protein (Saier *et al.*, 1994). Gram-positive bacteria utilise efflux systems from select single-component families (Figure 1.2b), while Gram-negatives can harbour any of the five families (Figure 1.2a).

### 1.1.2 The need for new antibiotic targets

Many current antibiotics were discovered by whole cell 'kill the bug' screening of natural products or synthetic chemical compounds. The golden era of antibiotic discovery was pioneered by Selman Waksman, who in the 1940s screened soil actinomycetes for their ability to suppress bacterial growth (Lewis, 2020). This Waksman platform for discovery brought about the first aminoglycoside antibiotics (Schatz, Bugie & Waksman, 2005) and was soon adopted by industry. Unfortunately, this platform very quickly became overmined, yielding frequent 'rediscovery' of existing drug classes. As a result, it is often said of antibiotic discovery that "the low hanging fruits are already picked" (Fair & Tor, 2014; Lewis, 2020). Synthetic chemistry brought about new classes of antibiotic, the most successful being the quinolones that target DNA gyrase and topoisomerase (type II and IV). Synthetic approaches were also essential to expanding existing antibiotic classes, through introduction of analogs with broader spectrum and ability to overcome resistance mechanisms (Lewis, 2020). However, since the discovery of quinolones in 1962, few new classes of antibiotic have been discovered, none of which have activity against Gram-negative species (Tacconelli *et al.*, 2018). The few established antibiotic classes target even fewer cellular targets – almost all target synthesis of DNA, RNA, protein, or the cell wall.

Focus must be placed on developing truly innovative antibiotic agents targeting priority pathogens. The WHO defines an innovative antibiotic lead as fulfilling at least one of the following criteria: belonging to a new chemical class, acting on a new target or by a new mechanism, or able to obviate resistance by mechanisms currently found in bacteria (World Health Organisation, 2017). While there has been growing interest in non-traditional antibiotic approaches, such as immunomodulating agents, antibodies and bacteriophage therapy, traditional small molecule antibiotics have a well-established regulatory pathway and therefore face fewer hurdles to clinical application (Theuretzbacher *et al.*, 2020). Critical analysis of the antibiotic development pipeline by the WHO has been ongoing since 2017. As of summer 2021, 12 new small molecule antibiotics have been approved worldwide since the WHO commenced this analysis. Five are active against at least one critical priority pathogen and the rest are active on a medium/ high priority pathogen. However, none have a novel mechanism of action and only one represents a new chemical class (Butler *et al.*, 2022).

One innovative approach is target-driven antibiotic discovery. Targeted approaches bias antibiotic discovery towards a particular mechanism of action, enabling researchers to filter out existing antibiotic classes. To ensure broad-spectrum activity, potential targets should be conserved across bacteria, particularly priority pathogens, and essential to viability. To avoid toxicity in humans, appropriate antibiotic targets should lack close human homologs. Comparative analyses of bacterial and human genomes have revealed approximately 300 essential and conserved proteins, non-homologous with human genes, that could be targeted with antibiotics (Sakharkar, Sakharkar & Chow, 2004; Fair & Tor, 2014). To reduce the possibility of bacterial cross-resistance to novel antibiotics by existing mechanisms, their targets should also be distinct from those of established antibiotics. Another consideration is that antibiotics targeting single enzymes are prone to evolution of resistance by single-step mutation of the gene encoding their target. To minimise target-based resistance, antibiotics or antibiotic cocktails with multiple targets could be developed. In this case, targets could be essential to virulence, pathogenicity or resistance, so their inhibition will attenuate affected bacteria and promote clearance by the immune system or potentiate the action of other antibiotics. Examples of such approaches are discussed in Chapter 5. To enable inhibitor development, selected targets should be well characterised, with known function, structure, mechanism of action and established assays for monitoring their activity.

### 1.1.3 Bacterial protein translocation as an antibiotic target

Correct protein synthesis, processing and turnover is essential to bacterial physiology and therefore a promising antibiotic target. Indeed, many approved antibiotics target bacterial ribosomes, impairing protein synthesis. While all bacterial proteins are synthesised in the cytoplasm, many perform their role outside this membrane-bound compartment. Extracytoplasmic proteins are vital to construction of the bacterial cell envelope and for bacterial communication with the environment. This includes uptake of compounds and efflux of toxins, both mechanisms playing a role in antibiotic resistance (Figure 1.2), as well as virulence and defence. Studies in *E. coli* revealed that 57 of its 356 essential proteins are extracytoplasmic (Loos *et al.*, 2019). To perform their function, each of these proteins must be transported across (or into) membranes to their destination compartment. This essential process could be targeted with antibiotics. However, there are no antibiotics targeting general protein translocation approved for use in the clinic, and until recently, very little research has been conducted on bacterial protein translocation as an antibiotic target (Segers & Anné, 2011; Rao *et al.*, 2014).

The first step to correct localisation of any cell envelope protein is passage across (or insertion into) the cytoplasmic membrane. The general machineries that carry out this process in bacteria are Sec (general secretory) and Tat (twin-arginine translocation). The mechanisms of Sec- and Tat-mediated protein translocation are fundamentally different: while protein substrates of the Sec-machinery must be unfolded (Arkowitz, Joly & Wickner, 1993), the Tat-machinery is involved in the transport of folded proteins. Many Tat substrates are proteins that noncovalently associate with cofactors in the cytoplasm (Berks, 1996; Santini *et al.*, 1998).

In *E. coli*, 96% of extracytoplasmic proteins are transported by the Sec-machinery (Orfanoudaki & Economou, 2014). The Sec-machinery is essential and conserved across bacteria, including priority pathogens (Oliver & Beckwith, 1981; Sadaie & Kada, 1985; Phillips & Silhavy, 1992; Tschauder, Driessen & Freudl, 1992). Sec complexes are also ubiquitous in eukaryotes (Hartmann *et al.*, 1994), where they translocate pre-secretory or membrane proteins across or into the endoplasmic reticulum membrane, but these are distinct from their bacterial counterpart (see Section 1.2 below). The Sec-machinery therefore meets the basic criteria of a good antibiotic target. The cellular location of Sec, being exposed in part to the periplasm, is also beneficial as it is more accessible to inhibitors (added extracellularly) than cytoplasmic targets. It is well-characterised in function and structure, with multiple assays available for studying its activity (see Chapter 3).

Where Tat is present, it always coexists with Sec. Unlike Sec, homologs of Tat have not been found in animals. However, compared with Sec, the composition and function of Tat is also less conserved across bacterial species (Dilks *et al.*, 2003; Yamada *et al.*, 2007; Palmer & Berks, 2012). It is even absent in some species of bacteria, including *Streptococcus pneumoniae* (Dilks *et al.*, 2003). Several human pathogens require Tat for export of virulence determinants (De Buck, Lammertyn & Anné, 2008), for example *tatC* mutants of *Pseudomonas aeruginosa* are attenuated in infection (Ochsner *et al.*, 2002). Nevertheless, the Tat-dependent proteome is substantially smaller than that dependent on Sec – there are approximately 30 potential Tat-dependent proteins encoded within the *E. coli* genome (Dilks *et al.*, 2003; Tullman-Ercek *et al.*, 2007). Consequently, Tat is not essential for viability in most clinically relevant bacteria. *Mycobacterium tuberculosis* is the only human pathogen in which Tat has been deemed essential in a laboratory setting (De Buck, Lammertyn & Anné, 2008; Palmer & Berks, 2012). Thus, compounds targeting the Tat-machinery may be useful as anti-virulence or anti-tuberculosis agents but are less likely to inhibit growth of critical priority pathogens. In comparison to Sec, structural information and biochemical assays for Tat are limited, which impedes efforts to establish Tat as an antibiotic target (Vasil, Tomaras & Pritchard, 2012).

## 1.2 Druggable targets in the Sec-machinery and their roles in translocation

Protein translocation occurs in three stages: substrate recognition and targeting to the translocation machinery, translocation through this machinery, then substrate release (Figure 1.4; Figure 1.7; Figure 1.9). Broadly, translocation through Sec can occur through two pathways: translationally coupled or uncoupled. Typically, the former pathway is reserved for integral cytoplasmic membrane protein insertion, while pre-secretory proteins (those destined for the periplasm, extracellular environment or outer membrane of Gram-negative bacteria) are transported by the latter (Ulbrandt, Newitt & Bernstein, 1997; Schibich *et al.*, 2016). Translationally coupled translocation requires co-translational targeting of substrate, usually by signal recognition particle (SRP). Through interaction with the SRP receptor, SRP targets translating ribosomes to the Sec channel (Powers & Walter, 1997). Membrane insertion is mediated by the Sec holotranslocon (Figure 1.4). On the other hand, translationally uncoupled translocation only requires the core translocon (Brundage *et al.*, 1990),

possibly in dimer form. Adenosine triphosphate (ATP) hydrolysis by the motor protein SecA provides the essential driving force (Economou & Wickner, 1994) and translocation is promoted by the proton-motive-force (PMF) across the membrane (Brundage *et al.*, 1990; Shiozuka *et al.*, 1990). SecA also acts as the targeting factor for this pathway (Brundage *et al.*, 1990). Targeting by SecA may be co- or post-translational; some pre-proteins may be fully synthesised before translocation begins (Figure 1.7). Proteolysis either during or after translocation releases mature protein on the extracytoplasmic side of the membrane (Josefsson & Randall, 1981).

Each of the recognition, translocation and release steps are governed by a fine balance of interactions, each of which could be targeted by novel antibiotics to perturb the bacterial secretome. Potential druggable targets in the Sec-machinery and the mechanisms by which they mediate protein translocation are outlined below.

## 1.2.1 Substrate recognition

### *1.2.1.1 Signal sequences*

A signal hypothesis for protein translocation into and across membranes was first proposed by Blobel and Dobberstein (1975). Nascent Sec and Tat substrates are synthesised as pre-proteins, with an N-terminal signal sequence (SS). This sequence contains all the information necessary for directing the passenger protein to translocation. SSs have a conserved general structure (Figure 1.3) but with significant variation in length and amino acid composition (von Heijne, 1985).

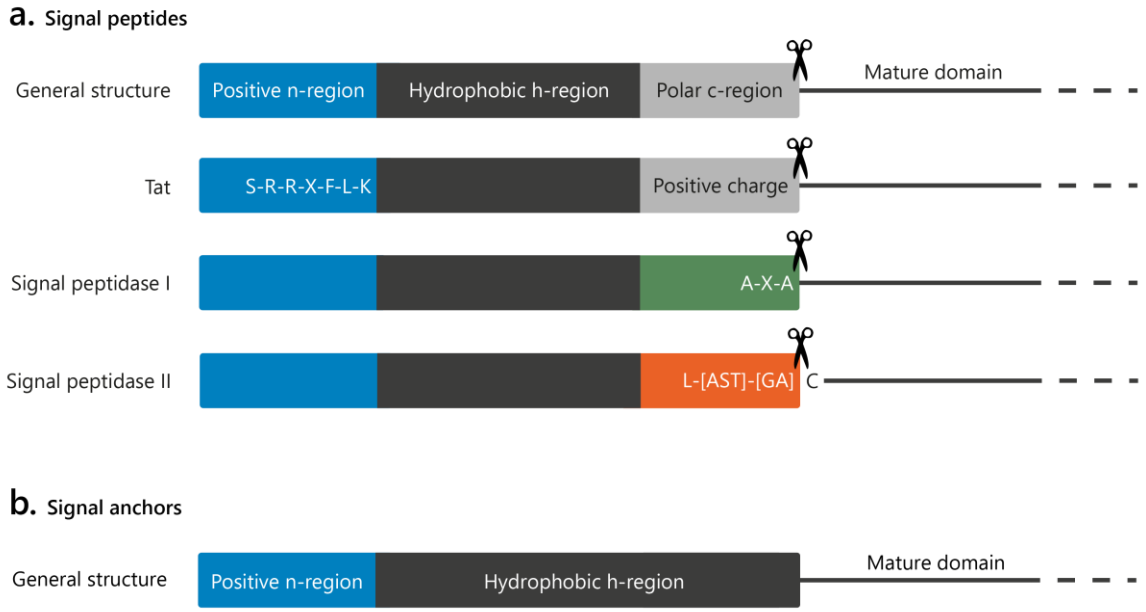


**Figure 1.3 Structure of signal sequences**
Schematic representation of signal sequence types (N- to C-terminus, left to right) with scissors indicating the signal peptidase cleavage site. The N-terminus of the mature domain is shown as a thin black line. Consensus motifs are shown in single-letter amino acid notation; X can be any amino acid and square brackets mean any of the listed amino acids may be present at that position.

Typically, SSs are 20 – 24 amino acids long (Cranford-Smith & Huber, 2018; Pradel *et al.*, 2009). They comprise a positively charged N-terminal region (n-region) containing one or more basic

amino acids and a hydrophobic core (h-region). Cleavable SSs, also termed signal peptides, are found on pre-secretory proteins. In addition to the n- and h-regions, these SSs possess a C-terminal region defining a cleavage site (c-region) for SS removal (Figure 1.3a). This cleavage reaction is important for release of mature protein from the membrane upon translocation. By contrast, integral cytoplasmic membrane proteins are directed to translocation by a transmembrane α-helix. This type of SS is also known as a signal anchor (Figure 1.3b), has a more hydrophobic h-region on average, lacks a c-region and is not cleaved upon translocation (von Heijne, 1985).

The amino acid composition of a SS determines the pathway by which the passenger protein will be translocated. Tat-specific SSs are distinguishable from their Sec-specific counterpart by their conserved twin-arginine motif, S-R-R-X-F-L-K, at the boundary of the n- and h-regions (Berks, 1996; Palmer & Stansfeld, 2020).In most cases, the eponymous twin arginines are essential for efficient recognition by Tat (Stanley, Palmer & Berks, 2000). Typically, the h-region of a Tat SS is less hydrophobic than that of Sec signals. Increasing hydrophobicity of a Tat-specific SS does not preclude translocation by Tat but may result in translocation by both Tat- and Sec-machineries (Cristóbal *et al.*, 1999). Tat-specific SSs also carry a positively charged amino acid in their c-region. While not essential for Tat-dependent transport, this – together with lower h-region hydrophobicity – serves as a Sec avoidance signal and likely prevents lethal jamming of the Sec channel with folded proteins (Bogsch, Brink & Robinson, 1997; Cristóbal *et al.*, 1999; Stanley, Palmer & Berks, 2000). The twin-arginine motif and cognate binding site on the Tat-machinery likely evolved as a means to strengthen substrate recognition in the presence of a weakly hydrophobic SS (Huang & Palmer, 2017).

The positively charged n-region interacts with the negatively charged cytoplasmic surface of the membrane and the h-region inserts into the hydrophobic phospholipid bilayer. The SS and early mature domain of Sec substrates form a hairpin loop within the translocon (Figure 1.4b), with the n-region at the cytoplasmic side of the membrane and the h-region resembling a transmembrane helix (von Heijne, 1992; Corey *et al.*, 2016; Ma *et al.*, 2019). The c-region of signal peptides is positioned at the periplasmic face of the membrane in a β-stranded conformation (Paetzel, Dalbey & Strynadka, 1998). By contrast, the positively charged c-region of Tat-specific SSs remains on the cytoplasmic side of the membrane and h-region penetrates halfway across the membrane as a hairpin-hinge. The SS must unhinge to allow translocation of the folded passenger protein across the membrane (Hamsanathan *et al.*, 2017).

As well as distinguishing pre-secretory proteins from integral membrane proteins, the c-region of SSs determines the fate of pre-secretory proteins following translocation. Type I cleavable SSs possess small, hydrophobic, neutral residues (generally alanines) at positions -3 and -1 relative to the cleavage site. This A-X-A consensus motif is recognised by signal peptidase I (von Heijne, 1984). By contrast, a L-[AST]-[GA] motif immediately preceding the cleavage site and cysteine in the +1 position (also known as a lipobox motif) denotes a pre-pro-lipoprotein. Such substrates are processed by signal peptidase II (von Heijne, 1989). Both Sec- and Tat-specific signal peptides can be processed by either enzyme.

Given the significant variation among SSs, a translocation inhibitor that acts by binding a SS is unlikely to have broad-spectrum activity. Alternatively, inhibitors of SS function could target the cytoplasmic factors responsible for SS recognition.

#### *1.2.1.2 Co-translational targeting by SRP*

Whereas Tat-dependent translocation does not require targeting factors (Palmer & Stansfeld, 2020), Sec SSs are recognised and targeted to translocation by cytoplasmic components, primarily SRP and SecA. While only 0.02% of Sec-specific SSs in *E. coli* possess twin arginines, half of them possess features that would allow productive engagement with Tat (Huang & Palmer, 2017; Palmer & Stansfeld, 2020). Given that the timing of interaction with cytoplasmic factors would be sooner than that with membrane-bound Tat, Sec substrates are likely triaged into the Sec pathway by SRP or SecA before they can engage Tat (Palmer & Stansfeld, 2020).

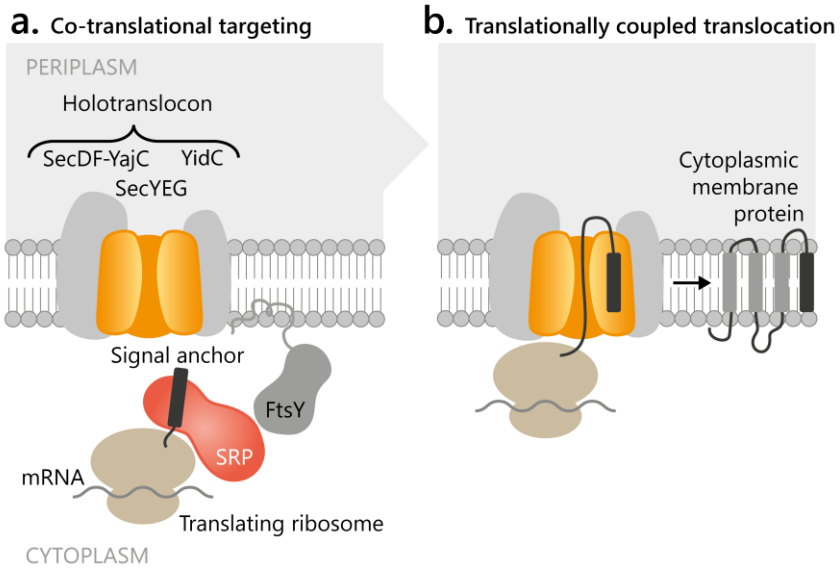


**Figure 1.4 Mechanism of co-translational targeting to Sec by SRP**
Integral cytoplasmic membrane proteins are translated from mRNA in ribosomes. **a.** As their signal anchor emerges from the ribosome exit site, they are recognised by SRP and directed to the holotranslocon via interactions of SRP with the membrane-bound SRP receptor, FtsY. **b.** Co-translational protein insertion is driven by ongoing protein synthesis. Substrate proteins are represented as a black line with signal anchors shown as a black rectangle and other transmembrane helices shown as grey rectangles. Black arrows indicate the direction of transport.

SRP is conserved across prokaryotes and essential for bacterial viability (Phillips & Silhavy, 1992). SRP is also found in eukaryotes, where it mediates protein translocation into the endoplasmic reticulum (Walter & Blobel, 1981). However, the prokaryotic and eukaryotic complexes differ in composition. Eukaryotic SRP comprises six proteins – SRP9, 14, 19, 54, 68 and 72 – alongside 7S RNA. Bacterial SRP is composed of a protein homologous to eukaryotic SRP54, named Fifty-Four Homologue (Ffh), and 4.5S (Gram-negative) or 6S (Gram-positive) RNA (Poritz, Strub & Walter, 1988; Bernstein *et al.*, 1993). Ffh has three domains: N, G and M (Romisch *et al.*, 1990; Zopf, Bernstein & Walter, 1993). The N-terminal N domain mediates ribosome binding, the G domain houses a Ras-like guanosine triphosphatase (GTPase) fold (Freymann *et al.*, 1997) and the C-

terminal methionine-rich M domain contains a SS-binding groove (Keenan *et al.*, 1998). A key feature of eukaryotic SRP that is absent from most bacteria is the Alu element on SRP RNA, that confers translational arrest activity on the complex (Siegel & Walter, 1988). Some Gram-positives, such as *Bacillus* and *Staphylococcus* species, do possess this element (Regalia, Rosenblad & Samuelsson, 2002).

*E. coli* SRP binds both translating and non-translating ribosomes with high affinity (Holtkamp *et al.*, 2012; Mercier *et al.*, 2017), positioning itself at the polypeptide exit tunnel. Bound SRP contacts the surface of the ribosome and positions its M domain at the ribosome exit tunnel (Figure 1.5a), where it can scan for presence of a SS (Schaffitzel *et al.*, 2006; Denks *et al.*, 2017). The SS-binding groove of the SRP M domain comprises a series of flexible hydrophobic residues forming a continuous surface along the groove. The nature of this groove may allow SRP to bind SSs of varying lengths and amino acid composition (Keenan *et al.*, 1998; Janda *et al.*, 2010). Upon elongation of nascent polypeptide to 40 – 50 residues such that its N-terminus is exposed outside the exit tunnel, only those possessing an SRP-specific signal maintain a high-affinity interaction with SRP (Mercier *et al.*, 2017). If an SRP-specific SS is not present, the affinity of SRP for the translating ribosome decreases leading to complex disassembly. The substrate pool of *E. coli* SRP is the majority (87%) of integral cytoplasmic membrane proteins and a small number (6%) of pre-secretory proteins (Schibich *et al.*, 2016).

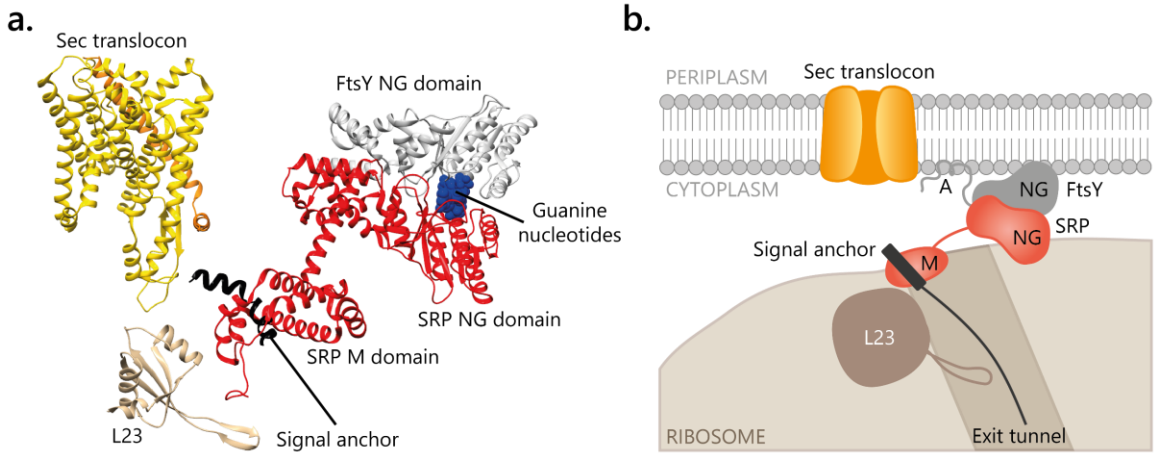


**Figure 1.5 The quaternary complex of ribosome, SRP, FtsY and Sec**
**a.** The structure (PDB 5NCO) of *E. coli* ribosomes (ribosomal protein L23 shown for reference) translating SRP substrate FtsQ in complex with SRP (protein component Ffh shown and SRP RNA omitted for simplicity), SRP receptor FtsY and the Sec translocon shown in cartoon format (Jomaa *et al.*, 2017). Guanine nucleotides (two total) bound to the NG domains of SRP and FtsY are shown in blue spheres format, highlighting the composite GTPase site. **b.** Schematic representation of **a**, shown in the context of the cytoplasmic membrane and polypeptide exit tunnel of the ribosome. The position of the FtsY A domain (which mediates most FtsY-Sec interactions) is shown.

When bound to ribosomes displaying SRP-specific SSs, the SRP NG domain has an increased affinity for guanosine triphosphate (GTP), a prerequisite for binding to the SRP receptor, FtsY in bacteria (Miller *et al.*, 1993). FtsY exists in equilibrium between membrane-associated and soluble, cytoplasmic states (Luirink *et al.*, 1994) and forms a complex with the Sec translocon via its N-terminal A domain (Angelini *et al.*, 2006). FtsY possesses N and G domains structurally similar to

those in SRP (Figure 1.5a). The NG domains of each protein mediate formation of a heterodimer in which both proteins share a composite GTPase active site. Upon dimerisation, the GTPase activities of both proteins are stimulated (Egea *et al.*, 2004). Formation of an active SRP-FtsY heterodimer increases the affinity of FtsY for its binding sites on the membrane. Reciprocally, membrane interaction drives conformation rearrangements in FtsY and SRP-FtsY, thus regulating the unloading of Sec substrates (Lam *et al.*, 2010).

Initially, FtsY binds proximal to the ribosomal exit tunnel. The Sec translocon is anchored near the exit tunnel through interactions with FtsY (Figure 1.5b). The SS extends from the SRP M domain, along the ribosome surface and towards the translocon (Jomaa *et al.*, 2017). Hydrolysis of GTP is necessary for complex disassembly, resulting in coupling of translating ribosomes to the translocon and regenerating free SRP and FtsY (Connolly & Gilmore, 1989; Miller *et al.*, 1993; Shan, Chandrasekar & Walter, 2007). Inhibitors of GTPase activity disrupt this process, blocking SRP-dependent protein translocation (Czech *et al.*, 2022). While such inhibitors are not clinically useful since they will also impact human GTPases, they demonstrate the potential druggability of SRP interactions.

#### *1.2.1.3 Co- and post-translational targeting by SecA*

Translationally coupled translocation using SRP ensures that pre-proteins cannot fold before passing through the Sec-machinery. However, it is limited by the rate of translation elongation. Bacteria lack specialised organelles (like the endoplasmic reticulum of eukaryotes) and membrane folding (like mitochondria) to increase the area available for protein translocation, thus the number of Sec translocons is also limiting. SecA likely exists in bacteria to increase translocation capacity, thus supporting the high rates of protein translocation needed for bacterial growth (Cranford-Smith & Huber, 2018). To maximise translocation capacity, only proteins absolutely requiring translationally coupled translocation (namely integral cytoplasmic membrane proteins) use SRP.

SecA is conserved across bacteria. Many bacteria have only one SecA, which is essential for viability (Oliver & Beckwith, 1981; Sadaie & Kada, 1985; Benson *et al.*, 2003). Some Gram-positives have two SecA homologs with non-overlapping functions: SecA1 and SecA2. SecA1 is a housekeeping protein with roles analogous to *E. coli* SecA, while SecA2 is generally nonessential for viability but plays an important role in virulence (Braunstein *et al.*, 2001; Bensing & Sullam, 2002; Bandara *et al.*, 2017). In some species, for example *Clostridium difficile*, SecA2 is essential (Fagan & Fairweather, 2011). Genomics approaches have frequently shown that SecA is absent in humans (Sakharkar, Sakharkar & Chow, 2004; Segers & Anné, 2011). The majority of cellular SecA is present as a peripheral protein on the cytoplasmic face of the membrane, and at some stages in its ATPase cycle, it inserts into the membrane. During these stages, accessibility for inhibitors of SecA may be increased (Economou & Wickner, 1994; Economou *et al.*, 1995; Eichler & Wickner, 1998; Rao *et al.*, 2014). Additionally, there are extensive structural, biochemical and biophysical data on SecA and assays to assess its activity. For this reason, SecA is an attractive target for antibiotic development, with multiple high throughput screens (HTSs) and inhibitors reported in the literature (see Chapter 3).

The large repertoire of intramolecular interactions, intermolecular interactions with various ligands and enzymatic activities of SecA provides a range of options for targeting its activity (Figure 1.6a). Each SecA molecule possesses two essential RecA-like nucleotide-binding domains (Walker *et al.*, 1982; Mitchell & Oliver, 1993). One nucleotide-binding domain comprises a high-affinity ATP-binding site, and the other is an intramolecular regulator of ATP hydrolysis which binds the former and stimulates ATP hydrolysis (Sianidis *et al.*, 2001). SecA also contains a helical wing domain, helical scaffold domain, pre-protein cross-linking domain and a C-terminal linker domain responsible for autoinhibition (Karamanou *et al.*, 1999). The helical scaffold domain contains both a long central helix, which provides a backbone for organisation of other domains, and a two-helix finger that contacts the translocon pore (Hunt *et al.*, 2002; Zimmer, Nam & Rapoport, 2008; Ma *et al.*, 2019).

Structural and biochemical studies of SecA have revealed an SS-binding site formed by regions of the two-helix finger and pre-protein cross-linking domain (Musial-Siwek, Rusch & Kendall, 2007; Gelis *et al.*, 2007; Auclair *et al.*, 2010; Grady, Michtavy & Oliver, 2012). The SS-binding site is large and complex, comprising negatively charged and hydrophobic residues for recognition of the n- and h-regions of an SS, respectively (Grady, Michtavy & Oliver, 2012). In the absence of SS, this site is occupied by 24 residues of the C-terminal linker domain (Gelis *et al.*, 2007). The cytoplasmic face of SecA houses a second site neighbouring the SS-binding site, responsible for interaction with the mature region of substrates. Interactions at both sites are necessary for activation of translocation (Chatzi *et al.*, 2017).

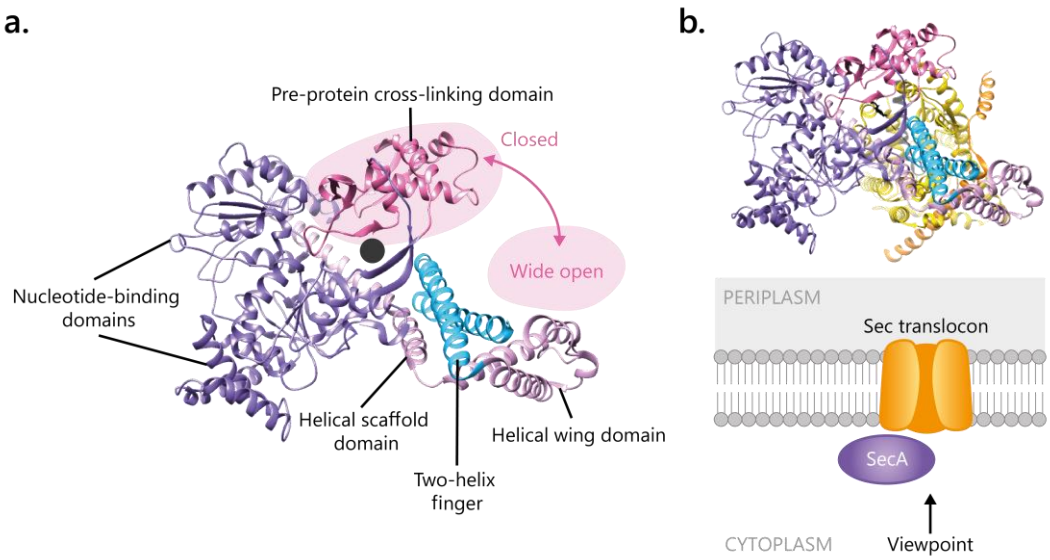


**Figure 1.6 Structure of SecA**
**a.** The structure of a SecA monomer (PDB 6ITC) is shown in cartoon format (Ma *et al.*, 2019). The pre-protein cross-linking domain and two-helix finger are shown in pink and blue, respectively. The pre-protein cross-linking domain is shown in the closed conformation; a pink curved arrow indicates the range of motion of this domain. The black dot indicates where pre-protein passes through this structure. **b.** The structure from **a** is shown in the context of the full PDB structure (top) and viewpoint relative to the membrane (bottom; indicated by black arrow). The Sec translocon (SecYE) is shown in shades of yellow.

For many years, it was accepted that the SecA targeting pathway entails pre-protein binding first to the cytoplasmic chaperone SecB. SecB is a homotetramer that interacts with pre-proteins through a large hydrophobic groove, thereby maintaining a translocation-competent conformation (Huang *et al.*, 2016). SecA has direct affinity for SecB through its C-terminal zinc-binding domain (Zhou & Xu, 2003). It was postulated that pre-protein is transferred from SecB to SecA and finally the channel complex (Hartl *et al.*, 1990). However, *secB* mutation does not affect bacterial growth and less than 5% of the *E. coli* secretome is SecB-dependent (Baars *et al.*, 2006).

More recently, it was revealed that SecA can co-translationally interact with ribosomes and nascent substrates via its N-terminus in a chaperone-independent manner (Figure 1.7a; Huber *et al.*, 2011; Chun & Randall, 1994; Huber *et al.*, 2017). Blocking the interaction between SecA and ribosomes slows translocation of SecA-dependent proteins. Interestingly, it also disrupts the interaction between SecB and substrate, suggesting that SecA binding to nascent substrate precedes SecB binding (Cranford-Smith & Huber, 2018; Huber *et al.*, 2017). Similarly to SRP, SecA scans the ribosomal exit tunnel for substrate (Knüpffer *et al.*, 2019). SecA engages substrates once they have reached a nascent chain length of approximately 100 amino acids (Zhu, Wang & Shan, 2022), far later than SRP engagement on its substrates.

Alongside its role in ribosome binding and co-translational substrate recognition, the SecA N-terminus mediates interactions with the Sec translocon and acidic phospholipids (Jilaveanu & Oliver, 2007; Cooper *et al.*, 2008; Das & Oliver, 2011; Knüpffer *et al.*, 2019). Thus, SecA can only perform co-translational targeting in its soluble, cytoplasmic state. For co-translational SecA substrates, SecA engagement precedes membrane association (Zhu, Wang & Shan, 2022). Given that SecA cannot simultaneously bind ribosomes and the translocon, the mechanism of how SecA targets ribosome-bound substrates to the translocon is unclear.

Given that the majority of cellular SecA is membrane-associated (Oliver & Beckwith, 1982), it is expected that only a small proportion of SecA is involved in co-translational substrate recognition. In line with this, only around half of pre-secretory proteins interact with SecA before release from the ribosome (Zhu, Wang & Shan, 2022). For those that are co-translationally targeted by SecA, timing of SecA engagement varies substantially. This spectrum of SecA engagement timing is due to a co-translational ribosome-binding chaperone called Trigger Factor (Figure 1.7b). The earliest interactions with Trigger Factor have the same timing as those with SecA (around 100 amino acids). In ribosome profiling experiments, pre-proteins that are post-translationally targeted by SecA and approximately half of co-translational SecA substrates were found to bind Trigger Factor first (Zhu, Wang & Shan, 2022). Together with SRP, SecA and Trigger Factor coordinate to sort Sec substrates into the appropriate targeting pathways.

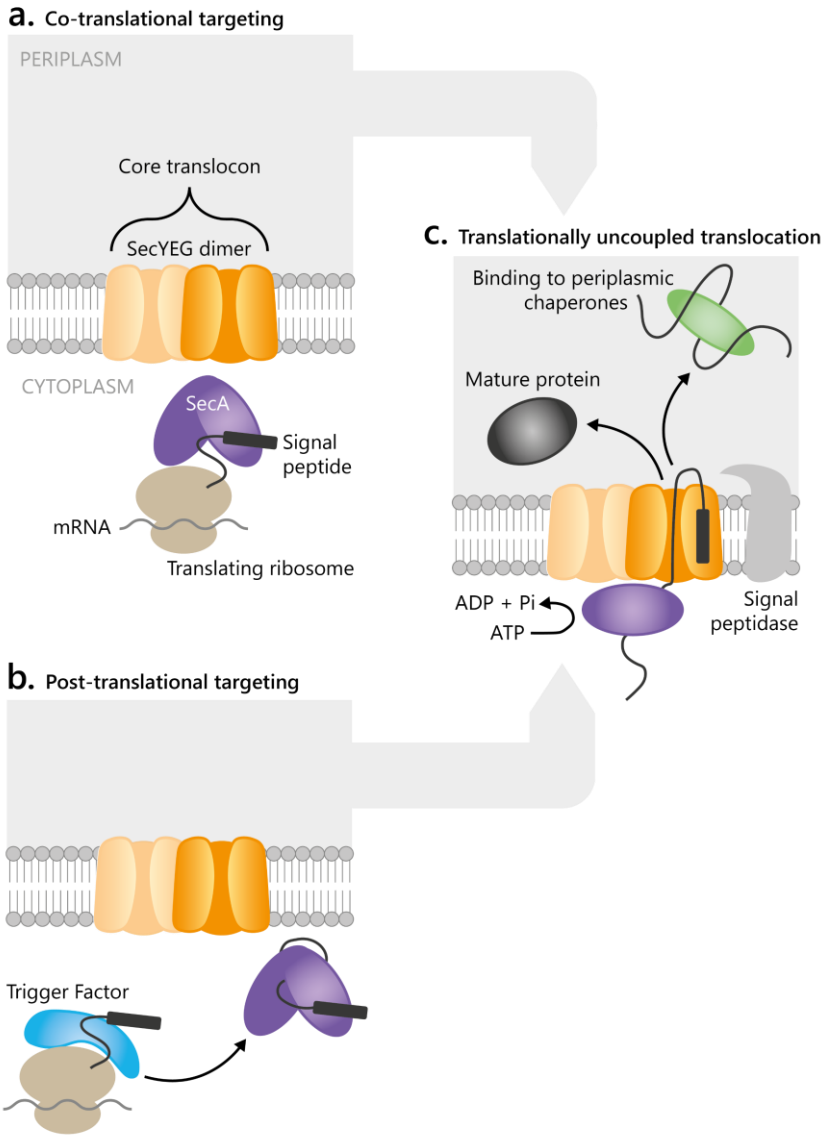


**Figure 1.7 Mechanism of co- and post-translational targeting to Sec by SecA**
Pre-proteins are translated from mRNA in ribosomes. As their signal peptide emerges from the ribosome exit site, they are recognised by **a.** SecA or **b.** Trigger Factor. Pre-proteins recognised by Trigger Factor engage SecA at a later stage of translation or after release from the ribosome. Pre-proteins, alone or within translating ribosomes, are targeted to the core translocon by SecA. **c.** Post-translational protein translocation is driven by ATP hydrolysis by SecA. Signal peptidase removes the signal peptide, releasing mature periplasmic protein or allowing transfer of outer membrane proteins to periplasmic chaperones. Substrate proteins are represented as a black line with signal peptides shown as a black rectangle. Black arrows indicate the direction of transport.

The major challenge of post-translational targeting to Sec-mediated protein translocation is preventing substrate folding, misfolding or aggregation prior to transport. SecA, SecB, Trigger Factor and cytoplasmic chaperones of the heat shock response maintain substrates in an unfolded, translocation-competent conformation. The bacterial chaperonin GroEL and its cofactor GroES have a strong affinity for pre-secretory protein (Zahn & Plückthun, 1992) and GroEL interacts with membrane-associated SecA (Bochkareva, Solovieva & Girshovich, 1998). While the chaperone system DnaK-DnaJ-GrpE preferentially interacts with cytoplasmic proteins, around 17% of DnaK interactors are putative extracytoplasmic proteins (Calloni *et al.*, 2012). The precise roles of each

chaperone system in protein translocation are substrate-specific and subject to functional redundancy. The chaperone requirements of model Sec substrate TEM β-lactamase are discussed in Chapter 5.

When SecA is bound to SS, the pre-protein cross-linking domain moves towards the nucleotide binding domains such that the polypeptide clamp transitions from a wide open to an open conformation (Hunt *et al.*, 2002; Gelis *et al.*, 2007; Zimmer, Nam & Rapoport, 2008). When substrate bound SecA binds the Sec translocon at the membrane, the pre-protein cross-linking domain undergoes a further conformational change, closing the clamp and activating the nucleotide binding domains (Figure 1.6a). The substrate is held by the pre-protein cross-linking domain clamp at its point of entry into SecA (Zimmer, Nam & Rapoport, 2008; Gold *et al.*, 2013; Collinson, Corey & Allen, 2015; Ma *et al.*, 2019). SecA binds cytoplasmic loops of SecY and the C-terminal SecY tail and contacts acidic phospholipids either side of the channel (Alami *et al.*, 2007; Zimmer, Nam & Rapoport, 2008; Gold *et al.*, 2010; Ma *et al.*, 2019). Post-translational SS handover from SecA may be mediated by the two-helix finger which inserts into the Sec channel (Figure 1.6b) and, alongside SecY cytoplasmic loops, guides the substrate into the translocon (Zimmer, Nam & Rapoport, 2008; Ma *et al.*, 2019).

### 1.2.2 Translocation through the Sec-machinery

#### *1.2.2.1 The core SecYEG translocon and Sec holotranslocon*

The core Sec components SecY and E are universally conserved in bacteria (Tschauder, Driessen & Freudl, 1992; Murphy & Beckwith, 1994). They are essential for translocation and bacterial viability (Brundage *et al.*, 1990; Hartl *et al.*, 1990; Murphy & Beckwith, 1994). SecG is not essential but promotes translocation through the channel (Duong & Wickner, 1997). SecY and E share significant similarity with eukaryotic Sec61α and γ, respectively (Hartmann *et al.*, 1994). By contrast, the β subunit of Sec61 bears no clear homology to SecG of bacteria (Van Den Berg *et al.*, 2004). Some antibiotics indirectly target SecY, suggesting that there is potential to exploit this protein as a target (Feltcher, Sullivan & Braunstein, 2010; Van Stelten *et al.*, 2009). Multiple inhibitors that bind the eukaryotic Sec61 complex have been discovered, offering insights into the possibility of targeting SecYEG (see Chapter 3).

In the SecYEG complex, SecY forms the channel (Van Den Berg *et al.*, 2004) It comprises ten transmembrane helices (TMHs), with cytoplasmic N- and C-termini and two large cytoplasmic loops (Figure 1.8a). The channel is situated between the two pseudo-symmetrical halves of SecY: TMH1-5 and TMH6-10. On the cytoplasmic side of the channel is a funnel-shaped pore serving as an entrance. When not engaged in translocation, this pore narrows to a close at a ring of six conserved hydrophobic residues in the middle of the lipid bilayer, and the external side of the channel is blocked by a ‘plug’ helix (Figure 1.8b). TMH5 and 6 act as a hinge for separation of the two halves of SecY. Reinforcing this hinge is SecE, comprising one conserved transmembrane helix and an amphipathic helix along the cytoplasmic face of the membrane (Figure 1.8a). Opposite the hinge region, TMH2 and TMH7 comprise the lateral gate. Separation of the two halves of SecY widens

the channel for protein translocation across the membrane, and opens the gate to the lipid bilayer for partitioning of integral membrane proteins (Van Den Berg *et al.*, 2004). Dimers of SecYEG form in a back-to-back arrangement, with SecE subunits proximal to one another (Kaufmann *et al.*, 1999). Dimerisation of SecYEG is required for optimal interaction with SecA (Figure 1.7; Deville *et al.*, 2011). However, only one copy of SecYEG is active in and essential for translocation (Osborne & Rapoport, 2007; Park & Rapoport, 2012; Schulze *et al.*, 2014).

A single copy of SecYEG may also associate with YidC, a membrane insertase. YidC can perform membrane protein insertion together with SecYEG or on its own; alone, it can insert mono or bitopic membrane proteins (Scotti *et al.*, 2000; Samuelson *et al.*, 2000; Serek *et al.*, 2004). It is conserved across bacteria and essential for viability (Scotti *et al.*, 2000; Samuelson *et al.*, 2000). It is a distant homolog of mitochondrial Oxa1p, widely conserved across eukaryotes (Bonnefoy *et al.*, 1994; Scotti *et al.*, 2000; Zhang, Tian & Wen, 2009). Downregulation of YidC production in *E. coli* increases susceptibility to antibacterial essential oils, validating it as a potential antibiotic target (Patil *et al.*, 2013).

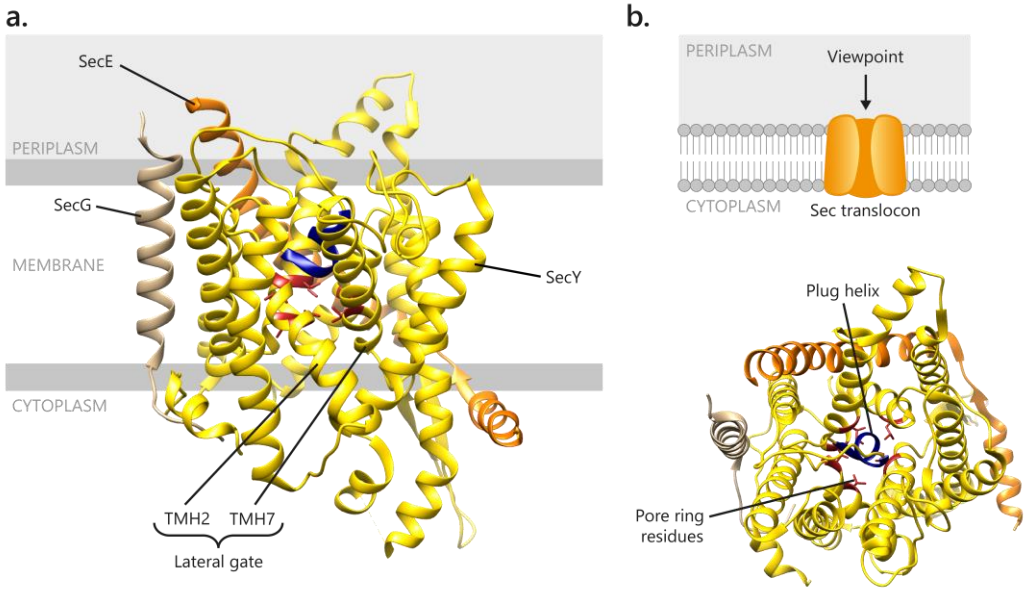


**Figure 1.8 Structure of SecYEG**
**a.** The structure of a SecYEG monomer (PDB 1RH5) is shown in cartoon with the lateral gate at the front. SecY is shown in yellow, SecE in orange and Secβ/ G in tan. **b.** The structure from **a** is shown from a periplasmic view. The plug helix is shown in blue and pore ring residues in red with side chains shown as sticks (Van Den Berg *et al.*, 2004).

YidC association with SecYEG requires the accessory subcomplex SecDF-YajC, together making up the HTL (Schulze *et al.*, 2014). The *secD*, *F* and *yajC* genes are encoded on the same operon. The individual role of YajC is unclear and it is not essential (Pogliano & Beckwith, 1994b). SecD and F are also not essential for viability or translocation, but mutation of *secD* or *F* inhibits translocation *in vivo* (Pogliano & Beckwith, 1994a). SecDF belongs to the resistance-nodulation-cell division superfamily (which includes the PMF-driven drug efflux systems, see section 1.1.1) and conducts protons across the membrane. The subcomplex has two major periplasmic domains, one of which binds unfolded protein and undergoes conformational changes important for SecDF

function (Tsukazaki *et al.*, 2011). These large periplasmic domains are accessible to inhibitors. Homologs of the accessory proteins SecD and F are absent in humans (Cao & Saier, 2003). However, these proteins are not universally conserved across bacteria (Cao & Saier, 2003) and SecDF-dependence is substrate-specific (Arkowitz & Wickner, 1994), so SecDF inhibitors are unlikely to have broad-spectrum activity.

Both HTL and the core SecYEG complex can induce SecA ATPase activity and mediate post-translational protein translocation across the membrane, although HTL is less efficient in this process (Figure 1.7). While SecYE alone is capable of transducing energy from the transmembrane PMF, HTL is more responsive to PMF stimulation, likely due to the presence of SecDF (Brundage *et al.*, 1990; Schulze *et al.*, 2014). Co-translational membrane protein insertion is more efficient through HTL than SecYEG (Figure 1.4; Schulze *et al.*, 2014). In HTL, YidC localises to the lateral gate of SecY (Sachelaru *et al.*, 2013), where it facilitates partitioning of substrate TMHs into the lipid bilayer.

#### *1.2.2.2 Translationally coupled translocation*

Upon handover to the translocon, the SS is inserted proximal to TMH2 and 7 of SecY. This triggers a conformational change in TMH7, opening the lateral gate (Wang *et al.*, 2004; Mitra *et al.*, 2005; Hizlan *et al.*, 2012; Corey *et al.*, 2016; Li *et al.*, 2016). From here, signal anchors and transmembrane domains of nascent membrane proteins may interact with YidC or partition into the lipid bilayer. The translocon pore is aligned with the ribosome exit tunnel, allowing passage of periplasmic domains (Mitra *et al.*, 2005). In eukaryotes, protein translocation initiated by SRP is driven by the energy of ongoing protein chain elongation. It is widely accepted that the driving force is the same for bacterial SRP substrates.

While SRP and co-translational translocation are sufficient for insertion of transmembrane domains, integral cytoplasmic membrane proteins with large periplasmic domains require additional machineries (typically SecA) for translocation (Neumann-Haefelin *et al.*, 2000; Zhu, Wang & Shan, 2022). During translationally coupled translocation, large regions of protein destined for the periplasm accumulate at the Sec channel entrance, likely disrupting the junction between Sec and the ribosome exit (Li *et al.*, 2016). SecA binds and resolves the protein build-up at the translocon, allowing recovery of the Sec-ribosome junction and continuation of translationally coupled translocation (Zhu, Wang & Shan, 2022).

Additionally, Sec and Tat can cooperate in membrane protein insertion. Actinobacterial Rieske proteins are the model substrates of this Sec and Tat dual transport pathway, possessing three to five transmembrane helices preceding an extracytoplasmic cofactor-containing domain. The first transmembrane domain comprises an SRP-specific signal anchor and the last resembles a Tat SS. Therefore, the Sec-machinery initiates translocation but disengages with substrate at the final transmembrane domain. The Tat-machinery takes over insertion of this domain and transport of the folded cofactor-containing domain (Keller *et al.*, 2012).

#### *1.2.2.3 SecA-mediated translocation*

Unlocking of the lateral gate by a SS primes SecYEG for translocation. Binding of ATP-bound SecA to the cytoplasmic loops of SecY and insertion of the SecA two-helix finger into the channel also causes partial opening of the lateral gate (Zimmer, Nam & Rapoport, 2008). Three of the six pore ring residues are located on TMH2 and 7, so lateral gate opening occurs concomitantly with widening of the channel (Figure 1.8). The plug is destabilised and moves towards the periplasm. The pre-protein cross-linking domain of SecA clamps around the substrate and SecA ATPase activity is fully activated (Zimmer, Nam & Rapoport, 2008; Collinson, Corey & Allen, 2015; Li *et al.*, 2016; Fessl *et al.*, 2018).

SecA-mediated SS insertion can occur in the absence of ATP hydrolysis, however plug opening and subsequent translocation requires the ATPase activity of SecA (Schiebel *et al.*, 1991; Collinson, Corey & Allen, 2015; Fessl *et al.*, 2018). Translocation of pre-protein through the channel occurs in a stepwise manner, requiring cycles of ATP hydrolysis and stimulated by the PMF. The Brownian ratchet model explains how ATP hydrolysis may promote protein translocation through Sec: i) polypeptides primarily pass through the channel by diffusion while SecA is in an ADP-bound state; ii) stretches of amino acids that cannot pass perturb the two-helix finger and trigger nucleotide exchange, opening the channel to allow passage and clamping the pre-protein cross-linking domain shut to prevent back-sliding; iii) hydrolysis of ATP closes the channel and traps these amino acid stretches on the periplasmic side of the membrane. The 'ratchet' biasing movement in the forward direction may be folding of translocated protein in the periplasm, interaction with periplasmic chaperones or protonation in the lower pH environment of the periplasm (Allen *et al.*, 2016; Corey *et al.*, 2019; Allen *et al.*, 2022). An alternative 'power stroke' model suggests that SecA binds substrate, pushes it forward through the channel, then releases substrate and retracts (Erlandson *et al.*, 2008; Bauer *et al.*, 2014). The evidence for either model, or a combination of the two, has been discussed previously (Bauer *et al.*, 2014; Allen *et al.*, 2016; Corey, Allen & Collinson, 2016). Inhibitors of the driving forces behind Sec-mediated transport may not only represent lead compounds for antibiotic development but could also help illuminate the mechanism of ATP-driven translocation.

### 1.2.3 Substrate release upon translocation

Type I and II signal peptidases represent different terminal branches of protein translocation. Signal peptidase I is responsible for the release of mature secretory proteins from the membrane following general protein translocation (Figure 1.9). Without signal peptidase I-mediated cleavage of the signal peptide, translocated proteins remain anchored to the membrane (Russel & Model, 1981; Dalbey & Wickner, 1985). Signal peptidase I is conserved across bacteria. Genetic and functional studies in *E. coli* and a range of human pathogens have shown that type I signal peptidase activity is essential to bacterial viability (Date, 1983; Cregg, Wilding & Black, 1996; Zhang, Greenberg & Lacks, 1997). Typically, Gram-negative bacteria have one chromosomal signal peptidase I gene, apart from *P. aeruginosa* which has two type I signal peptidases with distinct roles (Waite *et al.*, 2012), and Gram-positives commonly have multiple, redundant type I signal peptidases (Tjalsma

*et al.*, 1997; Parro *et al.*, 1999). Signal peptidase I also plays a role in virulence. As an example, the *Staphylococcus aureus* type I signal peptidase SpsB is required for processing of virulence proteins including extracellular proteases, lipases, superantigens and quorum sensing systems essential for biofilm formation (Kavanaugh, Thoendel & Horswill, 2007; Schallenberger *et al.*, 2012). Bacterial signal peptidase I is substantially different from the human counterpart in both structure and catalytic mechanism. For example, while human signal peptidases use a catalytic Ser/His/Asp triad or Ser/His dyad, the bacterial enzymes are serine proteases with an unconventional Ser/Lys dyad (Black, 1993; Paetzel, Dalbey & Strynadka, 1998). The numerous differences between bacterial and human signal peptidase make it possible to target the bacterial enzyme without side effects in human cells. Multiple screening attempts have validated signal peptidase I as a suitable antibiotic target. In addition, compounds targeting signal peptidase I are being developed as a potential new class of antibiotics (see Chapter 3).

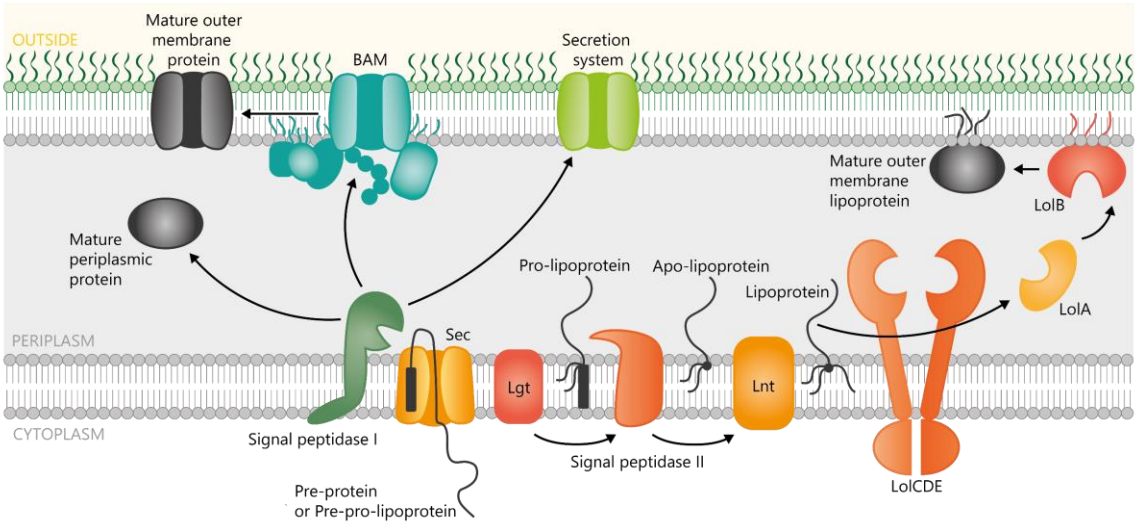


**Figure 1.9 Type I and II signal sequence processing following translocation**
Left, pre-proteins with type I signal sequences are recognised and cleaved by signal peptidase I, allowing release of mature periplasmic proteins, transfer of extracellular proteins to secretion systems, or outer membrane protein transfer to periplasmic chaperones and the β-barrel assembly machinery (BAM). Right, pre-pro-lipoproteins with a lipobox (type II signal sequence) are acylated by Lgt to pro-lipoprotein, cleaved by signal peptidase II then acylated further by Lnt. In Gram-negative bacteria, most lipoproteins are recognised by the Lol system and transferred to the inner leaflet of the outer membrane. Substrate proteins are represented as a black line with signal sequences shown as a black rectangle and lipobox cysteine as a small black circle. Black arrows indicate the direction of processing.

Signal peptidase II processes pre-pro-lipoproteins after their translocation (Figure 1.9). First, the phosphatidylglycerol/ prolipoprotein diacylglyceryl transferase Lgt attaches a diacylglycerol to the sulfhydryl group of the lipobox cysteine (Sankaran & Wu, 1994). The resulting pro-lipoprotein is recognised and cleaved by signal peptidase II (Dev & Ray, 1984), freeing up the amino group of the +1 cysteine for N-acylation by phospholipid/ apolipoprotein transacylase Lnt (Gupta & Wu, 1991). This gives mature lipoprotein. In Gram-negative bacteria, most lipoproteins are shuttled from the cytoplasmic membrane to the outer membrane by the Lol machinery. Gram-positive lipoproteins remain tethered to the outer leaflet of the cytoplasmic membrane. Signal peptidase II is an unconventional aspartic acid protease not found in eukaryotes, and lacks the conserved D-[ST]-G

motif found in eukaryotic aspartic acid proteases (Tjalsma *et al.*, 1999). While signal peptidase II is highly conserved and essential for viability in Gram-negative bacteria, it is not essential in Gram-positives (Gan *et al.*, 1993; Tjalsma *et al.*, 1999; Sander *et al.*, 2004; Stoll *et al.*, 2005). However, in some bacteria lacking the Gram-negative outer membrane like *M. tuberculosis*, the type II signal peptidase is important for virulence (Sander *et al.*, 2004). The cyclic peptide antibiotic globomycin inhibits signal peptidase II and growth of some Gram-negative bacteria including *E. coli* (Hussain, Ichihara & Mizushima, 1980; Dev, Harvey & Ray, 1985).

## 1.3 Aims

This introduction has presented the need for antibiotic innovation and proposed that antibiotics targeting the bacterial Sec-machinery could fulfil this need. It also gives an overview of the main components of the Sec-machinery, their function and their individual suitability as drug targets. The overarching aim of the following work is to further establish the bacterial Sec-machinery as a promising antibiotic target and to guide future discovery and development of Sec inhibitors. The work is divided into two objectives:

### 1.3.1 Objective 1: Develop a screening strategy for inhibitors of protein translocation by the bacterial Sec-machinery

Chapter 3 reviews existing screening strategies for Sec inhibitor discovery and the most promising antibiotic candidates inhibiting the Sec-machinery. Evaluation of the strengths and limitations of these previous approaches provides the rationale for design of a whole cell (*in vivo*) primary screen assay and counter assay based on the NanoLuc Binary Technology. The experimental portion of this chapter follows the validation of this assay setup using a model Sec substrate and commercially available inhibitors of Sec-mediated translocation, and deployment of the assay to screen a library of 5000 synthetic small molecules.

Chapter 4 discusses the downstream (secondary) assays needed to verify screen hits as *bona fide* Sec inhibitors. Two established *in vitro* assays for Sec-mediated translocation are compared for their ability to complement the primary and counter assays. Preliminary experiments are conducted to assess the antibacterial activity of hits. Together, chapters 3 and 4 propose a successful screening strategy.

### 1.3.2 Objective 2: Investigate the role of the Sec-machinery in a major mechanism of antibiotic resistance

Sec inhibitors lacking antibacterial activity may not provide useful antibiotic leads but – given the role of Sec in the correct localisation of proteins involved in virulence and resistance – could be used to potentiate current antibiotic treatments. Besides their clinical application, Sec inhibitors and the Sec inhibitor screen (Objective 1) are also valuable tools for investigating outstanding questions on Sec. Chapter 5 introduces a case study of β-lactamase enzymes: a major mechanism of antibiotic resistance in priority pathogens that relies on protein translocation often through the Sec-

machinery. Different Sec substrates can engage different accessory proteins and pathways for translocation, so how can researchers determine or predict the pathways used by diverse β-lactamases? Does inhibition of β-lactamase translocation translate to loss of β-lactamase activity? Which Sec components are the most useful targets for inhibition of β-lactamase translocation? The work presented here provides the tools to answer these questions.

# Chapter 2 Methods

## 2.1 General methods

### 2.1.1 Bacterial strains, culture, and transformation

MC4100 is an expression strain of *E. coli*, commonly used for translocation assays. All strains listed in the table below MC4100 are derivatives of this strain. Standard culture conditions are Miller's Lysogeny broth (LB; 10 g/l peptone 140, 5 g/l yeast extract, 10 g/l NaCl) with shaking at 200 rpm. Standard culture temperature for MM52 is 30°C to permit growth, and 37°C for all other strains. Under standard conditions, WAM121 cultures are supplemented with 50 µg/ml kanamycin and 0.2 % (w/v) arabinose. Unless stated otherwise, strains were grown under their respective standard conditions.

**Table 2.1 Bacterial strains used in this project**

| Strain | Genotype | Source |
|---|---|---|
| XL1-Blue | *E. coli* K-12 *recA1 endA1 gyrA96 thi-1 hsdR17($r_K^-$ $m_K^+$) supE44 relA1 lac [F´ proAB $lacI^qZ\Delta M15$ Tn10* (tetR)*]* | Agilent Technologies |
| BL21(DE3) | *E. coli* B $F^-$ *fhuA2 lon ompT dcm hsdS($r_B^-$ $m_B^-$) gal (λ DE3)* | New England Biolabs |
| C43(DE3) | *E. coli* B $F^-$ *ompT dcm hsdSB($r_B^-$ $m_B^-$) gal (λ DE3)* | Merck |
| MC4100 | *E. coli* K-12 $F^-$ *araD139 Δ(argF-lac)U169* $\lambda^-$ *$e14^-$ flhD5301 Δ(fruK-yeiR)725(fruA25) relA1 rpsL150*(strR) *rbsR22 Δ(fimB-fimE)632(::IS1) deoC1* | Coli Genetic Stock Centre |
| NR698 | MC4100 *lptD4213* | Kind gift of Prof. Thomas Silhavy (Ruiz *et al.*, 2005) |
| MM52 | MC4100 *secA51*(Ts) | Coli Genetic Stock Centre (Oliver & Beckwith, 1981) |
| WAM121 | MC4100 *$ara^+$ ffh::*kanR *attB::(oriR6K ParaBAD-$ffh^+$* tetR) | Weizmann Institute of Science (de Gier *et al.*, 1996) |

Chemically competent *E. coli* stocks were prepared as follows: overnight cultures were diluted 50-fold in fresh LB and grown under standard conditions until an optical density at 600 nm ($OD_{600}$) of 0.3 - 0.5; cells were harvested by centrifugation at 4500 x*g* for 10 min, resuspended in 1/2 volume ice-cold competency buffer (100 mM $CaCl_2$ + 10 % glycerol) and incubated on ice for 20 min; cells were pelleted by centrifugation as before and resuspended in 1/10 volume ice-cold competency buffer; after another 20 minute incubation on ice, suspensions were aliquoted and stored at -80°C.

Heat-shock was used for bacterial transformation. Chemically competent bacterial suspensions (10 - 50 µl) were thawed on ice, mixed with 20 - 100 ng purified plasmid DNA or 2 - 5 µl ligation reaction and incubated on ice for 10 min. Transformation reactions were transferred to 42°C for 45 s then placed back on ice for 5 min. Heat-shocked mixtures were supplemented with 200 - 500 µl LB and recovered for 1 h at the standard culture temperature for that strain. Recovered cells were plated on LB agar (1.6 % w/v) supplemented with 100 µg/ml ampicillin, 50 µg/ml kanamycin, 30 µg/ml chloramphenicol and/or 100 µg/ml spectinomycin as appropriate and cultured overnight in a static incubator under standard conditions. Single colonies from transformation plates were used to inoculate cultures for experiments.

### 2.1.2 SDS-PAGE analysis and immunoblotting

Unless stated otherwise, samples in 1X NuPAGE LDS sample buffer (Thermo Fisher Scientific) supplemented with 25 mM dithiothreitol (DTT) were heated to 95°C for 10 min. Samples (10 µl unless stated otherwise) were then resolved by sodium dodecyl sulfate-polyacrylamide gel electrophoresis (SDS-PAGE) on commercially sourced Bis-Tris protein gels (Invitrogen) according to the manufacturer's protocols. Bolt 12% Bis-Tris mini gels were used alongside Bolt MOPS running buffer for analysing β-lactamase constructs, while other proteins were resolved using Bolt 4 to 12%, Bis-Tris, Mini, 17-well gels with Bolt MES SDS running buffer or NuPAGE 4 to 12%, Bis-Tris, Midi, 26-well gels with NuPAGE MES SDS running buffer.

Protein gels were stained using InstantBlue Coomassie Protein Stain (Abcam) or blotted onto nitrocellulose membrane (Pierce) using a Power Blotter System (Invitrogen). Blots were developed with primary antibody – α-V5 (mouse monoclonal; GeneTex), α-TEM (mouse monoclonal; Insight Biotechnology), α-SecA C-terminus (rabbit polyclonal; laboratory stock), α-Ffh (rabbit polyclonal; laboratory stock), α-LacI (mouse monoclonal; Merck Millipore) – then DyLight-conjugated secondary antibody (Thermo Fisher Scientific). Blots were visualised using the Odyssey Fc System (LI-COR) and Image Studio (v 5.2).

### 2.1.3 Statistical analysis

Analysis of statistical significance was performed in RStudio (v 4.0.2). T-tests or one-way analysis of variance (ANOVA) tests followed by TukeyHSD tests were used for pairwise comparisons, as appropriate. For dose response assays, absolute $IC_{50}$ (X is concentration; Top=1; Baseline=0) was determined in GraphPad Prism (v 8.4.3).

## 2.2 Plasmid construction

Expression of β-lactamase constructs in the range of bacterial strains used required careful selection of an appropriate plasmid vector. Since WAM121 carries a kanamycin resistance gene on its chromosome, a plasmid using kanamycin for selection would be inappropriate. Other antibiotics to avoid include ampicillin, as this would complicate β-lactamase activity assays, and streptomycin, due to the *rpsL150*($Str^R$) mutation carried in strains with an MC4100 background.

MC4100 and MM52 carry the *araD139* mutation, which blocks arabinose metabolism and inhibits growth in the presence of arabinose (Englesberg *et al.*, 1962). This, alongside the arabinose-inducible *ffh* gene carried in WAM121, means that plasmids based on the arabinose expression system cannot be used. A T7 expression system would also be inappropriate as these strains do not produce the T7 polymerase.

pCDFT is a derivative of pCDFDuet-1 (Novagen, Sigma-Aldrich) that was generated by designing synthetic DNA of multiple cloning sites (MCS) 1 and 2 of pCDFDuet-1 with $P_{trp}$ promoters replacing the $P_{T7}$ promoter region but retaining the *lacO* region (Eurofins GeneStrand and Standard Gene, respectively). This gives a LacI/ $P_{tac}$ promoter system for each MCS, inducible by addition of isopropyl β-D-1-thiogalactopyranoside (IPTG). For exchanging the promoter of MCS1, the relevant synthetic DNA and pCDFDuet-1 were digested with New England Biolabs (NEB) restriction endonucleases EcoNI and BamHI (High-Fidelity versions were used where available). For MCS2, BsrGI and MfeI were used. Digested products were isolated by purification or gel extraction (QIAquick kits, QIAGEN), then ligated with T4 DNA ligase (NEB) and transformed into chemically competent XL1-Blue according to manufacturers' protocols. Constructs were verified by Eurofins Sanger sequencing with standard primers. pCDFT carries the *aadA* gene, which allows selection using streptomycin or spectinomycin. As MC4100 is resistant to streptomycin, spectinomycin was used.

The initial set of pCDFT-based β-lactamase constructs (encoding V5-tagged pTEM, pIMP-1 and pNDM-1) were generated by polymerase chain reaction (PCR) using Q5 Hot Start High-Fidelity DNA Polymerase (NEB), 1 ng template and 100 – 500 nM primer, following the manufacturer's guidelines. Plasmid pBAD/Myc-His B (Invitrogen, Thermo Fisher Scientific) was used as a template for amplification of *amp* (NCBI RefSeq WP_000027060.1) using primers pTEM-F and TEM-V5-R. Primers pIMP1-F and IMP1-V5-R were used to amplify $bla_{IMP-1}$ (NCBI RefSeq WP_003159548.1) from pSU2718-IMP1. Similarly, pNDM1-F and NDM1-V5-R were used for amplification of $bla_{NDM-1}$ (NCBI RefSeq WP_004201164.1) from pSU2718-NDM1. All pSU2718-based constructs were the kind gifts of Prof Matthew Avison (Cheung *et al.*, 2021). Primers were designed with 5' tails for addition of flanking restriction sites (BamHI – HindIII for TEM-181 and NDM-1; BamHI – SalI for IMP-1) and DNA encoding a C-terminal minimal V5 epitope, N - IPNPLLGL - C, codon-optimised for *E. coli* K-12. Purified PCR products and pCDFT were digested with the appropriate restriction endonucleases, purified, ligated, and transformed into XL1-Blue.

The resulting constructs formed the templates for generation of respective HiBiT-tagged constructs (pTEM-HiBiT, pIMP1-HiBiT and pNDM1-HiBiT) by PCR with universal primers BamHI-F and V5-HiBiT-R. These primers anneal to the regions flanking the β-lactamase insert in pCDFT. The 5' tail on V5-HiBiT-R was designed to add a codon-optimised DNA sequence encoding HiBiT, N - VSGWRLFKKIS – C, preceded by a GSG linker with a SalI restriction site following the stop codon. PCR products were inserted into pCDFT (BamHI – SalI) as above.

Mature versions of the resulting V5-HiBiT-tagged β-lactamase constructs (mTEM-HiBiT, mIMP1-HiBiT and mNDM1-HiBiT) were generated by PCR with the respective forward primer (mTEM-F,

mIMP1-F and mNDM1-F) and universal primer HindIII-R, which anneals to the HindIII restriction site downstream of the insert in pCDFT. The forward primers all anneal downstream of the codon corresponding to the -1 position on the cleavage site of the respective protein and contain a 5' tail for addition of a BamHI restriction site followed by an ATG start codon. PCR products were inserted into pCDFT (BamHI – SalI) as above.

SS-switched chimeric constructs iNDM1-HiBiT and nIMP1-HiBiT were generated by PCR of pCDFT-pNDM1-HiBiT and pCDFT-pIMP1-HiBiT, respectively. The former was achieved in one step using primers iNDM1-F and HindIII-R and template pCDFT-pNDM1-HiBiT. Primer iNDM1-F anneals downstream of the codon corresponding to the +6 position of NDM-1 and contains a 5' tail for addition of a BamHI restriction site followed by the first 24 codons of $bla_{IMP-1}$. By contrast, nIMP1-HiBiT was generated by two PCR steps: i) amplification of pCDFT-pIMP1-HiBiT using nIMP1-F and HindIII-R and ii) amplification of the resulting product with pNDM1-F and HindIII-R. Primer nIMP1-F anneals downstream of the codon corresponding to the +6 position of IMP-1 and contains a 5' tail for addition of the first 31 codons of $bla_{NDM-1}$. A BamHI site was added to the product by amplification with pNDM1-F and HindIII-R. PCR products were inserted into pCDFT (BamHI – SalI) as above.

The expanded set of pCDFT-based β-lactamase constructs includes pVIM1-HiBiT, pVIM2-HiBiT, pCTXM15-HiBiT and pKPC3-HiBiT. Gene synthesis of $bla_{VIM-1}$ (NCBI RefSeq WP_013263789.1) and $bla_{VIM-2}$ (NCBI RefSeq WP_003108247.1), with DNA encoding C-terminal V5 followed by HiBiT, was ordered from Eurofins Genomics. These genes were excised from their donor plasmids and inserted into pCDFT (BamHI – HindIII) as above. Primers pCTXM15-F and CTXM15-V5-HiBiT-R were used to amplify $bla_{CTX-M-15}$ (NCBI RefSeq WP_000239590.1) from pSU2718-CTXM15. Primers pKPC3-F and KPC3-V5-HiBiT-R were used for amplification of $bla_{KPC-3}$ (NCBI RefSeq WP_004152396.1) from pSU2718-KPC3. Primers were designed with 5' tails for addition of flanking restriction sites (BamHI and SalI) and DNA encoding C-terminal V5 followed by HiBiT. PCR products were inserted into pCDFT (BamHI – SalI) as above.

**Table 2.2 Primers used in this project**

| Primer name | Primer sequence (5' – 3') |
|---|---|
| pTEM-F | aga ctg gga tcc ATG AGT ATT CAA CAT TTC CGT GTC |
| TEM-V5-R | ctg aga aag ctt tta taa acc taa cag tgg gtt tgg aat CCA ATG CTT AAT CAG TGA GGC |
| pIMP1-F | aga ctg gga tcc ATG AGC AAG TTA TCT GTA TTC |
| IMP1-V5-R | ctg aga gtc gac tta taa acc taa cag tgg gtt tgg aat GTT GCT TGG TTT TGA TGG |
| pNDM1-F | aga caa gga tcc ATG GAA TTG CCC AAT ATT ATG CAC C |
| NDM1-V5-R | ctg aga aag ctt tca taa acc taa cag tgg gtt tgg aat GCG CAG CTT GTC GGC |

| | |
|---|---|
| BamHI-F | ACC ACA GCC AGG ATC CAT |
| V5-HiBiT-R | atc gaa gtc gac tta gct aat ttt ttt aaa cag gcg cca gcc gct cac gcc gga gcc TAA ACC TAA CAG TGG GTT TGG AAT |
| mTEM-F | aga ctg gga tcc atg CAC CCA GAA ACG CTG GTG |
| mIMP1-F | aga ctg gga tcc atg GCA GAG TCT TTG CCA GAT |
| mNDM-F | aga ctg gga tcc atG TGC ATG CCC GGT GAA ATC |
| iNDM1-F | aga ctg gat cca tga gca agt tat ctg tat tct tta tat ttt tgt ttt gca gca ttg cta ccg cag cag agt ctt tgc cag atC GCC CGA CGA TTG GCC AG |
| nIMP1-F | atg gaa ttg ccc aat att atg cac ccg gtc gcg aag ctg agc acc gca tta gcc gct gca ttg atg ctg agc ggg tgc atg ccc ggt gaa atc TTA AAA ATT GAA AAG CTT GAT GAA GGC |
| HindIII-R | TTA TGC GGC CGC AAG CTT |
| pCTXM15-F | aga ctg gga tCC ATG GTT AAA AAA TCA CTG CGC C |
| CTXM15-V5-HiBiT-R | aag ctt gtc gac tta gct aat ttt ttt aaa cag gcg cca gcc gct cac gcc gga gcc taa acc taa cag tgg gtt tgg aat CAA ACC GTC GGT GAC GAT |
| pKPC3-F | aga ctg gga tcc ATG TCA CTG TAT CGC CGT C |
| KPC3-V5-HiBiT-R | aag ctt gtc gac tta gct aat ttt ttt aaa cag gcg cca gcc gct cac gcc gga gcc taa acc taa cag tgg gtt tgg aat CTG CCC GTT GAC GCC |

Upper case letters denote annealing regions of the primer.

## 2.3 Protein preparations

Unless otherwise stated, all centrifugation steps were performed at 4°C.

### 2.3.1 LgBiT

BL21(DE3) was transformed with pBAD-$_{6H}$LgBiT. This plasmid, gifted by Dr. Daniel Watkins, encodes LgBiT with an N-terminal hexa-histidine tag under a AraC/ $P_{BAD}$ promoter and confers ampicillin resistance (Pereira *et al.*, 2019). A single colony was inoculated into 2xYT broth (16 g/l tryptone, 10 g/l yeast extract, 5 g/l NaCl) supplemented with 100 µg/ml ampicillin and cultured overnight at 37°C with shaking. Overnight cultures were diluted 1/ 50 (v/v) in fresh 2xYT containing ampicillin and grown at 37°C with shaking until $OD_{600}$ 0.6, then induced with 0.2% (w/v) arabinose for 3 h. Cells were harvested by centrifugation at 5000 x*g* for 15 min. Pellets were resuspended in buffer TKG (20 mM Tris, 50 mM KCl, 10% glycerol, pH 7.5), lysed with a cell disruptor (one pass at 25 kpsi; Constant Systems) then centrifuged at 40,000 x*g* for 30 min. The supernatant was loaded onto a HisTrap HP column (Cytiva), washed with 50 mM imidazole and eluted with 330 mM

imidazole. Using a spin concentrator with 3 kDa cut-off, the eluate was exchanged and concentrated into TKG.

### 2.3.2 GST-Dark

BL21(DE3) was transformed with pGEX-GST-Dark. This plasmid, gifted by Dr. Gonçalo Pereira, confers ampicillin resistance. It encodes Glutathione-S-transferase (GST) with a C-terminal dark peptide tag (N - VSGWALFKKIS – C) preceded by a SDPG linker under a LacI/ $P_{tac}$ promoter system (Pereira *et al.*, 2019). A single colony was inoculated into LB broth supplemented with 50 µg/ml ampicillin and cultured overnight at 37°C with shaking. Overnight cultures were diluted 1/ 100 (v/v) in fresh LB containing ampicillin and grown at 37°C with shaking until $OD_{600}$ 0.6 – 0.8. IPTG (1 mM) was added to induce expression and cells grown for a further 3 h. Cells were harvested by centrifugation at 4000 x*g* for 30 min, resuspended in TK buffer (20 mM Tris, 50 mM KCl, pH 7.5) then lysed with a cell disruptor. The supernatant was clarified by centrifugation at 167,000 x*g* for 45 min, then subjected to affinity chromatography using a GSTrap 4B column (GE Healthcare). The column was washed with TK buffer and GST-Dark eluted using TK + 20 mM reduced glutathione. The eluate was concentrated in a spin concentrator (10 kDa cut-off).

### 2.3.3 pSpy-HiBiT

Purified pSpy-HiBiT was a kind gift of Dr. Daniel Watkins. It was prepared as described previously (Pereira *et al.*, 2019). The protocol is as follows: MM52 was transformed with pBAD-pSpy-HiBiT-His. This plasmid encodes pre-secretory Spy (pSpy) with C-terminal minimal V5, HiBiT and hexa-histidine tags under an AraC/ $P_{BAD}$ promoter system and confers ampicillin resistance. A single colony was inoculated into 2xYT broth supplemented with 100 µg/ml ampicillin and cultured for 24 h at 30°C with shaking. Overnight cultures were diluted 1/ 10 (v/v) in fresh 2xYT containing ampicillin and grown at 39°C with shaking for 45 min. Expression was induced with 0.2% (w/v) arabinose for 2.5 h. Cells were harvested by centrifugation at 5000 x*g* for 15 min. Pellets were resuspended in buffer (50 mM Tris, 500 mM NaCl, 30 mM imidazole, pH 8.0) supplemented with cOmplete EDTA-free Protease Inhibitor Cocktail (Roche), lysed with a cell disruptor then centrifuged at 40,000 x*g* for 20 min. The soluble fraction was loaded onto a HisTrap column and washed with resuspension buffer. The eluate (300 mM imidazole) was exchanged into $TS_{130}$ buffer (20 mM Tris, 130 mM NaCl, pH 8.0), supplemented with 1 mM DTT, 0.5 mM ethylenediamine tetraacetic acid (EDTA) and 120 µg/ml TEV protease then incubated at room temperature for 3 h. The sample was then subjected to a second HisTrap step and the flow through was collected. Using a spin concentrator (3 kDa cut-off), this sample was exchanged into denaturing buffer (20 mM Tris, 6 M urea, pH 8.0) and concentrated.

### 2.3.4 pOmpA-V5

MM52 was transformed with pBAD-pOmpA-V5. This plasmid, gifted by Dr. William Allen, confers ampicillin resistance. It encodes full length pre-secretory OmpA (pOmpA), with its cysteines removed by mutagenesis and a C-terminal minimal V5 epitope, under an AraC/ $P_{BAD}$ promoter

system (Corey *et al.*, 2018). A single colony was inoculated into 2xYT broth supplemented with 100 µg/ml ampicillin and cultured for 24 h at 30°C with shaking. Overnight cultures were diluted 1/ 10 (v/v) in fresh 2xYT containing ampicillin and grown at 39°C with shaking for 45 min. Expression was induced with 0.2% (w/v) arabinose for 2.5 h. Cells were harvested by centrifugation at 5000 x*g* for 15 min. Pellets were resuspended in $TS_{130}$ buffer supplemented with cOmplete EDTA-free Protease Inhibitor Cocktail. Cells were lysed with a cell disruptor then centrifuged at 4000 x*g* for 15 min to collect inclusion bodies and cell debris. Pellets were rinsed with water then inclusion bodies solubilised in denaturing buffer by gentle mixing for 30 min at room temperature followed by homogenisation. Non-soluble material was removed by centrifugation at 200,000 x*g* for 60 min. The supernatant was loaded onto a HiTrap Q High Performance column (Cytiva) equilibrated in denaturing buffer and pOmpA eluted using an 80 ml linear gradient of 0 (Buffer A) – 200 mM KCl (20% Buffer B) at 4 ml/min. pOmpA was collected in the flow-through at approximately 10% B. Pooled fractions were spin concentrated (10 kDa cut-off).

### 2.3.5 SecA

BL21(DE3) was transformed with pET-SecA. This plasmid, gifted by Dr. William Allen, confers ampicillin resistance. It encodes SecA with its C-terminal domain replaced with a hexa-histidine tag under a LacI/ $P_{T7}$ promoter system (Gold *et al.*, 2007). A single colony was inoculated into LB broth supplemented with 50 µg/ml ampicillin and cultured overnight at 37°C with shaking. Overnight cultures were diluted 1/ 40 (v/v) in fresh LB containing ampicillin and grown at 37°C with shaking until $OD_{600}$ 0.6 – 0.8. IPTG (1 mM) was added to induce expression and cells grown for a further 1.5 h. Cells were harvested by centrifugation at 5000 x*g* for 15 min, resuspended in $TKM_{20,8.0}$ buffer (20 mM Tris, 50 mM KCl, 20 mM $MgCl_2$, pH 8.0) then lysed with a cell disruptor. The supernatant was clarified by centrifugation at 40,000 x*g* for 20 min, then loaded onto a column of Chelating Sepharose Fast Flow (Cytiva) resin charged with $NiSO_4$. The column was washed with 30 mM imidazole followed by a pulse of 6 M urea, then SecA was eluted in $TKM_{20,8.0}$ with 330 mM imidazole. The eluate was loaded onto a Q Sepharose Fast Flow (Cytiva) anion exchange column equilibrated in $TKM_{20,8.0}$ with 1 mM DTT and SecA eluted using a 40 ml linear gradient of 50 mM (Buffer A) – 1 M (Buffer B) KCl at 2 ml/min. After spin concentration (50 kDa cut-off), the fractions containing SecA (eluted at approximately 60% B) were subjected to size-exclusion chromatography (HiLoad 26/600 Superdex 200) in $TKM_{20,8.0}$ with 1 mM DTT. SecA was eluted approximately 60 ml after injection; desired fractions were pooled and concentrated as before.

### 2.3.6 SecYEG

C43(DE3) (Sigma-Aldrich) was transformed with pBAD22-SecYEG. This plasmid, gifted by Dr. William Allen, encodes SecYEG with an N-terminal hexa-histidine tag on SecE under an AraC/ $P_{BAD}$ promoter system and confers ampicillin resistance (Collinson *et al.*, 2001). A single colony was inoculated into 2xYT broth supplemented with 100 µg/ml ampicillin and cultured overnight at 37°C with shaking. Overnight cultures were diluted 3/ 200 (v/v) in fresh 2xYT containing ampicillin and grown at 37°C with shaking until $OD_{600}$ 0.8 – 1. Expression was induced by addition of 0.2% (w/v)

arabinose. After 3 h, cells were harvested by centrifugation at 5000 x*g* for 15 min, resuspended in $TSG_{300}$ buffer (20 mM Tris, 300 mM NaCl, 10% glycerol, pH 7.5) then lysed with a cell disruptor. The membrane fraction was pelleted by centrifugation at 167,000 x*g* for 45 min then resuspended in $TSG_{300}$ supplemented with 1% n-dodecyl β-D-maltoside (DDM). The suspension was mixed gently for 30 min at 4°C then clarified by centrifugation at 167,000 x*g* for 45 min. The supernatant was loaded onto a column of Chelating Sepharose Fast Flow resin charged with $NiSO_4$ and equilibrated in $TSG_{300}$ with 0.1% DDM. The column was washed with 30 mM imidazole then SecYEG was eluted with 330 mM imidazole. Fractions containing SecYEG were subjected to chromatography using HiLoad 26/600 Superdex 200 and Q Sepharose Fast Flow columns in combination. Columns were equilibrated in $TSG_{130}$ (20 mM Tris, 130 mM NaCl, 10% glycerol, pH 7.5) with 0.02% DDM. The injected sample was chased with a pulse of 5 M NaCl to determine the void volume of the column. SecYEG was eluted at 150 – 190 ml after injection; the desired fractions were pooled and spin concentrated (50 kDa cut-off).

### 2.3.7 SecYEG/ LgBiT and SecYEG proteoliposomes

*E. coli* polar lipids (4 mg/ml in 1% DDM) were treated with Bio-Beads until cloudy in appearance. Polar lipids (1 ml) were then mixed at room temperature with 20 µM purified LgBiT and 3.3 µM purified SecYEG. Bio-Beads were removed, and the mixture extruded into unilamellar liposomes by 11 passes through an Avanti Mini Extruder equipped with a 400 nm membrane. The extruded mixture was dialysed (12 – 14 kDa cut-off) in $TKM_{20,8.0}$ at 4°C overnight. Dialysis buffer was exchanged for fresh $TKM_{20,8.0}$ at 2 and 5 h dialysis. SecYEG/ LgBiT proteoliposomes (PLs) were pelleted by centrifugation at 345,000 x*g* for 20 min, washed once by resuspension in 2 ml denaturing buffer followed by centrifugation as before, then washed twice by resuspension in 2 ml $TKM_{20,8.0}$ then centrifugation as before. These wash steps are needed for removal of unencapsulated LgBiT. Harvested SecYEG/ LgBiT PLs were finally resuspended in $TKM_{20,8.0}$ to give 9.2 µM SecYEG. Empty SecYEG PLs were made in the same way, except omitting LgBiT and halving SecYEG concentration. Washing centrifugation steps were not required in this case. SecYEG may incorporate into PLs with its cytoplasmic face outside (correct orientation) or inside the vesicle; it is assumed that half the SecYEG present is correctly orientated and therefore active.

### 2.3.8 SecYEG/ Sec holotranslocon inverted inner membrane vesicles

pBAD22-SecYEG or pACEMBL-HTL3 (Botte *et al.*, 2016) were transformed into BL21(DE3). pACEMBL-HTL3, gifted by Sophie Williams, comprises genes encoding SecY, N-terminally His-tagged SecE, SecG and C-terminally calmodulin binding protein-tagged YajC under LacI/ $P_{trc}$ promoter systems, and C-terminally His-tagged YidC, C-terminally His-tagged SecD and SecF under control of AraC/ $P_{BAD}$. This plasmid confers ampicillin, kanamycin and chloramphenicol resistance. Single colonies were inoculated into 2xYT broth supplemented with 100 µg/ml ampicillin (SecYEG) or 50 µg/ml ampicillin, 25 µg/ml kanamycin and 25 µg/ml chloramphenicol (HTL) and cultured overnight at 37°C with shaking. Overnight cultures were diluted 3/ 200 or 3/100 (v/v) respectively in fresh 2xYT containing antibiotic and grown at 37°C with shaking until $OD_{600}$ 0.8 – 1.

Expression was induced by addition of 0.1% (w/v) arabinose or 0.2% (w/v) arabinose and 1 mM IPTG, respectively. After 2.5 h, cells were harvested by centrifugation at 5000 x*g* for 15 min, resuspended in $TKM_{2,7.5}$ (20 mM Tris, 50 mM KCl, 2 mM $MgCl_2$, pH 7.5) buffer then lysed by two passes through a cell disruptor. Supernatant was clarified by centrifugation at 20,000 x*g* for 20 min, then layered on top of 20% sucrose in $TKM_{2,7.5}$. Samples were centrifuged at 142,000 x*g* for 2 h, then the resulting pellet was resuspended in $TKM_{2,7.5}$. Sucrose gradients with equal volumes of $TKM_{2,7.5}$ with (from bottom to top) 1.6, 1.4, 1.2, 1.0 and 0.8 M sucrose were prepared, and the resuspended pellets layered on top. Gradients were centrifuged in a swing-out rotor at 174,000 x*g* overnight. Bands corresponding to the inner membrane fraction (bottom third of the gradient, omitting the pellet) were carefully removed and diluted at least two-fold in $TKM_{2,7.5}$. To pellet inverted inner membrane vesicles (IMVs), samples were centrifuged at 310,000 x*g* for 1.5 h. Pellets were resuspended in $TKM_{2,7.5}$. SecYEG concentrations were determined by anti-SecY immunoblot (with purified SecYEG as a standard) to be 5 and 3 µM in SecYEG and HTL IMV preparations, respectively.

## 2.4 Screening for inhibitors of protein translocation

### 2.4.1 Whole cell NanoBiT screen assay and counter assay

pBAD-pSpy-HiBiT or pBAD-mSpy-HiBiT were transformed into BL21(DE3). These plasmids, kind gifts of Dr. Daniel Watkins and Dr. William Allen, encode Spy variants with C-terminal minimal V5 and HiBiT tags under a $P_{BAD}$ promoter and confer ampicillin resistance. The former encodes the pre-protein form and the latter encodes mature Spy, lacking codons 2-23 encoding the signal peptide (Pereira *et al.*, 2019). Single colonies were inoculated into LB supplemented with 100 µg/ml ampicillin and cultured overnight at 37°C with shaking. Overnight cultures were diluted in fresh LB containing ampicillin to give expression cultures of $OD_{600}$ 0.05. Expression cultures were grown at 37°C with shaking until $OD_{600}$ 0.4, then diluted in fresh LB to $OD_{600}$ 0.1, with 100 µg/ml ampicillin, 0.1% (w/v) arabinose and inhibitor at the desired concentration. Diluted cultures (75 µl) were grown for 1.5 h in white-walled, clear flat-bottom 96-well plates (Corning 3610) at 37°C then stored at 4°C for 1 h. For low throughput assays, 100 µl buffer 1.6XTS (32 mM Tris, 32% w/v sucrose, pH 8.0) containing 2 nM LgBiT and 1/250 Nano-Glo Luciferase Assay Reagent (Promega) was added and luminescence read for 5 min. To assay NanoLuc activity from the periplasm of cells (primary assay) 25 µl of 1.6XTS containing 0.8 mg/ml lysozyme and 40 mM EDTA was injected, plates were shaken for 5 s and luminescence read for a further 55 min. For assays of NanoLuc activity from whole cells (counter assay) 1.6XTS was supplemented with Triton X-100 to a final concentration of 2% v/v. For hit discovery, this assay was used to screen a DiverSET compound library (ChemBridge) of 5000 compounds in 96-well plates. For higher throughput, plates were set up using a Tecan Freedom EVO 150 (in collaboration with BrisSynBio). In these assays, 125 µl 1.6XTS containing 1.6 nM LgBiT, 2/625 Nano-Glo Luciferase Assay Reagent, 0.16 mg/ml lysozyme and 8 mM EDTA was added, plates were shaken for 30 s then incubated for 1 h at 25°C before reading the luminescence endpoint. Plates were read using a CLARIOstar microplate reader (BMG Labtech) with an

integration time of 0.2 s/well, up to 3500 gain as required and no filter. Temperature was maintained at 25°C for the duration of the read.

### 2.4.2 *In vitro* translocation assays

#### *2.4.2.1 In vitro NanoBiT assays*

A master mix of reconstituted SecAYEG was prepared at 25°C in $TKM_{2,8.0}$ buffer (20 mM Tris, 50 mM KCl, 2 mM $MgCl_2$, pH 8.0) comprising all reaction components except test compound, substrate (pSpy-HiBiT) and ATP. The desired amount of test compound was added to empty wells of a solid white, U-bottom 96-well plate. Immediately before the reaction, pSpy-HiBiT was added to the master mix then the mix was added to wells containing compound (or $TKM_{2,8.0}$ as an untreated control). Luminescence was read for 10 min before injection of ATP (25 µl) and shaking (2 s), then luminescence was read for a further 10 - 25 min. Final reaction volume was 125 µl and composition was as follows: 0.1% Prionex, 0.1 mg/ml creatine kinase, 5 mM creatine phosphate, 1/1000 SecYEG/ LgBiT PLs (from stock with 9.2 µM SecYEG or 4.6 µM active SecYEG and 20 µM internal LgBiT), 1 µM SecA, 1/200 Nano-Glo Luciferase Assay Reagent, 10 µM GST-Dark, 2 µM pSpy-HiBiT and 1 mM ATP. Plates were read using a CLARIOstar microplate reader with an integration time of 0.1 s/well, 3500 gain and no filter. Temperature was maintained at 25°C for the duration of the read.

Resulting traces were analysed in pro Fit 7 (Quansoft) using a method adapted from earlier work (Allen *et al.*, 2020). Raw luminescence prior to ATP injection (background) was fitted to the following function:

```
function Three_Exp_plus_lag(A1, k1, C, S, A2, k2, A3, k3, lag: real);

inputs
A1 := 0, active;
A2 := 0, inactive;
A3 := 0, inactive;

k1 := 0, active;
k2 := 0, inactive;
k3 := 0, inactive;

C := 0, inactive;
S := 0, inactive;
lag := 0, active;

var
G1, G2, G3: real;
var xapp: real;



begin
xapp := x - lag;

if xapp < 0
then y := C
```

```
else
begin
G1 := A1 * (1 - exp(-xapp * k1));
G2 := A2 * (1 - exp(-xapp * k2));
G3 := A3 * (1 - exp(-xapp * k3));
y := G1 + G2 + G3 + C + (S * xapp);
end;


end;
```

For each run, this background fit was extrapolated to tabulate data post-injection and tabulated values subtracted from the respective data points. To account for the NanoLuc-quenching activity of test compound, the background-subtracted data were then normalised for 'brightness' through division by the amplitude (A1) determined in the background fit. The resulting transport signal data were fitted to the same function, except with `C := 0, active;` to give lag, apparent rate (k1, referred to herein as λ) and amplitude (A1).

#### *2.4.2.2 Protease protection assays*

Assays were performed similarly to previously described (Schulze *et al.*, 2014; Pereira *et al.*, 2019). A master mix of reconstituted Sec-machinery was prepared at 25°C in $TKM_{2,7.5}$ buffer comprising all reaction components except test compound and ATP. Final composition was as follows: 0.1 mg/ml creatine kinase, 5 mM creatine phosphate, SecYEG PLs at a concentration of 0.23 µM active SecYEG or IMVs at 0.28 µM SecYEG, 0.3 µM SecA and 0.7 µM pOmpA-V5. Master mix was added to eppendorfs containing the desired amount of compound (or $TKM_{2,7.5}$ as an untreated control) and equilibrated at 25°C for 5 min. ATP (to final concentration 1 mM) or $TKM_{2,7.5}$ for -ATP controls was added, and reactions allowed to proceed for up to 20 min. Reactions (50 µl) were quenched by addition to 200 µl of proteinase K mix (500 mM urea, 5 mM EDTA, pH 8.0 supplemented with 0.75 mg/ml proteinase K) and incubation on ice for 45 min. To precipitate successfully translocated pOmpA (protected from proteinase K activity), trichloroacetic acid was added to 20% (w/v) and reactions were incubated on ice for a further 30 min. To pellet precipitated protein, reactions were centrifuged at 18,000 x*g* at 4°C for 10 min. Pellets were resuspended in 30 µl 2.5X NuPAGE LDS buffer containing 2 M urea and resolved (10 µl) by SDS-PAGE. LDS samples were not heated prior to SDS-PAGE. The amount of translocated pOmpA-V5 from each reaction was analysed by α-V5 immunoblot.

### 2.4.3 Antimicrobial susceptibility testing by broth microdilution

Single colonies of the desired bacterial strain were inoculated into liquid medium (LB unless stated otherwise) supplemented with the appropriate antibiotic and cultured overnight at 37°C with shaking. Suspensions were prepared from overnight cultures. Serial two-fold dilutions of test compound were set up in a clear 96-well plate alongside a no compound control. Wells were inoculated with suspensions to a final volume of 150 µl and final $OD_{600}$ of 0.0004 - 0.0006. Plates were cultured for 18 h at 37°C with shaking. Growth was determined by measuring $OD_{600}$. For each

well, $OD_{600}$ was corrected by subtracting that of the respective blank. The minimum inhibitory concentration (MIC) was determined as the lowest concentration of compound at which $OD_{600}$ failed to reach a threshold of 0.1.

## 2.5 Interrogating β-lactamase translocation

### 2.5.1 *In silico* signal sequence analysis

β-lactamase protein sequences were analysed using SignalP 5.0 (Almagro Armenteros *et al.*, 2019) to detect Sec- or Tat-type signal peptides. This software can also distinguish between signal peptides processed by signal peptidase I and those processed by signal peptidase II. Sequences were also analysed using TatFind 1.4 (Rose *et al.*, 2002) and Phobius (Käll, Krogh & Sonnhammer, 2004). Predicted signal peptide sequences (consensus from the three different tools) were assessed for hydrophobicity using the algorithm described by Huber *et al.* (Huber *et al.*, 2005a) and the hydrophobicity scale derived by Wimley and White (Wimley & White, 1996).

### 2.5.2 Antimicrobial susceptibility testing by disc diffusion

Desired pSU2718 constructs were transformed into MC4100 and MM52. Single colonies were streaked onto LB agar (1.6%) supplemented with 30 µg/ml chloramphenicol and incubated overnight at 30 °C. Cells were suspended in phosphate-buffered saline (PBS; pH 7.4) to an $OD_{600}$ of 0.1, then streaked to lawn on Mueller Hinton (300 g/l beef infusion, 17.5 g/l casein hydrolysate, 1.5 g/l starch, pH 7.4) agar (1.6%). Cultures were challenged with 10 µg meropenem discs (Oxoid) and incubated for 16 - 18 h at 30, 37 or 42°C. Zones of growth inhibition (diameter in mm) were measured.

### 2.5.3 Whole cell NanoBiT assay for β-lactamases

MC4100 and derivative strains were transformed with pCDFT constructs. Single colonies were inoculated into LB supplemented with 100 µg/ml spectinomycin and cultured overnight under standard culture conditions for the respective strain. Overnight cultures were diluted in fresh LB containing spectinomycin to give expression cultures of $OD_{600}$ 0.05. Expression cultures were grown under desired conditions for 2 h, then induced with 10 µM IPTG. For comparison of different strains, expression cultures in falcon tubes were induced for 1.5 h, incubated on ice for 1 h then diluted to $OD_{600}$ 0.5 (final volume 75 µl) in solid white, U-bottom 96-well plates. For analysis of dose response to Sec inhibitors, cultures were diluted to $OD_{600}$ 0.05 (final volume 75 µl) in white-walled, clear, flat-bottom 96-well plates containing inhibitor at a range of concentrations at the time of induction, then grown for 1.5 h. Following growth, plates were stored at 4 °C for 1 h. NanoLuc activity from the periplasm of cells and from whole cells was assayed as described in section 2.4.1 for low throughput.

### 2.5.4 Nitrocefin hydrolysis assays

Cultures were grown as described above in section 2.5.3. After incubation on ice for 1 h, bacteria were resuspended to an $OD_{600}$ of 10 in Tris-sucrose buffer (20 mM Tris, 20% sucrose, pH 8.0). Lysozyme (0.1 mg/ml) and EDTA (5 mM) were added, and suspensions incubated on ice for 10 min. Then, 20 mM $MgCl_2$ was added, and suspensions centrifuged at 12,000 x*g* at 4 °C for 10 min. The supernatant (periplasmic fraction) was removed, and the pellet (spheroplasts plus membrane debris) was washed twice by centrifugation then resuspended in 1 volume Tris-sucrose buffer. Fractions (25 µl) were added to 50 µg/ml nitrocefin (APExBIO, 5 mg/ml stock in dimethyl sulfoxide, DMSO) in Tris-sucrose buffer (final volume 225 µl) and absorbance at 490 nm ($A_{490}$) monitored for 1 h at 25 °C, in clear, flat-bottom 96-well plates, using a CLARIOstar microplate reader. The rate of the colour change was calculated using pro Fit 7, by fitting the linear region of the resulting traces to a linear function ($y = mx + c$) to determine slope (m).

# Chapter 3 Screening for inhibitors of bacterial protein translocation

## 3.1 Introduction

Following identification of an appropriate antibiotic target, the next step in target-based antibiotic discovery is developing a bespoke assay. This assay will be adapted into a HTS for lead compounds. To provide the rationale behind the screen design proposed in this chapter, this introduction reviews existing strategies for developing a HTS against the bacterial Sec-machinery. The strengths and limitations of each approach are discussed, with the aim of providing insight into what makes a successful screen.

To be high quality, a HTS assay should identify hits – compounds that exhibit activity against the target – with confidence. The Z-factor is a measure of the integrity of the signal window, often used to assess HTS quality. It accounts for the difference in mean signal between uninhibited wells and positive control wells with reference inhibitor (dynamic range), and the signal variation (standard deviation, SD) at both extremes. Z-factor is calculated according to the equation below. A higher Z-factor of 0.5 – 1 indicates a better HTS assay (Zhang, Chung & Oldenburg, 1999).

$$Z = 1 - \frac{3SD\ of\ test\ wells + 3SD\ of\ positive\ control}{|\ mean\ of\ test\ wells - mean\ of\ positive\ control\ |}$$

Z-factors can be determined by comparing the positive and negative (untreated) controls, in which case they are referred to as Z'-factors. The preferred approach, however, is to use non-control-based normalisation. When unbiased compound libraries are used in HTSs, most compounds will have no or very weak biological activity. Thus, a typical histogram of activity from test compounds has a normal distribution centred around the mean signal of untreated samples (Figure 3.1) and the mean and SD of test wells can be taken to represent the uninhibited population. Whereas the Z-factor is useful for optimisation of compound library and concentration, the Z'-factor defines the quality of the assay itself without taking test compounds into consideration (Zhang, Chung & Oldenburg, 1999).

As well as achieving high Z-factors, assays must be optimised for speed, efficiency and low reagent consumption. They therefore require sensitivity, small sample volumes, minimal steps such as sample transfer, as well as reproducibility and accuracy (Zhang, Chung & Oldenburg, 1999). As an example, traditional *in vitro* assays of the Sec-machinery do not meet these criteria. In such assays, the Sec-machinery is reconstituted into membrane vesicles and pre-proteins are translocated into the vesicle interior (Schulze *et al.*, 2014; Brundage *et al.*, 1990). Translocation is assessed by monitoring protease protection (see Figure 4.6 for more details). This requires preparations of SecYEG in vesicles, purified SecA and purified, translocation-competent pre-protein. Preparation of these reagents is laborious, and a significant amount is consumed per reaction (see section 2.4.2.2). Vesicle-based assays for inhibitors are also susceptible to a high false positive rate due to

hydrophobic molecules that non-specifically bind membranes and affect their integrity. Assessment of protease protection by SDS-PAGE is slow and requires many steps in which error can be introduced, affecting reproducibility and accuracy. Platereader-based detection of absorbance, colorimetry, fluorescence or luminescence is often preferred for HTS.

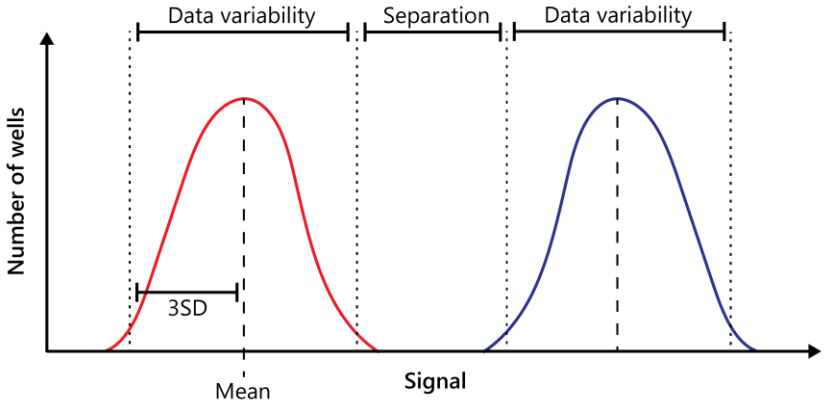


**Figure 3.1 Schematic of a signal window from a typical high throughput screen**
The red and blue traces are an abstract representation of inhibited and uninhibited populations, respectively. Traces show the number of wells in each population with a given signal. In a typical, unbiased screen with a sufficiently large number of samples, these distributions are assumed to be normal. The separation between these populations depends on their means and data variability (3 standard deviations, SD, in this case). Better separation gives a better signal window and higher Z-factor. Adapted from Zhang, Chung & Oldenburg, 1999.

### 3.1.1 Previous screens and inhibitors against protein translocation

The three major paradigms for drug discovery by target-based screening are *in vitro* using purified proteins, *in vivo* (whole bacterial cells) and *in silico* by structure-based virtual ligand screening. Previously, HTS efforts targeting bacterial Sec focused on developing assays for and identifying inhibitors against factors with enzymatic activity – SecA and signal peptidase. This was mostly achieved by *in vitro* strategies. With the transition to whole cell screening, screens against the activity of the Sec-machinery in its entirety have also been established.

#### *3.1.1.1 Screens and inhibitors against SecA*

The first demonstration of SecA as an antibiotic target occurred in the 1990s. In *E. coli* and *B. subtillis*, mutations conferring resistance to known antibacterial compound sodium azide ($NaN_3$) were primarily found in SecA (Oliver *et al.*, 1990). $NaN_3$ inhibits SecA ATPase activity during translocation by trapping SecA in a membrane-inserted, ADP-bound state (Economou *et al.*, 1995; Segers & Anné, 2011). However, $NaN_3$ is a general inhibitor of ATPases, also active against the $F_1$-ATPase, cytochrome c oxidase, superoxide dismutase and alcohol dehydrogenase (Bowler *et al.*, 2006; Li *et al.*, 2008). As a result, it has significant cytotoxicity in humans and is not a useful antibiotic.

Traditional screens for SecA inhibitors are performed *in vitro*, reporting on ATPase activity either of purified SecA alone (intrinsic ATPase), alongside reconstituted membranes (membrane ATPase) or with pre-protein substrate and membranes containing SecYEG (translocation ATPase). Release of phosphate during ATP hydrolysis can be followed colorimetrically using malachite green dye.

Pfizer adapted this method into a 96-well plate format suitable for screens against SecA translocation ATPase activity. Using this assay, the first natural product inhibitor of SecA, CJ-21058 (Figure 3.2a), was identified (Sugie *et al.*, 2002). Its half maximal inhibitory concentration ($IC_{50}$) against *E. coli* SecA translocation ATPase is 15 μg/ml (38.7 μM). Its effects on other ATPase activities of SecA are not reported. *In silico* docking of CJ-21058 into *E. coli* SecA reveals that it binds at the ATP-binding site (Huang *et al.*, 2012). CJ-21058 has strong antibacterial activity against select Gram-positives (MIC of 5 μg/ml) but not *E. coli* (Sugie *et al.*, 2002). The factors determining the spectrum of CJ-21058 antibacterial activity, for example whether it corresponds with inhibitory activity against SecA from different species, have not been explored in the literature. Crucially, CJ-21058 is moderately cytotoxic, giving 90% inhibition of HeLa cell growth at 32 μg/ml.

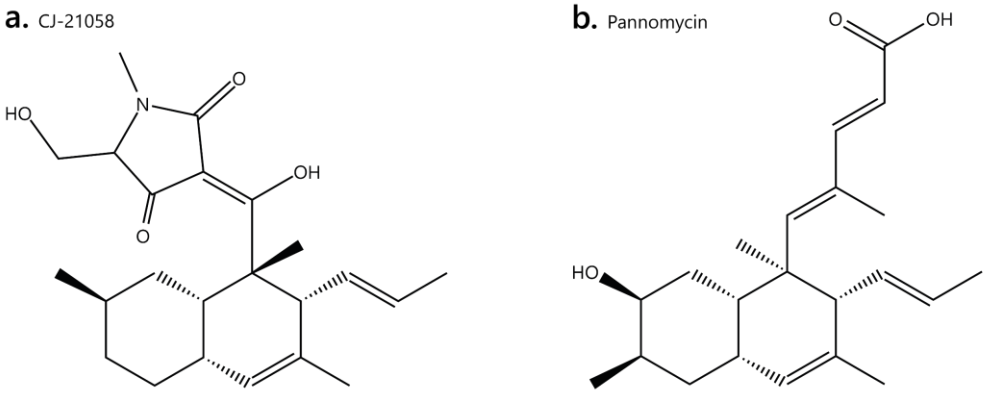


**Figure 3.2 Structures of SecA inhibitors CJ-21058 and Pannomycin**

Other *in vitro* screening approaches based on SecA ATPase assays exploit SecA mutants with elevated intrinsic activity, for example through mutation of residues (e.g. W775) involved in intramolecular regulation (Segers *et al.*, 2011) or truncation to remove the C-terminal domain involved in autoinhibition (Huang *et al.*, 2012). This circumvents the requirement for additional, more complex reagents (reconstituted membrane-bound Sec and purified, translocation-competent pre-protein) while still allowing sufficiently high ATPase activity to give a large dynamic range for the assay. The drawback of such assays is that they omit the (many) regulatory interactions of SecA and only identify active site inhibitors. An assay using W775A SecA was adapted to give a robust HTS with an average Z'-factor of 0.89 (using 50 mM EDTA as a positive control for inhibition) and identifying inhibitors of intrinsic, membrane and translocation ATPase activities of SecA. These inhibitors belong to a range of chemical classes, namely pyrrolo-pyrimidines and nipecotic acid derivatives (Segers *et al.*, 2011). *In vitro* low throughput screens using C-terminally truncated SecA identified the fluorescein analogs, including Rose Bengal (RB; Figure 3.3) and Erythrosin B (EB), as inhibitors of SecA. RB and EB yield $IC_{50}$ values of 0.9 and 10 μM against translocation ATPase, respectively. They bind at the ATP-binding site in the same position and orientation as CJ-21058 and are competitive inhibitors of ATP binding at low ATP concentrations. While wildtype *E. coli* is not susceptible to RB, the compound is antibacterial against outer membrane-permeable *E. coli* and Gram-positive bacteria (MIC 3.1 μM). This indicates that the antibacterial activity of RB is limited by its ability to penetrate the Gram-negative cell envelope (Huang *et al.*, 2012). Structure-activity

relationship studies (SARS) suggest the xanthene ring moiety of the compound is essential for activity – lower molecular weight analogs have comparable potency against SecA (Cui *et al.*, 2013).

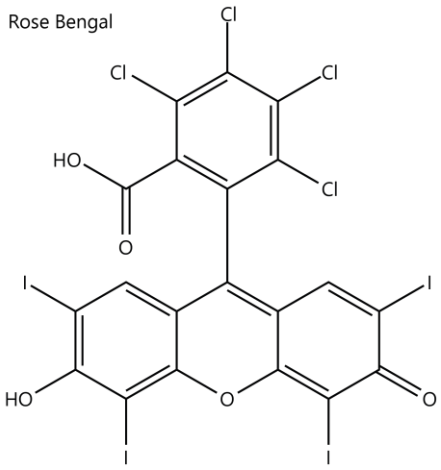


**Figure 3.3 Structure of SecA inhibitor Rose Bengal**

Elucidation of the structure of SecA paved the way for an *in silico* approach to inhibitor discovery. In this approach, compound structures are docked into the active site (or other ligand-binding sites) and the theoretical binding energy is calculated. Compounds giving high predicted binding energies are then evaluated in the laboratory (De Waelheyns *et al.*, 2015). Around 60,000 compounds were screened *in silico* against the active site cleft of *E. coli* SecA yielding 31 hits, of which the most potent had $IC_{50}$ values of 100 μM *in vitro* against truncated SecA. Chemical optimisation gave substituted thiouracils with improved *in vitro* activity against intrinsic ATPase ($IC_{50}$ < 60 μM) and modest antibacterial activity against outer membrane-permeable *E. coli* and Gram-positives, but no activity against wildtype *E. coli* (Li *et al.*, 2008; Chen *et al.*, 2010; Chaudhary *et al.*, 2015; Jin *et al.*, 2016). Based on the same *E. coli* structure (and later optimised using additional PDB structures) 3D homology models of SecA from the Gram-negative plant pathogen *Candidatus Liberibacter asiaticus* were built and used for screening. A small number of compounds selected based on predicted SecA active site binding were found to strongly inhibit intrinsic ATPase activity with $IC_{50}$ values as low as 0.25 μM. They additionally have antibacterial activity against another plant pathogen, the Gram-negative *Agrobacterium tumefaciens*, with minimum bactericidal concentrations (MBCs) of of 128 to 256 μg/ml (Akula *et al.*, 2011, 2012).

Despite these efforts, no potent and selective inhibitors of SecA have been found. Hits identified by anti-SecA screens are often ATPase inhibitors and, given the similarities between SecA ATPase domains and important eukaryotic ATPases, these hits are likely not selective enough to be useful antibiotic leads. While previous *in silico* approaches targeted the ATPase cleft of SecA, a more recent study identified two additional druggable pockets on the surface of SecA that are conserved across a range of bacterial species and important to SecA activity *in vivo*. One site was located at the pre-protein cross-linking domain and C-terminal domain interface, presumably involved in regulating ATPase activity and transmitting conformational changes, and the other was the SS-binding site. A library of 500,000 compounds were virtually screened against the SS-binding region, yielding 1040 small molecule hits for *in vitro* testing. The most potent gave $IC_{50}$ values of 24 to 65

μM against SecA translocation ATPase. The compounds display a moderate effect on growth of *S. aureus* ($IC_{50}$ <100 μM) and *P. aeruginosa* ($IC_{50}$ 31.8 μM), but even the most potent possess only weak activity against *E. coli* (De Waelheyns *et al.*, 2015).

As seen in the examples above, *in vitro* and *in silico* approaches for target-based antibiotic discovery have a low success rate. Hits often have high target-specific potency but are unsuited to bacterial uptake or evasion of efflux systems. This barrier is even more significant in Gram-negatives, due to the presence of the outer membrane and greater range of efflux systems available to these bacteria (Nikaido, 1976; Li & Nikaido, 2004). Target-based inhibitor screening in whole bacterial cells could help mitigate these issues. A frequently used platform for whole cell target-based screens exploits antisense RNA to downregulate translation of a target protein. Bacterial strains producing this RNA have increased sensitivity to inhibition of that protein or pathway. This technology was used at Merck in a strain of *S. aureus* that produces antisense RNA against *sec*A. Hits were identified in a two-plate agar-based differential sensitivity screen comparing the response of the hypersensitive strain to the wildtype. This screen of over 115,000 natural products identified a hit, Pannomycin (Figure 3.2b), that has weak antibacterial activity (in the mM range) against some Gram-positives (Parish *et al.*, 2009). It is structurally similar to CJ-21058, also possessing a decalin moiety. The greater antibacterial activity of CJ-21058 has been attributed to its tetramic acid group, presenting possible routes for optimisation of the decalin scaffold (Rao *et al.*, 2014). As this particular approach used a Gram-positive strain for the primary screen, the hits identified are not selected for uptake in Gram-negative cells. For discovery of broad-spectrum antibiotics, a Gram-negative test strain is more appropriate.

#### *3.1.1.2 Screens and inhibitors against signal peptidase*

Amongst the signal peptidase enzymes, signal peptidase I is the most attractive target for broad-spectrum agents. The 1990s saw the discovery of β-lactam type signal peptidase I inhibitors. These inhibitors include the monocyclic azedtinones, which inhibit *E. coli* signal peptidase I *in vitro* in the high mM range (Kuo *et al.*, 1994), and stereoisomers of 5 S-Penem, which are irreversible inhibitors with *in vitro* $IC_{50}$ values as low as 0.38 μM (Perry, Ashby & Elsmere, 1995; Rao *et al.*, 2014). They were validated on purified signal peptidase I *in vitro* using a continuous assay with fluorogenic substrate or quantification of cleavage products by high-performance liquid chromatography (HPLC), respectively. The latter method was used at GlaxoSmithKline in low throughput screening and optimisation efforts. The penem-type inhibitors screened had moderate antibacterial activity, with MICs against *E. coli* of 64 μg/ml and above (Perry, Ashby & Elsmere, 1995).

More scalable *in vitro* assays for type I signal peptidase activity include fluorescence resonance energy transfer (FRET)-based systems. These were developed using synthetic peptide substrates containing signal peptidase I recognition and cleavage sites and resembling signal peptides. The substrates are fluorescent, but internally quenched until cleavage by signal peptidase I. Such assays have achieved high average Z'-factors of 0.73 (Rao *et al.*, 2009, 2014). In the early 2000s, Eli Lilly and Company used a FRET system to screen 50,000 natural products for signal peptidase I inhibition (Peng *et al.*, 2001; Kulanthaivel *et al.*, 2004). As a result, Arylomycin C was identified as

an inhibitor with an *in vitro* $IC_{50}$ of 0.11 – 24.9 μM, depending on bacterial species, and some antibacterial activity (MICs of 4 – 8 μM against *E. coli*). At the same time, an academic research group reported that the A and B series of arylomycins possess anti-bacterial activity against Gram-positives but not *E. coli* (Schimana *et al.*, 2002). In total, there are 4 series of arylomycins, A – D. Their mechanism of action was elucidated by crystallography of the catalytic domain from *E. coli* signal peptidase I with Arylomycin A2 bound in the active site (Paetzel *et al.*, 2004). Structural studies were also used to characterise a major determinant of arylomycin resistance: a serine to proline substitution in a signal peptidase I substrate binding pocket, reducing the affinity of arylomycin binding (Smith *et al.*, 2018). Compared to their SecA counterpart, *in vitro* screens against signal peptidase I have shown greater success in discovering hits with activity in Gram-negative bacteria. This may be due to the periplasmic localisation of signal peptidase, which omits the additional permeability barrier of the cytoplasmic membrane, in contrast with cytoplasmic SecA.

As seen with the *sec*A antisense RNA system, whole cell assays for signal peptidase I inhibition typically involve up- or downregulation of the gene encoding this protein. One such system was used as a secondary assay to verify hits from an *in vitro* HTS. Underexpression of the signal peptidase I gene in *E. coli* increased susceptibility to an established penem inhibitor (used to validate the assay) while increased expression rescued growth. The novel hits had poor antibacterial activity against wildtype *E. coli*, but two were found to inhibit growth of *E. coli* in the presence of the outer membrane-permeabilising agent polymyxin B nonapeptide (Barbosa *et al.*, 2002). This system has since been adopted for inhibitor discovery against *M. tuberculosis* signal peptidase I, with the majority of hits belonging to the phenylhydrazone class of compounds (Bonnett *et al.*, 2016). In secondary testing, compounds gave MICs as low as 4 μM against wildtype *M. tuberculosis* and the most potent compound *in vitro* yielded an $IC_{50}$ of 12 μM against signal peptidase I activity (using internally quenched fluorescent substrate). However, there was no correlation observed between MIC and *in vitro* activity. None of the compounds tested affected membrane permeability or membrane potential, yet most compounds exhibited some cytotoxicity. The most potent compounds against *M. tuberculosis* tended to have greater cytotoxicity (Bonnett *et al.*, 2016).

In a similar vein, a screen developed at Merck employed 245 *S. aureus* antisense RNA strains, each with downregulated expression of a distinct essential gene. Compounds, usually with known antibacterial activity, are simultaneously screened against all strains to determine which are sensitised to each compound – informing on the compound's target and mechanism of action (Donald *et al.*, 2009). This strategy (termed *S. aureus* fitness testing, SaFT) identified several natural compounds with novel activities, including inhibitors of signal peptidase I. These signal peptidase I inhibitors, actinocarbasin and krisnomycin, were first discovered in high-throughput assays for compounds that potentiate β-lactam activity against methicillin-resistant *S. aureus* (MRSA). They have anti-MRSA activity, with MICs of 8 and 64 μg/ml, respectively. They both act as imipenem adjuvants at concentrations 16 times lower than their MIC, but this effect is specific to

MRSA (Therien *et al.*, 2012). Actinocarbasin represents the D series of arylomycins, while krisnomycin belongs to another structural class.

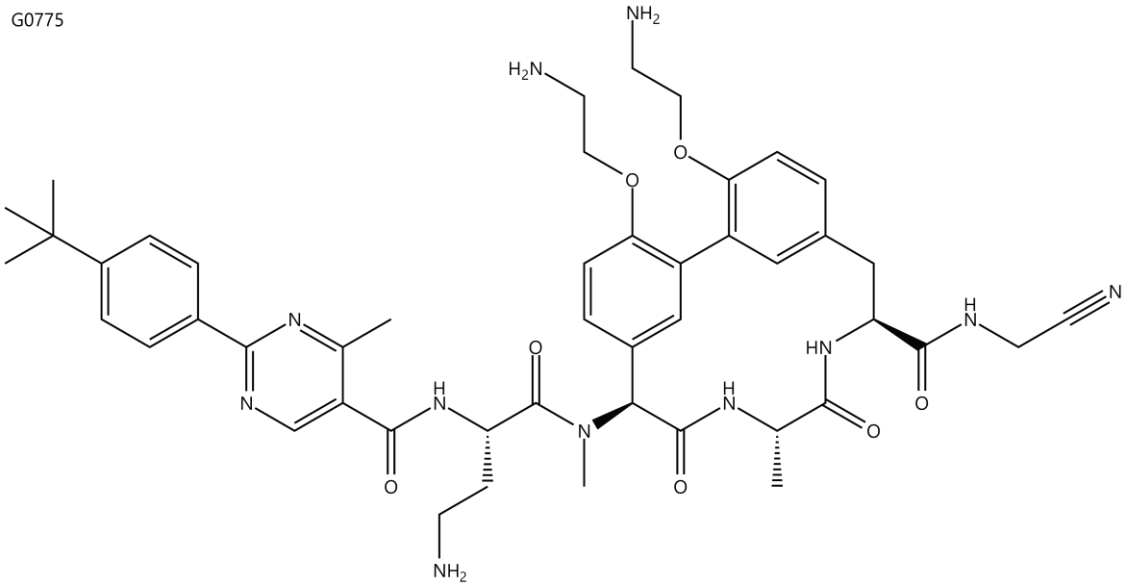


**Figure 3.4 Structure of type I signal peptidase inhibitor optimised arylomycin (G0775)**

Given the repeated detection of arylomycins in antibacterial or anti-signal peptidase I screens, they have attracted attention as a potential new class of antibiotic. A synthetic derivative of actinocarbasin in combination with β-lactam was shown to be effective in reducing bacterial counts in mouse models of MRSA infection. When used in this combination, emergence of antibiotic resistance was suppressed (Therien *et al.*, 2012). To improve anti-Gram-negative activity, arylomycin analogs were engineered for increased affinity for Gram-negative signal peptidase I and improved penetration through the outer membrane. An optimised arylomycin developed at Genentech (Figure 3.4) has strong antibacterial activity against a range of priority multidrug resistant Gram-negative pathogens, with MICs less than 0.5 μg/ml in 90% of *E. coli and Klebsiella pneumoniae* strains tested (Smith *et al.*, 2018). This demonstrates that the compound evades existing mechanisms of resistance, further validating the secretory pathway as a novel antibiotic target.

#### *3.1.1.3 Screens and inhibitors against the Sec-machinery as a whole*

The plethora of screens targeted at SecA and signal peptidase have demonstrated the sustained interest in inhibitors of bacterial protein translocation as potential antibiotics (including among major pharmaceutical companies Pfizer, Eli Lilly and GlaxoSmithKline). Some have yielded useful compounds for mechanistic studies or further lead optimisation. Other protein components of the Sec-machinery may be more druggable but targeting them is a greater challenge due to their lack of intrinsic enzymatic activity. As explained above, *in vitro* assays of protein translocation through Sec are not appropriate for HTS. However, screen assays using whole cells allow for targeting of complex machineries like Sec in their entirety, potentially identifying novel druggable sites on currently unexplored components.

While the antisense screens discussed above are focused on a single protein target, it is expected that they would respond to inhibitors of any step of the pathway in which that protein functions. However, comparison of growth of wildtype versus antisense bacterial strains can be a lengthy task: in the SecA-specific screen, this was achieved by measuring diameters of zones of inhibition on agar plates (Parish *et al.*, 2009), while SaFT requires optimisation of strain-specific primers, quantitative PCR and substantial data analysis (Donald *et al.*, 2009).

An alternative approach with an easier readout is to use genetic reporters of protein translocation inhibition. One genetic reporter-based screen exploited the autogenous upregulation of SecA synthesis under genetic and chemical conditions inhibiting translocation (Alksne *et al.*, 2000). A *sec*A-*lac*Z fusion was constructed in *E. coli* to report on hits that induce SecA production, either directly or indirectly by acting on other Sec components. Such hits would cause an increase in β-galactosidase activity, which can be measured as an increase in absorbance upon addition of a colorimetric substrate. A set of synthetic and natural compounds was screened, yielding six hits that increase SecA production by at least 1.4-fold and have MICs against *S. aureus* of less than 128 µg/ml. For half of these hits, secondary immunoassays of a model pre-protein could not rule out the possibility that they affected a metabolic or biosynthetic step prior to translocation (e.g. translation). Importantly, all the hits had a deleterious effect on membrane integrity, not only in bacteria but in eukaryotic cells. Many were cytotoxic, inhibiting growth of human cells by over 70% when used at just 10 µg/ml (Alksne *et al.*, 2000). Thus, this approach is inappropriate for antibiotic discovery since it preferentially identifies membrane active compounds.

A similar study identified other bacterial genes (with no prior links to Sec) that exhibited upregulation in response to SecA depletion and used these to drive the production of luciferase (*lux*CDABE) in *P. aeruginosa*. The proposed gain of signal screen using the ATP-dependent luciferase should be insensitive to compounds that damage cellular energy generating capacity, namely uncouplers and membrane active agents that marred the previous screen, and general protein synthesis inhibitors. Typical Z'-factors from a screen of over 70,000 natural and synthetic compounds were around 0.38. Of the 96 primary hits, only 9 were validated as specific inhibitors by direct measurements of secretion of reporter protein through Sec and type 2 secretion systems. None inhibited Sec-mediated translocation of β-lactamase. None inhibited bacterial growth, consistent with the non-essentiality of type 2 secretion systems in a laboratory setting (Moir *et al.*, 2011). The major limitation of gene reporter-based systems is that their readout of Sec inhibition is indirect; transcriptional and translational responses are complex and poorly understood. This increases the likelihood of false positives through non-specific effects. While efforts were made to confirm the luciferase reporter does not respond to stressors such as heat shock, peroxide and general growth inhibition (Moir *et al.*, 2011), they cannot feasibly cover the plethora of potential drug targets. As more direct measures of protein translocation, the secondary assays applied in this work were able to mitigate these false positives.

More recent screens take this direct approach from the start, reducing the amount of secondary testing required. Based on the knowledge that periplasmic β-galactosidase is enzymatically

inactive, a gain of signal screen assay was designed in *E. coli* using a fusion protein β-galactosidase with a Sec-specific SS. During normal protein translocation, the β-galactosidase is exported and inactive. When translocation is blocked, the enzyme accumulates in the cytoplasm and is able to mature to its active form. This system was validated against a panel of antibiotics that do not affect Sec, with each giving the expected effect (generally loss of signal) on β-galactosidase activity measured by absorbance (Crowther *et al.*, 2012). A library of 57,000 samples including natural product extracts was screened, using 0.25 mM $NaN_3$ as a reference inhibitor. Z'-factors were variable, ranging from 0 to 0.74. To offset this variability, compounds were screened in duplicate and signal from each well was corrected in post based on observed plate effect. This resulted in 367 primary hits, of which 211 were selected for retesting in the primary assay. Ten of these were abandoned as they interfered with absorbance readout and 67 were confirmed. A counter screen using β-galactosidase lacking a SS was performed to select against general enhancers of transcription or translation, eliminating all but 11 hits. The hit chosen for further study has a half maximal effective concentration ($EC_{50}$) of 25 µM in the primary assay. At 400 µM, it inhibits log phase growth of *E. coli* to 60% that of the untreated control. Unfortunately, the compound was more toxic to human cells than *E. coli*, with an $IC_{50}$ of just 101 µM. Secondary assays evaluated the effect of the hit on other reporter proteins *in vivo* – it caused similar reductions in periplasmic β-lactamase activity and activity of a cytoplasmic enzyme (Crowther *et al.*, 2015). This suggests that the compound has non-specific effects and is unlikely to represent a promising antibiotic lead. However, this work demonstrates the power of a thoroughly designed and optimised primary screen assay and suitable counter and secondary assays in narrowing down the search for Sec inhibitors.

An alternative protein reporter of Sec activity is alkaline phosphatase A (PhoA). This protein requires translocation into the periplasm, where it dimerises and undergoes disulfide oxidation, to function. PhoA activity in *E. coli* was assayed with a chemiluminescent substrate, so inhibition of Sec reduces luminescence. For screens based on PhoA, 4 mM $NaN_3$ was used as a positive control. Z'-factor was determined but is not specified. Counter assays involved incubation of hits with purified PhoA to measure their effects on enzymatic activity, alongside immunoblotting for PhoA production in treated bacteria. However, no fully quantitative assays of PhoA synthesis, nor assays of inhibition of PhoA dimerization or oxidation, were performed. Around 2000 primary hits were discovered amongst 240,000 small molecules screened. Eight hits (and six analogs) showed dose dependent inhibition ($IC_{50}$ < 50 µM in primary assay) and passed counter assay. Of these, five reduced growth of Gram-negative and/or -positive bacteria, with $IC_{50}$ values of 37 µM or lower. These compounds had relatively high cytotoxicity, with a 50% lethal dose towards HEK293T cells of 6.7 – 20.1 µM, so are not appropriate antibiotic leads. None of the compounds inhibited SecA activity *in vitro* (Hamed *et al.*, 2021). Given these findings alongside the lack of further secondary assays, it is not possible to conclude that hits from this screen are *bona fide* inhibitors of bacterial Sec.

Inhibitor discovery approaches for the analogous eukaryotic Sec61 complex also offer insights into screen design. Generally, inhibitors of the eukaryotic Sec-machinery have been discovered by screens for inhibitors of other cellular processes, such as cell adhesion (heptadepsipeptides),

endoplasmic-reticulum-associated protein degradation (eeyarestatin), cancers (decatransin) and viral infection (CADA). Eeyrastatin 24 and decatransin have been found to also inhibit SecYEG and possess antibacterial activity (Junne *et al.*, 2015; Steenhuis *et al.*, 2021). Sec61 inhibitors are often categorised into two types: broad ranging and specific inhibitors. The former inhibits translocation of all Sec61-dependent proteins and the latter impacts a specific subset of proteins, for example through SS interactions (Klein *et al.*, 2018b). At low concentrations, heptadepsipeptides like cotransin inhibit Sec61-mediated translocation of a small subset of proteins (Garrison *et al.*, 2005) yet higher concentrations inhibit almost all secretory proteins while integral membrane proteins remain unaffected (Klein *et al.*, 2015). These compounds are said to exhibit a mixed-type inhibition – selective, but not specific. By contrast, mycolactone is a mycobacterial toxin that non-selectively inhibits translocation through Sec61 (Hall *et al.*, 2014). Apratoxin A, produced by marine cyanobacteria, inhibits a subset of Sec61 substrates (Liu, Law & Luesch, 2009). No antibacterial activity has been reported for either bacterial toxin. Given that bacteria can deploy Sec inhibitors against eukaryotes, this gives further strength to antibiotic discovery approaches attempting the opposite. The multiple pathways for translocation through SecYEG make it probable that the two types of Sec inhibition also apply to bacteria. This highlights a key limitation of previous protein reporter-based assays for Sec inhibitors: they rely on the intrinsic activity of the reporter protein and are not readily adaptable to other proteins of interest. Therefore, previous screens may have identified specific inhibitors of reporter protein transport, which are unlikely to be useful in attenuating bacterial pathogens.

### 3.1.2 The proposed screen platform: NanoBiT

Based on these insights, it was decided that the most successful screen assays would be whole cell-based using Gram-negative bacteria, against the bacterial Sec-machinery in its entirety and using direct, adaptable protein reporters of translocation. Assays should be compatible with reference inhibitors, as well as robust counter and secondary assays for hit validation.

The chosen screen platform is the recently developed split-luciferase assay for monitoring protein translocation (Pereira *et al.*, 2019). This assay exploits a non-covalent complementation system based on NanoLuc, a small, bright luciferase (NanoLuc Binary Technology or NanoBiT; 27). Cleavage of the C-terminal β-strand of NanoLuc yields two non-luminescent fragments: Large BiT (LgBiT; 18 kDa) and Small BiT (SmBiT; 11 residues). Luciferase activity is restored upon interaction of LgBiT and SmBiT, giving luminescence in the presence of the substrate furimazine (Dixon *et al.*, 2016). For monitoring protein translocation, LgBiT is contained in the destination compartment and a high-affinity variant of SmBiT, HiBiT, is fused to a pre-protein of interest. Before translocation, NanoBiT fragments are separated by one or more membranes. Translocation of HiBiT-tagged pre-proteins allows complementation of NanoBiT fragments (Pereira *et al.*, 2019).

The NanoBiT reporter system has numerous advantages over previous systems. The use of a HiBiT tag allows the assay to be adapted to study any protein of interest, regardless of its (lack of) intrinsic enzymatic activity. The HiBiT peptide resembles a native Sec substrate (polypeptide), unlike

fluorescent dyes used in previous studies of protein translocation (Liang, Bageshwar & Musser, 2009), yielding more physiologically relevant results. Unlike dyes, HiBiT is produced and fused to proteins *in situ*, reducing cost and labour. It is smaller than other peptide tags used for this purpose – namely the 42-amino acid β-galactosidase fragment used in CAPT assay systems (Wehrman *et al.*, 2005) and the 3 kDa fragment of split-green fluorescent protein (GFP; Smoyer *et al.*, 2016) – so should have a negligible effect on biosynthesis of the attached protein. Moreover, while readouts using split-GFP require GFP maturation following translocation, HiBiT is a single β-strand that does not depend on folding for successful NanoBiT complementation. Thus, while the rate-limiting maturation of split-GFP following translocation impedes real-time measurements (Smoyer *et al.*, 2016), the rapid, high-affinity association of LgBiT and HiBiT is compatible with such analyses (Pereira *et al.*, 2019). Luminescence assays such as NanoBiT generally offer a greater dynamic range and sensitivity. Unlike absorbance and fluorescence readouts, luminescence is rarely affected by background absorbance or autofluorescence of reagents. Luminescence assays are also not constrained by the absorbance, fluorescence or quenching properties of compounds being screened (Moir *et al.*, 2011; Crowther *et al.*, 2012).

While the NanoBiT system has been established *in vitro* (Pereira et al., 2019), further development is necessary to establish a NanoBiT protein translocation assay for whole cells. This chapter describes the design and validation of a whole cell NanoBiT assay. To demonstrate its utility in development of HTSs for novel inhibitors of the Sec-machinery, the assay was deployed in a local screen of 5000 small, synthetic compounds, yielding a median Z'-factor of 0.71 and confirmed hit rate of 0.08%. These results are discussed in the context of previous, comparable screening strategies.

## 3.2 Design of the whole cell NanoBiT assay

Assay design was carried out in collaboration with Prof Ian Collinson and Dr. William Allen. Optimisation, validation and deployment of the assay as a HTS were performed by the author alone. Development of a whole cell system began by designing the major components of the assay: HiBiT-tagged pre-protein and LgBiT. The HiBiT tag should be added to the C-terminus of a protein of interest, to minimise the possibility of it interfering with translocation. The model protein from previous NanoBiT studies, Spy, was used to establish this assay (Figure 3.5a). Unlike the traditional model protein OmpA, which aggregates into inclusion bodies upon overexpression in *E. coli*, Spy is a small, globular, soluble protein that functions as a chaperone and is therefore suited to overexpression. Previous *in vitro* studies of HiBiT-tagged pre-secretory Spy show that it produces a strong luminescent signal in the presence of LgBiT and furimazine and it undergoes translocation by the core Sec-machinery (SecYEG and SecA alone) in a SS-dependent manner (Pereira *et al.*, 2019).

To achieve luminescent signal specifically under the correct condition (translocation of HiBiT-tagged pre-protein of interest into the periplasm), LgBiT was purified and added to the buffer surrounding cells. The outer membrane and cell wall were permeabilised (using 0.1 mg/ml lysozyme

and 5 mM EDTA) to release periplasmic contents, so extracellular LgBiT could bind HiBiT attached to exported Spy. Sucrose (20% w/v) was also added to suspensions, to maintain osmotic pressure and prevent spheroplasts from releasing cytoplasmic contents. This yields a luminescent signal that corresponds specifically to the amount of HiBiT construct exported (Figure 3.5b). A loss of signal would indicate inhibition of translocation.

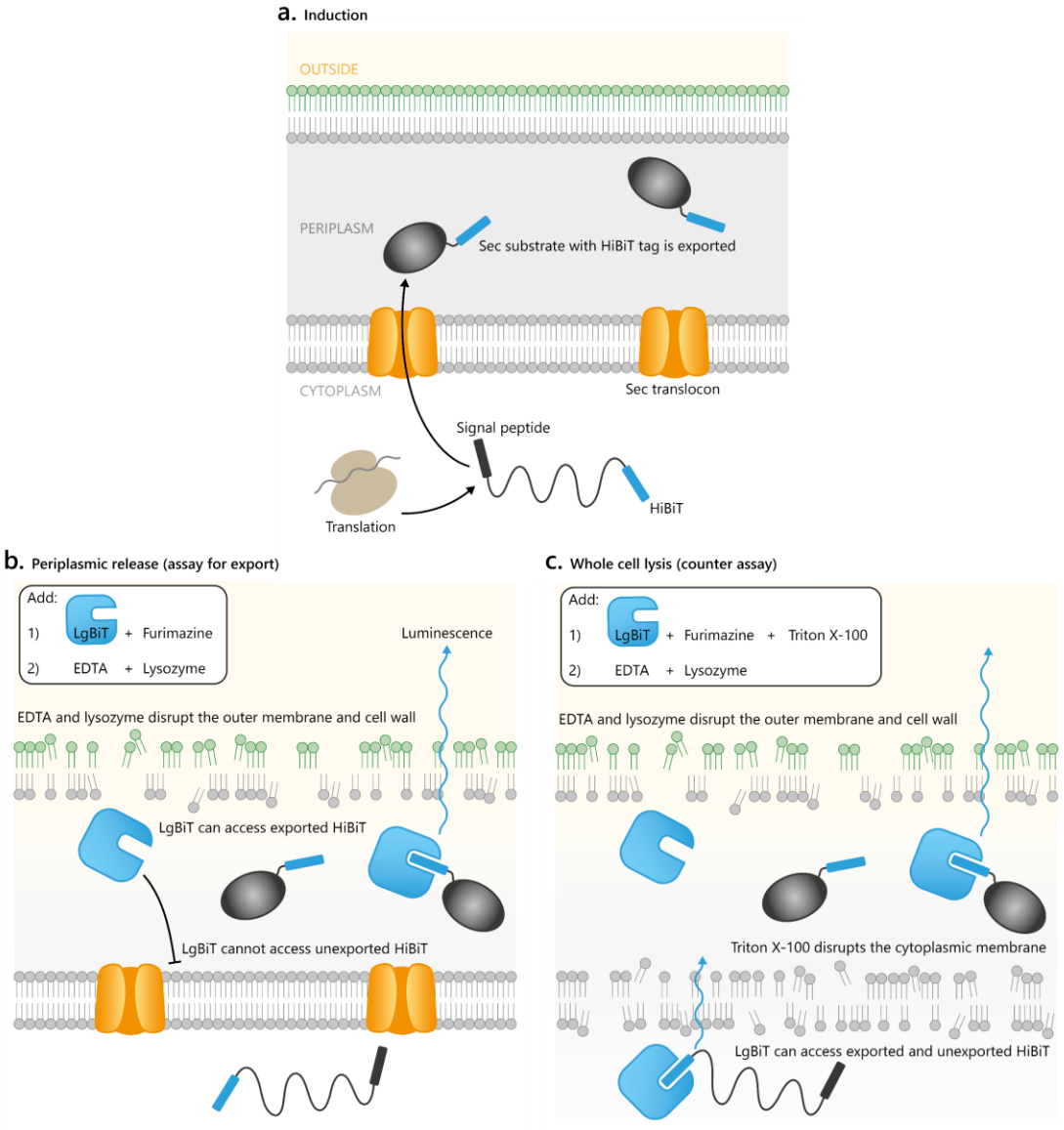


**Figure 3.5 Design of the whole cell NanoBiT assay for protein translocation**
Schematic of a Gram-negative bacterial envelope. This assay uses the native Sec-machinery. The NanoLuc luciferase is split into two non-luminescent fragments, LgBiT and HiBiT. Functional association of these fragments restores luciferase activity and gives luminescence. **a.** *E. coli* are transformed with a plasmid encoding pre-protein with an N-terminal Sec signal sequence and C-terminal HiBiT under control of an arabinose-inducible promoter. When cultured in the presence of arabinose and absence of inhibitor, *E. coli* synthesise this protein, which is then transported through the Sec-machinery. **b.** At the end of the growth period, LgBiT is added to the extracellular buffer, alongside NanoLuc substrate furimazine. EDTA and lysozyme are added for periplasmic extraction, to release exported HiBiT-tagged construct. **c.** LgBiT is added to the extracellular buffer, alongside NanoLuc substrate furimazine and Triton X-100. EDTA and lysozyme are added to release exported and unexported HiBiT-tagged construct (whole cell lysis). This gives active luciferase and a luminescent signal that informs on **b.** the level of export, or **c.** the level of synthesis, of the pre-protein of interest.

Designing a screen to report on target inhibition as a gain of signal would be a favourable choice, because such systems are impervious to common non-specific compounds that impact general protein synthesis and membrane integrity (Moir *et al.*, 2011; Crowther *et al.*, 2015). Since such compounds are more likely to have a negative impact by reducing viability or biosynthetic capacity of affected cells, they would result in a loss of signal and be filtered out by the primary assay. Inhibitors of reporter enzyme activity would also be deselected in this way. NanoBiT gain of signal assays were attempted through use of a NanoBiT-quenching peptide alongside HiBiT constructs. This peptide binds LgBiT in the same way as HiBiT but is catalytically inactive (Pereira *et al.*, 2019). However, these approaches require fine-tuning of the respective levels of HiBiT and quenching peptide. This complicates readouts, as compounds that simply offset this balance may show up as a false positive. To maintain simplicity in the primary screen, a loss of signal system was used.

An advantage of the NanoBiT design is the ease with which it can be adapted into a counter assay to control against conditions that inhibit periplasmic accumulation of Spy-HiBiT by non-specific mechanisms. In this counter assay, Triton X-100 (2% v/v) was also added to disrupt the cytoplasmic membrane. Here, LgBiT will be able to access the total amount of HiBiT constructs produced by the cell, giving a signal that corresponds to protein synthesis. If *E. coli* are treated with specific inhibitor of the Sec-machinery, the counter assay signal in this case will not differ substantially from the untreated control (Figure 3.5c).

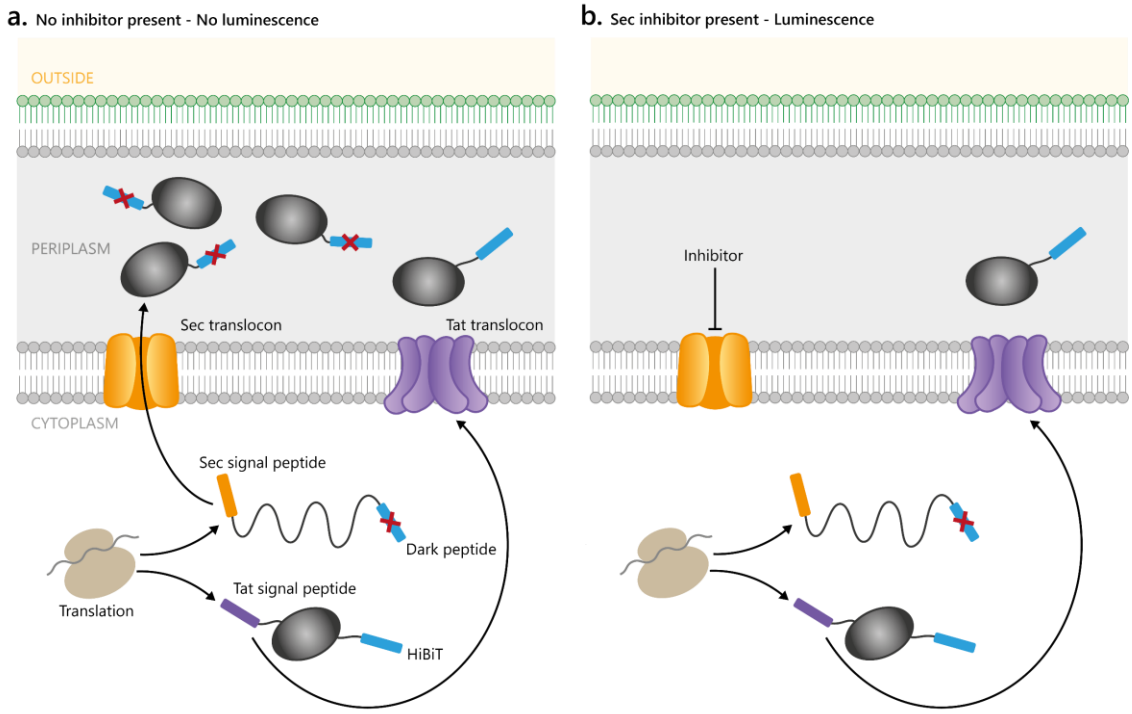


**Figure 3.6 Design of a gain of signal NanoBiT assay for protein translocation**
Schematic of a Gram-negative bacterial envelope. This assay uses the native Sec- and Tat-machineries. The NanoLuc luciferase is split into two non-luminescent fragments, LgBiT and HiBiT. Functional association of these fragments restores luciferase activity and gives luminescence. *E. coli* are transformed with plasmids encoding pre-protein with an N-terminal Tat signal sequence and C-terminal HiBiT, alongside plasmids encoding pre-protein with an N-terminal Sec signal sequence and C-terminal dark peptide. **a.** When cultured in the absence of inhibitor, *E. coli* synthesise and translocate both proteins through their respective machineries. The Sec-machinery is more abundant, so more dark peptide construct is translocated to the

periplasm than HiBiT. Dark peptide outcompetes HiBiT for binding LgBiT and there is no luminescence. **b.** In the presence of a specific Sec inhibitor, only HiBiT constructs reach the periplasm. Addition of LgBiT leads to luminescence. Inhibitors targeting protein synthesis or non-specific membrane active agents that will impair both Sec and Tat will not generate a luminescent signal.

The whole cell NanoBiT assay and counter assay were first validated using HiBiT-tagged pre-secretory (pSpy) and mature (mSpy, lacking the signal peptide) constructs, under control of an arabinose-inducible promoter. For each experiment, data were normalised by dividing by the mean maximum signal achieved by the respective pSpy sample (Figure 3.7). When arabinose is omitted (Uninduced pSpy) no HiBiT-tagged protein is synthesised and negligeable signal is observed upon addition of LgBiT, furimazine and either periplasmic release or whole cell lysis treatment (mean ± standard deviation of 0.0092±0.0011 and 0.011±0.0018 RLU, respectively). When *E. coli* carrying the gene encoding pSpy-HiBiT are induced, a substantial and reproducible luminescent signal occurs after both periplasmic release and whole cell lysis (1±0.15 and 1±0.066 RLU, respectively). Producers of mSpy-HiBiT give negligeable signal following periplasmic release (0.023±0.0023 RLU), but large signal (albeit lower than that of respective pSpy-HiBiT samples) following whole cell lysis (0.56±0.14 RLU). The requirement for lysozyme, EDTA and Triton X-100 for detection of signal from cells producing mSpy-HiBiT confirms that this protein remains in the cytoplasm. Since pSpy-HiBiT is known to be translocated by the Sec-machinery, while mSpy-HiBiT is not (Pereira *et al.*, 2019), these results verify that the signal observed upon periplasmic release results specifically from successful translocation of HiBiT-tagged construct.

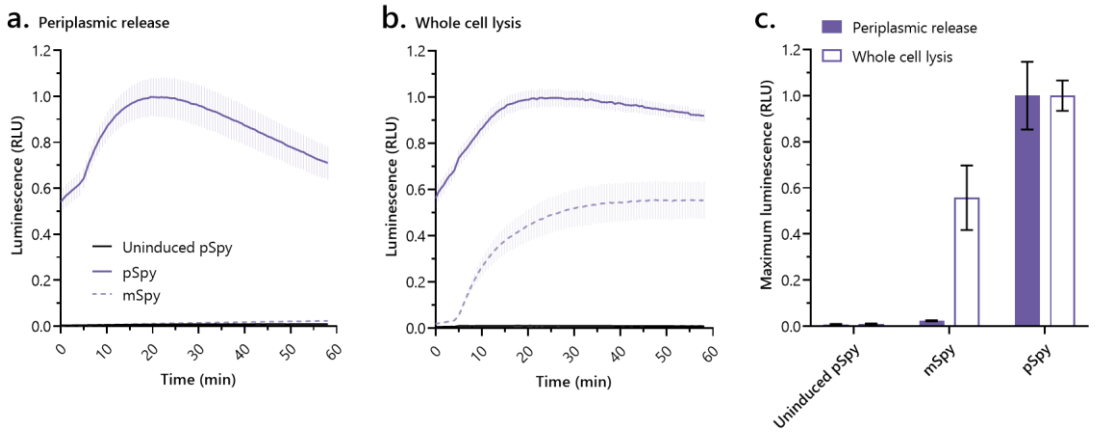


**Figure 3.7 *E. coli* producing pSpy-HiBiT exhibit luminescent signal after periplasmic release and whole cell lysis while those producing mSpy-HiBiT only exhibit activity after the latter**

LB cultures of BL21(DE3) producing pre-secretory Spy-HiBiT (pSpy) or mature Spy-HiBiT (mSpy) were diluted to $OD_{600}$ 0.1 in 96-well plates, supplemented with 0.1% (w/v) arabinose (except Uninduced pSpy), and incubated at 37 °C for 1.5 h then 4 °C for 1 h. **a**. LgBiT and furimazine (primary assay/ periplasmic release); **b**. LgBiT, furimazine and Triton X-100 (counter assay/ whole cell lysis) were added. Luminescence was measured for 5 min prior to and up to 1 h following injection of EDTA and lysozyme. Luminescence was normalised to the mean of maximum luminescence recorded for the respective pSpy samples. Data from three biological replicates are shown as mean ± standard error of the mean. **c**. The maximum normalised luminescence for each sample was calculated. Data from three biological replicates are shown as mean ± standard deviation.

Prior to injection of lysozyme and EDTA, pSpy-HiBiT-producing *E. coli* already present with high luminescence (Figure 3.7a, b). This is likely due to the greater than two-fold dilution of bacteria (from rich LB cultures) into salt-free buffer, which may cause osmotic shock and release periplasmic contents. In support of this suggestion, *E. coli* expressing the mSpy-HiBiT construct give almost no signal prior to treatment with EDTA and lysozyme, even in the presence of Triton X-100 (Figure 3.7b).

## 3.3 Assay validation using inhibitors of the Sec-machinery

Following initial validation, the effects of specific inhibitors of the Sec-machinery and expected non-specific inhibitors were investigated in the NanoBiT assay. Inhibitors were added to cultures of *E. coli* carrying pSpy-HiBiT constructs at the same time as induction. For each experiment, data were normalised by dividing by the maximum signal achieved by the respective untreated sample. CJ-21058, which inhibits SecA (Sugie *et al.*, 2002), was the first compound tested (Figure 3.8a). Consistent with its low antibacterial activity against *E. coli*, high concentrations of CJ-21058 (>100 µM) are needed to reduce luminescent signal from the periplasm. At concentrations over 200 µM, addition of CJ-21058 also diminishes luminescent signal during whole cell lysis. CJ-21058 is poorly soluble in water (Sugie *et al.*, 2002), so a 10 mM stock solution in DMSO was prepared for these experiments. At the high concentrations needed for CJ-21058 to inhibit Sec-dependent translocation of pSpy-HiBiT into the periplasm, the DMSO concentration is also high. DMSO concentrations above 2% (v/v; corresponding to 200 µM CJ-21058) decrease luminescent signal resulting from both periplasmic release and whole cell lysis (Figure 3.8b). The plots of maximum luminescence after whole cell lysis with increasing CJ-21058 concentrations and corresponding values for DMSO follow a similar trend, suggesting that the observed decrease is a due to the high levels of DMSO present and not due to CJ-21058. By contrast, luminescent signal upon periplasmic release exhibits a much steeper decline for *E. coli* treated with increasing concentrations of CJ-21058 ($IC_{50}$ of 227.1 µM; 95% confidence interval, CI, of 186.7 – 276.4 µM) than for DMSO ($IC_{50}$ could not reliably be calculated). This indicates that the SecA inhibitor CJ-21058 specifically inhibits periplasmic accumulation of pSpy-HiBiT and demonstrates the validity of this assay in identifying inhibitors of Sec-dependent translocation.

Carbonyl cyanide 3-chlorophenylhydrazone (CCCP) is an uncoupling ionophore. It equilibrates protons across the cytoplasmic membrane of bacteria, thereby dissipating the PMF required for Sec-dependent translocation (Brundage *et al.*, 1990; Economou *et al.*, 1995). The luminescent signal upon periplasmic release displays a dose-dependent response to treatment with CCCP (from a 4 mM stock in DMSO; Figure 3.8c). At concentrations greater than 0.2 µM, luminescence from the periplasm begins to decrease and CCCP concentrations of 50 µM or more abolish the signal. The $IC_{50}$ for CCCP on periplasmic signal is 1.82 µM (95% CI 1.45 – 2.31 µM). By contrast, the dose response curve of luminescence upon whole cell lysis is shifted to the right; concentrations over 5 µM are needed to reduce whole cell lysis signal, then signal rapidly declines with increasing concentration ($IC_{50}$ 18.6 µM, 95% CI 13.4 – 26.6 µM). This suggests that CCCP concentrations up

to 5 µM have a specific inhibitory effect on periplasmic accumulation of pSpy-HiBiT; total protein synthesised is unaffected by CCCP up to this concentration. However, at higher concentrations, CCCP has a non-specific effect on the assay. Given that AraE, the major transporter of arabinose (the inducer used in this assay) is a proton symporter dependent on the PMF (Daruwalla, Paxton & Henderson, 1981), it was considered that this non-specific effect might be due to CCCP inhibition of pSpy-HiBiT induction. Measurement of $OD_{600}$ following incubation with CCCP and prior to luminescence assay revealed that concentrations higher than 5 µM inhibit bacterial growth compared to the untreated control. This antibacterial effect of higher CCCP concentrations correlates with the decreased signal seen after whole cell lysis, suggesting that the lower signal observed is most likely due to reduced numbers of bacteria.

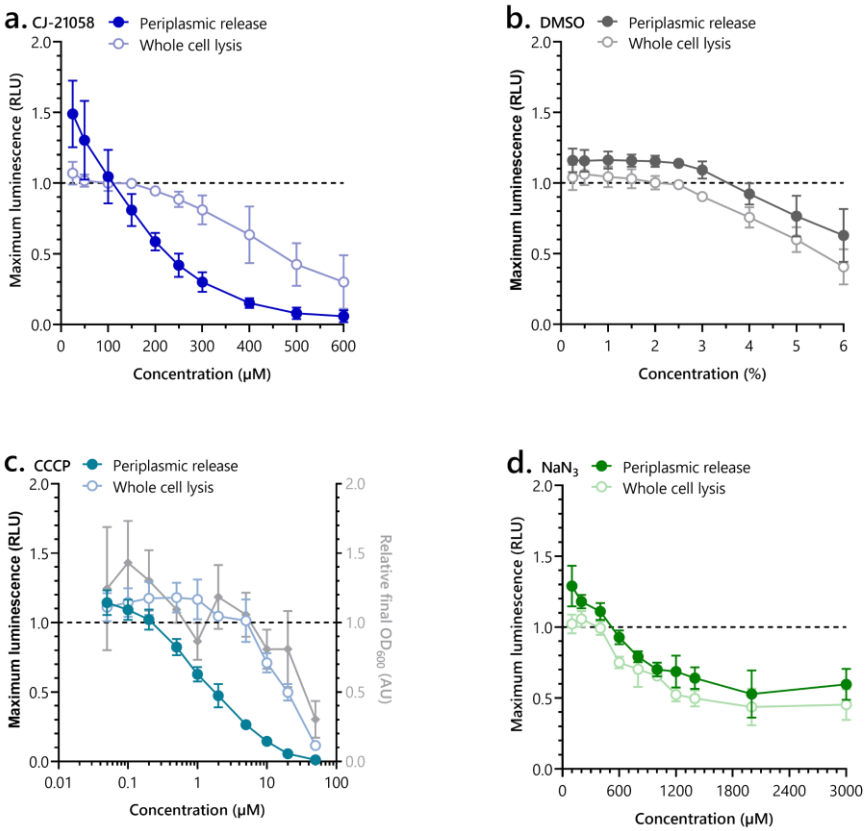


**Figure 3.8 Inhibitors of the Sec-machinery specifically reduce periplasmic NanoBiT signal in a dose-dependent manner**
LB cultures of BL21(DE3) producing pre-secretory Spy-HiBiT were diluted to $OD_{600}$ 0.1 in 96-well plates, supplemented with 0.1% (w/v) arabinose and varying concentrations of **a.** CJ-21058 in DMSO, **b.** DMSO, **c.** CCCP in DMSO, **d.** $NaN_3$, and incubated at 37 °C for 1.5 h then 4 °C for 1 h. LgBiT and furimazine were added in the absence (primary assay/ periplasmic release; solid circles) or presence (counter assay/ whole cell lysis; open circles) of Triton X-100, followed by EDTA and lysozyme. The maximum luminescence in each sample was normalised to the maximum signal in the respective untreated control (black dotted line) and plotted against concentration. **c.** The final optical density at 600 nm of cultures in plates prior to addition of buffer, normalised to that of the respective untreated control (no inhibitor added but EDTA and lysozyme added at endpoint; black dotted line), was recorded and plotted against concentration. Data from three independent replicates are shown as mean ± standard deviation.

$NaN_3$ is another inhibitor of SecA ATPase. It is more extensively characterised than CJ-21058 (Huang *et al.*, 2012) and has been used in previous screens for inhibitors of the Sec-machinery as

a positive control (Alksne *et al.*, 2000; Moir *et al.*, 2011; Crowther *et al.*, 2015; Hamed *et al.*, 2021). High concentrations of $NaN_3$ are needed to have an effect in the NanoBiT assay (Figure 3.8d). The dose response curves of luminescent signal arising from pSpy-HiBiT-producing *E. coli* to $NaN_3$ are comparable for both periplasmic release and whole cell lysis. At concentrations greater than 400 µM, signal begins to decrease to approximately half that of the untreated positive control (0.53±0.17 and 0.44±0.13 RLU for periplasmic and whole cell, respectively) before reaching a plateau.

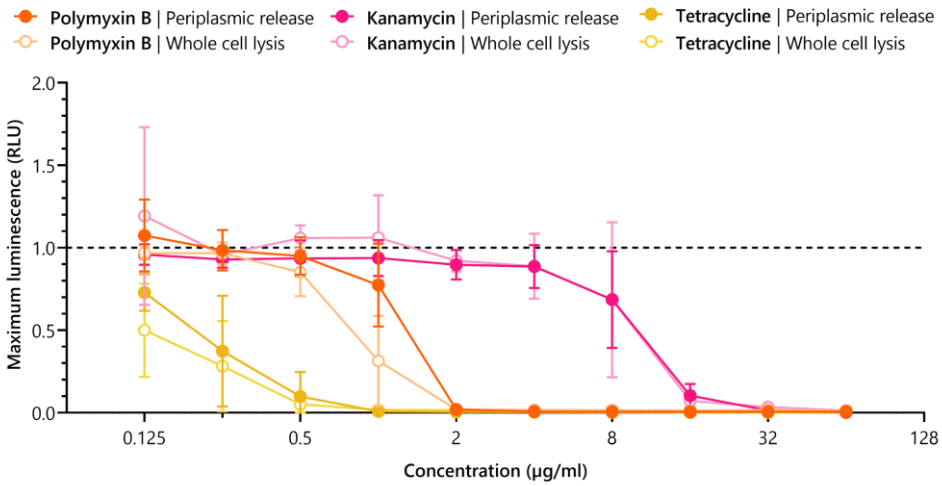


**Figure 3.9 Effect of non-specific inhibitors on the NanoBiT assay**
LB cultures of BL21(DE3) producing pre-secretory Spy-HiBiT were diluted to $OD_{600}$ 0.1 in 96-well plates, supplemented with 0.1% (w/v) arabinose and varying concentrations of polymyxin B (orange), kanamycin (pink) or tetracycline (yellow) and incubated at 37 °C for 1.5 h then 4 °C for 1 h. LgBiT and furimazine were added in the absence (primary assay/ periplasmic release; solid circles) or presence (counter assay/ whole cell lysis; open circles) of Triton X-100, followed by EDTA and lysozyme. The maximum luminescence in each sample was normalised to the maximum signal in the respective untreated control (black dotted line) and plotted against concentration. Data from three independent replicates are shown as mean ± standard deviation.

To further determine the capacity of the NanoBiT assay and counter assay to select against non-specific inhibitors, polymyxin B, which is a bactericidal antibiotic that primarily acts by destabilising the outer membrane, and antibacterial protein synthesis inhibitors kanamycin and tetracycline were also investigated in this system. Since these compounds are expected to indirectly interfere with bacterial protein secretion, they are commonly used as negative controls in Sec inhibitor screens (Crowther *et al.*, 2012). As was the case for $NaN_3$, the dose response curve for periplasmic release was comparable to that of whole cell lysis for all three antibiotics, consistent with a non-specific mechanism and validating the counter assay for exclusion of non-specific inhibitors (Figure 3.9).

## 3.4 Optimisation of local screen and initial hit discovery

As the condition that decreased luminescent signal upon periplasmic release the most, without impacting whole cell lysis signal, 5 µM CCCP (yielding 0.26±0.0091 RLU) was taken forward as the positive control for a hit. Screens were performed against 5000 ChemBridge DiverSET small synthetic compounds in 10 mM DMSO stocks in 96-well plates. Compared to natural product extracts, these compounds are more affordable and have simpler structures facilitating identification

of pharmacophores and subsequent lead optimisation. To further help optimisation, structural analogs are readily available through ChemBridge. To trial the HTS, one plate (62416) was screened at two concentrations by hand. For each plate or each independent experiment using the same plate, data were normalised by dividing by the mean luminescent signal reached by DMSO controls in column 1. A hit was defined as a compound that resulted in less than 0.8 RLU after normalisation. At 10 µM, a possible weak hit (position A11) which reduced luminescence to 0.74 RLU was identified (Figure 3.10a). At 100 µM, the effect of this compound was increased, giving a strong hit at 0.16 RLU (Figure 3.10b). At this concentration, several other compounds diminished luminescence to as low as 0.76 RLU, but this was not reproducible, suggesting that this screening concentration is high enough to detect compounds with non-specific inhibitory activity (false positives).

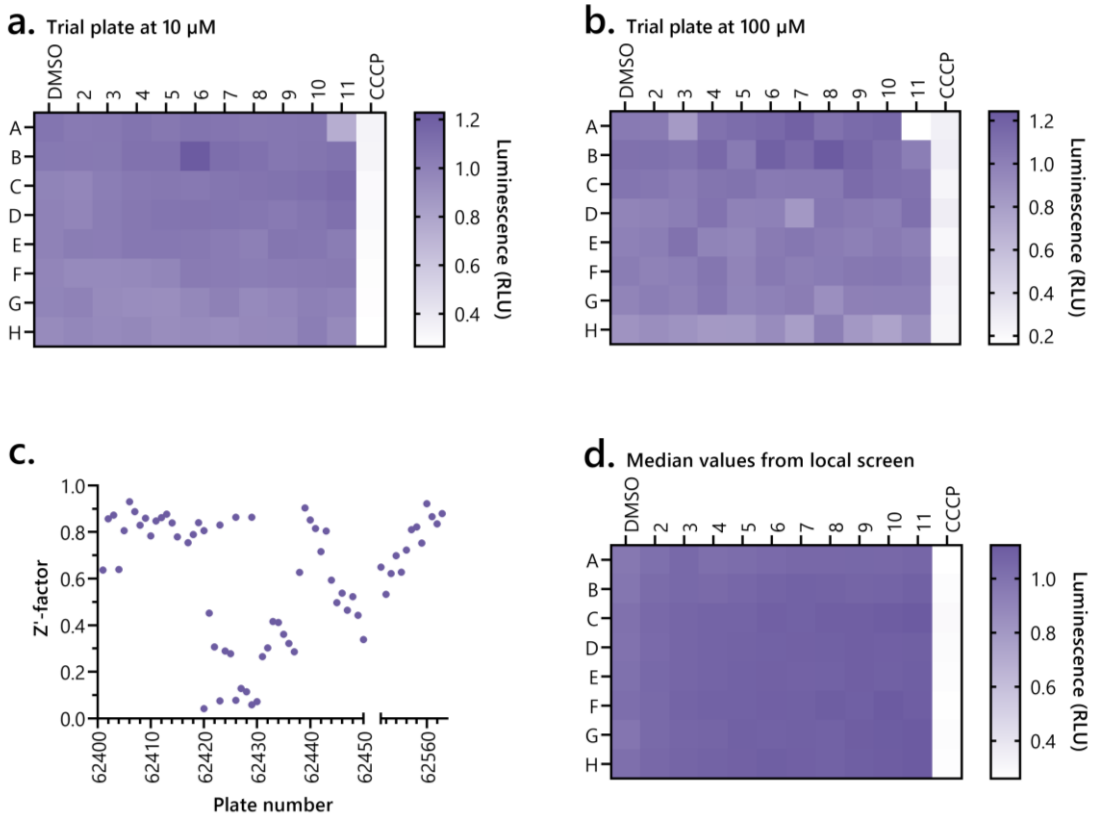


**Figure 3.10 Summary data for local screen of 5000 compounds**
LB cultures of BL21(DE3) producing pre-secretory Spy-HiBiT were diluted to $OD_{600}$ 0.1 in 96-well plates and supplemented with 0.1% (w/v) arabinose. Diluted cultures were treated with (Column 1) DMSO equivalent to the amount present in columns 2-11, (Column 12) 5 µM CCCP, (**a.** Columns 2-11) 10 µM compound library from 10 mM stock in DMSO, (**b.** Columns 2-11) 100 µM compound library, (**c, d.** Columns 2-11) 50 µM compound library. Plates were incubated at 37 °C for 1.5 h then 4 °C for 1 h. LgBiT and furimazine were added followed by EDTA and lysozyme (periplasmic release). **a, b.** The luminescence for each well after 1 h was normalised to the mean signal in the untreated controls and shown as a heatmap. **d.** The median normalised luminescence for each well position across all plates screened at 50 µM shown as a heatmap. A lighter shade of colour on the heatmap indicates lower luminescence (scale of colour vs. RLU given on the right of each graph). **c.** Z'-factor for each plate was calculated according to the equation derived by Zhang, Chung & Oldenburg (1999).

To facilitate screen optimisation, both Z- and Z'-factors were calculated (Zhang, Chung & Oldenburg, 1999). Both pilot runs had a Z'-factor over 0.5 (0.71 at 10 µM and 0.62 at 100 µM)

suggesting an excellent assay for screening compounds. Their Z-factors were comparable (0.63 and 0.65, respectively) indicating that test compound concentration has little effect on signal window. Moving forward, the first set of 6 plates were assayed at 10 µM, to avoid false positives. However, no further hits were detected, so the assay concentration was increased to 50 µM. All remaining plates were screened at this concentration, yielding a median Z'-factor of 0.71. While Z'-factors were high on average, this was dependent on liquid handling equipment; screens of plates 62420 to 62437 were subject to greater error, which was resolved upon servicing the equipment (Figure 3.10c). Overall, median well values for each plate position show minimal plate effect across test wells in columns 2 to 11 using this screen setup (Figure 3.10d). On average, column 1 yielded lower signal than columns 2 to 11, when it is expected to give comparable signal. This suggests that the outermost wells are subject to some plate effect – likely evaporation of cultures during the 1.5 h incubation step – but this effect is subtle and does not affect interpretation of results.

In addition to a pre-determined threshold for hit selection (<0.8 RLU compared to the positive control), a second condition for hit selection from the local screen was defined. This condition requires that hits yield signal less than $\bar{x}$-3SD, where $\bar{x}$ is the mean signal and SD is the standard deviation of signal from columns 2 to 11 in the respective plate. This condition accounts for plates with low Z'-factors and high standard deviation due to erroneous liquid handling – false positives from such errors are less likely to generate a hit (Makarenkov *et al.*, 2007). Using these criteria, 11 hits were taken forward for confirmatory testing. The hit rate from the primary screen is 0.22%.

## 3.5 Hit confirmation by dose response and counter assay

Compounds taken as hits from the primary screen were re-tested by the primary assay at a range of concentrations, to assess whether their activity is reproducible and to determine the $IC_{50}$ of each compound under these assay conditions. Counter selection was performed in parallel using the whole cell lysis counter assay. Only one compound (Figure 3.11a) had no activity when re-tested. For five compounds, re-testing confirmed activity, but counter assay revealed that their effects were predominantly non-specific; the dose response curves for the counter assay were comparable to those for the primary assay (Figure 3.11b - f). For the six compounds that did not pass confirmatory testing and counter assay, $IC_{50}$ for the primary assay could not reliably be calculated from the dose response data.

On the other hand, the response of the primary assay to each of the confirmed hits follows a sigmoidal shape when plotted against compound concentration on a logarithmic scale (base 10). This enables estimation of $IC_{50}$; under these assay conditions, the $IC_{50}$ values of all confirmed hits against periplasmic accumulation of pSpy-HiBiT in intact *E. coli* are less than 20 µM. For these hits, the plotted dose response of the counter assay is shifted to the right compared to the primary assay, suggesting the compounds exhibit specific inhibitory activity against periplasmic accumulation of Spy constructs.

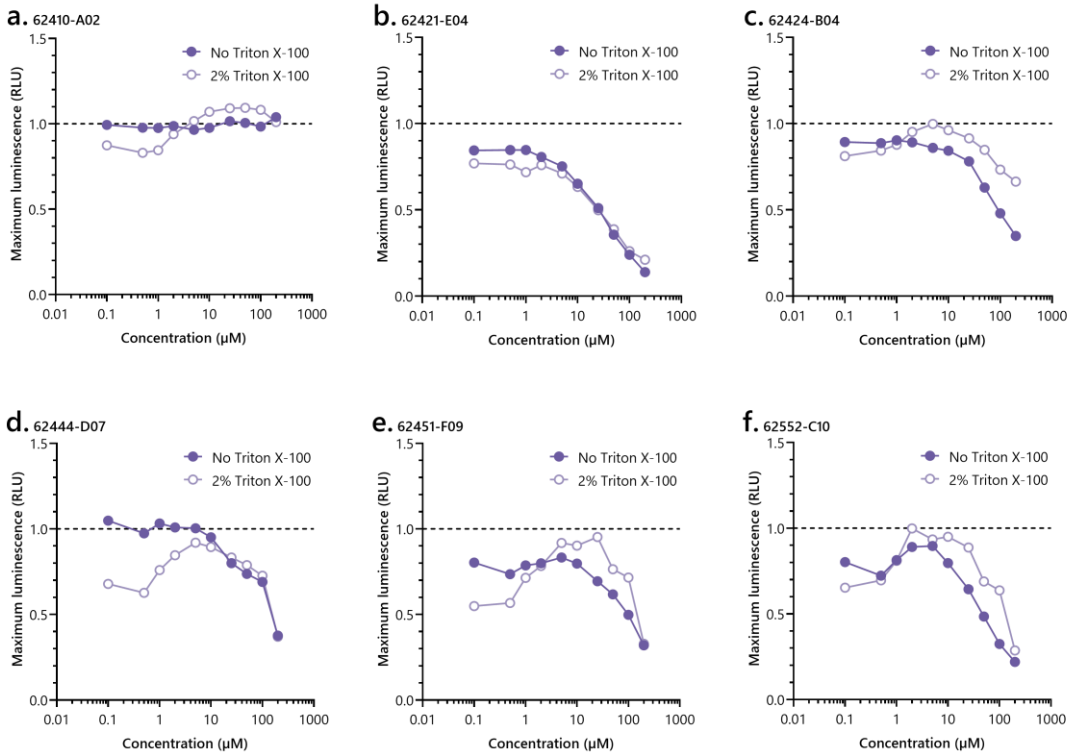


**Figure 3.11 Dose response of rejected hits in primary and counter assays**
LB cultures of BL21(DE3) producing pre-secretory Spy-HiBiT were diluted to $OD_{600}$ 0.1 in 96-well plates and supplemented with 0.1% (w/v) arabinose and varying concentrations of compounds from 10 mM DMSO stocks at the following positions from the compound library **a.** 62410-A02, **b.** 62421-E04, **c.** 62424-B04, **d.** 62444-D07, **e.** 62451-F09, **f.** 62552-C10. Following incubation at 37 °C for 1.5 h then 4 °C for 1 h, LgBiT and furimazine were added in the absence (primary assay/ periplasmic release; solid circles) or presence (counter assay/ whole cell lysis; open circles) of Triton X-100, followed by EDTA and lysozyme. The maximum luminescence in each sample was normalised to the maximum signal in the respective untreated control (black dotted line) and plotted against concentration. Data from one replicate are shown.

Initially, the compound from 62416-A11 (Hit1) gave an $IC_{50}$ of 18.1 μM in the primary assay (95% CI 15.9 – 20.8 μM; Figure 3.12a). However, upon ordering more compound, subsequent batches have no activity ($IC_{50}$ could not reliably be calculated; Figure 3.12b). Liquid chromatography mass spectrometry analysis revealed that the initial batch of compound differed from the subsequent batches, and from the supplier's mass spectrometry analysis, but could not determine its identity. Hit2 (62431-G04 in the compound library) has an $IC_{50}$ of 5.23 μM (95% CI 3.73 – 7.40 μM) on periplasmic accumulation of pSpy-HiBiT (Figure 3.12c). Like CCCP, its $IC_{50}$ for whole cell levels of the construct is approximately one order of magnitude greater than its specific activity (53.5 μM; 95% CI 39.2 – 72.1 μM). Hit2 has a molecular weight of 370 Da and is lipophilic, with a positive LogP (4.61, calculated by ChemBridge) indicating a preference for octanol as a solvent over water. Its structure is shown in Figure 3.12d.

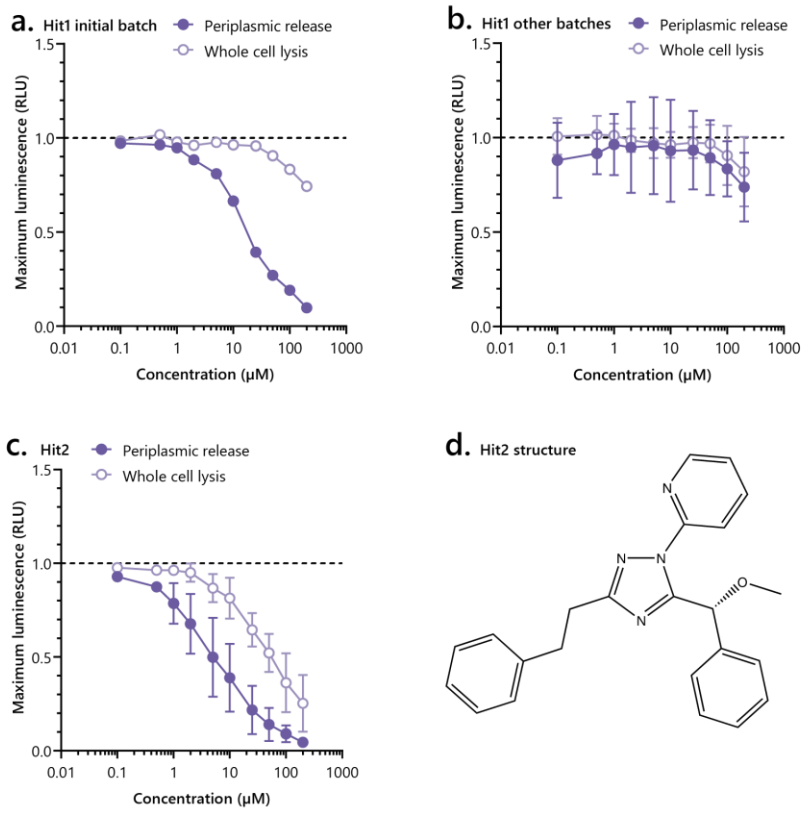


**Figure 3.12 Dose response of Hit1 and Hit2 in primary and counter assays**
LB cultures of BL21(DE3) producing pre-secretory Spy-HiBiT were diluted to $OD_{600}$ 0.1 in 96-well plates and supplemented with 0.1% (w/v) arabinose and varying concentrations of compounds from 10 mM DMSO stocks of **a.** Hit1 from the initial compound library; **b.** Hit1 from subsequent batches; **c.** Hit2. Following incubation at 37 °C for 1.5 h then 4 °C for 1 h, LgBiT and furimazine were added in the absence (primary assay/ periplasmic release; solid circles) or presence (counter assay/ whole cell lysis; open circles) of Triton X-100, followed by EDTA and lysozyme. The maximum luminescence in each sample was normalised to the maximum signal in the respective untreated control (black dotted line) and plotted against concentration. Data from up to three independent replicates are shown as mean ± standard deviation. **d.** Chemical structure of Hit2.

In the periplasmic release assay, Hit3 (62556-A06) yields an $IC_{50}$ of 6.79 µM (95% CI 6.09 – 7.59 µM; Figure 3.13b). By contrast, its $IC_{50}$ in the counter assay is approximately twenty times greater at 145.0 µM (95% CI 113.3 – 197.5 µM). Hit3 has a similar molecular weight and lipophilicity to Hit2 (398 Da and logP of 4.16). Assessment of structural analogs of Hit3 helped elucidate characteristics of the compound that are required for its activity in the assay (structures shown in Figure 3.13a, d, e, h). Only analog Hit3-c retains comparable activity ($IC_{50}$ in primary assay 16.4 µM; 95% CI 15.0 – 18.0 µM; $IC_{50}$ in counter assay could not be calculated) to Hit3 (Figure 3.13g). Hit3-a has no activity in primary or counter assays (Figure 3.13c) and Hit3-b activity is similar in the primary and counter assays, suggesting that it only has a non-specific inhibitory effect (Figure 3.13f). Hit3-a, b and c are all smaller (355, 369 and 377 Da) and have lower logP (3.02, 3.27 and 3.74) than Hit3. Based on qualitative assessment of the region that differs in structure across the four analogs, attachment of the amide nitrogen to a $CH_2$ group bound to a ring structure appears essential for specific inhibitory activity. All four compounds were received as racemic samples; it is important for future development of these into promising drug leads to determine which enantiomers have activity.

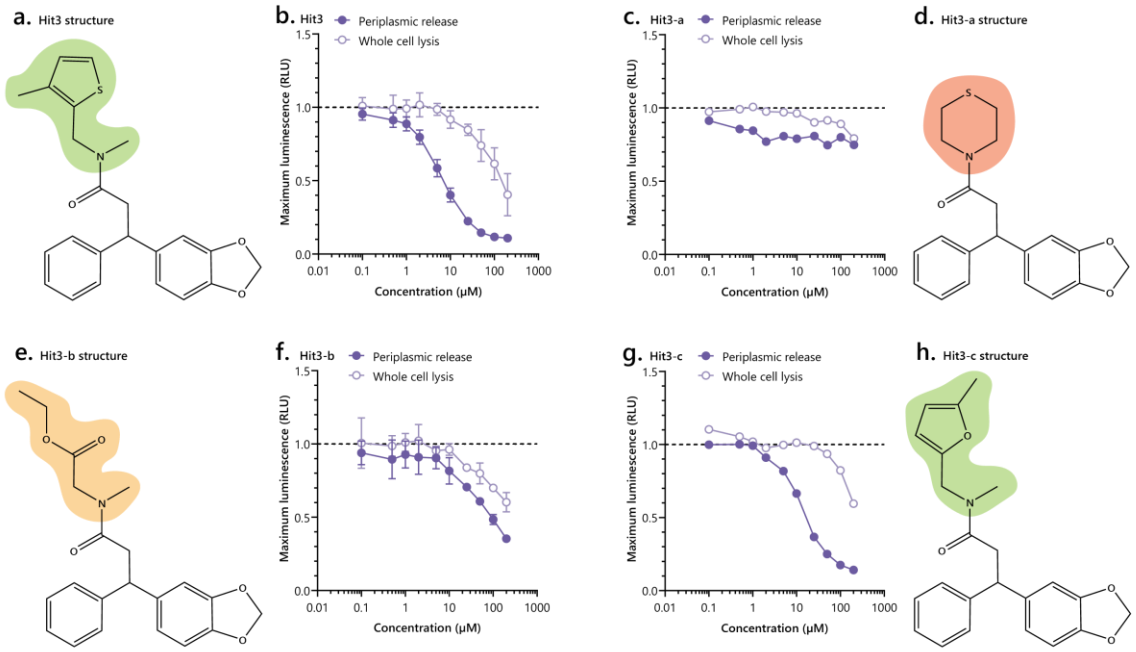


**Figure 3.13 Dose response of Hit3 and structural analogs in primary and counter assays** LB cultures of BL21(DE3) producing pre-secretory Spy-HiBiT were diluted to $OD_{600}$ 0.1 in 96-well plates and supplemented with 0.1% (w/v) arabinose and varying concentrations of compounds from 10 mM DMSO stocks of **b.** Hit3, **c.** Hit3-a, **f.** Hit3-b, **g.** Hit3-c. Following incubation at 37 °C for 1.5 h then 4 °C for 1 h, LgBiT and furimazine were added in the absence (primary assay/ periplasmic release; solid circles) or presence (counter assay/ whole cell lysis; open circles) of Triton X-100, followed by EDTA and lysozyme. The maximum luminescence in each sample was normalised to the maximum signal in the respective untreated control (black dotted line) and plotted against concentration. Data from up to three independent replicates are shown as mean ± standard deviation. Chemical structure of **a.** Hit3, **d.** Hit3-a, **e.** Hit3-b, **h.** Hit3-c. Regions that differ between analogs are highlighted in colour: green for compounds more active in primary assay than counter assay, orange-red for compounds with no activity and yellow for compounds with comparable activity in primary and counter assays.

Hit4 (62558-C08) inhibits periplasmic accumulation of pSpy-HiBiT with $IC_{50}$ 16.1 μM (95% CI 14.0 – 18.4 μM; Figure 3.14a). Its non-specific inhibitory activity is just under ten times its specific activity ($IC_{50}$ 110.4 μM, 95% CI could not reliably be calculated). It has LogP 3.42 and molecular weight 330 Da and was received as a racemic mixture (structure shown in Figure 3.14b). Strikingly, the compound from position 62562-A02 (Hit5) has very little non-specific activity (Figure 3.14c). After treatment with 200 μM of compound, luminescent signal upon whole cell lysis remains high at 0.77±0.023 RLU. In contrast, its $IC_{50}$ against periplasmic signal is low at 12.2 μM (95% CI 10.0 – 14.9 μM). Removal of the trifluoromethyl group from, and attachment of a chlorine atom to, its benzyl ring abolishes this activity (Figure 3.14d, e). Hit5 and the Hit5-a analog have LogP 3.32 and 2.98, respectively, and their molecular weights are 420 and 387 Da, respectively.

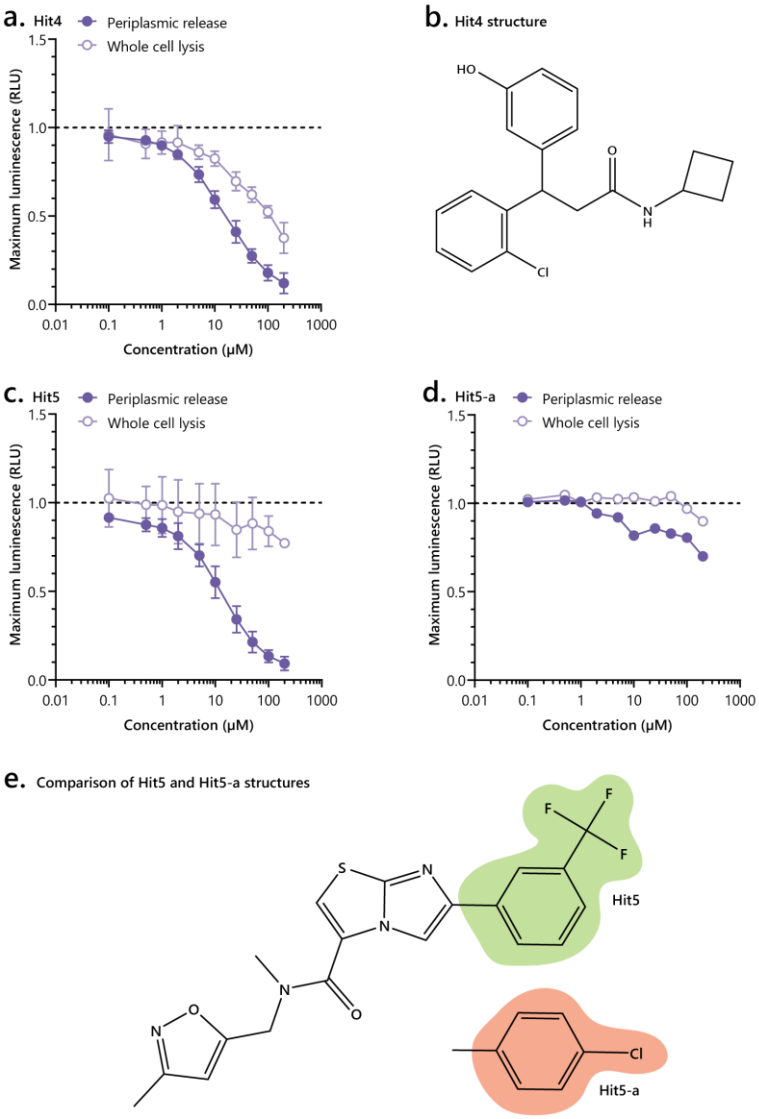


**Figure 3.14 Dose response of Hit4, Hit5 and structural analogs in primary and counter assays**
LB cultures of BL21(DE3) producing pre-secretory Spy-HiBiT were diluted to $OD_{600}$ 0.1 in 96-well plates and supplemented with 0.1% (w/v) arabinose and varying concentrations of compounds from 10 mM DMSO stocks of **a.** Hit4, **c.** Hit5**, d.** Hit5-a. Following incubation at 37 °C for 1.5 h then 4 °C for 1 h, LgBiT and furimazine were added in the absence (primary assay/ periplasmic release; solid circles) or presence (counter assay/ whole cell lysis; open circles) of Triton X-100, followed by EDTA and lysozyme. The maximum luminescence in each sample was normalised to the maximum signal in the respective untreated control (black dotted line) and plotted against concentration. Data from up to three independent replicates are shown as mean ± standard deviation. **b**. Chemical structure of Hit4. **e**. Chemical structure of Hit5 (top) with the region that differs in Hit5-a (bottom). Regions that differ between analogs are highlighted in colour: green for compounds more active in primary assay than counter assay and orange-red for compounds with no activity. The region that is not highlighted is common to Hit5 and Hit5-a.

## 3.6 Discussion

This chapter demonstrates the design, validation, optimisation and small-scale deployment of a novel whole cell-based screen for inhibitors of the Sec-machinery. Based on the NanoBiT assay for

protein translocation (Pereira *et al.*, 2019), this screen system is straightforward, offering high sensitivity and adaptability to any Sec-dependent protein of interest (demonstrated in Chapter 5).

The screen assay designed here is a loss-of-signal system. As non-specific inhibitors are not deselected in such a system, this created a need for a high throughput counter assay for rapid identification of these agents. In previous screens, this was achieved using cells producing SS-less reporter protein that remains in the cytoplasm. Specific inhibitors of translocation would not impact cytoplasmic reporter activity, while non-specific inhibitors would do so (Crowther *et al.*, 2015; Klein *et al.*, 2018b). The advantage of this approach over screening primary hits against purified reporter enzyme (Hamed *et al.*, 2021) is that it will identify inhibitors of cellular functions as well as reporter activity. The drawback of both options is that they require incubation of compounds with additional samples to the primary assay. It was shown above that the HiBiT-tagged reporter protein remains capable of complementing LgBiT in the absence of its SS. However, the periplasmic release and whole cell lysis methods developed in this work enable parallel assessment of hit activity in primary and counter assays from the same samples, significantly increasing throughput of hit confirmation.

In the counter assay, mSpy-HiBiT yields a lower signal compared to the respective pSpy-HiBiT sample. One explanation is that upon whole cell lysis, LgBiT may not be able to access HiBiT on unfolded cytoplasmic Spy constructs as efficiently as those that have been translocated and matured in the periplasm. If this were true, a decrease in whole cell signal would be expected following treatment of pSpy-HiBiT producers with secretion inhibitors, since these would also result in accumulation of HiBiT in the cytoplasm. However, the SecA inhibitor CJ-21058 does not reduce whole cell signal of such cells compared to a DMSO control. Alternatively, SS-less mSpy may occupy different conformations in the cytoplasm than unexported pSpy, rendering HiBiT less accessible for LgBiT. This is unlikely, as folding transitions of the Spy mature domain are not affected by the presence or absence of SS (Tsirigotaki *et al.*, 2018). Therefore, the most plausible explanation is that deletion of the Spy SS results in lower expression or stability of the protein, resulting in decreased whole cell levels of mSpy-HiBiT compared to pSpy-HiBiT. Importantly, validation with CJ-21058 confirms that HiBiT activity is unaffected by the subcellular location or conformation of associated Spy constructs.

Thorough assay validation using a panel of compounds with known activities is important both for assay optimisation and for uncovering any weaknesses in the assay design. Dose response of the primary assay to $NaN_3$ reveals that even the highest concentrations (3 mM) only achieve approximately 50% inhibition. This poor activity may explain the low and variable Z'-factors resulting from earlier screens using up to 0.5 mM $NaN_3$ as a positive control for inhibition (Moir *et al.*, 2011; Crowther *et al.*, 2015). Interestingly, in assays of periplasmic PhoA activity, 4 mM $NaN_3$ inhibited signal by over 90% (Hamed *et al.*, 2021). With different assay systems and different Sec substrates, sensitivity to a given inhibitor will vary. The contrasting results with $NaN_3$ demonstrate the importance of optimising positive controls for each assay system, to improve the signal window.

The comparable response of both primary and counter assays to $NaN_3$ suggest that it predominantly affects periplasmic accumulation of pSpy-HiBiT by a non-specific mechanism. This

is consistent with the general ATPase inhibitor activity of $NaN_3$ and its known impact on the respiratory chain (Bowler *et al.*, 2006). The counter assay was also effective in deselection of two different classes of protein synthesis inhibitor as well as a non-specific membrane active agent. Uncouplers like CCCP also impact membrane integrity, increasing proton permeability. Ideally, uncouplers would also be deselected, but up to 5 mM CCCP was determined to have a specific effect on the periplasmic levels of reporter protein without affecting whole cell levels. Nevertheless, this is not a shortcoming of the specific assay setup described here, but an unavoidable property of the native Sec-machinery. The transmembrane proton gradient is a major driving force of translocation through Sec, so uncouplers like CCCP specifically inhibit this process as well as other cellular functions (Brundage *et al.*, 1990; Economou *et al.*, 1995; Schulze *et al.*, 2014; Allen *et al.*, 2022). These results confirm that the assay specifically reports on translocation of pSpy-HiBiT but demonstrate the importance of screening compounds at a range of concentrations to identify off-target effects.

A typical screening concentration for a high-purity, diverse small molecule library is 10 µM. Unbiased libraries will generally give a hit rate of up to 1% under these conditions. When challenged with 10 µM compound, the NanoBiT screen assay gave a primary hit rate substantially lower than 1%. A concentration of 50 µM was used instead, yielding a primary hit rate of 0.22%. Indeed, previous whole cell screens of synthetic compounds also used higher than standard concentrations, ranging from 20 – 100 µM (Alksne *et al.*, 2000; Moir *et al.*, 2011; Crowther *et al.*, 2012, 2015; Hamed *et al.*, 2021). Their primary hit rates were similar to this work: 0.14, 0.64 and 0.83% (Moir *et al.*, 2011; Crowther *et al.*, 2015; Hamed *et al.*, 2021, respectively). The need for a higher screening concentration is not surprising, given that for effective use, current antibiotics require concentrations up to a thousand times larger than drugs with a eukaryotic target. The binding of antibiotics to their respective targets is comparable to that of eukaryotic drugs; the major constraint of activity is poor permeation in bacteria (Lewis, 2013). Commercial synthetic compound libraries are optimised for physicochemical properties that promote oral bioavailability and absorption into the gastrointestinal tract (Lewis, 2020). Attempts to screen synthetic libraries for compounds with bacterial targets would therefore be aided by establishment of an equivalent set of rules for bacterial uptake.

Previously, lower primary hit rates were associated with greater rates of hit confirmation by retesting and counter assays, showing that more stringent primary assay selection results in fewer false positives. Confirmation rates were 9.3, 5.2 and 0.4%, respectively (Moir *et al.*, 2011; Crowther *et al.*, 2015; Hamed *et al.*, 2021). Given the small size of the local screen in this work, thresholds for hit confirmation were more lenient. While only one primary hit (Hit5) specifically inhibited the primary assay with negligeable effect on the counter assay, four hits were taken as true positives due to their demonstration of a reproducible dose response and lower activity in counter assays (36% of hits were confirmed). More typical confirmation criteria would still allow a high true positive rate (9.1%), comparable to previous work with a similar primary hit rate (Moir *et al.*, 2011).

The identified hits had strong activity in the primary assay, with $IC_{50}$ values ranging 5 – 20 µM. These values were substantially lower than that of CJ-21058 (227.1 µM) and closer to that of CCCP

(1.82 µM). This $IC_{50}$ range appears typical for whole cell screens against the Sec-machinery; hits from other systems had a half-maximal effect on their respective primary assay at 3 – 57 µM (Crowther *et al.*, 2015; Hamed *et al.*, 2021). Similarity searches (2D and 3D, standard parameters) on the Hit2Lead website (ChemBridge) confirmed that the hits identified in this work all belong to distinct chemotypes. Where available, structural analogs of each hit were obtained from Hit2Lead and tested in primary and counter assays to elucidate the chemical substructures that affect their observed activity. Amide bonds, resembling peptide structures, and bulky ring moieties are common to the majority of active compounds. It would be interesting to know whether the differences in activity between analogs are target-specific or due to differences in bacterial uptake and efflux. Furthermore, it would be useful from a medicinal chemistry perspective to determine whether the identified hits are analogous to known promiscuous binders or pan-assay interference compounds that often show up as false positives (Klein *et al.*, 2018b). From a biochemical standpoint, hits from the primary screen can be validated in a range of secondary assays instead.

# Chapter 4 Secondary assays for translocation inhibitor screens

## 4.1 Introduction

The introduction to the previous chapter summarises published target-based screening approaches for discovery of bacterial Sec inhibitors. Where full information is available, the combinations of primary screen platform and secondary assays (including counter assays) used in these approaches are summarised in Table 4.1. Each of the primary screens enrich for compounds that impact Sec-mediated protein translocation, either through specific inhibition of SecA/ signal peptidase I or by interfering with the broader pathway. The different primary screening strategies employed necessitate different counter and secondary assays to demonstrate the utility of identified inhibitors. It is important to assess the strengths of the chosen primary screen and design secondary assays to mitigate any limitations. Overall, all approaches should show i) direct interaction with the Sec pathway *in vitro*; ii) lack of off-target effects; and iii) cellular activity, ideally on translocation in whole cells as well as growth inhibition.

### 4.1.1 Existing secondary assays for Sec inhibitors

With the exception of the whole cell differential sensitivity approach, all strategies targeting SecA investigated whether hits directly interact with SecA *in vitro* by assessment of ATPase activity in either primary or secondary assays (Li *et al.*, 2008; Segers *et al.*, 2011; Akula *et al.*, 2011, 2012; Huang *et al.*, 2012; De Waelheyns *et al.*, 2015). Of these, only one considered the off-target activity of identified inhibitors, reporting cytotoxicity on eukaryotic cells, but still failed to identify the mechanisms of off-target activity (De Waelheyns *et al.*, 2015). This is particularly troublesome for SecA-targeted screens, given the tendency for SecA inhibitors to inhibit other ATPases. While three of the five strategies included secondary assays for inhibitory activity on bacterial growth (Akula *et al.*, 2012; Huang *et al.*, 2012; De Waelheyns *et al.*, 2015), none assessed the impact of inhibitors on protein translocation in cells. Overall, none of these approaches satisfy all three of the criteria above.

The advantage of whole cell screens over *in vitro* systems is that hit compounds have confirmed inhibitory activity against translocation in a cellular context. Nevertheless, this does not guarantee an inhibitory effect on bacterial growth, which is also investigated in the majority of cases (Alksne *et al.*, 2000; Parish *et al.*, 2009; Crowther *et al.*, 2015; Hamed *et al.*, 2021). Additionally, whole cell assays are more prone than *in vitro* systems to non-specific inhibitors and do not confirm a direct interaction with the desired target. Successful counter assays will rule out inhibition of reporter transcription and translation, as well as reporter activity (Crowther *et al.*, 2015). It is important to note that, unlike SecA, homologs of core channel SecYE are present in both bacteria and eukaryotes. As illustrated by pan-Sec inhibitors eeyarestatin 24 and decatransin, it is possible that *bona fide* inhibitors of the core bacterial Sec-machinery may also inhibit eukaryotic Sec. Therefore,

**Table 4.1 Combinations of primary and secondary assays used in previous Sec inhibitor screens**

| Target | Primary assay | Secondary assays | Reference |
|---|---|---|---|
| **SecA** | ***In vitro*** intrinsic ATPase activity (activated mutant) | 1. ***In vitro*** intrinsic, membrane and translocation ATPase activity (wildtype *E. coli* SecA)<br>2. ***In vitro*** translocation of pPhoA (protease protection) | (Segers *et al.*, 2011) |
| | ***In vitro*** intrinsic ATPase activity (activated mutant) | 1. ***In vitro*** intrinsic, membrane and translocation ATPase activity (wildtype *E. coli* SecA)<br>2. ***In vitro*** translocation of pOmpA (protease protection)<br>3. **Bacterial growth inhibition and bactericidal activity** (wildtype and outer membrane permeable *E. coli*, *B. subtilis*)<br>4. ***In silico*** docking into ATPase cleft | (Huang *et al.*, 2012) |
| | ***In silico*** docking into ATPase cleft | 1. ***In vitro*** intrinsic ATPase activity (activated mutant) | (Li *et al.*, 2008) |
| | ***In silico*** docking into ATPase cleft | 1. ***In vitro*** intrinsic ATPase activity (*Ca. L. asiaticus* SecA)<br>2. **Bactericidal activity** (*A. tumefaciens*) | (Akula *et al.*, 2011, 2012) |
| | ***In silico*** docking into signal sequence-binding site | 1. ***In vitro*** intrinsic, membrane and translocation ATPase activity (wildtype *E. coli* SecA)<br>2. **Bacterial growth inhibition** (*E. coli*, *P. aeruginosa*¸ *B. subtilis* and *S. aureus*)<br>3. **Cytotoxicity** (growth inhibition of human T lymphoblasts) | (De Waelheyns *et al.*, 2015) |
| | **Whole cell** differential sensitivity | 1. **Bacterial growth inhibition** (*E. coli*, *B. subtilis*, *S. aureus*, *E. faecalis*, *S. pneumoniae* and *Haemophilus influenzae*)<br>2. **Cytotoxicity** (growth inhibition of *C. albicans*) | (Parish *et al.*, 2009) |
| **Signal peptidase I** | ***In vitro*** fluorogenic substrate | 1. ***In vitro*** accumulation of cleavage products (HPLC)<br>2. **Bacterial growth inhibition** (*E. coli*, *S. aureus*, *S. pneumoniae* and *H. influenzae*)<br>3. **β-lactamase secretion** (into medium by *S. aureus*) | (Peng *et al.*, 2001; Kulanthaivel *et al.*, 2004) |
| | **Whole cell** differential sensitivity | 1. **Bacterial growth inhibition** (*M. tuberculosis*)<br>2. ***In vitro*** fluorogenic substrate | (Bonnett *et al.*, 2016) |

| Target | Primary assay | Secondary assays | Reference |
|---|---|---|---|
| | | 3. **Membrane permeability** and **potential** (*M. tuberculosis*)<br>4. **Cytotoxicity** (growth inhibition of Vero cells) | |
| **Entire Sec pathway** | **Whole cell** genetic reporter (gain of signal) | 1. **Bacterial growth inhibition** (*S. aureus*)<br>2. **Protein production and secretion** (into medium by *S. aureus*) measured by immunoblot/ enzyme-linked immunoassay<br>3. **Pre-protein accumulation** (in *E. coli*) measured by pulse-chase labelling and immunoprecipitation<br>4. **Cytotoxicity** (growth inhibition of human cell lines)<br>5. **Membrane disruption** (outer membrane permeable *E. coli* and human red blood cells) | (Alksne *et al.*, 2000) |
| | **Whole cell** genetic reporter (gain of signal) | 1. **Counter assay** of reporter signal when under stress-inducible promoters unrelated to Sec<br>2. **β-lactamase translocation** (into *P. aeruginosa* periplasm)<br>3. **Elastase and phospholipase C secretion** (into medium by *P. aeruginosa* type 2 secretion systems) and **counter assay** against enzyme activity | (Moir *et al.*, 2011) |
| | **Whole cell** protein reporter (cytoplasmic, gain of signal) | 1. **Counter assay** of reporter transcription, translation and activity<br>2. **Bacterial growth inhibition** (*E. coli*)<br>3. **Cytotoxicity** (growth inhibition of human B lymphocytes)<br>4. **Protein production and processing** measured by immunoblot<br>5. **β-lactamase translocation** (into *E. coli* periplasm)<br>6. **Counter assay of cytoplasmic enzyme production**<br>7. **Thermal shift assay** of SecA binding | (Crowther *et al.*, 2015) |
| | **Whole cell** protein reporter (periplasmic, loss of signal) | 1. **Counter assay** of reporter activity and expression (immunoblot)<br>2. **Cytotoxicity** (killing of HEK293T cells)<br>3. **Bacterial growth inhibition** (wildtype, outer membrane permeable and efflux-deficient *E. coli*, *B. subtilis*, *S. aureus*, WHO priority pathogens)<br>4. ***In vitro*** intrinsic, membrane and translocation ATPase activity (activated mutant and wildtype *E. coli* SecA) | (Hamed *et al.*, 2021) |

cytotoxicity assays are not useful for identification of off-target activity in this case. Instead, methods to deselect non-specific inhibitors include measuring biosynthetic capacity (Alksne *et al.*, 2000; Crowther *et al.*, 2015), studying induction of known stress-response pathways (Moir *et al.*, 2011) or checking for membrane disruption (Alksne *et al.*, 2000; Bonnett *et al.*, 2016). With the exception of the *M. tuberculosis* signal peptidase I screen (Bonnett *et al.*, 2016), all of the previous whole cell-based screening approaches lack confirmation of inhibitor interaction with the Sec pathway *in vitro* (Alksne *et al.*, 2000; Parish *et al.*, 2009; Moir *et al.*, 2011; Crowther *et al.*, 2015; Hamed *et al.*, 2021). Those that attempted to achieve this focused only on SecA as the target site, despite these screens targeting the pathway as a whole (Crowther *et al.*, 2015; Hamed *et al.*, 2021). This shows that *in vitro* assays incorporating the broader Sec-machinery – other components as well as SecA – are better suited for this purpose.

All assays risk interference of reporter activity, which can result in false positives. In the absence of counter assays, a frequently used method for deselecting compounds that interfere with readout is through use of secondary assays based on a different reporter system. For example, *in vitro* screens of SecA ATPase activity using a colorimetric reporter were accompanied by *in vitro* protease protection assays, involving detection by radiography or immunoblot (Segers & Anné, 2011; Huang *et al.*, 2012). Whole cell-based screens strategies similarly employed immunoblot-based secondary assays (Alksne *et al.*, 2000; Crowther *et al.*, 2015) or alternative protein reporters of translocation, such as β-lactamase (Moir *et al.*, 2011; Crowther *et al.*, 2015). The additional impact of testing hits against a range of Sec substrates is that this will elucidate whether they operate as substrate-selective or broad inhibitors.

### 4.1.2 Proposed secondary assays to complement whole cell NanoBiT

Considering the successes and limitations of past searches for inhibitors of Sec, priorities for secondary assays to complement the whole cell NanoBiT screen were determined. First, *in vitro* assays should confirm a direct interaction with the broader Sec-machinery. After this, more targeted *in vitro* systems, such as SecA ATPase assays could be employed. Alongside counter assays, *in vitro* assays are expected to deselect compounds that act through non-target-specific mechanisms. Therefore, the second priority is determination of antibacterial activity. To differentiate between bacteria-specific Sec inhibitors that are promising antibiotic leads and pan-Sec inhibitors, cytotoxicity assays could then be performed.

*In vitro* assays for activity of the broader Sec-machinery require, at a minimum, SecA and lipid vesicles containing SecY, E and optionally G (Brundage *et al.*, 1990). Translocation-competent pre-proteins are added and translocated into the vesicle interior in an ATP-dependent reaction (Figure 4.1a; Figure 4.6a). There are broadly two types of vesicles used in these assays: proteoliposomes (PLs) and inverted inner membrane vesicles (IMVs). While PLs are made by mixing purified integral membrane proteins of Sec with commercial preparations of phospholipids, IMVs are isolated from bacteria overexpressing *sec* genes and house the Sec-machinery in its native lipid environment. As an example, anionic lipids like cardiolipin bind Sec *in vivo* so may be enriched around the Sec-

machinery in IMVs compared to PLs (Corey *et al.*, 2018). Cardiolipin is important for SecA recruitment and ATPase activity (Gold *et al.*, 2010) and PMF stimulation of Sec (Corey *et al.*, 2018). Furthermore, PLs and IMVs may be prepared with additional components of the Sec-machinery (SecDF-YajC and YidC, yielding HTL) or separate protein machineries such as bacteriorhodopsin, a light-driven proton pump that produces a PMF (Schulze *et al.*, 2014). In IMVs, other membrane proteins (namely ATP synthase which generates the PMF) will be present in trace amounts. Each of these factors can impact Sec activity. Thus, analysis of inhibitor activity against different *in vitro* preparations of the Sec-machinery can help elucidate their mode of action. Do they target the core machinery or auxiliary proteins? Do they require a specific lipid environment? Are they non-specific membrane active agents that interfere with the PMF?

The traditional method of monitoring protein translocation *in vitro* is by assessing protease protection (Figure 4.6a, b). The *in vitro* NanoBiT system is a more recent alternative (Figure 4.1a). As expressed in Chapter 3, the traditional assays can be laborious. NanoBiT assays have higher throughput and give continuous reads with far higher time resolution compared to protease protection assays (Pereira *et al.*, 2019). Such precise monitoring of protein transport allows extraction of more data informing on the kinetics of transport (Allen *et al.*, 2020, 2022). The drawback of this system is that it uses the same reporter as the primary screen, so will be susceptible to hits that impair readout. On the other hand, counter assays were used to deselect against such hits. This chapter compares the two assay systems to determine the most suitable approach for confirming inhibitor activity *in vitro*.

Additionally, efforts were made to determine antibacterial activity of hit compounds by standard antimicrobial susceptibility testing. None have detectable inhibitory activity on growth of *E. coli* strains under the conditions studied. Results suggest that hit antibacterial activity is due to insufficient inhibition of target, rather than bacterial cell envelope permeability constraints, but further experimentation is needed to confirm this. The implications of this on whether hits represent useful antibiotic leads are discussed.

## 4.2 *In vitro* NanoBiT assays for hit validation

For NanoBiT-based assays of translocation *in vitro*, pre-protein is tagged with HiBiT, and vesicles contain LgBiT. Transport of HiBiT-tagged pre-protein via Sec into the vesicle lumen, analogous to the Gram-negative periplasm, allows complementation of NanoBiT fragments, giving luminescence in the presence of furimazine (Figure 4.1a). Signal is fit to a lag phase followed by a single exponential (Figure 4.1b). Alongside lag, the apparent rate constant (λ) and amplitude (A) of the signal can be derived (Allen *et al.*, 2020).

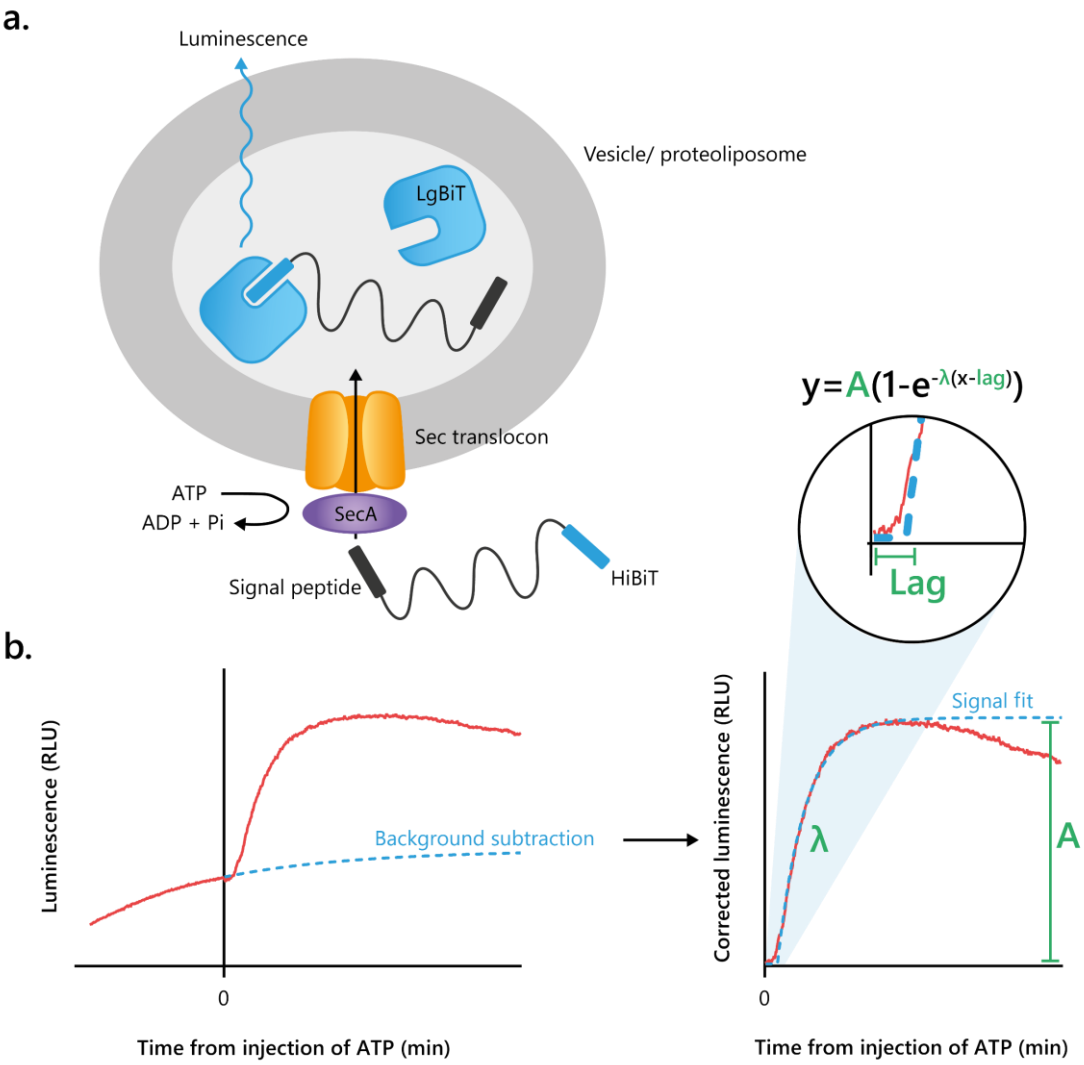


**Figure 4.1 Design of *in vitro* NanoBiT assays for protein translocation**
**a.** Proteoliposomes or inverted inner membrane vesicles containing the membrane-bound Sec-machinery and LgBiT are combined with purified SecA, agents for regeneration of ATP from ADP, furimazine and translocation-competent, C-terminally HiBiT-tagged Sec substrate. Upon addition of ATP, SecA drives translocation of substrate from outside to inside the vesicle. HiBiT attached to substrate can access LgBiT inside liposomes, giving luminescence. **b.** Luminescent signal from the reaction is monitored in a platereader. Signal prior to ATP injection is fit to a single exponential and extrapolated values are subtracted from post-ATP signal (background subtraction). Corrected luminescence, omitting signal decay, is fit to a single exponential plus lag (equation shown) and parameters lag, A (amplitude) and λ (indicated in green) are derived.

Lag is the minimum time taken for signal to be generated. Since reaction components are equilibrated together prior to initiation of translocation with ATP, lag corresponds to the time taken for pre-formed complexes of Sec and substrate to complete translocation. It is therefore a measure of transport rate; longer lag means slower transport. Amplitude is proportional to the amount of substrate that has been translocated upon reaction completion. Under the assay conditions used here, translocation is largely single turnover, so amplitude is proportional to the number of active Sec-machinery sites (Allen *et al.*, 2022). The most complex parameter is λ, which contains information not only on transport rates, but on probability of translocation stalling or failure (Allen *et al.*, 2020, 2022). Data from *in vitro* NanoBiT assays have facilitated elucidation of the number and size of transport steps (Allen *et al.*, 2020) and how they are impacted by different polypeptide

sequences and exposure to inhibitors (Allen *et al.*, 2022). It follows that the mode of action of primary hits can be uncovered based on their effect on each of these three transport parameters.

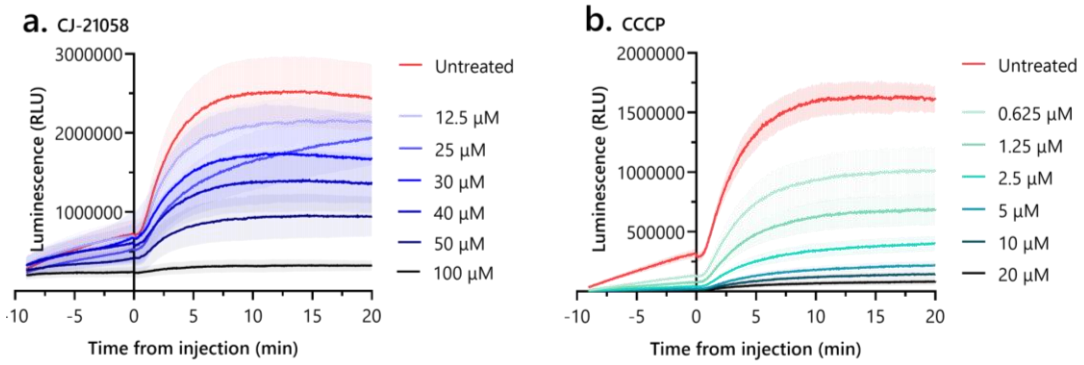


**Figure 4.2 Activity of control inhibitors assessed by *in vitro* NanoBiT assay**
Proteoliposomes containing SecYEG and LgBiT were combined with purified SecA, ATP regeneration reagents, furimazine, translocation-competent pSpy-HiBiT and varying concentrations of **a.** CJ-21058 or **b.** CCCP. Luminescence was measured for approximately 10 min prior to, and 20 min after, reaction initiation by injection of ATP. Data from 3 – 6 technical replicates are shown as mean ± SEM.

As the simplest possible reconstitution of Sec, SecYEG PLs containing LgBiT were challenged with inhibitor. They were mixed with purified SecA, ATP regeneration reagents, furimazine and translocation-competent pSpy-HiBiT (the same substrate as in primary screen assays). CJ-21058 is a known SecA inhibitor, so should hinder pSpy-HiBiT translocation into SecYEG PLs and reduce NanoBiT complementation. By contrast, CCCP abrogates the PMF, which is absent in this system, so should have no effect on signal generation. In primary NanoBiT assays, up to 100 µM CJ-21058 (which corresponds to 37.5 µM during the endpoint read) has no effect on recorded signal (Figure 3.8). In the reconstituted system, 25 µM or more CJ-21058 decreases the maximal signal reached within 20 min of reaction initiation with ATP (Figure 4.2a). This response is dose dependent. Interestingly, the apparent rate for samples treated with 25 µM CJ-21058 is noticeably (and reproducibly) slower compared to the untreated control and adjacent tested concentrations; signal fails to reach a plateau in the 20 min time window. Final signal reached is approximately half-maximal during 40 µM treatment (mean ± standard error of the mean, SEM of 1,367,000±376,500 compared to 2,437,000±430,400 for the untreated control). Treatment with 100 µM CJ-21058 almost completely abolishes signal.

However, these treatments also impair signal formation prior to ATP addition (Figure 4.2a). This background signal is caused by complementation of HiBiT with any LgBiT that may have leaked out of vesicles or not been washed from their external surface after vesicle preparation. It acts as an internal control against compounds that quench luminescence from NanoBiT or impair NanoBiT complementation. This suggests that, under the conditions used in these experiments, NanoBiT itself is sensitive to CJ-21058. From these signal traces, it is not possible to conclude the specific effect of CJ-21058 on Sec-mediated translocation *in vitro*.

CCCP similarly affects signal generation before and after addition of ATP in a dose-dependent manner (Figure 4.2b). Qualitatively, the shape of the signal curve appears unchanged regardless

of CCCP treatment; the only noticeable difference is in amplitude. It is possible that the NanoBiT enzyme is also quenched by CCCP. To confirm that the apparent NanoBiT quenching activities of CJ-21058 and CCCP are not due to the presence of DMSO from their respective stock solutions, DMSO concentrations up to 0.5% (equivalent to 50 µM CJ-21058, 50 µM hit compound or 20 µM CCCP) were assayed. DMSO treatment did not result in a reproducible, dose-dependent decrease in luminescence before or after ATP addition (Appendix 1).

All four primary hit compounds affected both background and signal in the *in vitro* NanoBiT assay (Figure 4.3). This response is dose dependent in all cases; the highest concentration of compound yields the lowest signal pre- and post-addition of ATP. The untreated signal trace has lower amplitude than expected in all three replicates of the Hit4 treatment series (Figure 4.3c).

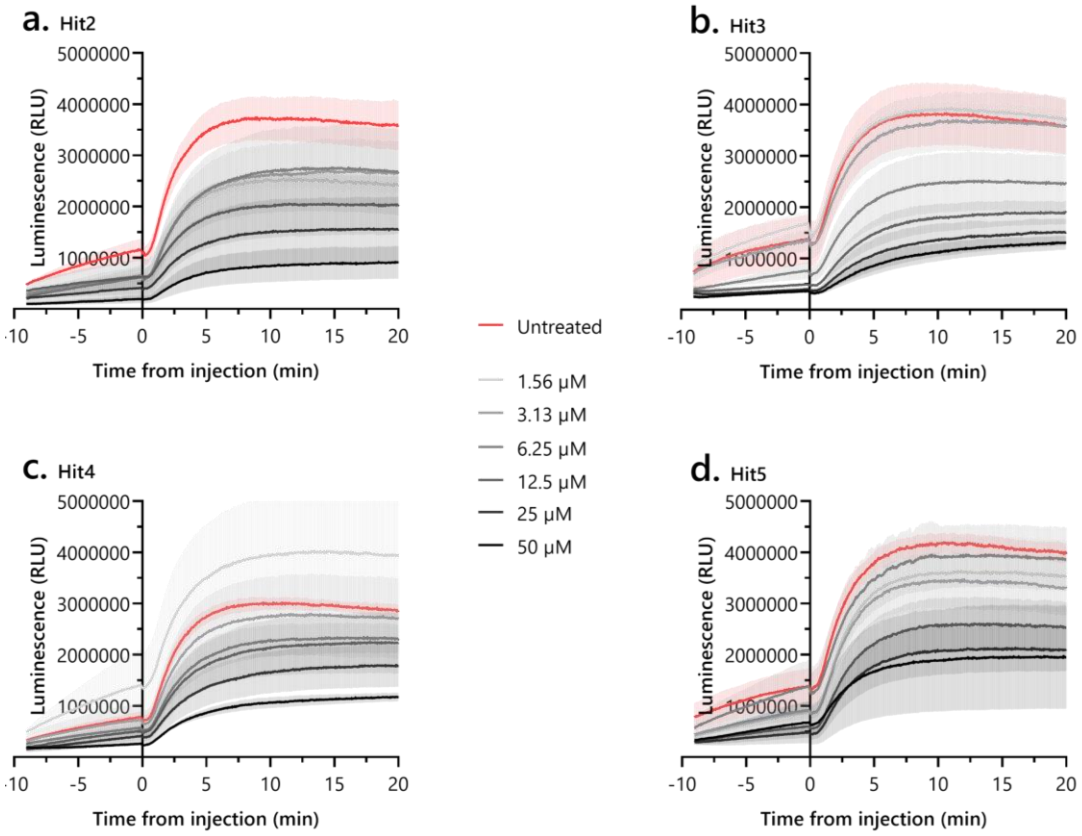


**Figure 4.3 Activity of hits on SecYEG proteoliposomes assessed by *in vitro* NanoBiT assay**
Proteoliposomes containing SecYEG and LgBiT were combined with purified SecA, ATP regeneration reagents, furimazine, translocation-competent pSpy-HiBiT and varying concentrations of **a.** Hit2, **b.** Hit3, **c.** Hit4 or **d.** Hit5. Luminescence was measured for approximately 10 min prior to, and 20 min after, reaction initiation by injection of ATP. Data from three technical replicates are shown as mean ± SEM.

For all *in vitro* NanoBiT traces, raw luminescence is plotted as mean ± SEM of the replicates. The error in all cases is considerable, giving overlap between signal traces from consecutive concentrations of CJ-21058 or hit compounds. This error is due in part to the sensitivity of the signal amplitude (maximum possible NanoBiT luciferase brightness) to inhibitor, as mentioned above, as well as small differences in experimental setup and is a common occurrence in such assays (Allen *et al.*, 2020). To mitigate against this, the same batch of PLs were used for all experiments.

However, to obtain useful quantitative data, each signal trace should be normalised by its respective NanoBiT brightness. This was achieved by fitting the background to a single exponential and not only subtracting tabulated background from post-ATP signal (as seen in Figure 4.1b) but also normalising signal by the respective background amplitude. Additionally, the injection carried out by the platereader takes longer than each read step, introducing error to the measured time post-injection of ATP. For accurate calculation of lag, a time correction factor must be calculated for each well based on its position.

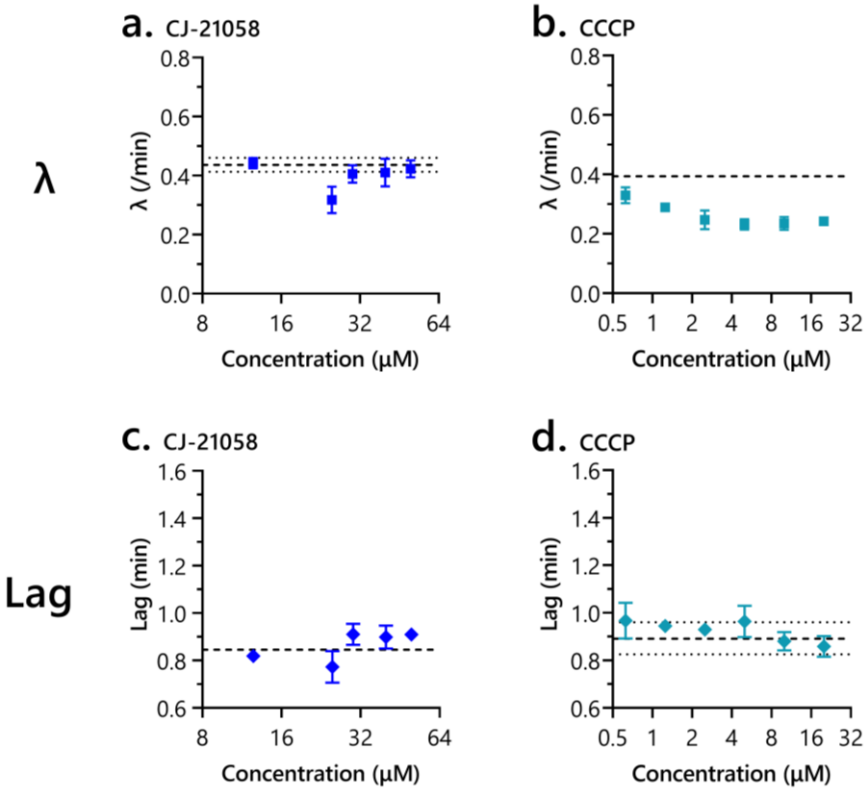


**Figure 4.4 Fits of control activity on *in vitro* NanoBiT**
Signal traces shown in Figure 4.2 were normalised by background amplitude, time-corrected and fit to the equation shown in Figure 4.1. Parameters λ (**a.**, **b.**) and lag (**c.**, **d.**) are shown over different concentrations of each control compound: CJ-21058 (**a.**, **c.**) and CCCP (**b.**, **d.**). Data from 3 – 6 technical replicates are shown as mean ± SEM. Data from untreated controls are shown as dashed (mean) and dotted (± SEM) black lines.

These corrections substantially decreased error for each of the three parameters. However, error in amplitude remained too great for confident assessment of dose response (Appendix 2). For CJ-21058, neither apparent rate (λ) nor lag values (Figure 4.4a and c, respectively) deviate appreciably from those of the untreated control at any concentration of inhibitor. The λ resulting from 25 μM treatment is lower than all other concentrations tested, consistent with its raw luminescence trace (Figure 4.2a). Overall, these data indicate that CJ-21058 does not affect the kinetics of Sec-mediated transport in this system in a dose-dependent manner. Surprisingly, given the lack of PMF in PLs, CCCP treatment results in a dose-dependent decrease in λ from approximately 0.39 /min to approximately 0.23 /min for CCCP concentrations of 6.25 μM or greater (Figure 4.4b). Contrary to the hypothesis, this suggests that CCCP does impact Sec-mediated translocation in PLs, either by decreasing rate or increasing probability of stalling or failure. Lag does not increase with CCCP

concentration, suggesting CCCP does not impact translocation rate (Figure 4.4d). To assess whether this inhibitory effect of CCCP is related to dissipation of the PMF, *in vitro* NanoBiT was performed with ionophores valinomycin and nigericin. Valinomycin is a potassium ionophore that diminishes the electrical component of PMF and nigericin is an electroneutral antiporter of potassium ions and protons that dissipates the pH component of PMF. When used in combination, their effects on PMF-dependent Sec-mediated translocation mimic those of CCCP (Yamane, Ichihara & Mizushima, 1987). The NanoBiT signal trace was unaffected by valinomycin/ nigericin treatment (Appendix 3). This suggests that the observed effect of CCCP on these assays is unrelated to PMF.

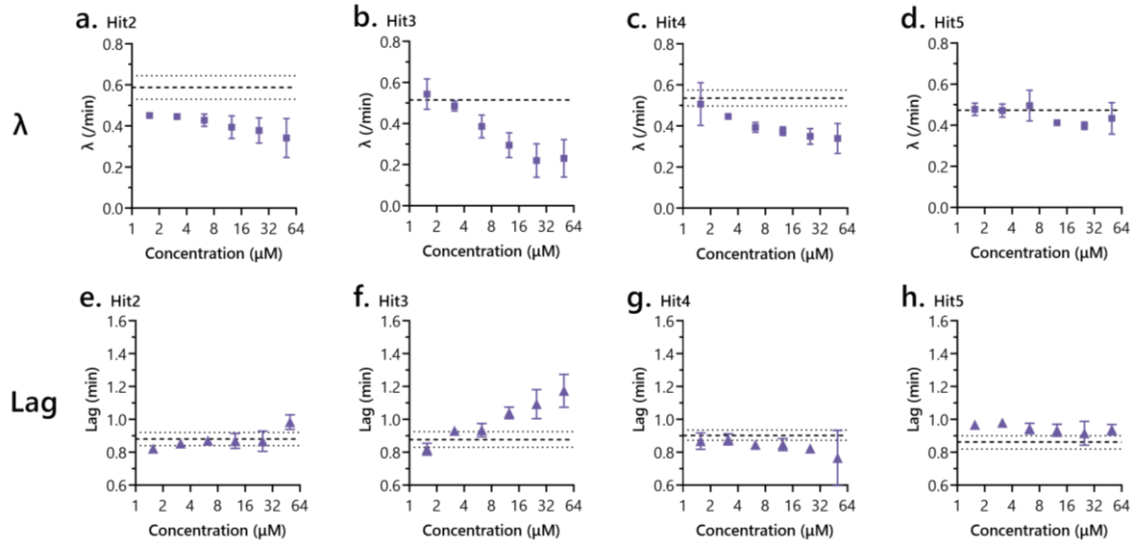


**Figure 4.5 Fits of hit activity on *in vitro* NanoBiT**
Signal traces shown in Figure 4.3 were normalised by background amplitude, time-corrected and fit to the equation shown in Figure 4.1. Parameters λ (**a.**, **b.**, **c.**, **d.**) and lag (**e.**, **f.**, **g.**, **h.**) are shown over different concentrations of each primary hit compound: Hit2 (**a.**, **e.**), Hit3 (**b.**, **f.**), Hit4 (**c.**, **g.**) and Hit5 (**d.**, **h.**). Data from three technical replicates are shown as mean ± SEM. Data from untreated controls are shown as dashed (mean) and dotted (± SEM) black lines.

When comparing λ from untreated controls for each series of experiments (different compounds), that of Hit2 is greater than for the other series. Even when this is considered, there is a noticeable (although small) tendency for λ to decrease with increasing concentrations of Hit2 (Figure 4.5a). Hit4 decreases λ to a similar extent (Figure 4.5c) while treatment with increasing concentrations of Hit3 results in the most dramatic decrease in λ (Figure 4.5b). Treatment with up to 50 μM Hit5 does not give a significant (based on error bars) difference in λ (Figure 4.5d). This suggests that Hit2 – 4 (but not Hit5) either decrease translocation rate or probability of successful translocation in this system. Moreover, there is a clear upwards trend in lag with increasing concentrations of Hit3 (Figure 4.5f); concentrations of 12.5 μM or higher give substantially different lag values compared to the untreated control. By contrast, lag resulting from treatment with up to 50 μM Hit2, 4 or 5 does not deviate considerably from that of untreated controls (Figure 4.5e, g, h). It is therefore likely that Hit3 decreases the rate of translocation, while Hit2 and 4 reduce apparent rate through another mechanism.

## 4.3 Alternative *in vitro* assays for hit validation

The setup for protease protection assays is largely similar to *in vitro* NanoBiT: they require all the same components, except LgBiT and HiBiT (Figure 4.6a). At defined time points after reaction initiation with ATP, samples are taken and treated with proteinase K. Pre-proteins translocated by Sec are protected from proteolysis while untranslocated proteins are degraded (Figure 4.6b). The progress of translocation is monitored by SDS-PAGE against substrate protein, giving traces similar to NanoBiT (Figure 4.6c – e).

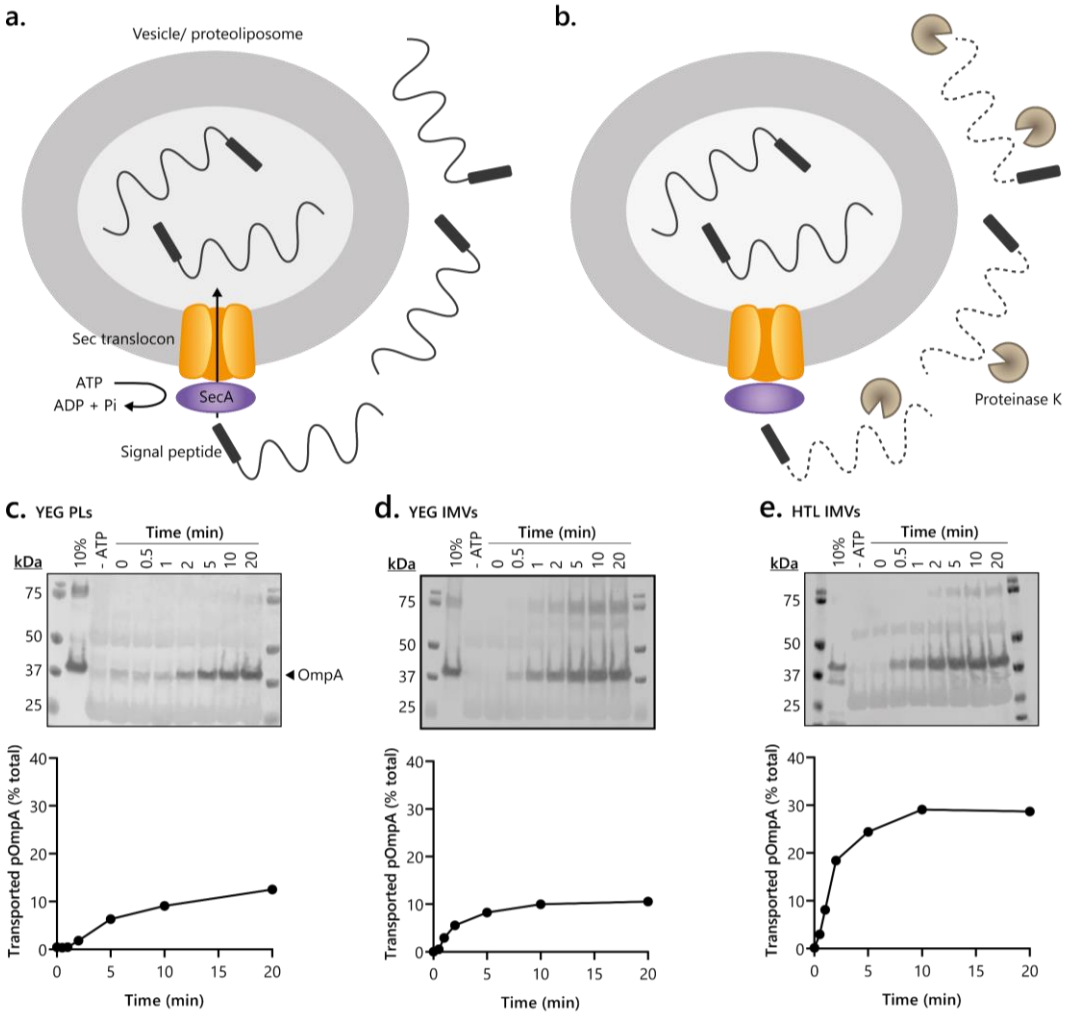


**Figure 4.6 Design of *in vitro* protease protection assays for protein translocation**
**a.** Proteoliposomes or inverted inner membrane vesicles containing the membrane-bound Sec-machinery are combined with purified SecA, agents for regeneration of ATP from ADP and translocation-competent Sec substrate. Upon addition of ATP, SecA drives translocation of substrate from outside to inside the vesicle. **b.** At desired time intervals after initiation, samples of reaction are quenched with buffer (lane 1) or proteinase K. Translocated substrate is protected from proteolysis while untranslocated protein is degraded. Proteins are resolved by immunoblot. **c. – e.** Translocation-competent V5-tagged pOmpA was subjected to protease protection assay in **c.** Proteoliposomes (PLs) containing SecYEG or **d.**, **e.** inner membrane vesicles (IMVs) from bacteria overexpressing **d.** genes encoding SecYEG only or **e.** genes encoding the Sec holotranslocon (HTL). Protease protection over time was assessed by anti-V5 immunoblot and bands corresponding to pOmpA (indicated with arrow) were quantified. Lane 1, 10% of the total pOmpA present in each sample prior to proteinase K treatment (loading control). Lane 2, sample taken from 20 min reaction in the absence of ATP (negative control). For lanes 3 – 9, the percentage of total pOmpA translocated was calculated. Data from one replicate are shown.

Whereas NanoBiT assays were optimised using pSpy as the substrate protein, protease protection assays typically use pre-secretory OmpA (pOmpA). Attachment of a V5 tag to the pOmpA C-terminus allows protease protection to be assessed by V5 immunoblot. Due to constraints on time and reagents, it was not possible to assess the full dose response with each compound with time resolution. Protease protection assays were instead carried out as endpoint experiments. An additional caveat is that only one replicate of each condition could be obtained. However, preliminary results are sufficient to evaluate whether this system is worth pursuing as a secondary assay.

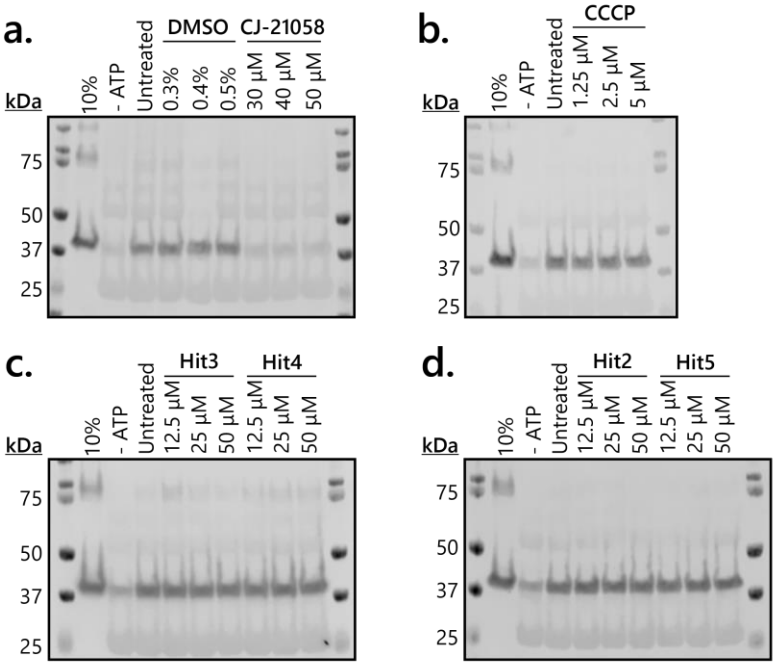


**Figure 4.7 Activity of controls and hits on SecYEG proteoliposomes assessed by *in vitro* protease protection assay**
Proteoliposomes containing SecYEG were combined with purified SecA, ATP regeneration reagents, translocation-competent pOmpA-V5 and **a.** DMSO, CJ-21058, **b.** CCCP, **c.** Hit3, Hit4, **d.** Hit2 or Hit5, as indicated. Reaction was initiated by addition of buffer (lanes 1 and 2) or ATP. After 5 min, samples were quenched with buffer (lane 1) or proteinase K and resolved by immunoblot. Lane 1, 10% of the total pOmpA present in each sample prior to proteinase K treatment (loading control). Lane 2, sample taken from 5 min reaction in the absence of ATP (negative control). Data from one replicate are shown.

SecYEG PLs were the first system to be challenged with inhibitor in protease protection assays. Using time-resolved data of pOmpA protection (Figure 4.6c) it was decided that 5 min was a suitable reaction window. Signal at 5 min is substantially greater than that of the -ATP control, but the signal trace is just starting to plateau at this point. This should give the maximum possible dynamic range while avoiding signal saturation. The highest three concentrations of CJ-21058 used for *in vitro* NanoBiT, encompassing its reported $IC_{50}$ against translocation ATPase *in vitro* (38.7 µM, Sugie *et al.*, 2002), were assessed in this system. All three concentrations of CJ-21058 reduced the degree of pOmpA protection to -ATP levels (Figure 4.7a). The respective concentrations of DMSO had no effect, confirming that this inhibition is specific to CJ-21058 activity.

For CCCP, 5 µM was selected as the highest concentration for protease protection assays. In the primary whole cell assay, 5 µM CCCP gives over 70% inhibition and is the highest concentration that exhibits no activity in counter assay (Figure 3.8). As expected for a system lacking PMF, treatment with up to 5 µM CCCP does not impact protease protection of pOmpA compared to the untreated control (Figure 4.7b). This further supports the suggestion that the sensitivity of *in vitro* NanoBiT assays with pSpy-HiBiT and PLs is related to an off-target activity of CCCP, potentially on the NanoBiT enzyme, rather than its function as a PMF uncoupler.

Hit compounds at 12.5 – 50 µM were also assessed in this system; for all four compounds, this concentration range encompasses or exceeds their $IC_{50}$ in the primary assay. Contrary to NanoBiT assays on YEG PLs, even the highest concentration of each primary hit had a negligeable effect on pOmpA transport into YEG PLs (Figure 4.7c, d).

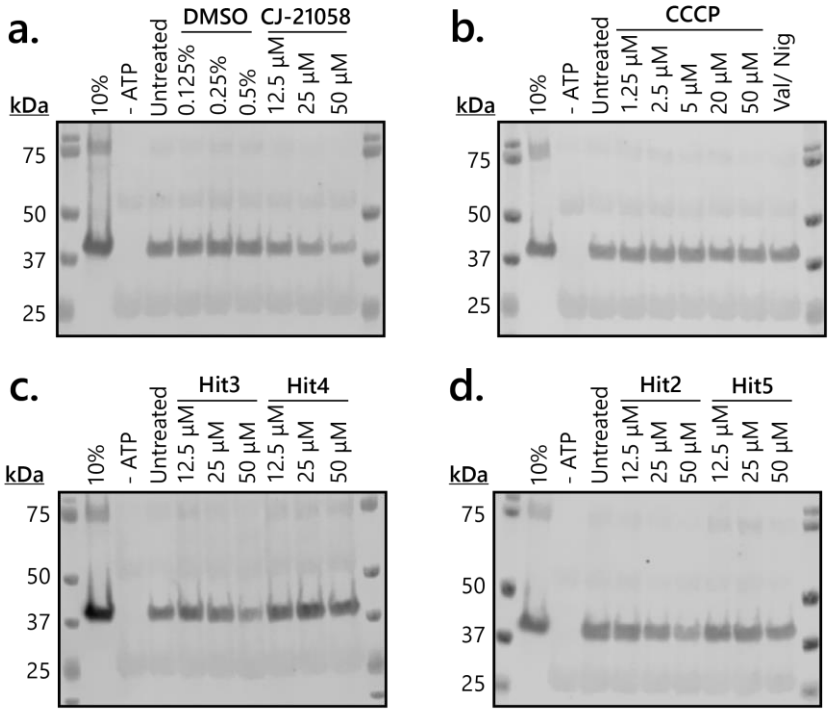


**Figure 4.8 Activity of controls and hits on SecYEG inner membrane vesicles assessed by *in vitro* protease protection assay**
Inverted inner membrane vesicles from bacteria overexpressing SecYEG genes were combined with purified SecA, ATP regeneration reagents, translocation-competent pOmpA-V5 and **a.** DMSO, CJ-21058, **b.** CCCP, valinomycin and nigericin at 1 and 2 µM respectively, **c.** Hit3, Hit4, **d.** Hit 2 or Hit5, as indicated. Reaction was initiated by addition of buffer (lanes 1 and 2) or ATP. After 1 min, samples were quenched with buffer (lane 1) or proteinase K and resolved by immunoblot. Lane 1, 10% of the total pOmpA present in each sample prior to proteinase K treatment (loading control). Lane 2, sample taken from 1 min reaction in the absence of ATP (negative control). Data from one replicate are shown.

Initial experimentation with IMVs from *E. coli* overexpressing *secY*, *E* and *G* – at comparable concentrations of SecYEG (0.28 µM) to YEG PLs (0.23 µM correctly orientated SecYEG) and identical conditions otherwise – did not detect any difference in the amount of pOmpA translocated into a protease-protected environment over 5 min upon CJ-21058 treatment. The apparent rate of pOmpA transport is noticeably faster in YEG IMVs compared to YEG PLs (Figure 4.6c, d). As a

result, for PLs there is a considerable difference between band intensities at 2 and 5 min, but this difference is much smaller for IMVs. Thus, 5 min is not the optimal reaction time for a good signal window when using IMVs. Instead, reactions were quenched after 1 min.

Using a 1 min endpoint, it was found that 50 µM CJ-21058 does noticeably impair translocation of pOmpA (Figure 4.8a). However, the amount of translocated, protease-protected pOmpA is still higher upon 50 µM treatment than in the -ATP control. This suggests that YEG IMVs are less sensitive to CJ-21058 than YEG PLs. Since the same degree of inhibition was observed for YEG PLs treated with 30 and 40 µM CJ-21058 compared to 50 µM (Figure 4.7a), a broader concentration range was tested for IMVs. Some inhibition is seen at 12.5 µM CJ-21058 and the response of YEG IMVs appears dose-dependent. Treatment with respective concentrations of DMSO did not reduce levels of transported pOmpA.

IMVs made from wildtype bacteria contain some ATP synthase. Upon addition of ATP, the reverse action of ATP synthase generates a PMF, which stimulates the Sec-machinery. Previous NanoBiT studies found that YEG IMVs translocating pSpy-HiBiT are sensitive to uncouplers such as valinomycin and nigericin (Allen *et al.*, 2022). However, neither a combination of valinomycin and nigericin (at 1 and 2 µM respectively, the same concentrations as in previous studies) nor 50 µM CCCP visibly inhibit pOmpA transport measured by protease protection in YEG IMVs (Figure 4.8b). This may reflect a lower PMF requirement for pOmpA transport compared to pSpy, or the decreased sensitivity of endpoint protease protection assays compared to *in vitro* NanoBiT.

Intriguingly, treatment of YEG IMVs with 50 µM Hit2 or 3 reduces levels of pOmpA detected following protease treatment, suggesting that these compounds inhibit translocation (Figure 4.8c, d). This is consistent with the observed decreases in λ and/ or increases in lag observed in NanoBiT assays with either compound. Lower concentrations of these compounds have a negligeable effect on observed pOmpA band intensity. Translocation by YEG IMVs appears unaffected by treatment with up to 50 µM Hit4 or 5 under these conditions.

IMVs from *E. coli* overexpressing *secY, E, G, D* and *F* alongside *yajC* and *yidC* (HTL IMVs) give a fast apparent rate and short lag when assessed for pOmpA protection over time, similarly to YEG IMVs (Figure 4.6e). When translocated pOmpA is normalised by the loading control, the amplitude of HTL IMV transport is over twice that of YEG transport. For protease protection experiments, an equivalent final concentration of SecYEG (0.28 µM) was used in reactions with YEG and HTL IMVs. However, active HTL is known to carry one copy of SecYEG, while SecYEG in the absence of auxiliary factors is expected to function in dimers (Schulze *et al.*, 2014). The difference in amplitude observed in the work presented here is consistent with this stoichiometry. However, more replicates are needed to confirm whether this is a real result or loading error.

As with YEG IMVs, translocation reactions with HTL IMVs were quenched after 1 min. Lower levels of translocated pOmpA are seen in HTL IMVs treated with CJ-21058 compared to the untreated control (Figure 4.9a). These IMVs present a similar dose response to CJ-21058 to YEG IMVs and are insensitive to DMSO. Unlike YEG IMVs, however, HTL IMVs are sensitive to inhibition by CCCP

in a dose-dependent manner (Figure 4.9b). Treatment with 20 µM or more CCCP reduces pOmpA protection in HTL IMVs to -ATP levels, suggesting translocation is completely inhibited under these conditions. Valinomycin and nigericin in combination has a similar effect, confirming that pOmpA transport by HTL IMVs is sensitive to PMF uncouplers.

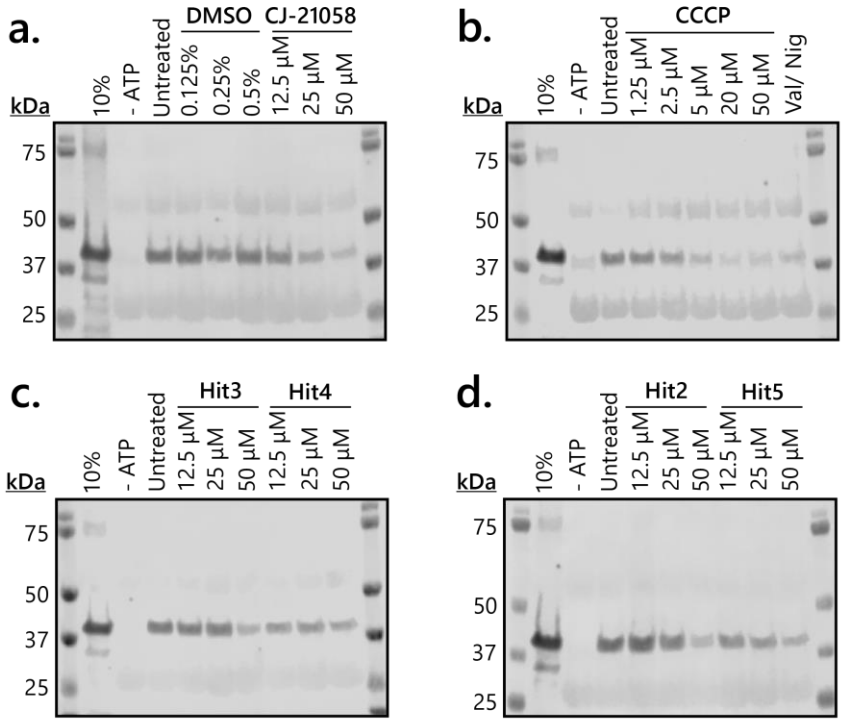


**Figure 4.9 Activity of controls and hits on holotranslocon inner membrane vesicles assessed by *in vitro* protease protection assay**
Inverted inner membrane vesicles from bacteria overexpressing Sec holotranslocon genes were combined with purified SecA, ATP regeneration reagents, translocation-competent pOmpA-V5 and **a.** DMSO, CJ-21058, **b.** CCCP, valinomycin and nigericin at 1 and 2 µM respectively, **c.** Hit3, Hit4, **d.** Hit 2 or Hit5, as indicated. Reaction was initiated by addition of buffer (lanes 1 and 2) or ATP. After 1 min, samples were quenched with buffer (lane 1) or proteinase K and resolved by immunoblot. Lane 1, 10% of the total pOmpA present in each sample prior to proteinase K treatment (loading control). Lane 2, sample taken from 1 min reaction in the absence of ATP (negative control). Data from one replicate are shown.

On the other hand, YEG and HTL IMVs exhibit comparable levels of translocation inhibition upon treatment with Hit2 and 3 (Figure 4.9c, d). Unlike YEG IMVs, HTL IMVs may also be sensitive to Hit4 and 5 – all three tested concentrations of these compounds yield lower pOmpA band intensities in immunoblot. For Hit5 but not Hit4, a slight dose-dependent decrease in detected pOmpA levels is seen. While both IMV preparations give a response to Hit2 and 3, improving confidence that the observed effects are real, more experiments are needed, especially for Hit4 and 5, to confidently conclude whether any of these compounds inhibit transport measured by *in vitro* protease protection assays.

## 4.4 Effect of hit compounds on growth of *E. coli*

Given that hits were identified in a cell-based assay, it is known that they can access their target in intact cells. However, this does not always translate into bacteriostatic or bactericidal activity.

Sufficient amounts of compound would need to accumulate in bacterial cells to inhibit target activity to sufficiently low levels to affect viability.

Treatment with 400 µM CJ-21058 inhibits transport of pSpy-HiBiT in BL21(DE3) to 15.2±3.5% that of the untreated control (mean ± SEM, Figure 3.8). However, 400 µM CJ-21058 does not inhibit growth of *E. coli* MC4100 (Table 4.2). This corroborates earlier characterisation of this inhibitor, where it was found to inhibit growth of some Gram-positive bacteria but not Gram-negatives (Sugie *et al.*, 2002). The cause of *E. coli* insensitivity to CJ-21058 has not yet been investigated. Here, the MC4100 derivative NR698 was also challenged with compounds of interest. NR698 harbours an *lptD4213* mutation and is defective in its outer membrane permeability barrier (Ruiz *et al.*, 2005). This strain was substantially more susceptible to CJ-21058, with a MIC of 3.1 µM, consistent with failure of CJ-21058 to cross the Gram-negative outer membrane.

The MIC of CCCP could be determined for both *E. coli* strains (Table 4.2). As expected for a compound that enters cells by diffusion through lipid bilayers, CCCP has a lower MIC against the more outer membrane permeable NR698 (6.3 µM) compared to MC4100 (78.2 µM). The CCCP concentration required for killing of MC4100 is marginally higher than that required for maximal inhibition of pSpy-HiBiT translocation in BL21(DE3) cells (50 µM, 0.012±0.003 signal compared to the untreated control, Figure 3.8).

**Table 4.2 Minimum inhibitory concentrations of translocation inhibitors for *E. coli***

| Strain | Compound | MIC (µM) |
|---|---|---|
| MC4100 | CJ-21058 | >400 |
| | CCCP | 78.2 |
| | Hit2 | >200 |
| | Hit3 | >200 |
| | Hit4 | >200 |
| | Hit5 | >200 |
| NR698 | CJ-21058 | 3.1 |
| | CCCP | 6.3 |
| | Hit2 | >200 |
| | Hit3 | >200 |
| | Hit4 | >200 |
| | Hit5 | >200 |

Data from one replicate are shown.
MIC, minimum inhibitory concentration
NR698 (MC4100 *lpt*D4213) outer membrane permeable

The MICs of primary hits were too high to be determined (Table 4.2). Both MC4100 and NR698 grew to a similar $OD_{600}$ when left untreated or treated with up to 200 µM of Hit2 – 5. Beyond 200 µM, most hit compounds have limited solubility in water. Culturing MC4100 in minimal media – to

upregulate outer membrane porin levels – did not reduce MIC to detectable levels. This suggests that the activity of these compounds against *E. coli* cannot be increased by increasing permeability of the outer membrane lipid bilayer or porin overproduction. In primary assays, 200 µM Hit2, 3, 4 and 5 inhibit periplasmic accumulation of pSpy-HiBiT to 4.5±2.2, 10.8±1.3, 12.0±5.8 and 9.3±3.9 % compared to untreated controls, respectively (Figure 3.12, Figure 3.13, Figure 3.14). Thus, for all hit compounds, inhibition at 200 µM is greater than that of 400 µM CJ-21058 but less than that of 50 µM CCCP. This suggests there may be a threshold level of translocation below which bacterial growth is affected. Alternatively, hit compounds may be unstable under culture conditions for extended periods of time.

## 4.5 Discussion

Past attempts at finding potential inhibitors targeting the Sec-machinery demonstrate the utility of secondary assays for validating screen hits (Alksne *et al.*, 2000; Moir *et al.*, 2011; Crowther *et al.*, 2015; Bonnett *et al.*, 2016; Hamed *et al.*, 2021). To study the target pathway more directly, *in vitro* secondary assays are adopted. The time-resolution of *in vitro* NanoBiT assays allows acquisition of large quantities of data with minimal effort (Pereira *et al.*, 2019; Allen *et al.*, 2020, 2022). However, unlike the whole cell NanoBiT assay used for primary screens, the reconstituted system is highly sensitive to off-target effects resulting in substantial noise. Some noise could be mitigated by data correction and normalisation, but this is a complicated and laborious process. Also, to confidently deselect compounds that act on the reporter enzyme rather than the desired target, it is preferable to have secondary assays that rely on different reporters than the primary assay. For this reason, protease protection assays were evaluated as an alternative. As this system uses a different Sec substrate compared to whole cell and *in vitro* NanoBiT, it can also be used to help determine the substrate specificity of putative inhibitors.

The responses of different assay systems to known and putative Sec inhibitors are summarised in Table 4.3. From *in vitro* NanoBiT data, plots of λ and lag against CJ-21058 concentration suggest that pSpy-HiBiT transport into PLs is insensitive to this inhibitor. By contrast, when assessed by protease protection, CJ-21058 treatment drastically inhibits pOmpA transport into PLs (Table 4.3). This discrepancy may reflect the different Sec substrates used, suggesting that pOmpA is more SecA-dependent for transport than pSpy. However, it is possible that CJ-21058 treatment affected the total amount of pSpy-HiBiT translocated, proportional to amplitude of NanoBiT signal, but noise in the data impeded assessment of this. YEG PLs used for protease protection assays also show greater sensitivity to CJ-21058 treatment than either type of IMV. The presence of cardiolipin in the latter, known to stimulate SecA ATPase activity (Gold *et al.*, 2010), may dampen the effects of CJ-21058.

HTL IMVs present with higher sensitivity to uncouplers of transmembrane proton gradients than their YEG counterpart (Table 4.3). This is consistent with studies of bacteriorhodopsin PLs where HTL had a greater dependence on the PMF for optimal translocation compared to SecYEG alone (Schulze *et al.*, 2014). Under the experimental conditions explored here, pOmpA transport by YEG

IMVs is not inhibited by uncoupling ionophores. This contradicts previous studies of pOmpA transport in bacteriorhodopsin PLs with SecYE(G) (Brundage *et al.*, 1990; Schulze *et al.*, 2014) and *in vitro* NanoBiT studies of pSpy-HiBiT transport in YEG IMV preparations equivalent to those used in this work (Allen *et al.*, 2022). PMF generation in IMVs is comparable to that in whole cells (Allen *et al.*, 2022). In such IMVs, where ATP synthase is not overexpressed, PMF generation will likely be less than that of bacteriorhodopsin PLs. The improved sensitivity of *in vitro* NanoBiT compared to protease protection may be necessary to detect PMF-dependent differences in translocation in YEG IMVs.

**Table 4.3 Summary of inhibitor activities against translocation *in vitro***

| | | Activity | | | |
|---|---|---|---|---|---|
| | **$IC_{50}$ in primary** | pSpy NanoBiT | pOmpA protease protection | | |
| **Inhibitor** | **assay (μM)** | YEG PLs | YEG PLs | YEG IMVs | HTL IMVs |
| CJ-21058 | 227.1 | - | ++ [c] | + | + |
| CCCP | 1.82 | + [a] | - | - | + |
| Hit2 | 5.23 | + | - | + | + |
| Hit3 | 6.79 | ++ [b] | - | + | + |
| Hit4 | 16.1 | + | - | - | ? [d] |
| Hit5 | 12.2 | - | - | - | ? [d] |

Inhibitor activity: -, not active; +, active; ++, very active; ?, possibly active/ data inconclusive.
[a] This is likely an off-target effect, unrelated to its uncoupling ionophore activity.
[b] Hit3 both reduced rate and increased lag of translocation in a dose-dependent manner, whereas other active inhibitors only reduced λ.
[c] CJ-21058 (50 μM) inhibited translocation of pOmpA to a greater extent in YEG PLs than either type of IMVs.
[d] Translocation into HTL IMVs is reduced at all tested concentrations of Hit4 and 5 compared to untreated control; more experiments are needed to confirm a dose-dependent response.

The comparable responses of relatively PMF-independent YEG IMVs and PMF-dependent HTL IMVs to Hit2 and 3 suggest that these compounds are not uncouplers and do not target auxiliary Sec proteins (Table 4.3). In addition, both Hit2 and 3 are active on systems using distinct pre-secretory proteins: globular, periplasmic pSpy and β-barrel outer membrane protein OmpA. This indicates that they are not substrate specific. Although IMVs translocating pOmpA are inhibited by Hit2 and 3, YEG PLs do not display sensitivity to these inhibitors under the conditions tested. Hit4 is also active against pSpy *in vitro* NanoBiT, however pOmpA protease protection assays on this compound (and Hit5) are inconclusive. YEG PLs/ IMVs transporting pOmpA are insensitive to Hit4 and 5 while HTL IMVs may be sensitive to these compounds. The limited range of concentrations and endpoint setup of the protease protection assays mean that the effects of compounds on translocation may have been missed. It is therefore not possible to conclude that any compound is entirely inactive on any protease protection system. To rule out inactive compounds with greater certainty, transport of pOmpA in each sample should be monitored over time and using a greater range of concentrations.

Because multiple factors vary between YEG PLs, YEG IMVs and HTL IMVs, it is not possible to draw conclusions on the precise mode of action of hits by comparison of transport assays alone. Additional secondary assays that would be useful for this project include assays for membrane integrity and membrane potential, *in vitro* ATPase assays on SecA and binding assays such as fluorescence resonance energy transfer. Membrane-active compounds (including but not limited to uncouplers) often present as hits in screens for Sec inhibitors (Alksne *et al.*, 2000; Segers & Anné, 2011). Fluorescent membrane potential indicator dyes such as diethyloxacarbocyanine (Novo *et al.*, 1999) can be used to determine whether compounds are membrane-active. Whereas the above *in vitro* assays for specific translocation inhibitors are laborious and require purified reaction components, fluorescent dye-based testing of membrane potential can be performed at high throughput in whole bacteria. Therefore, it would be practical to filter out membrane-active agents using the PMF indicator dyes before moving on to *in vitro* assays. Following confirmation of translocation inhibition *in vitro*, validated compounds should then be assessed in a more target-specific manner by SecA ATPase assays or binding studies with particular Sec components.

To determine whether hits are promising antibiotic leads, MICs were assessed by broth microdilution against two laboratory strains of *E. coli*: MC4100 and the outer membrane-permeable NR698. None of the primary hits identified by the NanoBiT-based screen inhibit growth of either strain. Hit compounds inhibit translocation to as low as 4.5±2.2% maximum capacity in primary whole cell NanoBiT assays against whole BL21(DE3) cells. Confirming translocation inhibition in MC4100 and NR698 by whole cell NanoBiT would be useful. The different susceptibilities of MC4100 and NR698 to these compounds may be detectable using more sensitive growth assays, such as calculation of log-phase growth rates (Crowther *et al.*, 2015). Alternatively, MICs could be determined in environments that better mimic conditions of infection. For example, *tatC* deletion mutants of *P. aeruginosa* grow under laboratory conditions but not under oxygen restriction or increased osmolarity, conditions often seen in cystic fibrosis-associated mucoid infection (Ochsner *et al.*, 2002). To fully understand why hit compounds lack antibacterial activity, it is important to confirm specific Sec inhibitory activity and stability in overnight culture. Nevertheless, target accessibility is unlikely to be the major limiting determinant of antibacterial activity for these hits. Crowther *et al.* (2015) similarly found a potent hit of translocation *in vivo*, but found that the growth rate of *E. coli* treated with the compound only begins to decline at concentrations at which the compound has maximal activity in the primary assay. It is hypothesised that almost complete inhibition of the Sec-machinery is needed for inhibition of growth.

If this is the case, then the hunt for a Sec inhibitor sufficiently potent for use as a standalone antibiotic will be challenging. Previous screens against SecA or the Sec-machinery as a whole often employ far larger compound libraries than used here – up to 100 times more compounds (De Waelheyns *et al.*, 2015; Hamed *et al.*, 2021). This increases the possibility of discovering compounds with strong activity against translocation. Additionally, screens may be used in conjunction with hit expansion studies, including analog searches and SARS development for improved activity (Crowther *et al.*, 2015; Bonnett *et al.*, 2016; Hamed *et al.*, 2021). Conversely, inhibitors of Sec-mediated translocation may need a secondary mechanism of bacterial killing to be

promising antibiotic leads. Indeed, the most promising translocation inhibitor currently in antibiotic development – signal peptidase I inhibitor arylomycin – exhibits antibacterial activity through two mechanisms. As well as reducing translocation of essential extracytoplasmic proteins, arylomycins cause the accumulation of pro-lipoproteins in the cytoplasmic membrane, thereby compromising membrane structure (Smith & Romesberg, 2012).

However, Sec inhibitors may still be clinically useful even if they have high MICs under laboratory conditions. Unlike existing classes of antibiotic, sub-MIC arylomycin treatment inhibits translocation-dependent virulence mechanisms such as flagellum biogenesis, biofilm formation, motility and horizontal gene transfer mediated by type IV secretion systems (Walsh et al., 2019). Arylomycins also disrupt the function of extracytoplasmic antibiotic resistance determinants (Therien *et al.*, 2012). This illustrates how, alongside potential bactericidal and bacteriostatic activities, inhibitors of protein translocation can (re)-potentiate existing antibiotics or disarm pathogens to improve clearance by the immune system. In the absence of antibacterial killing, compounds showing up as hits in screens for Sec inhibitors could also be pursued as antibiotic adjuvants or anti-virulence drugs.

# Chapter 5 Role of protein translocation in β-lactamase mediated resistance

## 5.1 Introduction

Antibiotic adjuvants, also known as resistance breakers or antibiotic potentiators, have limited or no antibacterial activity on their own. However, when used alongside antibiotics, they either block mechanisms of resistance to the drug or potentiate the antibacterial activity of the drug. Well-explored antibiotic adjuvant strategies include efflux pump inhibitors and outer membrane permeabilisers. By far the most clinically successful type of antibiotic adjuvant is β-lactamase inhibitors. However, as discussed in more depth below, the non-essential, highly mutable single enzyme target of these inhibitors has enabled bacterial evolution to overcome their activity. The relative immutability of the strongly conserved Sec-machinery offers a more robust target for antibiotic adjuvant approaches. The role of Sec in biogenesis of efflux pumps, outer membranes and β-lactamases points to a potential application of Sec inhibitors as adjuvants of a broad range of antibiotics.

This chapter focuses on the possibility of inhibiting Sec-mediated translocation of β-lactamases as an approach to (re-)potentiate and prolong the lifespan of β-lactam antibiotics. The success of β-lactamase inhibitors has hinged on extensive studies on the structure, biochemistry and mechanism of action of their enzyme target (reviewed in Tooke *et al.*, 2019). Conversely, knowledge on the mechanisms of β-lactamase translocation is lacking.

### 5.1.1 The β-lactam arms race

Since the discovery of the first β-lactam antibiotic, benzylpenicillin, as a natural product from *Penicillium* species in 1929 (Fleming, 1929) and its first use in a clinical setting in the 1940s (Tooke *et al.*, 2019), the β-lactam class of drugs has played a central role in medicine. The β-lactams are attributed with more prescriptions and sales than any other antibiotic class (Klein *et al.*, 2018a). All four β-lactam subclasses feature on the WHO list of critically important antibiotics in human medicine (Collignon *et al.*, 2016). Their position at the forefront of antibiotic chemotherapy, even after over 70 years of clinical use, has been put down to their potency, broad spectrum of activity and low toxicity in humans (King, Sobhanifar & Strynadka, 2016).

Besides the penicillins, three other subclasses of β-lactam have been uncovered, each having a natural origin: cephalosporins (Newton & Abraham, 1954), the last resort antibiotics carbapenems (Rolinson, 1976) and monobactams (Sykes *et al.*, 1981; Imada *et al.*, 1981). Common to these four classes of β-lactam is the eponymous four-membered cyclic amide ring. In penicillins, cephalosporins and carbapenems, the β-lactam ring forms part of a bicyclic structure, while monobactams are monocyclic. Over the years, chemical modification of these core structures has yielded semi-synthetic β-lactam derivatives with altered uptake, potency, spectrum of activity and ability to evade resistance (Tooke *et al.*, 2019).

### *5.1.1.1 Mechanisms of β-lactam action and β-lactam resistance*

β-lactams target bacterial cell wall synthesis and maintenance. The cell wall, found in the periplasm, is composed of a mesh-like peptidoglycan network. Peptidoglycan comprises polysaccharide chains with short peptide branches. Crosslinking between peptides from adjacent chains by transamidation forms the peptidoglycan network. This is mediated by peptidoglycan transpeptidase/ transamidase (Izaki, Matsuhashi & Strominger, 1966), also known as penicillin binding protein (PBP). A PBP attacks the terminal two residues (D-alanyl-D-alanine) of the "donor" chain, releasing one D-alanine residue and forming an acyl-enzyme intermediate. A neighbouring "acceptor" chain attacks the intermediate, forming a covalent link between the two peptidoglycan chains (Tipper & Strominger, 1965; Sauvage *et al.*, 2008). The β-lactam ring structure resembles the D-alanyl-D-alanine moiety of the donor chain. Thus, β-lactams react with the PBP transamidase active site. The β-lactam ring opens up and irreversibly acylates the enzyme (Tipper & Strominger, 1965; Tooke *et al.*, 2019). This inhibits further transamidation, compromising the structural integrity of the peptidoglycan cell wall and eliciting bacterial cell death (Figure 5.1).

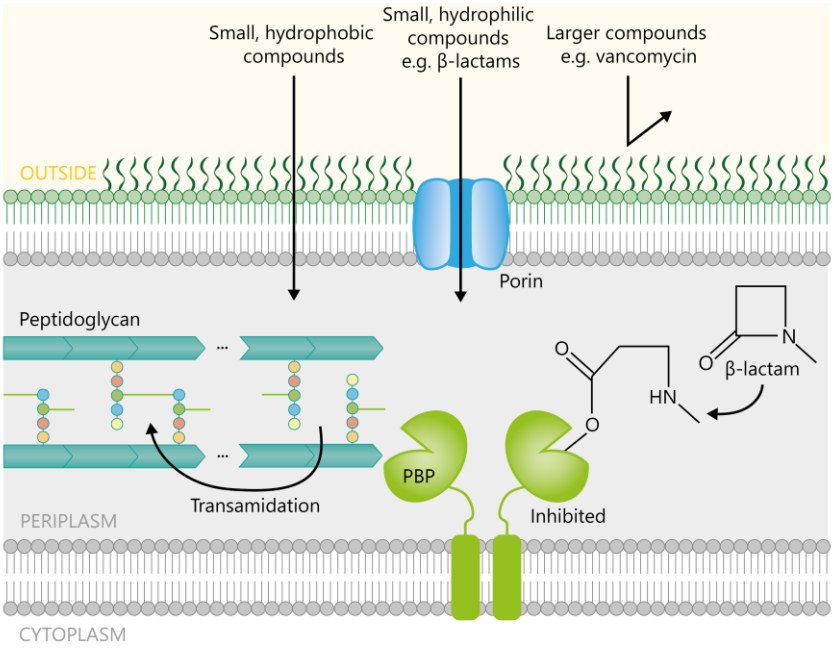


**Figure 5.1 Entry and mechanism of action of β-lactams in Gram-negative bacteria**
Straight, black arrows indicate the path of entry of different types of antibiotics. Once in the periplasmic space, β-lactams bind and irreversibly acylate penicillin binding proteins (PBPs) that catalyse the transamidation of adjacent peptidoglycan strands (indicated by curved arrows).

This extracytoplasmic target is a major advantage of β-lactams; they do not need to cross the cytoplasmic membrane to function. For this reason, β-lactams are some of the few antimicrobials that can be deployed against both Gram-positive and Gram-negative bacteria. Despite their initially broad-spectrum activity, the β-lactams now face diverse bacterial mechanisms of resistance (Figure 5.2). The mechanisms adopted differ between Gram-positive and -negative bacteria. Often, a combination of these mechanisms interplay to produce a resistant phenotype.

Gram-positive strains including MRSA, penicillin-resistant *S. pneumoniae* and multi-drug resistant *C. difficile* were the first to emerge as a β-lactam resistance threat (Fair & Tor, 2014). Often, Gram-positive strains exhibit β-lactam resistance through acquisition of modified PBP genes (Figure 5.2). For example, MRSA possesses a *mecA* gene that encodes a PBP with reduced reactivity with β-lactams (Hartman & Tomasz, 1984; Matsuhashi *et al.*, 1986). Up until recently, antibiotic development has focused on Gram-positive bacteria. However, Gram-negatives have emerged as a threat, now ranking higher than MRSA on the WHO global priority pathogens list (Tacconelli *et al.*, 2018; Figure 1.1). These strains may adopt any of the β-lactam resistance mechanisms shown in Figure 5.2. However, the primary mechanism of β-lactam resistance in Gram-negative bacteria is the deployment of β-lactamases (King, Sobhanifar & Strynadka, 2016).

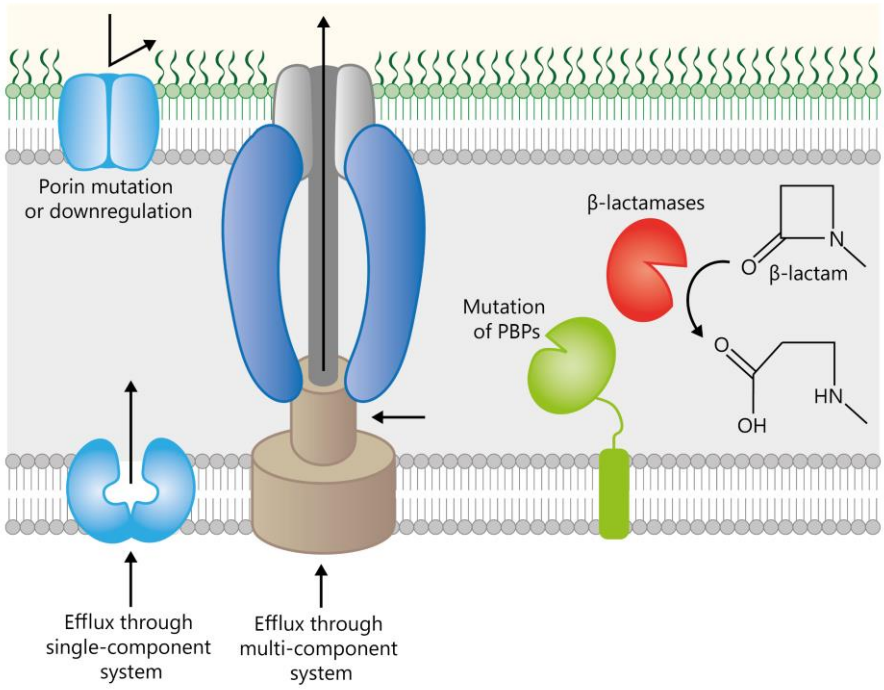


**Figure 5.2 Mechanisms of β-lactam resistance in Gram-negative bacteria**
Top left, the porins through which β-lactams enter the cell may be downregulated or mutated to restrict entry as indicated by the straight, black arrow. Bottom left, production of single-component and multi-component efflux systems allows bacteria to expel antibiotics from the cell (direction of efflux shown by black arrows). Right, bacteria may acquire mutant penicillin binding proteins (PBPs) that no longer recognise and react with β-lactams, or β-lactamase enzymes that bind β-lactams, open the β-lactam ring and can release the inactivated drug and regenerate active enzyme (indicated by curved arrow).

### *5.1.1.2 β-lactamases*

The β-lactamases are enzymes that hydrolyse the β-lactam ring (Figure 5.2). Shortly after the discovery of the first β-lactam benzylpencillin, and before its introduction to clinical use, a β-lactamase capable of its inactivation was discovered (Abraham & Chain, 1940). The frequent use (and misuse) of β-lactams has driven the evolution and dissemination of β-lactamases; there are now over 4000 such enzymes, encoded by homologous but diverse genes and found in many different microbial communities (Naas *et al.*, 2017). Together, the β-lactamases can inactivate all β-lactam drugs currently approved for use in the clinic (King, Sobhanifar & Strynadka, 2016; Naas

*et al.*, 2017). β-lactamases may be carried on bacterial chromosomes but most clinically relevant enzymes are found on mobile DNA elements, which facilitate dissemination and often carry additional resistance factors for other antimicrobial classes (Bush & Bradford, 2020).

Two systems for β-lactamase classification exist: molecular classification based on protein sequence (Ambler, 1980; Jaurin & Grundström, 1981; Ouellette, Bissonnette & Roy, 1987; Philippon *et al.*, 2019) and functional classification based on substrate and inhibitor profiles (Bush, Jacoby & Medeiros, 1995; Bush & Jacoby, 2010). There are four molecular classes of β-lactamase: A, B, C and D. Classes A, C and D are serine-β-lactamases (SBLs) that utilise a catalytic serine, while class B are metallo-β-lactamases (MBLs) with a zinc centre.

Many important Gram-negative bacteria carry chromosomal *ampC* genes encoding a class C SBL. AmpC is capable of hydrolysing penicillins and first generation cephalosporins (Bush & Jacoby, 2010; Tooke *et al.*, 2019). Extended-spectrum β-lactamases (ESBLs), including members of the class A TEM, SHV and CTX-M families and class D OXA family, later emerged. These hydrolyse later generation cephalosporins. Dissemination of ESBLs drove up the use of carbapenems, which in turn led to the spread of carbapenemases (Tooke *et al.*, 2019; Bush & Bradford, 2020). These include the class A SBLs of the KPC family (Yigit *et al.*, 2001) and the MBLs, namely the IMP (Osano *et al.*, 1994; Laraki *et al.*, 1999), VIM (Lauretti *et al.*, 1999) and NDM (Yong *et al.*, 2009; Li *et al.*, 2013) families. KPCs can degrade all β-lactam subclasses and MBLs can break down all β-lactams except monobactams (Tooke *et al.*, 2019; Bush & Bradford, 2020). Since carbapenems are often used as a last resort antibiotic, the dissemination of carbapenemases is a particularly pressing concern. Infections with carbapenem-resistant Enterobacteriaceae have been associated with mortality rates as high as 71% (Friedman, Temkin & Carmeli, 2016).

Alongside use of different subclasses of β-lactam or development of semi-synthetic derivatives, a major approach against β-lactamase-mediated resistance is the administration of β-lactams alongside β-lactamase inhibitors (Bush & Fisher, 2011; King, Sobhanifar & Strynadka, 2016; Tooke *et al.*, 2019). However, broad spectrum inhibitor development is difficult to achieve. For example, the inhibitors sulbactam, clavulanate and tazobactam are β-lactam-based inhibitors developed to target class A β-lactamases. They have no activity against class A carbapenemases like KPCs and limited activity against other classes (Bush & Bradford, 2016). Avibactam, a bridged diazabicyclo[3.2.1]octanone (DBO) non-β-lactam β-lactamase inhibitor, is also approved for clinical use, having shown activity against class A, C and some class D SBLs including the KPCs (Tuon, Rocha & Formigoni-Pinto, 2018). Despite the recent introduction of DBO inhibitors to the clinic, KPC and AmpC variants with reduced susceptibility have been generated in the laboratory and some clinical isolates have been found possessing DBO-resistant KPC variants (Tooke *et al.*, 2019).

Of major concern is the lack of inhibitors against MBLs in or close to clinical use. To make matters worse, evidence has arisen that MBLs may degrade DBOs (Tooke *et al.*, 2019). Attempts at MBL inhibitor discovery include compounds that displace or chelate zinc active site ions and compounds that bind the active site (Tooke *et al.*, 2019). The most promising class of MBL inhibitor is the bicyclic boronates that mimic a tetrahedral oxyanion intermediate of hydrolysis (Brem *et al.*, 2016).

However, their spectrum of activity may not even cover all MBLs. For example, the subclass B3 enzyme L1 is not inhibited by bicyclic boronates (Calvopiña *et al.*, 2017).

The divergence of not only the molecular classes of β-lactamases, but the subclasses and families within them, makes it difficult to track which combinations of drug and inhibitor will work for a given enzyme. This issue is exacerbated by the fact that bacteria can carry multiple β-lactamases with complementary substrate and inhibitor profiles. In a particularly alarming case, a clinical isolate was found carrying at least 8 different β-lactamase genes (Moland *et al.*, 2007; King, Sobhanifar & Strynadka, 2016). Given the limitations of mechanism-based inhibitor discovery, focus has recently shifted to understanding and targeting β-lactamase biogenesis.

### 5.1.2 A new paradigm: Targeting β-lactamase translocation

In both Gram-positive and -negative bacteria, the PBPs that build the peptidoglycan cell wall are situated on the extracytoplasmic side of the cytoplasmic membrane. As a result, β-lactamases must also exit the cytoplasm, where they can bind β-lactam antibiotics in the PBP enzymes' stead. For full activity, β-lactamases from all classes require disulfide bridges (Furniss *et al.*, 2021). Disulfide bridge formation only occurs in the oxidising conditions of the periplasm. The MBLs require acquisition of one or more zinc ions for catalytic activity and stability; this is not favoured in the relatively zinc-depleted cytoplasm (Morán-Barrio, Limansky & Viale, 2009). An essential step of β-lactamase biogenesis is therefore translocation across the cytoplasmic membrane.

Mobilisation of β-lactamase genes allowed their spread by horizontal gene transfer between diverse bacterial hosts, but different β-lactamases have different host ranges. Their dissemination and subsequent evolution are largely dictated by their compatibility with host machinery (Socha, Chen & Tokuriki, 2019). To confer a β-lactam resistance phenotype, newly acquired β-lactamases need to be present in the correct subcellular location at a high enough concentration. This depends on gene copy number and efficiency of transcription, translation, folding and translocation of the resulting protein (Bharathwaj *et al.*, 2021). However, these processes rely on host machineries that did not co-evolve with the newly acquired gene. Failure to translocate nascent β-lactamase, resulting in accumulation of pre-protein, is associated with a high fitness cost (López *et al.*, 2019). The N-terminal SS of β-lactamases has been shown to contribute substantially to their ability to confer resistance to antibiotic or a fitness cost in its absence (López *et al.*, 2019; Zalucki *et al.*, 2020). However, the exact mechanism by which the translocation system of one organism could be incompatible with a SS that evolved in another species is unknown. Both the SBLs and MBLs exhibit low sequence similarity outside of their active site – pairwise amino acid identities for the MBLs are as low as 20%. This is especially true of their N-terminal SSs (Socha, Chen & Tokuriki, 2019). Phylogenetic analysis of β-lactamase SS does not reveal any clustering according to their host range (López *et al.*, 2019). Elucidating the relationship between β-lactamase SSs and the machineries required for their translocation is crucial to anticipating the spread of these enzymes between different bacterial species.

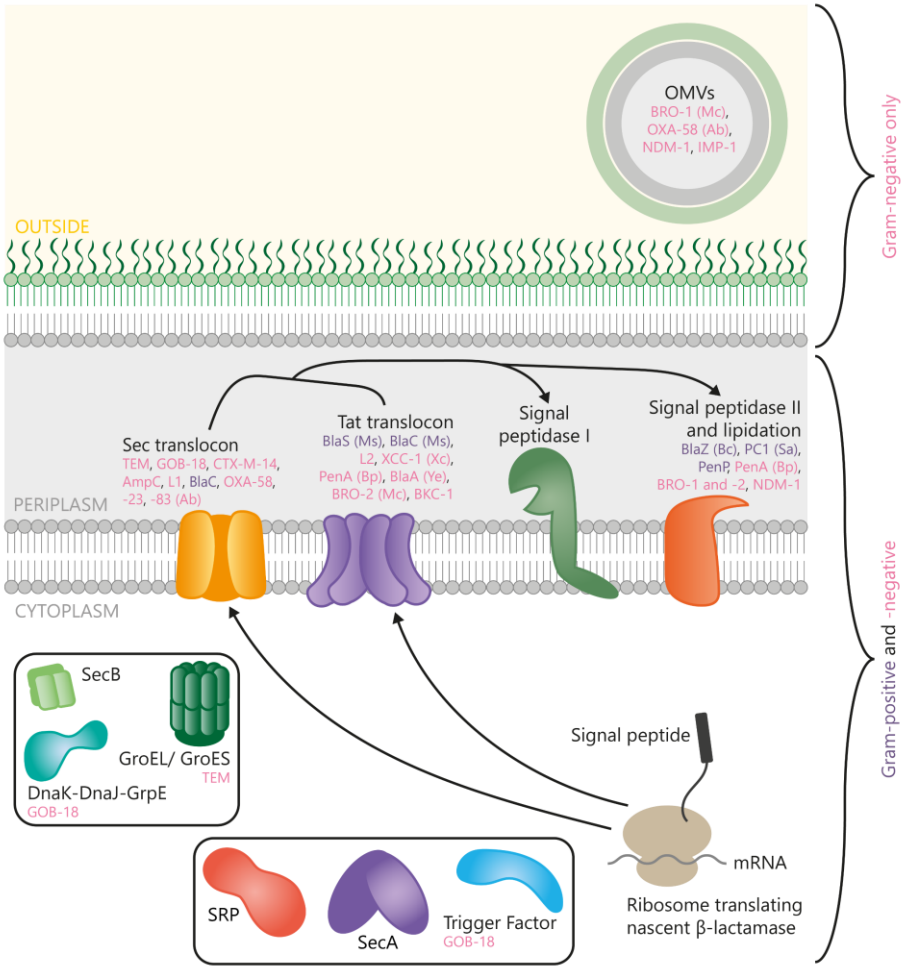


**Figure 5.3 Summary of published data on the translocation pathways of β-lactamases**
During translation by ribosomes in the cytoplasm, β-lactamase precursors associate with co-translational chaperones, either SRP, SecA or Trigger Factor. Pre-β-lactamases are either translocated co-translationally by Sec, post-translationally by Sec or by Tat after translation and folding. Post-translational Sec substrates may associate with cytoplasmic chaperones including SecB, DnaK-DnaJ-GrpE or GroEL/ GroES. Following or during translocation, pre-β-lactamases are processed to their mature form by signal peptidases I or II. In Gram-negative bacteria, some β-lactamases are exported in outer membrane vesicles (OMVs). For each machinery involved in translocation, the β-lactamases shown to be dependent on that machinery are listed next to it. β-lactamases of Gram-negative or -positive origin are written in pink or purple, respectively. The species from which experimental data were obtained was *E. coli* unless given in brackets. Abbreviations: Ab, *Acinetobacter baumannii*; Ms, *Mycobacterium smegmatis*; Xc, *Xanthomonas campestris*; Bp, *Burkholderia pseudomallei*; Ye, *Yersinia enterocolitica*; Mc, *Moraxella catarrhalis*; Bc, *Bacillus cereus*; Sa, *Staphylococcus aureus*.

#### *5.1.2.1 β-lactamase translocation: Sec or Tat*

Multiple studies have looked at the propensity of β-lactamases to undergo translocation by either of the two major machineries: Sec and Tat (summarised in Figure 5.3). A bioinformatic analysis of 400 β-lactamase SSs predicted that few β-lactamases (16%) are likely to be translocated by the Tat-machinery. Of the known Tat-dependent β-lactamases, only one is found on a mobile DNA element, while most are the products of chromosomal genes (Mcdonough *et al.*, 2005; Pradel *et al.*, 2009; Lee *et al.*, 2012; Schriefer *et al.*, 2013; Balder, Shaffer & Lafontaine, 2013; Randall *et al.*, 2016; Bharathwaj *et al.*, 2021). Notably, the exception – class A enzyme BKC-1 – is not exclusively dependent on Tat (see below). Together with the relatively low conservation of Tat across bacterial

species (Dilks *et al.*, 2003; Yamada *et al.*, 2007), this suggests that Sec-dependent β-lactamases are more compatible with mobilisation across a range of host species.

There is some overlap between Tat and Sec. Previous research has shown that TEM-type enzymes are strictly Sec-dependent upon expression in *E. coli* (Pradel *et al.*, 2009) but their mature protein domains are compatible with translocation through the Tat machinery (McCann *et al.*, 2007). The class A SBL BlaC is Tat-dependent in its native genus *Mycobacterium* but Sec-dependent in *E. coli*; this may be due to differences in the Tat machineries of each species (Mcdonough *et al.*, 2005; Pradel *et al.*, 2009). Not only can a β-lactamase use different translocation pathways in different species, but it may also exploit multiple pathways in the same organism. In bacteria producing BKC-1, the Tat-machinery is required for full conferral of β-lactam resistance, but Tat deletion mutants can still export the enzyme presumably via Sec (Bharathwaj *et al.*, 2021). BKC-1 contains a Tat-specific motif but acquired a duplication in its h-region. While BKC-1 is encoded on a mobile genetic element similar to KPC-2, related enzymes have only been identified in one clinical isolate suggesting limits to its dissemination. This duplication might have been selected to allow compatibility of the BKC-1 gene with expression in Enterobacteriaceae and may represent an interim stage of evolution (towards Sec-specificity) for more effective translocation of the protein in a broader host range (Bharathwaj *et al.*, 2021). Another example of dual-targeted transport is the class A CTX-M-15 found in a pathogenic strain of *E. coli*. In this strain, CTX-M-15 is translocated to the extracellular environment either by the type 1 secretion system that spans the entire Gram-negative envelope or by Sec followed by the type 2 secretion system (Rangama *et al.*, 2021). Together, these studies support Sec as the default mechanism of translocation for mobilisable β-lactamases, but bacteria can also evolve specialised pathways for β-lactamase transport.

#### *5.1.2.2 β-lactamase sorting after translocation*

An important step of β-lactamase sorting either during or after export is removal of the SS by signal peptidase (Josefsson & Randall, 1981). While most β-lactamases are predicted to be cleaved by signal peptidase I, both SBLs and MBLs exist with a lipobox motif for processing by signal peptidase II (Figure 5.3). Lipidated β-lactamases are particularly common in the cytoplasmic membrane of Gram-positive bacteria, presumably because lipidation prevents diffusion of the enzyme away from the producer bacterium, but are also found in the Gram-negative outer membrane (Bootsma *et al.*, 1996; Balder, Shaffer & Lafontaine, 2013; González *et al.*, 2016; Randall *et al.*, 2016). The most notable example is the class B NDM family of enzymes. NDM-1 is lipidated following SS cleavage and becomes localised to the inner leaflet of the outer membrane. This localisation protects the lipoprotein from degradation in zinc-limited conditions, which otherwise destabilises MBL structures (González *et al.*, 2016). Lipobox-containing β-lactamases including NDM-1, the class A enzyme BRO-1 and class D OXA-58, are found in both soluble and membrane-bound forms, suggesting processing by both signal peptidase I- and II-type enzymes. The ratios of soluble enzyme and lipoprotein vary depending on host (González *et al.*, 2016; Zalucki *et al.*, 2020; Bootsma *et al.*, 1996; Liao *et al.*, 2015).

Lipidated β-lactamases are often packaged into outer membrane vesicles (OMVs), spherical structures formed from the outer lipid bilayer of Gram-negative bacteria, sometimes along with DNA coding for these enzymes (Liao *et al.*, 2015; González *et al.*, 2016; López *et al.*, 2019). Soluble periplasmic enzymes can also associate with OMVs; their packaging into vesicles is mediated by electrostatic interactions with the outer membrane (López *et al.*, 2021). These OMVs both protect neighbouring susceptible bacteria from β-lactam treatment through their β-lactamase activity and promote dissemination of these β-lactam resistance determinants through horizontal gene transfer. This complicates β-lactam therapy and has been cited as a reason for treatment failure (Bielaszewska *et al.*, 2021). By targeting translocation of such β-lactamases, the deleterious effects of Gram-negative OMVs will also be reduced.

The processes following translocation also affect the levels of active β-lactamase in the periplasm. Mutation of *mreB*, which encodes a bacterial actin homologue important for maintenance of rod-shaped cells and thought to play a role in sorting of PBPs, causes accumulation of the pre-protein form of TEM (Pradel *et al.*, 2009). In the periplasm of Gram-negative bacteria, many β-lactamases are processed by thiol-disulfide oxidoreductases from the disulfide bond formation (DSB) system. DsbA catalyses the formation of disulfide bonds between cysteine side chains. All four Ambler classes A – D include enzymes possessing pairs of cysteines. Mutation of *dsbA* significantly increases β-lactam susceptibility in bacteria producing cysteine-containing class A, B or D β-lactamases, including the inhibitor-resistant KPC and OXA families (Furniss *et al.*, 2021). Since inhibiting β-lactamase translocation would also prevent acquisition of disulfide bonds in these proteins, it is similarly expected to be a viable adjuvant approach that reverses β-lactam resistance.

#### *5.1.2.3 β-lactamase sorting before Sec-mediated translocation: how does protein sequence determine targeting?*

As discussed in Chapter 1, a complex network of chaperones is involved in Sec substrate recognition, targeting and maintenance of a translocation-competent conformation. Experimental data on the pathways utilised by different Sec-dependent β-lactamases are limited, and the majority of existing knowledge is on TEM β-lactamase (Figure 5.3). TEM is translocated across the cytoplasmic membrane and processed to its mature form after completion of its translation (Josefsson & Randall, 1981; Koshland & Botstein, 1982). Consistent with a post-translational translocation mechanism, TEM does not bind SRP or depend on SRP for translocation *in vitro* (Beha *et al.*, 2003). The post-translational nature of TEM as a Sec substrate raises the question of how it maintains a translocation-competent state. In the absence of chaperones, the pre-protein form of TEM (pTEM) folds significantly slower than the mature enzyme (Laminet & Pluckthun, 1989). This suggests that its SS delays folding. However, SS-stabilised folding intermediates can be aggregation prone due to exposure of hydrophobic patches, requiring chaperones to shield them (Tsirigotaki *et al.*, 2018). Ribosome profiling has revealed that the co-translational chaperone Trigger Factor interacts with nascent pre-β-lactamases (Oh *et al.*, 2011; Kaderabkova *et al.*, 2022). Deletion of *secB* or depletion of DnaK-DnaJ-GrpE alone do not affect translocation of TEM, but absence of both SecB and DnaK-DnaJ-GrpE impairs translocation (Laminet, Kumamoto &

Plückthun, 1991; Wild *et al.*, 1996). This suggests that these two chaperone systems are functionally redundant in sorting of TEM. More severe defects in translocation of TEM are seen when GroEL or GroES are inactivated by mutation (Kusakawa *et al.*, 1989). The GroEL/ GroES system recognises early folding intermediates of pTEM, but not mature TEM, preventing misfolding steps that would otherwise lead to aggregation of the protein (Zahn & Plückthun, 1992). TEM may be targeted post-translationally to the translocon through GroEL interaction with SecA at the membrane (Bochkareva, Solovieva & Girshovich, 1998).

However, insights into the translocation of other β-lactamases show that the chaperone network involved in TEM translocation does not apply to all β-lactamases. Processing of Sec-dependent AmpC by signal peptidase, and therefore AmpC translocation, is entirely co-translational (Josefsson & Randall, 1981; Pradel *et al.*, 2009). Translocation of class B3 MBL GOB-18 is Sec-dependent and reduced in cells lacking Trigger Factor. Similar to TEM, GOB-18 is unaffected by *secB* deletion alone. Contrary to TEM, however, GOB-18 translocation is dependent on the DnaK-DnaJ-GrpE pathway and not GroEL/ GroES (Morán-Barrio, Limansky & Viale, 2009). Unlike Tat-specific substrates and pre-pro-lipoproteins, which possess clear motifs in their SS allowing them to be predicted bioinformatically, consensus motifs for substrates of different Sec targeting pathways and chaperones do not exist.

The most commonly cited predictor of targeting pathway for Sec substrates is SS hydrophobicity. Generally, substrates with a sufficiently hydrophobic SS (usually integral cytoplasmic membrane proteins) will be targeted to the Sec channel co-translationally by SRP, while proteins with lower SS hydrophobicity are targeted by SecA (Lee & Bernstein, 2001; Huber *et al.*, 2005a). Recently, it has become clear that SecA targeting itself exists as a hierarchy of co- to post-translational, where substrates with the least hydrophobic SSs tend to be targeted to translocation entirely post-translationally (Zhu, Wang & Shan, 2022). Newer research has also demarcated SRP substrates from the broader pool of SRP-dependent proteins. As an example, DsbA has a highly hydrophobic SS and was assumed to be an SRP substrate because translocation directed by its SS is co-translational and impaired in cells depleted for SRP (Schierle *et al.*, 2003). However, DsbA was found not to associate with SRP in ribosome profiling studies (Schibich *et al.*, 2016). Instead, DsbA is an early, co-translational substrate of SecA (Zhu, Wang & Shan, 2022). DsbA is therefore SRP-dependent for optimal translocation *in vivo*, but not an SRP substrate. It follows that other early co-translational substrates of SecA would be similarly SRP-dependent.

The dependence of a given β-lactamase on different chaperones and pathways for translocation will affect the types of translocation inhibitors that can be deployed against it. Effective inhibitors would reduce extracytoplasmic levels of active enzyme to a sufficient extent to abrogate β-lactamase resistance and potentiate the clinically important β-lactam class of antibiotics. Given the thousands of different β-lactamase enzymes in circulation, it is not possible to determine translocation requirements on a case-by-case basis. Elucidation of protein sequence properties associated with different types of Sec substrates would therefore be beneficial. With a focus on determining SRP and SecA dependence, the following work is a step towards understanding the

requirements of diverse β-lactamases for translocation. The whole cell NanoBiT assay described in previous chapters is adapted to follow the translocation of β-lactamases from different molecular classes and with different substrate profiles. In previous studies, the intrinsic activity of β-lactamase enzymes was exploited to track their export using traditional antimicrobial susceptibility testing or assays with chromogenic β-lactam substrate. The NanoBiT-based assay complements these traditional assays, with greater specificity and signal: noise ratio, and the counter assay allows differentiation between conditions that specifically inhibit export and those that affect other stages of β-lactamase biogenesis. This work reveals that IMP-1 and NDM-1 are sensitive not only to inhibition of SecA but also depletion of SRP, while translocation of TEM is SecA-dependent and SRP-independent.

## 5.2 Signal sequence prediction and hydrophobicity analysis

Previous work determined the SRP dependence of SSs with a range of hydrophobicities (Huber *et al.*, 2005a). Figure 5.4a is a histogram representing the distribution of hydrophobicity scores of SSs included in that work, based on the Wimley-White scale (Wimley & White, 1996). From this histogram, a minimum threshold score for SRP dependence was determined as 4.56, and it was postulated that no pre-secretory protein with a score below this threshold will depend on SRP for export in *E. coli*. The model protein DsbA, which is SRP-dependent but not an SRP substrate, has a SS hydrophobicity score of 4.66. β-lactamase SSs (81 total) were extracted from UniProt and scored by Dr. Damon Huber and Prof Ian Collinson. β-lactamase SS scores span a range of hydrophobicities, both above and below the threshold (Figure 5.4b). The median SS hydrophobicity score for the β-lactamases is in the 4.5 – 4.56 range, compared to a median score of 4.44 – 4.5 for the previous dataset of proteins with diverse functions. This suggests that β-lactamases are targeted to translocation by a range of pathways, with a tendency towards SRP dependence compared to the general *E. coli* secretome.

There is no noticeable correlation between the SS hydrophobicity of a β-lactamase and the bacterial species from which it was first isolated. Molecular classes A to D are represented at both extremes of the spectrum. One such example is the molecular subclass B1 enzymes IMP-1 and NDM-1, which have SS hydrophobicities of 4.76 and 4.37, respectively (Figure 5.4b). Based on the proposed SS hydrophobicity threshold, it was hypothesised that IMP-1 is SRP-dependent while NDM-1 does not depend on SRP for translocation.

First isolated from *Serratia marcescens*, IMP-1 is encoded on a transferable class 1 integron and has been found in multiple species (Osano *et al.*, 1994; Laraki *et al.*, 1999). NDM-1 was discovered in *K. pneumoniae*. It is mobilised by an insertion sequence element, IS*Aba*125, and has been found on broad host range plasmids enabling its spread (Yong *et al.*, 2009; Toleman *et al.*, 2012; Li *et al.*, 2013). NDM-1-positive strains have been reported across the globe (Li *et al.*, 2013; Bush & Fisher, 2011). While $bla_{IMP-1}$ is more common in *P. aeruginosa*, $bla_{NDM-1}$ has seen a more successful spread amongst Enterobacterales (Cheung *et al.*, 2021). Both IMP-1 and NDM-1 are able to inactivate a range of β-lactams – penicillins, cephalosporins, the last resort carbapenems, but not monobactams

– and to overcome conventional inhibitors (Yong *et al.*, 2009; Osano *et al.*, 1994). This makes them ideal targets for translocation inhibitors.

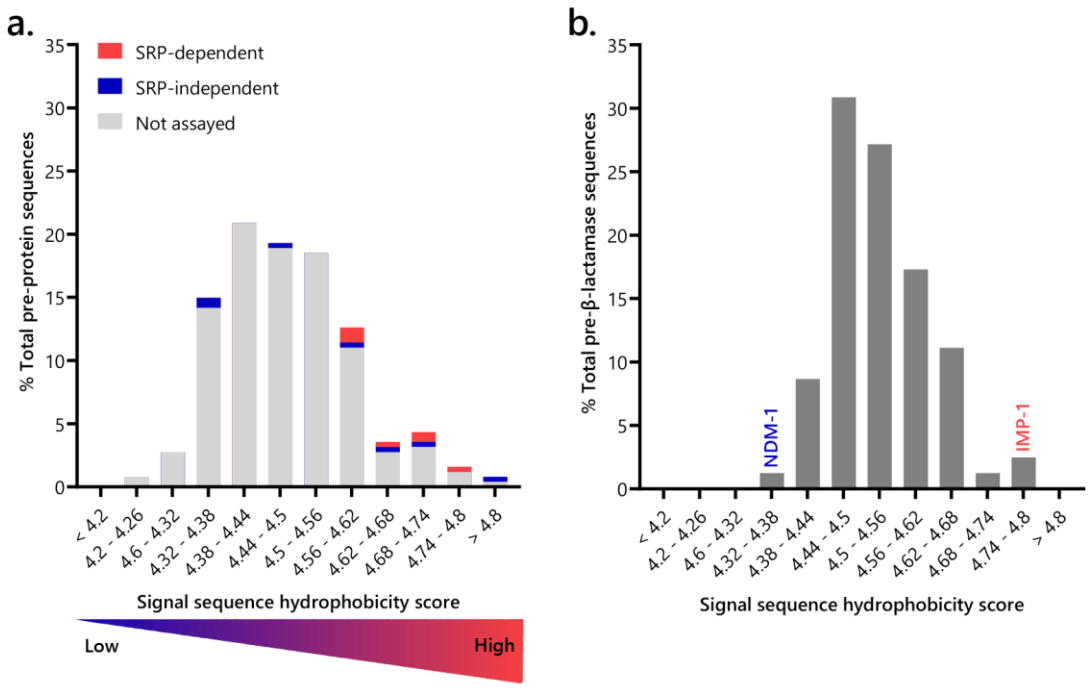


**Figure 5.4 β-lactamase signal sequences span a range of hydrophobicities**
**a.** Signal sequences (SSs) extracted from UniProt by Huber *et al.* (2005). Each bar corresponds to the percentage of total extracted sequences that have a given hydrophobicity. The percentages of total extracted sequences corresponding to SRP-dependent and -independent proteins (as determined in Huber *et al.*, 2005) or proteins that were not assayed are represented in red, blue and grey, respectively. **b.** Pre-β-lactamase SSs extracted from UniProt for this study. Each bar corresponds to the percentage of total extracted pre-β-lactamase sequences that have a given SS hydrophobicity. The approximate hydrophobicity scores of NDM-1 and IMP-1 SSs are indicated.

## 5.3 Meropenem susceptibility of β-lactamase-producing *E. coli* with a SecA defect

Since β-lactamases require transport into the periplasm to fold to their native state and access substrate, their translocation can be assessed by measuring β-lactam susceptibility or β-lactamase activity of whole cells. Where β-lactamase export is diminished, producing bacteria would be more susceptible to β-lactam treatment (Pradel *et al.*, 2009; Liao *et al.*, 2015; Morán-Barrio, Limansky & Viale, 2009; Mcdonough *et al.*, 2005). Historically, *E. coli* strain MC4100 is used for protein translocation assays (Ferenci *et al.*, 2009). There are numerous MC4100 derivative strains with mutations in the Sec-machinery. MM52 possesses a temperature-sensitive *secA* mutation (*secA51*$^{ts}$) that impairs export of SecA-dependent pre-proteins. The defect is more pronounced at higher temperatures, so raising temperature would reduce export of SecA-dependent pre-proteins further (Oliver & Beckwith, 1981).

As IMP-1 and NDM-1 are proteins destined for the periplasm like DsbA (Schierle *et al.*, 2003), it is expected that both would depend on SecA for translocation following targeting. Yet IMP-1 may meet

the threshold SS hydrophobicity for SRP-dependent targeting, while NDM-1 has a weakly hydrophobic SS so its targeting is expected to be strictly SecA-dependent. This would render NDM-1 more sensitive to defects in SecA function compared to IMP-1. SecA-dependence of IMP-1 and NDM-1 was first assessed by expression of $bla_{IMP-1}$ and $bla_{NDM-1}$ genes under their native, constitutive promoters in MM52. β-lactamase export by MM52 (SecA51$^{ts}$) was compared to that of its parent strain MC4100, which possesses wildtype (WT) SecA.

Antibiotic susceptibility was first assessed by meropenem disc diffusion, in which a bigger zone of growth inhibition indicates greater susceptibility. Due to the essentiality of SecA for growth, MM52 exhibits robust growth at 30 °C (permissive temperature for growth) but upon a switch to 37 or 42 °C (non-permissive temperatures) growth ceases after a few hours (Oliver & Beckwith, 1981). Initially, experiments were attempted at 42 °C, but there was no visible growth of MM52 at 42 °C. When MM52 is incubated at 37 °C, resulting lawns are thinner than those of MM52 at 30 °C and all MC4100 cultures.

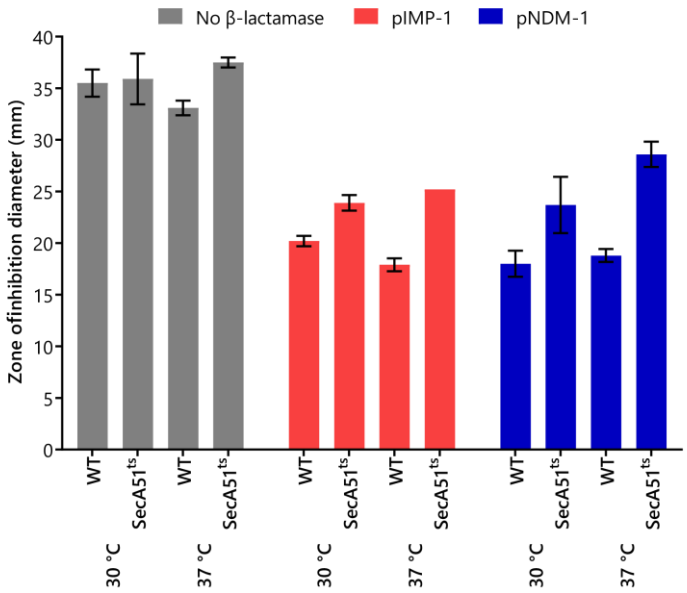


**Figure 5.5 Meropenem susceptibility of β-lactamase-producing *E. coli* is increased in a SecA-defective background**
MC4100 (WT) and MM52 (SecA51$^{ts}$) carrying empty pSU2718 (EV) or β-lactamases under their native promoters (as indicated) were suspended in PBS ($OD_{600}$ 0.1). Suspensions were streaked to lawn on Mueller Hinton agar and challenged with 10 µg meropenem discs. Plates were incubated overnight at 30 °C or 37 °C then the zones of growth inhibition were measured. Data from five independent experiments are shown as mean ± standard deviation.

Across all strains at both temperatures, a one-way analysis of variance (ANOVA) test yielded significant variation in zone of inhibition diameter (adjusted R-squared = 0.9733, $F_{11, 48} = 196.2$, $p < 0.001$). At 30 °C, MC4100 and MM52 transformed with empty pSU2718 (EV; negative control for β-lactamase) have similar susceptibility (with mean ± standard deviation diameters of 35.5±1.2 and 35.9±2.2 mm, respectively; Figure 5.5). Contrastingly, at 37 °C, the susceptibility increases for MM52 carrying EV (37.5±0.5 mm) and decreases for MC4100 (33.1±0.7 mm). There was no significant difference in growth inhibition with increased temperature for either strain ($p>0.05$).

β-lactamase production decreases meropenem susceptibility compared to the EV control; this difference was significant in all cases (Figure 5.5). MM52 cells producing β-lactamase all have higher susceptibility than corresponding MC4100 cells at 30 °C (MC4100 $bla_{IMP-1}$ 20.2±0.4 mm, MM52 $bla_{IMP-1}$ 23.9±0.7 mm, p<0.001; MC4100 $bla_{NDM-1}$ 18.0±1.2 mm, MM52 $bla_{NDM-1}$ 23.7±2.4 mm, p<0.001). This suggests that both IMP-1 and NDM-1 are dependent on functional SecA for efficient production of active enzyme. A further increase in susceptibility at 37 °C only occurs in MM52 producing NDM-1 (28.6±1.1 mm, p<0.001), suggesting that NDM-1 is more sensitive to SecA defects than IMP-1.

It is unexpected that MC4100 expressing $bla_{IMP-1}$ and $bla_{NDM-1}$ from pSU2718 exhibit comparable susceptibility (17.9±0.5 and 18.8±0.6 mm at 37 °C, respectively; p>0.05) since previously $bla_{NDM-1}$ expression was far more likely to confer meropenem resistance than $bla_{IMP-1}$ in Enterobacterales such as *E. coli* MG1655. It was found that, when encoded on pSU plasmids under their native promoters, production of NDM-1 exceeded that of IMP-1 by up to 6-fold (Cheung *et al.*, 2021). This high gene expression of $bla_{NDM-1}$ imparts a significant fitness cost associated with amino acid starvation. Thus, in the absence of selective pressure for elevated NDM-1 production, mutations accumulate to reduce $bla_{NDM-1}$ expression (Cheung *et al.*, 2021). Such mutations may have occurred in the strains used for this experiment. Given the potential artefacts of expression of these β-lactamases under their (relatively uncharacterised) native promoter regions, constructs for investigation of β-lactamase translocation were redesigned.

## 5.4 NanoBiT assays reveal SRP dependence of β-lactamase translocation

To enable fine-tuning of β-lactamase expression level and control for its effects on export, $bla_{IMP-1}$ and $bla_{NDM-1}$ were cloned under the well-characterised, titratable tac promoter. The inducer of this promoter (IPTG) is actively transported into cells by lactose permease (LacY), which will be dependent on Sec for its insertion into the membrane. However, MC4100 has a *lacY* deletion so IPTG uptake is exclusively by diffusion (Peters, Thate & Craig, 2003; Fernández-Castané *et al.*, 2012). Therefore, IPTG induction of β-lactamase constructs will be unaffected by inhibition of Sec. Preliminary results using antimicrobial susceptibility testing suggest that impairment of SecA function reduces the amount of active β-lactamase in the periplasm, however they do not clarify whether this effect occurs at the level of translocation (as hypothesised) or elsewhere. Since the whole cell NanoBiT assay developed for inhibitor screening is capable of distinguishing between specific and non-specific effects, as well as being a direct measure of protein localisation independent of folding to an active enzyme, it was adapted for studying the β-lactamases.

**Table 5.1 Signal sequences of β-lactamases studied in this work**

| β-lactamase | Signal sequence (N to C-terminus) |
|---|---|
| TEM | MSIQHFR VALIPFFAAF CLPVFA |
| IMP-1 | MSK LSVFFIFLF CSIATA |
| NDM-1 | MELPNIMHPVAKLST ALAAALM LSG |

Further experimentation included the class A TEM β-lactamase as a control. TEM has previously been determined as SRP-independent and completely post-translational despite its moderately high SS hydrophobicity (4.60). The SSs of TEM, IMP-1 and NDM-1 are given in Table 5.1. Constructs encoding pre-secretory (pTEM) and mature (mTEM) forms of this β-lactamase C-terminally tagged with HiBiT were transformed into MM52 and MC4100 (Figure 5.6a). A one-way ANOVA test yielded significant variation in luminescence between samples (adjusted R-squared = 0.9897, $F_{5, 12} = 327.4$, $p < 0.001$). Both MM52 and MC4100 carrying empty pCDFT (EV), which do not produce TEM-HiBiT, give no luminescent signal. *E. coli* producing mTEM-HiBiT yield negligeable luminescence upon periplasmic release, which confirms that TEM transport into the periplasm requires its signal peptide. After periplasmic release, the maximum signal reached by MM52 producing pTEM-HiBiT is substantially decreased compared to MC4100 pTEM-HiBiT (mean ± standard deviation of 1.00 RLU for MC4100 and 0.26±0.09 RLU for MM52; $p<0.001$), which could suggest that pTEM-HiBiT translocation is dependent on SecA. However, MM52 producing pTEM-HiBiT also yields dramatically decreased signal compared to the respective MC4100 strain following whole cell lysis (1.00 RLU for MC4100 and 0.36±0.07 RLU for MM52; $p<0.001$) which suggests that the decreased periplasmic accumulation of pTEM-HiBiT in MM52 is related to decreased expression of TEM constructs in this strain.

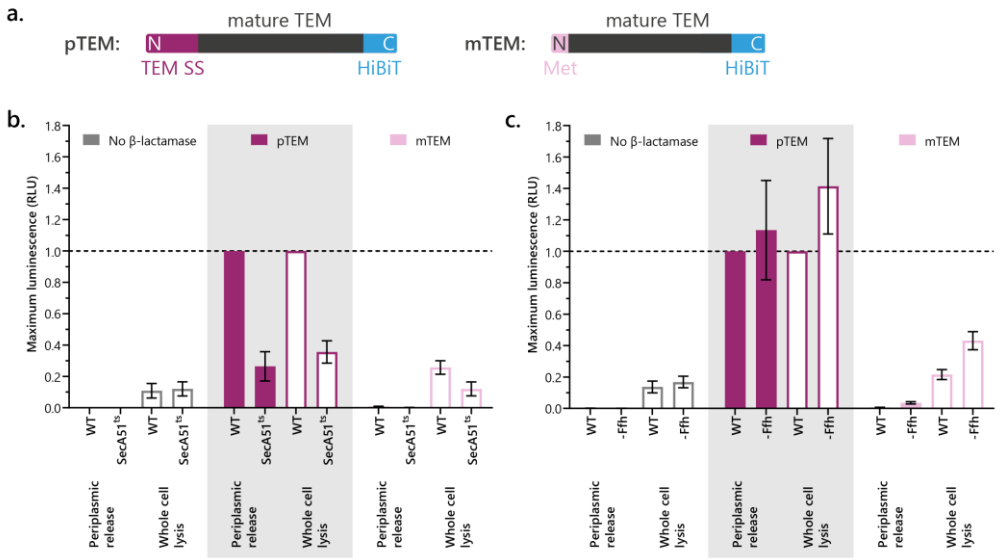


**Figure 5.6 pTEM-HiBiT production and export is decreased in a SecA-defective background but not by Ffh depletion**
LB cultures of *E. coli* carrying empty pCDFT (EV), or pCDFT encoding pre-secretory (pTEM) or mature TEM (mTEM) tagged with HiBiT under $P_{Tac}$ (as indicated) were induced with 10 µM IPTG for 1.5 h, incubated at 4 °C for 1 h then diluted to $OD_{600}$ 0.5 in LB. LgBiT and furimazine (periplasmic release; solid bars) or LgBiT, furimazine and Triton X-100 (whole cell lysis; bars with outline only) were added. NanoLuc activity (luminescence) was measured for 5 min prior to and up to 1 h following addition of EDTA and lysozyme. The maximum luminescence for each sample was recorded and normalised to the maximum luminescence recorded for the respective MC4100 pTEM-HiBiT samples (dotted line at y = 1.0). Data from three independent experiments are shown as mean ± standard deviation. **a.** Schematic of TEM-HiBiT constructs. **b.** Data from MC4100 (WT) and MM52 ($SecA51^{ts}$) grown at 30 °C. **c.** Data from MC4100 and WAM121 (-Ffh) washed three times by resuspension in fresh LB then grown at 37 °C.

pTEM- and mTEM-HiBiT were also studied as above in WAM121 (Figure 5.6b). This strain has an MC4100 background but its *ffh* gene, which encodes the protein component of SRP, is under control

of an arabinose-inducible promoter. Growth in the absence of arabinose depletes Ffh, impairing SRP-dependent translocation. A one-way ANOVA test of NanoBiT data indicated significant variation in luminescence (adjusted R-squared = 0.9358, $F_{5, 12} = 50.5$, $p < 0.001$). After the growth period, WAM121 carrying EV give no signal and those producing mTEM-HiBiT yield negligeable signal upon periplasmic release. After Ffh depletion (confirmed by immunoblot) and induction of pTEM-HiBiT production, MC4100 and WAM121 reach similarly high maximum signal upon periplasmic release (1.00 RLU and 1.13±0.31 RLU, respectively; $p>0.05$), showing that pTEM-HiBiT transport into the periplasm is not affected by SRP.

In MC4100 and MM52 producing mTEM-HiBiT following whole cell lysis, the maximum luminescent signal reached is either the same as, or only marginally greater than the respective EV strain (Figure 5.6b). After whole cell lysis, WAM121 pTEM-HiBiT and mTEM-HiBiT reach higher signal than the corresponding MC4100 strains. This difference is statistically significant for the former (1.00 RLU for MC4100 pTEM-HiBiT and 1.41±0.30 RLU for WAM121 pTEM-HiBiT; $p=0.02$) and not significant for the latter (0.22±0.03 RLU for MC4100 mTEM-HiBiT and 0.43±0.06 RLU for WAM121 mTEM-HiBiT; $p>0.05$). These results could suggest that WAM121 produces more TEM or cytoplasmic TEM is more stable in WAM121 compared to cells with wildtype Ffh.

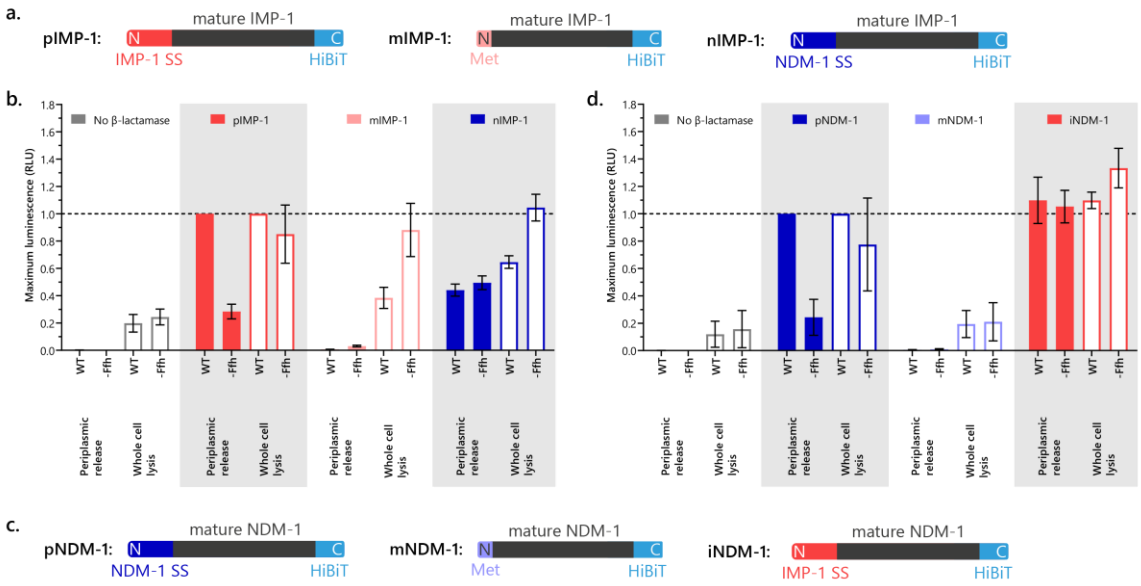


**Figure 5.7 Export of both pIMP-1-HiBiT and pNDM-1-HiBiT, but not their SS-switched chimeras, is decreased by Ffh depletion**
LB cultures of MC4100 (WT) and WAM121 (-Ffh) carrying empty pCDFT (EV), or pCDFT encoding HiBiT-tagged constructs under $P_{Tac}$ (as indicated) were washed three times by resuspension in fresh LB then grown at 37 °C. Cultures were induced with 10 µM IPTG for 1.5 h, incubated at 4 °C for 1 h then diluted to $OD_{600}$ 0.5 in LB. LgBiT and furimazine (periplasmic release; solid bars) or LgBiT, furimazine and Triton X-100 (whole cell lysis; bars with outline only) were added. NanoLuc activity (luminescence) was measured for 5 min prior to and up to 1 h following addition of EDTA and lysozyme. The maximum luminescence for each sample was recorded and normalised to the maximum luminescence recorded for the respective MC4100 **b.** pIMP-1-HiBiT or **d.** pNDM-1-HiBiT samples (dotted line at y = 1.0). Data from three independent experiments are shown as mean ± standard deviation. **a.** Schematic of IMP-1-HiBiT constructs. **b.** IMP-1-HiBiT export with different SS. **c.** Schematic of NDM-1-HiBiT constructs. **d.** NDM-1-HiBiT export with different SS.

For whole cell NanoBiT assays of IMP-1 and NDM-1 constructs (Figure 5.7), one-way ANOVA tests gave significant variation in luminescence (adjusted R-squared = 0.9924 and 0.9754 respectively, $F_{7, 22}$ = 539.9 and 124.6, $p < 0.001$ in both cases). *E. coli* strains producing HiBiT-tagged mIMP-1 give negligeable signal upon periplasmic release, confirming that IMP-1 export requires the SS (Figure 5.7b). Following periplasmic release, WAM121 producing pIMP-1-HiBiT yields lower signal than the respective MC4100 sample (1.00 RLU for MC4100 and 0.28±0.05 RLU for WAM121; $p<0.001$). After whole cell lysis using Triton X-100, WAM121 producing pIMP-1-HiBiT reaches a marginally lower maximum signal than MC4100, but this difference is not significant (MC4100 1.00 RLU; WAM121 0.85±0.21 RLU; $p>0.05$). This suggests that SRP depletion specifically impacts periplasmic levels of IMP-1.

Interestingly, while the luminescent signal resulting from whole cell lysis of MC4100 producing mIMP-1-HiBiT is only slightly greater than that from MC4100 carrying EV, WAM121 producing mIMP-1-HiBiT yields a whole cell signal comparable to that seen in strains producing pIMP-1-HiBiT (Figure 5.7b). The difference in signal between MC4100 and WAM121 producing mIMP-1-HiBiT is significant (0.38±0.08 RLU and 0.88±0.20 RLU respectively; $p=0.002$).

As observed for TEM and IMP-1, periplasmic release of mNDM-1-HiBiT producing strains yields negligeable signal (Figure 5.7d). This is in line with the expectation that the NDM-1 SS is required for export, however whole cell lysis of these strains also yields comparable levels of luminescence to strains producing no HiBiT constructs. Therefore, it is possible that low periplasmic signal is due to greatly reduced mNDM-1-HiBiT production or stability, or because this construct does not interact well with LgBiT. Contrary to the hypothesis that NDM-1 is SRP-independent, WAM121 producing pNDM-1-HiBiT reaches lower signal than MC4100 pNDM-1-HiBiT upon periplasmic release (1.00 RLU for MC4100 and 0.24±0.13 RLU for WAM121; $p<0.001$). WAM121 pNDM-1-HiBiT also yields a lower signal upon whole cell lysis than MC4100 pNDM1-HiBiT, but statistical tests did not confirm a significant difference (MC4100 1.00 RLU; WAM121 0.78±0.34 RLU; $p>0.05$).

To further elucidate whether the IMP-1 and NDM-1 SSs determine SRP dependence, SS-switched chimeras iNDM-1 (NDM-1 with the putative SRP-dependent IMP-1 SS) and nIMP-1 (IMP-1 with the putative SRP-independent NDM-1 SS) were generated (Figure 5.7). Both periplasmic and whole cell signal from MC4100 nIMP-1-HiBiT (0.44±0.04 RLU and 0.65±0.05 RLU, respectively) is lower than that of MC4100 producing pIMP-1-HiBiT (periplasmic release, $p<0.001$; whole cell lysis, $p=0.01$), suggesting that replacement of the IMP-1 SS with the NDM-1 SS results in sub-optimal synthesis and/ or translocation of the IMP-1 construct (Figure 5.7b). Upon periplasmic release, WAM121 producing nIMP-1-HiBiT gives comparable signal (0.49±0.05 RLU) to MC4100 nIMP-1-HiBiT ($p>0.05$) suggesting that Ffh depletion does not further impair IMP-1 export when directed by the NDM-1 SS. However, whole cell lysis of WAM121 nIMP-1-HiBiT yields higher signal (1.04±0.10 RLU) than that of MC4100 nIMP-HiBiT ($p=0.02$). By contrast, replacement of the NDM-1 SS with that of IMP-1 (Figure 5.7d) did not have a significant effect on luminescence following periplasmic release or whole cell lysis in MC4100 compared to pNDM-1 (1.10±0.17 RLU and 1.10±0.06 RLU, respectively; $p>0.05$). WAM121 iNDM-1-HiBiT gives comparable periplasmic signal (1.05±0.12

RLU) and whole cell signal (1.33±0.14) to MC4100 iNDM-1-HiBiT ($p>0.05$), suggesting that this chimeric construct is insensitive to Ffh depletion.

## 5.5 Traditional assays for β-lactamase activity complement NanoBiT data

To validate NanoBiT results, assays based on classical methods for β-lactamase detection were adopted. WAM121 cannot be cultured for long periods (i.e. overnight) in the absence of arabinose, making it impossible to evaluate the β-lactamase activity of Ffh-depleted *E. coli* by susceptibility testing. Instead, the chromogenic β-lactam, nitrocefin was used. An additional advantage of this method is its greater sensitivity; often subtle differences in periplasmic β-lactamase levels are not detected by susceptibility testing (Pradel *et al.*, 2009). Hydrolysis of nitrocefin by β-lactamase causes a change in colour from yellow to red and an increase in absorbance at 490 nm ($A_{490}$).

Cultures of MC4100 and WAM121 producing HiBiT-tagged β-lactamases were grown as above. When resuspended in Tris-sucrose buffer and added to nitrocefin, whole cells of *E. coli* producing pTEM, pIMP-1 or pNDM-1 constructs cause a comparable increase in $A_{490}$ to those carrying EV. However, upon disruption of the outer membrane and cell wall by EDTA and lysozyme treatment, the extracytoplasmic contents of the cell (i.e. outer leaflet of the inner membrane, periplasm and inner leaflet of the outer membrane) are exposed and available for nitrocefin hydrolysis.

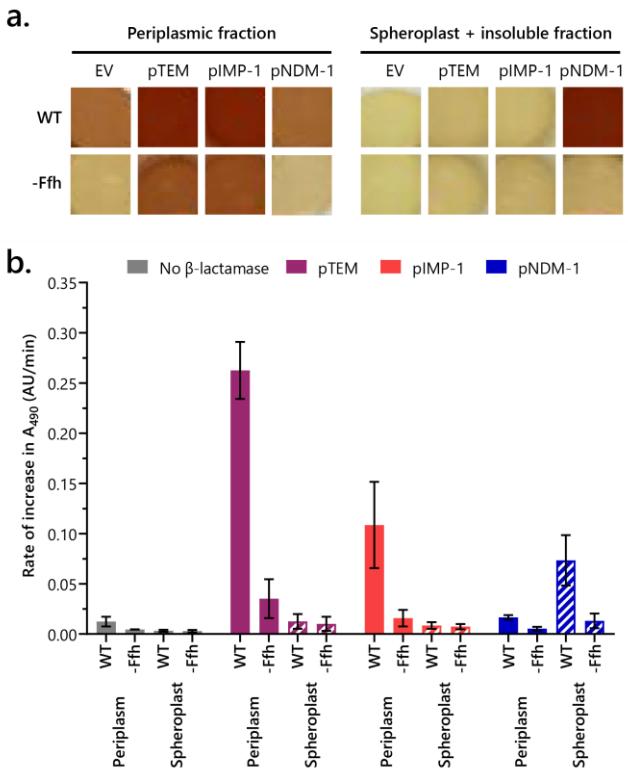


**Figure 5.8 β-lactamase activity of fractions from *E. coli* producing HiBiT-tagged pTEM, pIMP-1 or pNDM-1**
LB cultures of MC4100 (WT) and WAM121 (-Ffh) carrying empty pCDFT (EV), or pCDFT encoding HiBiT-tagged constructs under $P_{Tac}$ (as indicated) were washed three times by resuspension in fresh LB then grown at 37 °C. Cultures were induced with 10 µM IPTG for 1.5 h, incubated at 4 °C for 1 h then resuspended in Tris-sucrose buffer to $OD_{600}$ 10. Spheroplasts were separated from the periplasmic fraction by treatment with EDTA and lysozyme followed by

centrifugation, then resuspended in 1 volume Tris-sucrose. Fractions (25 µl) were added to nitrocefin (final concentration 50 µg/ml, final reaction volume 225 µl). Absorbance at 490 nm was monitored for 1 h. **a.** The final colour of respective wells at the end of 1 h period. A representative replicate is shown. **b.** The rate of the colour change was calculated. Data from three independent experiments are shown as mean ± standard deviation.

The soluble periplasm was separated from the inner membrane-bound spheroplasts and insoluble cell envelope debris by centrifugation. The periplasmic fraction of MC4100 carrying empty pCDFT caused a slight colour change from yellow to orange (Figure 5.8a, left). This nitrocefin hydrolysis activity is likely the result of low-level expression of the chromosomal *amp*C gene, found in *E. coli* K-12 strains such as MC4100 (Jaurin & Grundström, 1981). The periplasm of MC4100 producing pTEM and pIMP-1 exhibited additional nitrocefin hydrolysis activity, causing the reaction to turn red in colour. However, the final colour of reaction with the periplasm of pNDM-1-producing MC4100 is comparable to that of EV-carrying MC4100. Instead, the insoluble fraction from MC4100 producing NDM-1 causes a colour change to red, unlike the other two β-lactamases, which give a comparable result to EV (Figure 5.8a, right). This is consistent with reports than mature NDM-1 exists as a membrane-anchored lipoprotein (González *et al.*, 2016).

The periplasmic fraction of Ffh-depleted WAM121 producing pTEM and pIMP-1 gives a less intense red colour than respective MC4100 fractions (Figure 5.8a, left). However, the extent of the colour change resulting from the periplasm of EV-carrying WAM121 is also reduced compared to that of MC4100. This suggests that endogenous AmpC is SRP-dependent, consistent with the co-translational nature of AmpC signal peptide removal (Josefsson & Randall, 1981). It also makes it difficult to qualitatively assess whether the nitrocefin hydrolysis activity attributable to TEM or IMP-1 production is decreased in WAM121 compared to MC4100. On the other hand, the insoluble fraction of EV-carrying WAM121 results in a yellow colour comparable to MC4100 carrying EV (Figure 5.8a, right). Insoluble fractions of WAM121 producing pNDM-1 give a negligeable colour change in complete contrast to the respective MC4100 fraction. This can be taken to show that NDM-1 is impaired by Ffh depletion, consistent with NanoBiT data.

To facilitate comparison of the periplasmic fractions of bacteria producing pTEM and pIMP-1, the rate of nitrocefin hydrolysis was calculated based on the rate of increase in $A_{490}$ (Figure 5.8b). Endogenous AmpC activity – determined from MC4100 carrying EV as 0.012±0.0048 AU/min – contributes very little to the overall rate of nitrocefin hydrolysis in the periplasm of MC4100 producing pTEM (0.26±0.028 AU/min) and pIMP-1 (0.10±0.043 AU/min). The difference in rate between EV and pTEM or pIMP-1 is significant ($p<0.001$ in both cases). WAM121 producing pIMP-1 has substantially lower periplasmic activity (0.015±0.0082 AU/min) than MC4100 pIMP-1 ($p<0.001$) consistent with NanoBiT results. Contrary to NanoBiT data, and suggestive of SRP dependence, extracytoplasmic nitrocefin hydrolysis activity is lower in WAM121 producing pTEM (0.035±0.019 AU/min) compared to MC4100. This difference is very significant ($p<0.001$). Consistent with qualitative analysis, the spheroplast fraction of MC4100 producing pNDM-1 yields greater activity than MC4100 EV (0.073±0.025 and 0.0032±0.00099 AU/min for MC4100 pNDM-1 and EV, respectively; $p<0.001$) and WAM121 producing pNDM-1 (0.013±0.0073 AU/min, $p=0.004$).

Activity from the periplasmic fractions of MC4100 producing pNDM-1 (0.016±0.0022 AU/min) does not differ significantly from MC4100 carrying EV ($p>0.05$).

## 5.6 Off-target effects of SRP depletion on β-lactamase biosynthesis

Further β-lactamases were selected to test the hypothesis that a more hydrophobic SS confers SRP dependence, using the assays established above. IMP-1 and NDM-1 are only two examples from a whole spectrum of thousands of diverse β-lactamases. As a lipoprotein with a unique SS – possessing a negative charge in its n-region (González *et al.*, 2016; Zalucki *et al.*, 2020) – NDM-1 may represent an exception to the rule. Additionally, these enzymes are both MBLs; different rules may exist for sorting of SBLs (as seen for the class A SBL TEM). A larger, more diverse and representative subset of β-lactamases should be interrogated before conclusions are drawn.

Like IMP-1 and NDM-1, VIM-1 and -2 are molecular class B1 enzymes (MBLs). They have similarly broad substrate specificities. The $bla_{VIM-1}$ gene, first found on the chromosome of a *P. aeruginosa* strain, is situated on a class 1 integron (much like $bla_{IMP-1}$). More recently, $bla_{VIM-1}$ has been found on the highly mobile, broad host range IncA plasmid in a range of Enterobacterales species (Arcari *et al.*, 2020). VIM-2 shares 90% amino acid identity with VIM-1. Its gene was also first discovered in *P. aeruginosa*, on a plasmid-borne class 1 integron weakly related to that of $bla_{VIM-1}$ (Poirel *et al.*, 2000). CTX-M-15 was found concomitantly in multiple Enterobacterales species on a range of large size plasmids. In all cases, its gene was situated downstream of insertion sequence *ISEcp1* (Karim *et al.*, 2001). CTX-M-15 is a class A SBL, and (unlike previous CTX-M enzymes) it can hydrolyse extended spectrum cephalosporins like ceftazidime. It is susceptible to inhibition by clavulanic acid and tazobactam (Poirel, Gniadkowski & Nordmann, 2002). KPC-3 is also a class A SBL. However, it has a broader spectrum than CTX-M-15, conferring resistance to extended spectrum cephalosporins, carbapenems (when present alongside other resistance mechanisms) and monobactams (Woodford *et al.*, 2004). KPC enzymes are also resistant to clinically available β-lactamase inhibitors (Tooke *et al.*, 2019). The $bla_{KPC-3}$ gene was first found in *K. pneumoniae*, carried on a conjugative plasmid (Woodford *et al.*, 2004).

In each of the TEM, IMP, NDM, VIM, CTX-M and KPC enzyme families, there is diversity in SS (Naas *et al.*, 2017). The VIM family has particularly striking divergence in SS. VIM enzymes are broadly divided into two clades: VIM-1-type and VIM-2-type. The majority of the sequence differences between VIM-1 and -2 are in their SS (Chen, Fowler & Tokuriki, 2020), suggesting that these clades may have evolved to undergo translocation using different machineries or in different hosts. The VIM-1 SS is weakly hydrophobic (scoring 4.46) whereas VIM-2 has a moderately hydrophobic SS (4.58; Figure 5.9a). If targeting to translocation is indeed determined by SS hydrophobicity, as hypothesised earlier in this work, then the VIM clades may differ in SRP or SecA-dependence. CTX-M-15 (4.43) and KPC-3 (4.63) have weakly and moderate-highly hydrophobic SSs, respectively (Figure 5.9a). It is postulated that the latter would be SRP-dependent, whereas the former would be strictly SecA-dependent.

Luminescence upon periplasmic release or whole cell lysis of cultures producing each HiBiT-tagged β-lactamase was normalised by the respective MC4100 signal (Figure 5.9b). Thus, signal from MC4100 producing each enzyme is taken to be 1.0 RLU. This allows the difference in periplasmic or whole cell accumulation of each β-lactamase upon Ffh depletion to be assessed by one sample t-test in which the reference value is 1.0 RLU. Consistent with earlier ANOVA tests, t-tests found that Ffh depletion is not associated with a significant difference in periplasmic release or whole cell lysis signal from pTEM-HiBiT-producing bacteria ($p>0.05$ in both cases). As before, WAM121 producing pIMP-1- and pNDM-1-HiBiT give lower periplasmic release signal than MC4100 ($p<0.001$) but there is no significant difference in whole cell lysis signal between the two strains when producing these β-lactamases ($p>0.05$; Figure 5.9b).

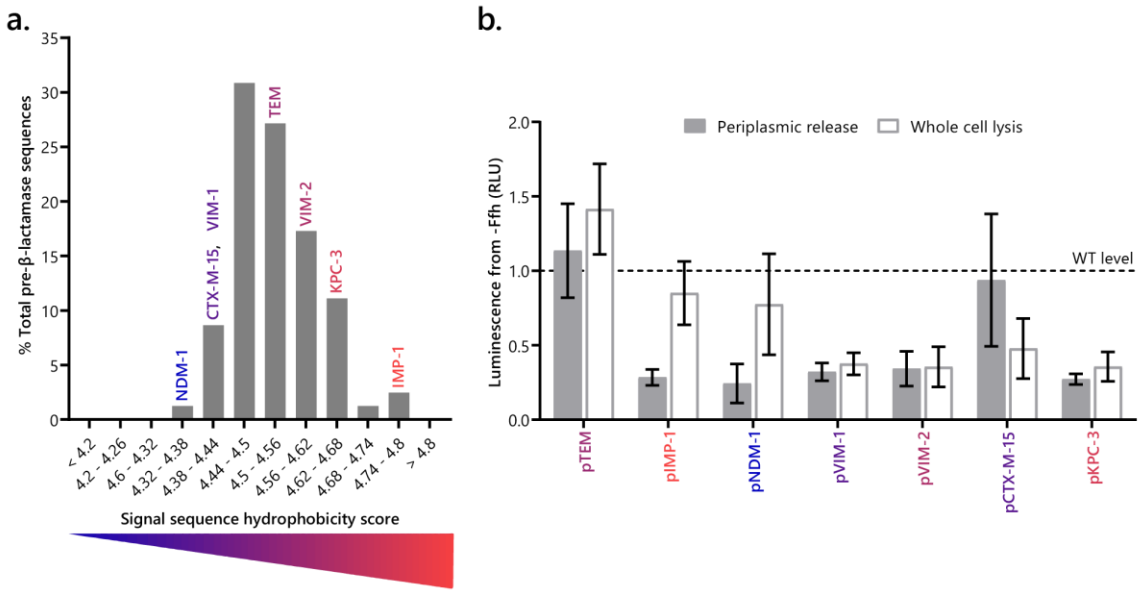


**Figure 5.9 Investigation of further β-lactamases reveals off-target effects of Ffh depletion**
**a.** Pre-β-lactamase SSs extracted from UniProt for this study. Each bar corresponds to the percentage of total extracted pre-β-lactamase sequences that have a given SS hydrophobicity. The approximate hydrophobicity scores of NDM-1, CTX-M-15, VIM-1, TEM, VIM-2, KPC-3 and IMP-1 SSs are indicated. **b.** LB cultures of MC4100 (WT) and WAM121 (-Ffh) carrying empty pCDFT (EV), or pCDFT encoding HiBiT-tagged constructs under $P_{Tac}$ (as indicated) were washed three times by resuspension in fresh LB then grown at 37 °C. Cultures were induced with 10 µM IPTG for 1.5 h, incubated at 4 °C for 1 h then diluted to $OD_{600}$ 0.5 in LB. LgBiT and furimazine (periplasmic release; solid bars) or LgBiT, furimazine and Triton X-100 (whole cell lysis; bars with outline only) were added. NanoLuc activity (luminescence) was measured for 5 min prior to and up to 1 h following addition of EDTA and lysozyme. The maximum luminescence for each sample was recorded and normalised to the maximum luminescence recorded for the respective MC4100 (WT) samples (dotted line at y = 1.0). Data from three independent experiments are shown as mean ± standard deviation.

In stark contrast to the first subset of β-lactamase constructs tested, the second set all yield lower whole cell signal when produced in WAM121 compared to MC4100 (pVIM-1-HiBiT 0.38±0.074 RLU, $p=0.005$; pVIM-2-HiBiT 0.36±0.13 RLU, $p=0.01$; pCTX-M-15-HiBiT 0.48±0.20 RLU, $p=0.05$; pKPC-3-HiBiT 0.36±0.10, $p=0.008$; Figure 5.9b). This suggests that their biogenesis is dependent on SRP, either at the level of protein synthesis or pre-protein stability in the cytoplasm. WAM121 producing HiBiT-tagged pVIM-1, -2 and pKPC-3 all give lower periplasmic signal than MC4100 (0.32±0.060 RLU, $p=0.003$; 0.34±0.12 RLU, $p=0.01$; 0.27±0.036 RLU, $p<0.001$, respectively)

consistent with their relatively low whole cell signal. By contrast, the periplasmic accumulation of CTX-M-15-HiBiT does not differ significantly in Ffh-depleted bacteria compared to MC4100 (0.94±0.45 RLU, p>0.05). This suggests that accumulation of this protein in the periplasm is uncoupled from its accumulation in the cell as a whole, consistent with a post-translational translocation mechanism. Overall, the data from testing further β-lactamases suggest that the effects of SRP on β-lactamase biogenesis are not clear cut, and inhibition by mutation has off-target effects that complicate interpretations of translocation pathway.

## 5.7 Response of β-lactamases to chemical inhibition of Sec measured by NanoBiT

Given the dramatic effects of mutating essential genes in bacteria, attention was turned to chemical inhibition of these machineries. Known inhibitors of the Sec-machinery, CJ-21058 and CCCP, were added to cultures of MC4100 carrying HiBiT-tagged β-lactamase constructs at the same time as induction. High concentrations of CJ-21058 (>50 µM) were needed to reduce luminescent signal upon periplasmic release for all three of pTEM, pIMP-1 and pNDM-1 (Figure 5.10a). At concentrations >250 µM, addition of CJ-21058 also diminished luminescent signal from whole cell lysis – as before with pSpy-HiBiT, this is due to the high DMSO concentrations needed to retain CJ-21058 in solution. The plots of maximum luminescence upon periplasmic release with increasing CJ-21058 concentrations for each β-lactamase were used to calculate the $IC_{50}$ for each enzyme. The CJ-21058 $IC_{50}$ for export of pIMP-1-HiBiT is 123.6 µM and for pNDM-1-HiBiT is 102.9 µM. These values are comparable, with 95% CI of 108.1 – 140.5 µM and 90.7 – 115.7 µM, respectively. Contrastingly, the $IC_{50}$ for pTEM-HiBiT is higher at 202.9 µM CJ-21058 (95% CI 186.3 – 220.6 µM), suggesting it is less sensitive to SecA inhibition.

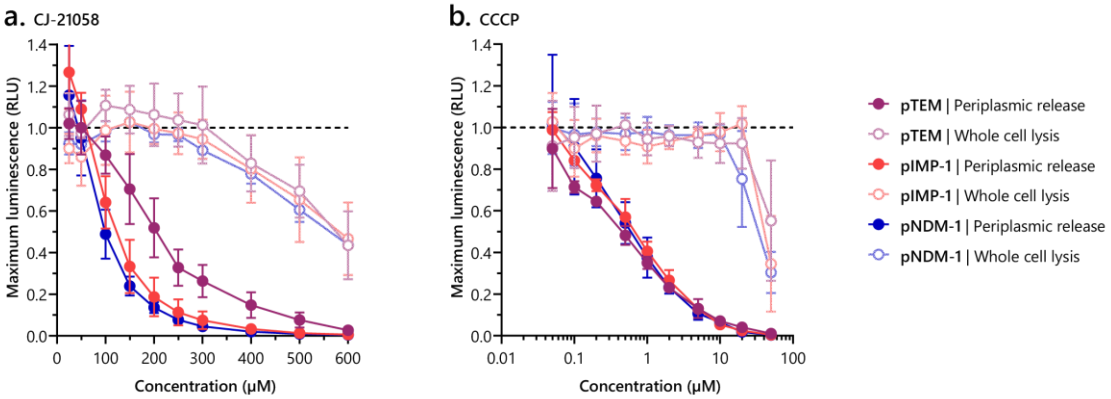


**Figure 5.10 Export of β-lactamase is sensitive to SecA inhibitor CJ-21058 and proton motive force uncoupler CCCP**
LB cultures of MC4100 carrying pCDFT encoding HiBiT-tagged pTEM (purple), pIMP-1 (red) or pNDM-1 (blue) under $P_{Tac}$ (as indicated) were diluted to $OD_{600}$ 0.05 in LB supplemented with **a.** CJ-21058 or **b.** CCCP at a range of concentrations, induced with 10 µM IPTG for 1.5 h then incubated at 4 °C for 1 h. LgBiT and furimazine (periplasmic release; filled circles) or LgBiT, furimazine and Triton X-100 (whole cell lysis; open circles) were added. NanoLuc activity (luminescence) was measured for 5 min prior to and up to 1 h following addition of EDTA and lysozyme. The maximum luminescence for each sample was recorded and normalised to the

maximum luminescence recorded for the respective untreated sample. Data from three independent experiments are shown as mean ± standard deviation.

The luminescent signal upon periplasmic release of MC4100 producing HiBiT-tagged β-lactamase exhibits a dose-dependent response to treatment with CCCP (Figure 5.10b). At concentrations >0.05 μM, luminescent signal begins to decrease and [CCCP] ≥50 μM abolishes the signal. HiBiT-tagged pTEM, pIMP-1 and pNDM-1 have comparable CCCP $IC_{50}$ values of 0.44 μM (95% CI 0.37 – 0.54 μM), 0.66 μM (95% CI 0.58 – 0.76 μM) and 0.63 μM (95% CI 0.45 – 0.87 μM) respectively. By contrast, the dose response curve of luminescence upon whole cell lysis is shifted to the right; concentrations >10 μM are needed to reduce whole cell lysis signal, then signal rapidly declines with increasing concentration. Therefore [CCCP] up to 10 μM have a specific inhibitory effect on periplasmic accumulation of β-lactamase-HiBiT, but total protein produced is unaffected by CCCP up to this concentration. This inhibition suggests that all three β-lactamases are similarly dependent on an intact PMF for translocation. However, at higher concentrations, CCCP impairs other cellular functions such as respiration so has a non-specific effect on the assay.

## 5.8 Discussion

The observed sensitivities of TEM, IMP-1 and NDM-1 to SecA inhibitor demonstrate that they each require the core Sec-machinery (SecA) for full transport in *E. coli*. This supports bioinformatic predictions of their translocation pathway asserting that they are unlikely to be translocated by the Tat-machinery due to absence of a twin-arginine motif. As enzymes encoded on mobile elements, the TEM, IMP-1 and NDM-1 β-lactamases studied here follow the tendency for mobilisable β-lactamases to utilise Sec (Pradel *et al.*, 2009). Nevertheless, while the data presented here demonstrate the requirement of Sec for translocation of these enzymes, they cannot rule out the possibility that Tat also plays a role as seen for BKC-1 (Bharathwaj *et al.*, 2021).

**Table 5.2 Summary of signal sequence hydrophobicity and SRP dependence of β-lactamase constructs**

| β-lactamase | Signal sequence hydrophobicity score | SRP-dependent? | |
|---|---|---|---|
| | | NanoBiT assay | Nitrocefin assay |
| TEM | 4.60 | No | Yes |
| IMP-1 | 4.76 | Yes | Yes |
| NDM-1 | 4.37 | Yes | Yes |
| IMP-1 with NDM-1 SS | 4.37 | No | ND |
| NDM-1 with IMP-1 SS | 4.76 | No | ND |

Abbreviations: SS, signal sequence; ND, not determined.

The SRP dependence of β-lactamases, determined by depletion of the protein component of SRP (Ffh), is summarised in Table 5.2. When measured by NanoBiT, the translocation of TEM into the periplasm is entirely independent of SRP, consistent with previous reports of TEM interaction with alternative chaperone pathways (Wild *et al.*, 1996; Kusakawa *et al.*, 1989; Zahn & Plückthun, 1992)

and the post-translational timing of TEM translocation (Josefsson & Randall, 1981). By contrast, NanoBiT assays of protein translocation highlight the specific decrease in periplasmic accumulation of native IMP-1 and NDM-1 upon depletion of Ffh. The IMP-1 SS is more hydrophobic than the model SecA- and SRP-dependent periplasmic protein DsbA, so the observed SRP dependence of this protein is expected. However, NDM-1 – which possesses a signal sequence with substantially lower hydrophobicity than the post-translational Sec substrate TEM – also relies on SRP for optimal translocation. This is contrary to previous studies stipulating that secretory proteins dependent on SRP require highly hydrophobic signal sequences (Schierle et al., 2003; Zhou, Ueda & Müller, 2014) and indicates that signal sequence hydrophobicity is not the sole predictor of SRP dependence. The NDM-1 SS has a unique structure, with a long n-region possessing a negatively charged residue (Zalucki *et al.*, 2020). This may explain why it behaves as an exception to the SS hydrophobicity rule.

Given the negligeable number of pre-secretory proteins that co-translationally interact with SRP – just 6% of proteins destined for the periplasm or outer membrane in *E. coli* (Schibich *et al.*, 2016) – it is unlikely that IMP-1 and NDM-1 are *bona fide* substrates of the SRP pathway. Ribosome profiling studies in bacteria producing IMP-1 or NDM-1 would confirm whether they are SRP substrates, or co-translational SecA substrates hindered by SRP deletion as seen for DsbA (Schierle *et al.*, 2003; Schibich *et al.*, 2016; Zhu, Wang & Shan, 2022).

When IMP-1 and NDM-1 SSs are switched, both β-lactamases are rendered insensitive to Ffh depletion, further supporting that SS alone does not determine SRP dependence (Table 5.2). The results from chimeric variants also indicate that the NDM-1 SS is sub-optimal for IMP-1 targeting to translocation. On the other hand, maximal transport of NDM-1 occurs with both its own SS and the IMP-1 SS. The recently established hierarchy of Sec substrate targeting pathways provides an explanation for these results. On this hierarchy, pre-proteins most in need of targeting to translocation during translation are SRP substrates, followed by co-translational SecA substrates and finally post-translational Sec substrates (Zhu, Wang & Shan, 2022). The timing of co-translational SecA engagement exists on a spectrum of early to late translation, with later co-translational and post-translational SecA substrates engaging Trigger Factor first. Deletion of *tig*, encoding Trigger Factor, causes translocation of post-translational SecA substrates to become more co-translational. Given the limited pool of cytoplasmic SecA, this reduces the availability of SecA for its native co-translational substrates (Zhu, Wang & Shan, 2022). Reciprocally, it is expected that SRP depletion would redirect the available pool of SecA to SRP-dependent substrates, rendering the translocation of co-translational SecA substrates more post-translational. As a post-translational SecA substrate, TEM is unaffected by the absence of SRP. On the other hand, IMP-1 and NDM-1 are likely co-translational substrates (either of SRP or SecA). Targeting mediated by the IMP-1 SS may occur sooner than that of NDM-1, and the mature domain of IMP-1 may be incompatible with the more post-translational mode of targeting enforced by the NDM-1 SS. Further delays in nIMP-1 targeting upon SRP depletion may be negligeable compared to those due to the SS switch. Conversely, SS switch would render the targeting of NDM-1 more co-translational, and the maximal amount of translocation-competent protein still reaches Sec. A shift to more post-

translational targeting would not impact translocation efficiency of iNDM-1, as the passenger β-lactamase is not strictly dependent on this degree of co-translational targeting. In this manner, it is the mature domain of the protein that determines dependence on SRP/ co-translational targeting but the SS that ensures targeting by the correct pathway.

It is proposed that the SS co-evolved with the folding kinetics of the mature domain of a pre-protein. Only the most rapid-folding substrates, strictly dependent on a certain level of co-translational targeting, utilise a co-translational pathway (Schierle *et al.*, 2003; Huber *et al.*, 2005b; Zhu, Wang & Shan, 2022). To further assess this hypothesis, absolute contact order for TEM, IMP-1 and NDM-1 were calculated as described by Zhu, Wang & Shan (2022). Absolute contact order provides a measure of primary sequence separation between all contacting residues in the native state; proteins with a lower absolute contact order have a propensity to fold more quickly (Plaxco, Simons & Baker, 1998). Based on AlphaFold predictions for their pre-secretory forms (Jumper *et al.*, 2021), IMP-1 (14.03) and NDM-1 (14.96) have a far lower absolute contact order than TEM (25.45). The IMP-1 and NDM-1 values are more in line with absolute contact order for more co-translational SecA substrates (~20) versus substrates that engage Trigger Factor first (~30) according to previous analyses (Zhu, Wang & Shan, 2022). Calculated absolute contact order of these β-lactamases (IMP-1 lowest, TEM highest) also correlate with SRP dependence as interpreted from NanoBiT data (IMP-1 most dependent, TEM least dependent). This suggests that protein folding propensity is a better predictor of SRP dependence compared to SS hydrophobicity.

It is important to note that studies comparing translocation of pre-secretory proteins in secretion mutants of *E. coli* are prone to off-target effects. For example, SecY is inserted into the cytoplasmic membrane using SRP (Koch et al., 1999). The Ffh depletion strain used in this study may therefore possess fewer active Sec translocons than wildtype *E. coli*, which could in turn impair translocation of β-lactamase regardless of SRP dependence or independence of the β-lactamase itself. The data presented above demonstrate that this is not the case, as known SRP-independent β-lactamase TEM is unaffected by Ffh depletion in the NanoBiT assay.

The NanoBiT counter assay uncovers off-target effects that affect whole cell levels of protein. The counter assay revealed that wildtype *E. coli* does not stably express mature β-lactamase constructs (mTEM, mIMP-1 or mNDM-1) compared to the full, pre-secretory form. This was seen previously, although to a smaller extent, with model protein Spy used to establish the NanoBiT assay. Cytoplasmic proteases such as Lon recognise and degrade aberrant, untranslocated secretory proteins (Jiang, Wynne & Huber, 2021). Aggregation and subsequent degradation of cytoplasmic mTEM, mIMP-1 and mNDM-1 likely explains the observed low levels of these constructs. On the other hand, whole cell levels of mature β-lactamase constructs are higher in Ffh-depleted *E. coli* compared to the wildtype. This difference is particularly striking for IMP-1. Translocation defects due to lack of SRP will cause accumulation of untranslocated Sec substrates in the cytoplasm, which could saturate protease systems. This would increase retention of the mature β-lactamase constructs. Importantly, NanoBiT counter assays revealed that, unlike TEM, IMP-1 and NDM-1, the

whole cell levels of VIM-1, -2, CTX-M-15 and KPC-3 are all reduced in Ffh-depleted cells. This confounds judgement of SRP dependence from NanoBiT data for these proteins.

NanoBiT assays are less prone to off-target effects than more traditional assays for β-lactamase export, namely antibiotic susceptibility testing and nitrocefin assays. This newer system provides a direct measure of protein translocation, independent of folding of the protein of interest. By contrast, traditional systems give readouts of β-lactamase export based on β-lactamase activity. For some β-lactamases, folding and full activity require disulfide bridges (Furniss *et al.*, 2021). A major constituent of the disulfide bridge formation system, DsbA, is SRP-dependent (Schierle *et al.*, 2003). Thus, depletion of Ffh would have the additional effect of inhibiting disulfide bridge formation. In their mature domain, IMP-1 and NDM-1 only have one cysteine available for oxidation. However, TEM has two such residues and has been shown to contain a disulfide bond in its mature form (Pollitt & Zalkin, 1983). The disulfide bridge of TEM-1 is important for its function under stress conditions (Schultz et al., 1987) and inhibition of the disulfide bridge formation system has been shown to increase β-lactam susceptibility of an *E. coli* strain carrying TEM-15 (Furniss et al., 2021). A decrease in periplasmic DsbA may explain the apparent reduction of periplasmic TEM in Ffh-depleted *E. coli* when measured by nitrocefin hydrolysis activity, while NanoBiT assays show no such reduction.

Upon periplasmic extraction for nitrocefin assays, TEM and IMP-1 are found in the supernatant while NDM-1 activity localises to the insoluble fraction. Nitrocefin hydrolysis activity of the soluble fraction from *E. coli* producing NDM-1 does not differ significantly from *E. coli* without β-lactamase. This is consistent with reports than mature NDM-1 exists as a membrane-anchored lipoprotein (González *et al.*, 2016). This characteristic of NDM-1 did not impair detection of the protein by NanoBiT assay, demonstrating the adaptability of the assay to lipoproteins as well as soluble Sec substrates.

The results presented here give an insight into how translocation inhibitors could be developed to combat β-lactamases. The sensitivity of all β-lactamases tested to CJ-21058 demonstrates that SecA, or the core Sec-machinery more generally, could be targeted to attenuate a broad range of β-lactamases. The reduced sensitivity of TEM to SecA inhibitor CJ-21058, compared to IMP-1 and NDM-1, suggests that there may be substrate-specific differences in SecA-dependence. This may be related to the post-translational nature of TEM transport, compared to the predicted co-translational targeting of IMP-1 and NDM-1. Each of these proteins also exhibited sensitivity to PMF uncoupler CCCP, suggesting that proteins responsible for coupling PMF to the Sec-machinery are also a promising anti-β-lactamase target. Given the SRP independence of periplasmic accumulation of TEM and CTX-M-15, compounds targeting SRP are less likely to be broad-spectrum inhibitors of β-lactamase translocation.

# Chapter 6 Concluding remarks and future perspectives

## 6.1 Objective 1: Develop a screening strategy for inhibitors of protein translocation by the bacterial Sec-machinery

Chapter 3 presents the design of a primary assay reporting on Sec inhibition *in vivo* and a counter assay for non-specific inhibitors. These assays can be performed in parallel on the same samples (split into two plates at time of assay) and are both scalable to high throughput. Bacterial growth in these same samples can also be assessed by measuring $OD_{600}$. This could serve as an extra level of selection – for translocation inhibitors that also inhibit growth – or inform on possible mechanisms of observed non-specific activity, as seen for CCCP. The primary assay yields a robust screen, giving a median Z'-factor of 0.71 across over 60 plates and 5000 small synthetic compounds. The primary hit rate was 0.22%, comparable with previous screen approaches (Moir *et al.*, 2011; Crowther *et al.*, 2015; Hamed *et al.*, 2021), and dose response and counter assay confirmed specific activity in four hits (36% of all primary hits). The built-in counter assay and adaptability of NanoBiT technology to any Sec substrate of interest are the major benefits of this screening strategy over previous approaches.

A fully developed screening strategy requires suitably matched secondary assays. Previous approaches to Sec inhibitor discovery were reviewed, allowing establishment of a set of essential inhibitor properties that should be examined in a successful screening approach: i) direct interaction with Sec *in vitro*; ii) lack of off-target effects; and iii) cellular activity. The primary assay confirms cellular activity, in that hit compounds impede translocation in whole cells. Traditional antibiotic susceptibility testing was employed to ascertain antibacterial activity. The majority of Chapter 4 focused on evaluation of the suitability of two different *in vitro* translocation assay systems as secondary assays for direct inhibitor-target interaction. The protease protection system has been employed in previous Sec inhibitor discovery work (Segers *et al.*, 2011; Huang *et al.*, 2012), is sensitive to specific inhibitors of the Sec-machinery and insensitive to inhibitors of the primary screen readout (NanoLuc luminescence). This system is determined to be a suitable complementary assay in the present screening strategy. By contrast, *in vitro* NanoBiT assays displayed insensitivity to SecA inhibitor and non-specific, PMF-independent sensitivity to CCCP. Due to time constraints, it was not possible to explore methods – beyond counter assay – to determine off-target effects of hit compounds, however established techniques exist for analysing membrane integrity/ PMF dissipation upon inhibitor treatment (Novo *et al.*, 1999; Alksne *et al.*, 2000). The more bespoke assays developed in this work, alongside previously established assays, give an overall robust strategy for Sec inhibitor discovery.

## 6.2 Objective 2: Investigate the role of the Sec-machinery in a major mechanism of antibiotic resistance

The use of antibiotic adjuvants or cocktails of antibiotics that synergise with each other is an increasingly popular approach for preserving the antibiotic arsenal (González-Bello, 2017). The Sec-machinery is responsible for correct localisation of over 90% of extracytoplasmic proteins in *E. coli* (Orfanoudaki & Economou, 2014; Tsirigotaki *et al.*, 2017). This includes virulence factors and proteins involved in antibiotic resistance, including an estimated over 80% of β-lactamases (Pradel *et al.*, 2009). There are a range of different pathways for protein translocation through Sec, which may result in inhibitor selectivity for certain types of Sec substrate, as seen for inhibitors of eukaryotic Sec61 (Van Puyenbroeck & Vermeire, 2018; Klein *et al.*, 2018b). Therefore, understanding the precise pathways taken by clinically relevant β-lactamases will help determine which Sec inhibitors will be useful β-lactam adjuvants. As SS has a major impact on the fitness cost of β-lactamase production (Socha, Chen & Tokuriki, 2019; Zalucki *et al.*, 2020), knowledge of a β-lactamase's requirements for translocation would also help anticipate its spread across pathogenic species.

Besides the observation that mobilisable β-lactamases tend to require the Sec-machinery for export, no relationship has been found between an enzyme's host range and its SS characteristics (Pradel *et al.*, 2009; Socha, Chen & Tokuriki, 2019). Similarly, the present study found that β-lactamase SS hydrophobicities do not cluster based on the species from which the enzymes were first isolated. If SS hydrophobicity of Sec substrates does determine targeting by SecA or SRP, then this would suggest that Sec targeting pathway does not influence dissemination or host compatibility. Given the strong conservation of all targeting factors Trigger Factor, SecA and SRP across Gram-negative species (Oliver & Beckwith, 1981; Phillips & Silhavy, 1992; Lyon, Gibson & Caparon, 1998; Rao *et al.*, 2014), this is not surprising.

However, the present study could not confirm a correlation between SS and SRP dependence. Of the three β-lactamases assessed in detail, all exhibit SecA dependence for translocation, but only two (IMP-1 with highly hydrophobic SS and NDM-1 with weakly hydrophobic SS) require SRP for maximal translocation. For the third, TEM with moderately hydrophobic SS, removal of SRP indirectly affected active levels of β-lactamase, likely due to inhibition of the DSB system (Schierle *et al.*, 2003; Furniss *et al.*, 2021). These findings indicate that SecA inhibitors are more likely to be broad-spectrum inhibitors of β-lactamase translocation, but SRP inhibitors may prove useful on a subset of enzymes.

It would be useful to predict from a β-lactamase's primary sequence whether it is susceptible to SRP inhibition. For the limited number of β-lactamases tested in this work, SS hydrophobicity proved to be a poor indicator of SRP dependence. A stronger relationship was observed between SRP dependence and folding kinetics. It has been suggested that rapid-folding Sec substrates evolve SRP dependence or more co-translational translocation to prevent folding in the cytoplasm (Schierle *et al.*, 2003). In turn, these substrates likely evolved more hydrophobic SSs to strengthen

recognition by targeting factors. Thus, the relationship between folding kinetics and SRP dependence is more direct than that between SS hydrophobicity and SRP dependence. Historically, bioinformatic prediction of folding kinetics was not as accessible as assessing SS hydrophobicity. Folding kinetics can be accurately estimated based on contact order in the protein's native structure (Plaxco, Simons & Baker, 1998). While previously, this required structural determination of the protein, this can now be calculated based on primary sequence through use of AlphaFold (Jumper *et al.*, 2021; Zhu, Wang & Shan, 2022). Using this novel tool, future work should investigate further whether folding kinetics is a better predictor of targeting pathway to Sec.

## 6.3 Overarching aim: Establish the bacterial Sec-machinery as a promising antibiotic target and guide future discovery and development of Sec inhibitors

The work presented here further strengthens the body of work that claims the Sec-machinery is a promising antibiotic target. Chapters 3 and 4 demonstrate that the Sec-machinery has screenable activity, particularly in whole cells, and establish a diverse toolkit of assays for Sec activity to facilitate identification and development of Sec-specific antibiotics. Chapter 5 underscores the critical role of the Sec-machinery in mediating a major mechanism of antibiotic resistance, paving the way for development of antibiotic cocktails based on Sec inhibition.

While the primary objective of chapters 3 and 4 is screen design, exploration of secondary assays gave insights into the mechanisms of established and putative inhibitors of Sec. All four hits discovered in this work have comparable size (370, 398, 330 and 420 Da for Hit2, 3, 4 and 5, respectively) to known SecA inhibitor CJ-21058 (388 Da) and are similarly poorly soluble in water (limited solubility at 400 - 800 µM). All hits are over ten times more active against translocation in live *E. coli* cells, when measured by primary assay, than CJ-21058 ($IC_{50}$ 5.23, 6.79, 16.1, 12.2 µM for Hit2, 3, 4 and 5, respectively, and CJ-21058 $IC_{50}$ 227.1 µM). By contrast, when assessed in Chapter 4 for their ability to inhibit pOmpA translocation *in vitro*, all hit compounds were less active than CJ-21058 against PLs. Against IMVs, Hit2 and 3 brought about similar levels of inhibition to CJ-21058, but Hit4 and 5 were noticeably less active than the SecA inhibitor. For Hit2 and 3, this suggests that their activity is dependent on the native environment of Sec.

Consistent with the potent anti-Gram-positive activity of CJ-21058 (Sugie *et al.*, 2002), the current work demonstrated that CJ-21058 activity is restricted by the presence of the Gram-negative outer membrane – this compound has greater activity against outer membrane-permeable NR698. By contrast, all four hits have comparable activity against wildtype and outer membrane-deficient *E. coli*. This could suggest that, unlike CJ-21058, these novel compounds are not limited by permeation across the outer membrane. This is consistent with the fact they were discovered in a whole cell screen. However, despite their inhibitory activity in the primary assay, none of these compounds have a measurable MIC against *E. coli*.

Assessing the degree of Sec inhibition by CCCP at approximately MIC levels, it is hypothesised that a threshold level of Sec inhibition is necessary for antibacterial effects. Similar suggestions have been made in previous Sec inhibitor studies (Crowther *et al.*, 2015). According to data presented here, bacteria may be viable with as low as 1% Sec capacity. To test this hypothesis further, it would be useful to assess the level of protein translocation inhibition in NR698 cells treated with CJ-21058 at its MIC. Insights into how much protein translocation inhibition is needed to inhibit bacterial growth are crucial to future discovery and development of Sec inhibitors as antibiotics.

While around 1% protein translocation capacity may be sufficient to support cell growth, such low levels of β-lactamase export are unlikely to sustain β-lactam resistance. Multiple studies have shown that sub-lethal reductions in protein translocation can significantly reduce β-lactamase-mediated resistance (Mcdonough *et al.*, 2005; Morán-Barrio, Limansky & Viale, 2009; Pradel *et al.*, 2009; Liao *et al.*, 2015; Chiu *et al.*, 2016). The present work supplements such studies, showing that inhibition of Sec reduces extracytoplasmic β-lactamase activity of *E. coli* producing the clinically important MBLs IMP-1 and NDM-1. This confirms that Sec inhibitor development is a viable method for re-potentiating important β-lactam drugs. Future work into protein translocation inhibitors as β-lactam adjuvants should determine the degree of translocation inhibition required to significantly decrease β-lactam resistance. The whole cell NanoBiT assay is unique in that provides a fully quantitative and direct measure of translocation, independent of substrate protein folding or activity. This assay should therefore be utilised in concert with antibiotic susceptibility testing to answer this important research question. In turn, these findings will improve Sec inhibitor discovery pipelines by providing an empirical minimum threshold for a hit.

# Chapter 7 Appendices

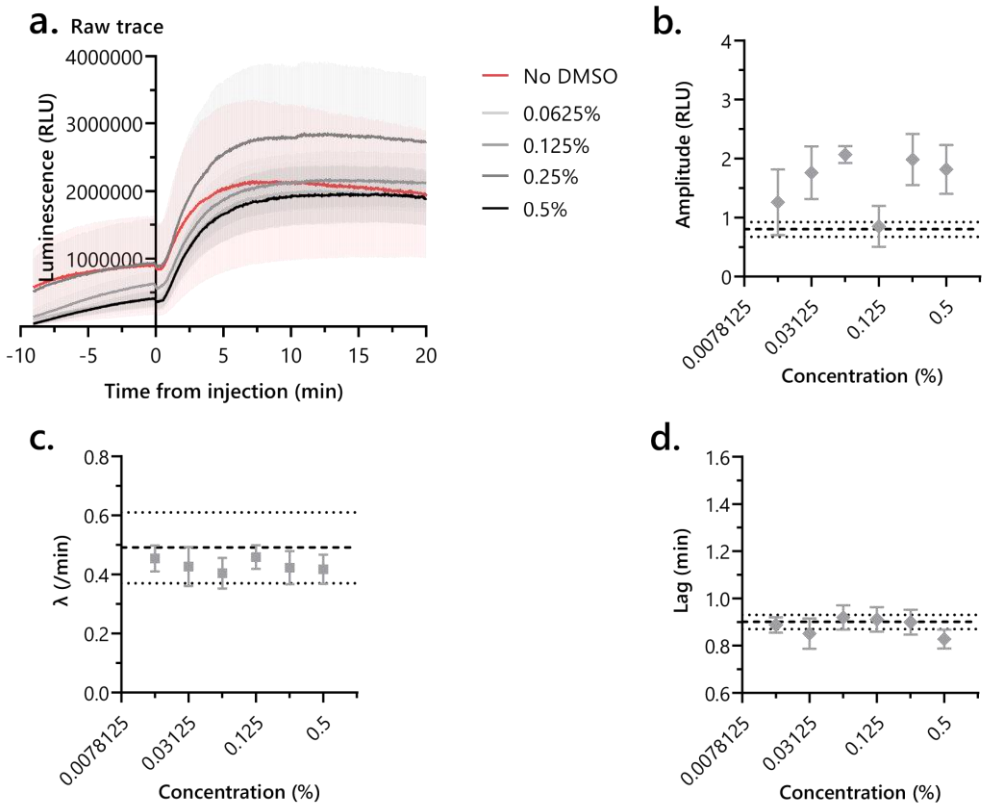


**Appendix 1 Activity of DMSO assessed by *in vitro* NanoBiT assay**
Proteoliposomes containing SecYEG and LgBiT were combined with purified SecA, ATP regeneration reagents, furimazine, translocation-competent pSpy-HiBiT and varying concentrations of DMSO. Luminescence was measured for approximately 10 min prior to, and 20 min after, reaction initiation by injection of ATP. Signal traces shown in **a.** were normalised by background amplitude, time-corrected and fit to the equation shown in Figure 4.1. **b.** Amplitude, **c.** λ and **d.** lag are shown over different concentrations of DMSO. Data from three technical replicates are shown as mean ± SEM. Data from untreated controls are shown as dashed (mean) and dotted (± SEM) black lines.

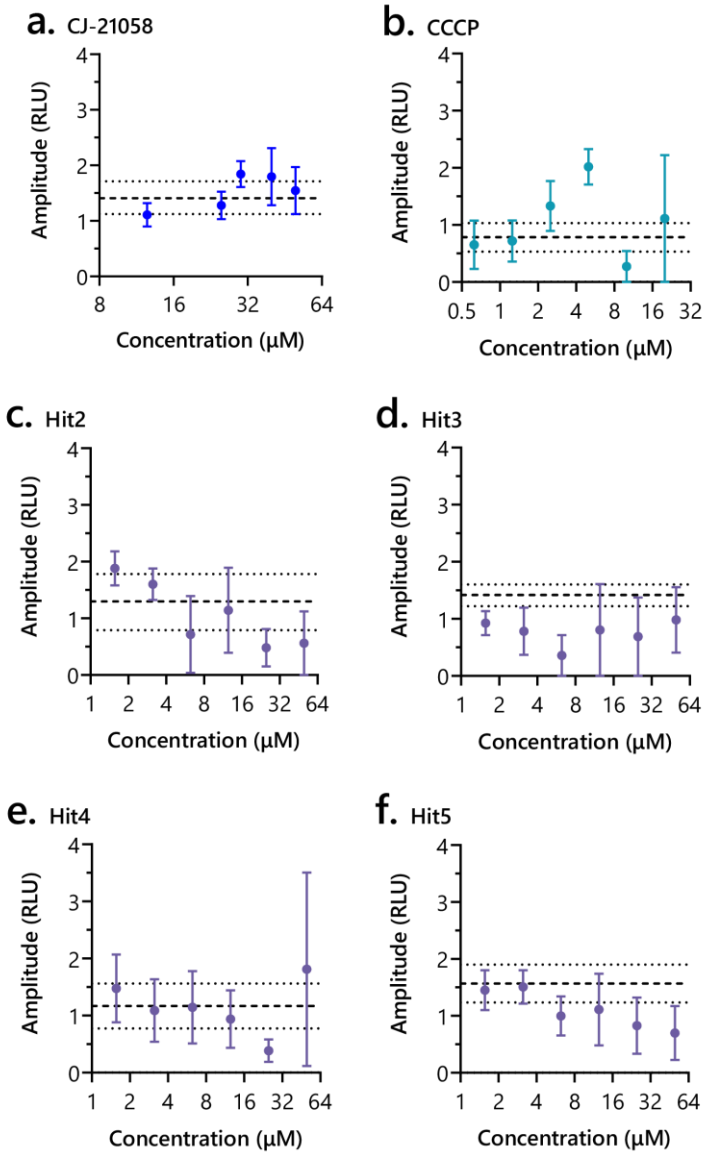


**Appendix 2 Fits of control and hit activity on *in vitro* NanoBiT amplitude**
Signal traces shown in Figure 4.3 were normalised by background amplitude, time-corrected and fit to the equation shown in Figure 4.1. Amplitude is shown over different concentrations of each compound: **a.** CJ-21058, **b.** CCCP, **c.** Hit2, **d.** Hit3, **e.** Hit4 and **f.** Hit5. Data from three technical replicates are shown as mean ± SEM. Data from untreated controls are shown as dashed (mean) and dotted (± SEM) black lines.

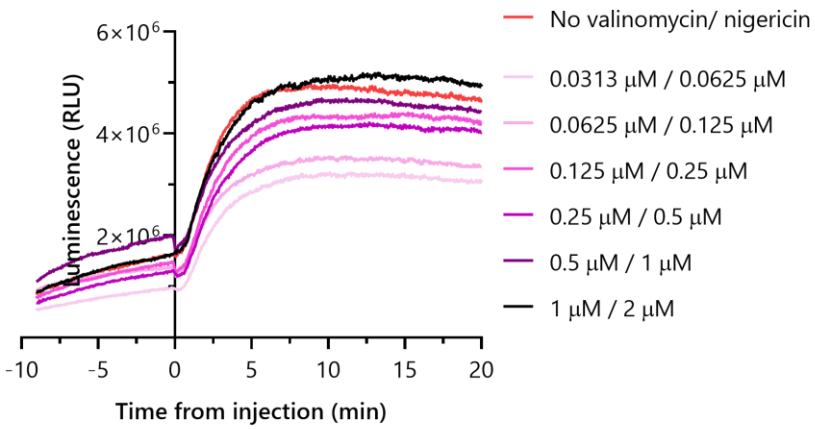


**Appendix 3 Activity of valinomycin/ nigericin assessed by *in vitro* NanoBiT assay**
Proteoliposomes containing SecYEG and LgBiT were combined with purified SecA, ATP regeneration reagents, furimazine, translocation-competent pSpy-HiBiT and varying concentrations of valinomycin and nigericin in a 1:2 ratio. Luminescence was measured for approximately 10 min prior to, and 20 min after, reaction initiation by injection of ATP. Data from one replicate are shown.

# Chapter 8 References

Abraham, E.P. & Chain, E. (1940) An enzyme from bacteria able to destroy penicillin. *Nature*. [Online] 146, 837. Available from: doi:10.1038/146837a0.

Akula, N., Trivedi, P., Han, F.Q. & Wang, N. (2012) Identification of small molecule inhibitors against SecA of *Candidatus Liberibacter asiaticus* by structure based design. *European Journal of Medicinal Chemistry*. [Online] 54, 919–924. Available from: doi:10.1016/J.EJMECH.2012.05.035.

Akula, N., Zheng, H., Han, F.Q. & Wang, N. (2011) Discovery of novel SecA inhibitors of *Candidatus Liberibacter asiaticus* by structure based design. *Bioorganic & Medicinal Chemistry Letters*. [Online] 21 (14), 4183–4188. Available from: doi:10.1016/J.BMCL.2011.05.086.

Alami, M., Dalal, K., Lelj-Garolla, B., Sligar, S.G., et al. (2007) Nanodiscs unravel the interaction between the SecYEG channel and its cytosolic partner SecA. *The EMBO Journal*. [Online] 26 (8), 1995. Available from: doi:10.1038/SJ.EMBOJ.7601661 [Accessed: 13 December 2022].

Alksne, L.E., Burgio, P., Hu, W., Feld, B., et al. (2000) Identification and analysis of bacterial protein secretion inhibitors utilizing a SecA-LacZ reporter fusion system. *Antimicrobial Agents and Chemotherapy*. [Online] 44 (6), 1418–1427. Available from: doi:10.1128/AAC.44.6.1418-1427.2000 [Accessed: 24 August 2020].

Allen, W.J., Corey, R.A., Oatley, P., Sessions, R.B., et al. (2016) Two-way communication between SecY and SecA suggests a Brownian ratchet mechanism for protein translocation. *eLife*. [Online] 5 (MAY2016), e15598. Available from: doi:10.7554/eLife.15598 [Accessed: 8 October 2018].

Allen, W.J., Corey, R.A., Watkins, D.W., Oliveira, A.S.F., et al. (2022) Rate-limiting transport of positively charged arginine residues through the Sec-machinery is integral to the mechanism of protein secretion. *eLife*. [Online] 11, 592543. Available from: doi:10.7554/ELIFE.77586 [Accessed: 26 May 2022].

Allen, W.J., Watkins, D.W., Dillingham, M.S. & Collinson, I. (2020) Refined measurement of SecA-driven protein secretion reveals that translocation is indirectly coupled to ATP turnover. *Proceedings of the National Academy of Sciences of the United States of America*. [Online] 117 (50), 31808–31816. Available from: doi:10.1073/pnas.2010906117 [Accessed: 2 June 2021].

Almagro Armenteros, J.J., Tsirigos, K.D., Sønderby, C.K., Petersen, T.N., et al. (2019) SignalP 5.0 improves signal peptide predictions using deep neural networks. *Nature Biotechnology*. [Online] 37 (4), 420–423. Available from: doi:10.1038/s41587-019-0036-z.

Ambler, R.P. (1980) The structure of beta-lactamases. *Philosophical transactions of the Royal Society of London. Series B, Biological sciences*. 289, 321–331.

Angelini, S., Boy, D., Schiltz, E. & Koch, H.G. (2006) Membrane binding of the bacterial signal

recognition particle receptor involves two distinct binding sites. *Journal of Cell Biology*. [Online] 174 (5), 715–724. Available from: doi:10.1083/JCB.200606093 [Accessed: 13 December 2022].

Arcari, G., Di Lella, F.M., Bibbolino, G., Mengoni, F., et al. (2020) A Multispecies Cluster of VIM-1 Carbapenemase-Producing Enterobacterales Linked by a Novel, Highly Conjugative, and Broad-Host-Range IncA Plasmid Forebodes the Reemergence of VIM-1. *Antimicrobial Agents and Chemotherapy*. [Online] 64 (4). Available from: doi:10.1128/AAC.02435-19 [Accessed: 29 September 2022].

Arkowitz, R.A., Joly, J.C. & Wickner, W. (1993) Translocation can drive the unfolding of a preprotein domain. *The EMBO journal*. [Online] 12 (1), 243–253. Available from: doi:10.1002/J.1460-2075.1993.TB05650.X [Accessed: 13 December 2022].

Arkowitz, R.A. & Wickner, W. (1994) SecD and SecF are required for the proton electrochemical gradient stimulation of preprotein translocation. *The EMBO Journal*. [Online] 13 (4), 954. Available from: doi:10.1002/J.1460-2075.1994.TB06340.X [Accessed: 15 November 2022].

Auclair, S.M., Moses, J.P., Musial-Siwek, M., Kendall, D.A., et al. (2010) Mapping of the signal peptide-binding domain of *Escherichia coli* SecA using förster resonance energy transfer. *Biochemistry*. [Online] 49 (4), 782–792. Available from: doi:10.1021/bi901446r.

Baars, L., Ytterberg, A.J., Drew, D., Wagner, S., et al. (2006) Defining the role of the *Escherichia coli* chaperone SecB using comparative proteomics. *Journal of Biological Chemistry*. [Online] 281 (15), 10024–10034. Available from: doi:10.1074/jbc.M509929200 [Accessed: 13 December 2022].

Balder, R., Shaffer, T.L. & Lafontaine, E.R. (2013) *Moraxella catarrhalis* uses a twin-arginine translocation system to secrete the β-lactamase BRO-2. *BMC Microbiology*. [Online] 13 (1), 140. Available from: doi:10.1186/1471-2180-13-140 [Accessed: 23 August 2022].

Bandara, M., Skehel, J.M., Kadioglu, A., Collinson, I., et al. (2017) The accessory Sec system (SecY2A2) in *Streptococcus pneumoniae* is involved in export of pneumolysin toxin, adhesion and biofilm formation. *Microbes and Infection*. [Online] 19 (7–8), 402–412. Available from: doi:10.1016/j.micinf.2017.04.003.

Barbosa, M.D.F.S., Lin, S., Markwalder, J.A., Mills, J.A., et al. (2002) Regulated Expression of the *Escherichia coli lepB* Gene as a Tool for Cellular Testing of Antimicrobial Compounds That Inhibit Signal Peptidase I In Vitro. *Antimicrobial Agents and Chemotherapy*. [Online] 46 (11), 3549. Available from: doi:10.1128/AAC.46.11.3549-3554.2002 [Accessed: 22 July 2022].

Bauer, B.W., Shemesh, T., Chen, Y. & Rapoport, T.A. (2014) A 'push and slide' mechanism allows sequence-insensitive translocation of secretory proteins by the SecA ATPase. *Cell*. [Online] 157 (6), 1416–1429. Available from: doi:10.1016/j.cell.2014.03.063.

Beha, D., Deitermann, S., Müller, M. & Koch, H.-G. (2003) Export of beta-lactamase is independent of the signal recognition particle. *The Journal of Biological Chemistry*. [Online] 278 (24),

22161–22167. Available from: doi:10.1074/jbc.M300929200.

Bensing, B.A. & Sullam, P.M. (2002) An accessory *sec* locus of *Streptococcus gordonii* is required for export of the surface protein GspB and for normal levels of binding to human platelets. *Molecular microbiology*. [Online] 44 (4), 1081–1094. Available from: doi:10.1046/J.1365-2958.2002.02949.X [Accessed: 13 December 2022].

Benson, R.E., Gottlin, E.B., Christensen, D.J. & Hamilton, P.T. (2003) Intracellular expression of peptide fusions for demonstration of protein essentiality in bacteria. *Antimicrobial Agents and Chemotherapy*. [Online] 47 (9), 2875–2881. Available from: doi:10.1128/AAC.47.9.2875-2881.2003.

Benveniste, R. & Davies, J. (1973) Aminoglycoside antibiotic-inactivating enzymes in actinomycetes similar to those present in clinical isolates of antibiotic-resistant bacteria. *Proceedings of the National Academy of Sciences of the United States of America*. [Online] 70 (8), 2276–2280. Available from: doi:10.1073/PNAS.70.8.2276 [Accessed: 13 December 2022].

Van Den Berg, B., Clemons, W.M., Collinson, I., Modis, Y., et al. (2004) X-ray structure of a protein-conducting channel. *Nature*. [Online] 427 (6969), 36–44. Available from: doi:10.1038/nature02218.

Berks, B.C. (1996) A common export pathway for proteins binding complex redox cofactors? *Molecular Microbiology*. [Online] 22 (3), 393–404. Available from: doi:10.1046/J.1365-2958.1996.00114.X [Accessed: 7 December 2022].

Bernstein, H.D., Zopf, D., Freymann, D.M. & Walter, P. (1993) Functional substitution of the signal recognition particle 54-kDa subunit by its *Escherichia coli* homolog. *Proceedings of the National Academy of Sciences of the United States of America*. [Online] 90 (11), 5229–5233. Available from: doi:10.1073/PNAS.90.11.5229 [Accessed: 13 December 2022].

Bharathwaj, M., Webb, C.T., Vadlamani, G., Stubenrauch, C.J., et al. (2021) The Carbapenemase BKC-1 from *Klebsiella pneumoniae* Is Adapted for Translocation by Both the Tat and Sec Translocons. *mBio*. [Online] 12 (3), e0130221. Available from: doi:10.1128/MBIO.01302-21 [Accessed: 11 October 2021].

Bielaszewska, M., Daniel, O., Nyč, O. & Mellmann, A. (2021) In Vivo Secretion of β-Lactamase-Carrying Outer Membrane Vesicles as a Mechanism of β-Lactam Therapy Failure. *Membranes*. [Online] 11 (11), 806. Available from: doi:10.3390/MEMBRANES11110806 [Accessed: 7 December 2021].

Black, M.T. (1993) Evidence that the catalytic activity of prokaryote leader peptidase depends upon the operation of a serine-lysine catalytic dyad. *Journal of Bacteriology*. [Online] 175 (16), 4957–4961. Available from: doi:10.1128/JB.175.16.4957-4961.1993 [Accessed: 14 December 2022].

Blobel, G. & Dobberstein, B. (1975) Transfer of proteins across membranes: I. Presence of

proteolytically processed and unprocessed nascent immunoglobulin light chains on membrane-bound ribosomes of murine myeloma. *Journal of Cell Biology*. [Online] 67 (3), 835–851. Available from: doi:10.1083/jcb.67.3.835.

Bochkareva, E.S., Solovieva, M.E. & Girshovich, A.S. (1998) Targeting of GroEL to SecA on the cytoplasmic membrane of *Escherichia coli*. *Proceedings of the National Academy of Sciences of the United States of America*. [Online] 95 (2), 478. Available from: doi:10.1073/PNAS.95.2.478 [Accessed: 9 September 2022].

Bogsch, E., Brink, S. & Robinson, C. (1997) Pathway specificity for a delta pH-dependent precursor thylakoid lumen protein is governed by a 'Sec-avoidance' motif in the transfer peptide and a 'Sec-incompatible' mature protein. *The EMBO Journal*. [Online] 16 (13), 3851. Available from: doi:10.1093/EMBOJ/16.13.3851 [Accessed: 7 December 2022].

Bonnefoy, N., Chalvet, F., Hamel, P., Slonimski, P.P., et al. (1994) *OXA1*, a *Saccharomyces cerevisiae* nuclear gene whose sequence is conserved from prokaryotes to eukaryotes controls cytochrome oxidase biogenesis. *Journal of Molecular Biology*. [Online] 239 (2), 201–212. Available from: doi:10.1006/jmbi.1994.1363 [Accessed: 10 November 2022].

Bonnett, S.A., Ollinger, J., Chandrasekera, S., Florio, S., et al. (2016) A Target-Based Whole Cell Screen Approach to Identify Potential Inhibitors of *Mycobacterium tuberculosis* Signal Peptidase. *ACS Infectious Diseases*. [Online] 2 (12), 893–902. Available from: doi:10.1021/ACSINFECDIS.6B00075/SUPPL_FILE/ID6B00075_SI_001.PDF [Accessed: 16 December 2022].

Bootsma, H.J., van Dijk, H., Verhoef, J., Fleer, A., et al. (1996) Molecular characterization of the BRO beta-lactamase of *Moraxella (Branhamella) catarrhalis*. *Antimicrobial Agents and Chemotherapy*. [Online] 40 (4), 966–972. Available from: doi:10.1128/AAC.40.4.966 [Accessed: 23 April 2020].

Botte, M., Zaccai, N.R., Nijeholt, J.L. à., Martin, R., et al. (2016) A central cavity within the holo-translocon suggests a mechanism for membrane protein insertion. *Scientific Reports*. [Online] 6 (1), 38399. Available from: doi:10.1038/srep38399.

Bowler, M.W., Montgomery, M.G., Leslie, A.G.W. & Walker, J.E. (2006) How azide inhibits ATP hydrolysis by the F-ATPases. *Proceedings of the National Academy of Sciences of the United States of America*. [Online] 103 (23), 8646. Available from: doi:10.1073/PNAS.0602915103 [Accessed: 15 July 2021].

Braunstein, M., Brown, A.M., Kurtz, S. & Jacobs, J. (2001) Two nonredundant SecA homologues function in mycobacteria. *Journal of Bacteriology*. [Online] 183 (24), 6979–6990. Available from: doi:10.1128/JB.183.24.6979-6990.2001 [Accessed: 13 December 2022].

Brem, J., Cain, R., Cahill, S., McDonough, M.A., et al. (2016) Structural basis of metallo-β-lactamase, serine-β-lactamase and penicillin-binding protein inhibition by cyclic boronates. *Nature Communications*. [Online] 7. Available from: doi:10.1038/NCOMMS12406 [Accessed:

29 July 2022].

Brundage, L., Hendrick, J.P., Schiebel, E., Driessen, A.J.M., et al. (1990) The purified *E. coli* integral membrane protein SecY/E is sufficient for reconstitution of SecA-dependent precursor protein translocation. *Cell*. [Online] 62 (4), 649–657. Available from: doi:10.1016/0092-8674(90)90111-Q.

De Buck, E., Lammertyn, E. & Anné, J. (2008) The importance of the twin-arginine translocation pathway for bacterial virulence. *Trends in Microbiology*. [Online] 16 (9), 442–453. Available from: doi:10.1016/J.TIM.2008.06.004.

Bush, K. & Bradford, P.A. (2020) Epidemiology of β-Lactamase-Producing Pathogens. *Clinical Microbiology Reviews*. [Online] 33 (2). Available from: doi:10.1128/CMR.00047-19 [Accessed: 15 December 2022].

Bush, K. & Bradford, P.A. (2016) β-Lactams and β-Lactamase Inhibitors: An Overview. *Cold Spring Harbor Perspectives in Medicine*. [Online] 6 (8), a025247. Available from: doi:10.1101/cshperspect.a025247.

Bush, K. & Fisher, J.F. (2011) Epidemiological Expansion, Structural Studies, and Clinical Challenges of New β-Lactamases from Gram-Negative Bacteria. *Annual Review of Microbiology*. [Online] 65, 455–478. Available from: doi:10.1146/annurev-micro-090110-102911.

Bush, K. & Jacoby, G.A. (2010) Updated functional classification of beta-lactamases. *Antimicrobial Agents and Chemotherapy*. [Online] 54 (3), 969–976. Available from: doi:10.1128/AAC.01009-09.

Bush, K., Jacoby, G.A. & Medeiros, A.A. (1995) A functional classification scheme for beta-lactamases and its correlation with molecular structure. *Antimicrobial agents and chemotherapy*. [Online] 39 (6), 1211–1233. Available from: doi:10.1128/AAC.39.6.1211 [Accessed: 15 December 2022].

Butler, M.S., Gigante, V., Sati, H., Paulin, S., et al. (2022) Analysis of the Clinical Pipeline of Treatments for Drug-Resistant Bacterial Infections: Despite Progress, More Action Is Needed. *Antimicrobial Agents and Chemotherapy*. [Online]. 66 (3). Available from: doi:10.1128/aac.01991-21 [Accessed: 8 September 2022].

Calloni, G., Chen, T., Schermann, S.M., Chang, H.C., et al. (2012) DnaK Functions as a Central Hub in the *E. coli* Chaperone Network. *Cell Reports*. [Online] 1 (3), 251–264. Available from: doi:10.1016/j.celrep.2011.12.007 [Accessed: 9 November 2022].

Calvopiña, K., Hinchliffe, P., Brem, J., Heesom, K.J., et al. (2017) Structural/mechanistic insights into the efficacy of nonclassical β-lactamase inhibitors against extensively drug resistant *Stenotrophomonas maltophilia* clinical isolates. *Molecular microbiology*. [Online] 106 (3), 492–504. Available from: doi:10.1111/MMI.13831 [Accessed: 29 July 2022].

Cao, T.B. & Saier, M.H. (2003) The general protein secretory pathway: phylogenetic analyses leading to evolutionary conclusions. *Biochimica et Biophysica Acta (BBA) - Biomembranes*. [Online] 1609 (1), 115–125. Available from: doi:10.1016/S0005-2736(02)00662-4.

Chatzi, K.E., Sardis, M.F., Tsirigotaki, A., Koukaki, M., et al. (2017) Preprotein mature domains contain translocase targeting signals that are essential for secretion. *Journal of Cell Biology*. [Online] 216 (5), 1357–1369. Available from: doi:10.1083/jcb.201609022.

Chaudhary, A.S., Jin, J., Chen, W., Tai, P.C., et al. (2015) Design, syntheses and evaluation of 4-oxo-5-cyano thiouracils as SecA inhibitors. *Bioorganic & Medicinal Chemistry*. [Online] 23 (1), 105–117. Available from: doi:10.1016/J.BMC.2014.11.017 [Accessed: 10 October 2022].

Chen, J.Z., Fowler, D.M. & Tokuriki, N. (2020) Comprehensive exploration of the translocation, stability and substrate recognition requirements in VIM-2 lactamase. *eLife*. [Online] 9, 1–31. Available from: doi:10.7554/eLife.56707.

Chen, W., Huang, Y. ju, Gundala, S.R., Yang, H., et al. (2010) The first low μM SecA inhibitors. *Bioorganic & Medicinal Chemistry*. [Online] 18 (4), 1617–1625. Available from: doi:10.1016/J.BMC.2009.12.074.

Cheung, C.H.P., Alorabi, M., Hamilton, F., Takebayashi, Y., et al. (2021) Trade-Offs Between Antibacterial Resistance and Fitness Cost in the Production of Metallo-β-Lactamases by Enteric Bacteria Manifest as Sporadic Emergence of Carbapenem Resistance in a Clinical Setting. *Antimicrobial Agents and Chemotherapy*. [Online] 2020.10.24.353581. Available from: doi:10.1128/aac.02412-20 [Accessed: 2 June 2021].

Chiu, C.-H., Liu, Y.-H., Wang, Y.-C., Lee, Y.-T., et al. (2016) In vitro activity of SecA inhibitors in combination with carbapenems against carbapenem-hydrolysing class D b-lactamase-producing *Acinetobacter baumannii*. *Journal of Antimicrobial Chemotherapy*. [Online] 71, 3441–3448. Available from: doi:10.1093/jac/dkw331.

Chun, S.-Y. & Randall, L.L. (1994) In vivo studies of the role of SecA during protein export in *Escherichia coli. Journal of Bacteriology*. 176 (14), 4197–4203.

Collignon, P.C., Conly, J.M., Andremont, A., McEwen, S.A., et al. (2016) World Health Organization Ranking of Antimicrobials According to Their Importance in Human Medicine: A Critical Step for Developing Risk Management Strategies to Control Antimicrobial Resistance from Food Animal Production. In: *Clinical Infectious Diseases*. [Online]. 15 October 2016 Oxford Academic. pp. 1087–1093. Available from: doi:10.1093/cid/ciw475 [Accessed: 15 December 2022].

Collinson, I., Breyton, C., Duong, F., Tziatzios, C., et al. (2001) Projection structure and oligomeric properties of a bacterial core protein translocase. *The EMBO Journal*. [Online] 20 (10), 2462. Available from: doi:10.1093/EMBOJ/20.10.2462 [Accessed: 5 July 2022].

Collinson, I., Corey, R.A. & Allen, W.J. (2015) Channel crossing: how are proteins shipped across the bacterial plasma membrane? *Philosophical Transactions of the Royal Society of London.*

*Series B, Biological Sciences*. [Online] 370 (1679), 20150025. Available from: doi:10.1098/rstb.2015.0025.

Connolly, T. & Gilmore, R. (1989) The signal recognition particle receptor mediates the GTP-dependent displacement of SRP from the signal sequence of the nascent polypeptide. *Cell*. [Online] 57 (4), 599–610. Available from: doi:10.1016/0092-8674(89)90129-3.

Cooper, D.B., Smith, V.F., Crane, J.M., Roth, H.C., et al. (2008) SecA, the Motor of the Secretion Machine, Binds Diverse Partners on One Interactive Surface. *Journal of Molecular Biology*. [Online] 382 (1), 74–87. Available from: doi:10.1016/j.jmb.2008.06.049.

Corey, R.A., Ahdash, Z., Shah, A., Pyle, E., et al. (2019) ATP-induced asymmetric pre-protein folding as a driver of protein translocation through the Sec machinery. *eLife*. [Online] 8, 1–25. Available from: doi:10.7554/eLife.41803.

Corey, R.A., Allen, W.J. & Collinson, I. (2016) Protein translocation: what's the problem? *Biochemical Society Transactions*. [Online] 44 (3), 753–759. Available from: doi:10.1042/BST20160047 [Accessed: 26 May 2022].

Corey, R.A., Allen, W.J., Komar, J., Masiulis, S., et al. (2016) Unlocking the Bacterial SecY Translocon. *Structure*. [Online] 24 (4), 518–527. Available from: doi:10.1016/j.str.2016.02.001 [Accessed: 8 October 2018].

Corey, R.A., Pyle, E., Allen, W.J., Watkins, D.W., et al. (2018) Specific cardiolipin–SecY interactions are required for proton-motive force stimulation of protein secretion. *Proceedings of the National Academy of Sciences of the United States of America*. [Online] 115 (31), 7967–7972. Available from: doi:10.1073/pnas.1721536115.

Cranford-Smith, T. & Huber, D. (2018) The way is the goal: How SecA transports proteins across the cytoplasmic membrane in bacteria. *FEMS Microbiology Letters*. [Online] 365 (11). Available from: doi:10.1093/femsle/fny093.

Cregg, K.M., Wilding, E.I. & Black, M.T. (1996) Molecular cloning and expression of the *spsB* gene encoding an essential type I signal peptidase from *Staphylococcus aureus*. *Journal of Bacteriology*. [Online] 178 (19), 5712–5718. Available from: doi:10.1128/JB.178.19.5712-5718.1996 [Accessed: 14 December 2022].

Cristóbal, S., De Gier, J.W., Nielsen, H. & Von Heijne, G. (1999) Competition between Sec- and TAT-dependent protein translocation in *Escherichia coli*. *EMBO Journal*. [Online] 18 (11), 2982–2990. Available from: doi:10.1093/emboj/18.11.2982.

Crowther, G.J., Quadri, S.A., Shannon-Alferes, B.J., Van Voorhis, W.C., et al. (2012) A mechanism-based whole-cell screening assay to identify inhibitors of protein export in *Escherichia coli* by the sec pathway. *Journal of Biomolecular Screening*. [Online] 17 (4), 535–541. Available from: doi:10.1177/1087057111431606 [Accessed: 31 January 2020].

Crowther, G.J., Weller, S.M., Jones, J.C., Weaver, T., et al. (2015) The bacterial sec pathway of

protein export: Screening and follow-up. *Journal of Biomolecular Screening*. [Online] 20 (7), 921–926. Available from: doi:10.1177/1087057115587458 [Accessed: 14 April 2021].

Cui, J., Jin, J., Hsieh, Y.H., Yang, H., et al. (2013) Design, Synthesis and Biological Evaluation of Rose Bengal Analogues as SecA Inhibitors. *ChemMedChem*. [Online] 8 (8), 1384–1393. Available from: doi:10.1002/CMDC.201300216 [Accessed: 29 April 2022].

Czech, L., Mais, C.N., Kratzat, H., Sarmah, P., et al. (2022) Inhibition of SRP-dependent protein secretion by the bacterial alarmone (p)ppGpp. *Nature Communications*. [Online] 13 (1), 1–14. Available from: doi:10.1038/s41467-022-28675-0 [Accessed: 13 September 2022].

Dalbey, R.E. & Wickner, W. (1985) Leader peptidase catalyzes the release of exported proteins from the outer surface of the *Escherichia coli* plasma membrane. *Journal of Biological Chemistry*. [Online] 260 (29), 15925–15931. Available from: doi:10.1016/S0021-9258(17)36347-0.

Daruwalla, K.R., Paxton, A.T. & Henderson, P.J.F. (1981) Energization of the transport systems for arabinose and comparison with galactose transport in *Escherichia coli. The Biochemical Journal*. [Online] 200 (3), 611–627. Available from: doi:10.1042/BJ2000611 [Accessed: 18 November 2022].

Das, S. & Oliver, D.B. (2011) Mapping of the SecA·SecY and SecA·SecG interfaces by site-directed in vivo photocross-linking. *Journal of Biological Chemistry*. [Online] 286 (14), 12371–12380. Available from: doi:10.1074/jbc.M110.182931.

Date, T. (1983) Demonstration by a Novel Genetic Technique That Leader Peptidase Is an Essential Enzyme of *Escherichia coli*. *Journal of Bacteriology*. [Online] 154 (1), 76–83. Available from: doi:10.1128/JB.154.1.76-83.1983 [Accessed: 14 December 2022].

Davies, J. & Davies, D. (2010) Origins and evolution of antibiotic resistance. *Microbiology and Molecular Biology Reviews*. [Online] 74 (3), 417–433. Available from: doi:10.1128/MMBR.00016-10.

Denks, K., Sliwinski, N., Erichsen, V., Borodkina, B., et al. (2017) The signal recognition particle contacts uL23 and scans substrate translation inside the ribosomal tunnel. *Nature Microbiology*. [Online] 2 (4), 1–10. Available from: doi:10.1038/nmicrobiol.2016.265.

Dev, I.K., Harvey, R.J. & Ray, P.H. (1985) Inhibition of prolipoprotein signal peptidase by globomycin. *Journal of Biological Chemistry*. 260 (10), 5891–5894.

Dev, I.K. & Ray, P.H. (1984) Rapid assay and purification of a unique signal peptidase that processes the prolipoprotein from *Escherichia coli* B. *Journal of Biological Chemistry*. [Online] 259 (17), 11114–11120. Available from: doi:10.1016/s0021-9258(18)90629-0 [Accessed: 14 December 2022].

Deville, K., Gold, V.A.M., Robson, A., Whitehouse, S., et al. (2011) The oligomeric state and arrangement of the active bacterial translocon. *Journal of Biological Chemistry*. [Online] 286

(6), 4659–4669. Available from: doi:10.1074/jbc.M110.175638 [Accessed: 10 November 2022].

Dilks, K., Rose, R.W., Hartmann, E. & Pohlschröder, M. (2003) Prokaryotic utilization of the twin-arginine translocation pathway: A genomic survey. *Journal of Bacteriology*. [Online] 185 (4), 1478–1483. Available from: doi:10.1128/JB.185.4.1478-1483.2003 [Accessed: 31 March 2020].

Dixon, A.S., Schwinn, M.K., Hall, M.P., Zimmerman, K., et al. (2016) NanoLuc Complementation Reporter Optimized for Accurate Measurement of Protein Interactions in Cells. *ACS Chemical Biology*. [Online] 11 (2), 400–408. Available from: doi:10.1021/acschembio.5b00753.

Donald, R.G.K., Skwish, S., Forsyth, R.A., Anderson, J.W., et al. (2009) A *Staphylococcus aureus* Fitness Test Platform for Mechanism-Based Profiling of Antibacterial Compounds. *Chemistry and Biology*. [Online] 16 (8), 826–836. Available from: doi:10.1016/J.CHEMBIOL.2009.07.004.

Duong, F. & Wickner, W. (1997) Distinct catalytic roles of the SecYE, SecG and SecDFyajC subunits of preprotein translocase holoenzyme. *The EMBO Journal*. [Online] 16 (10), 2756–2768. Available from: doi:10.1093/emboj/16.10.2756.

Economou, A., Pogliano, J.A., Beckwith, J., Oliver, D.B., et al. (1995) SecA membrane cycling at SecYEG is driven by distinct ATP binding and hydrolysis events and is regulated by SecD and SecF. *Cell*. [Online] 83 (7), 1171–1181. Available from: doi:10.1016/0092-8674(95)90143-4.

Economou, A. & Wickner, W. (1994) SecA promotes preprotein translocation by undergoing ATP-driven cycles of membrane insertion and deinsertion. *Cell*. [Online] 78 (5), 835–843. Available from: doi:10.1016/S0092-8674(94)90582-7.

Egea, P.F., Shan, S.O., Napetschnig, J., Savage, D.F., et al. (2004) Substrate twinning activates the signal recognition particle and its receptor. *Nature*. [Online] 427 (6971), 215–221. Available from: doi:10.1038/NATURE02250 [Accessed: 13 December 2022].

Eichler, J. & Wickner, W. (1998) The SecA subunit of *Escherichia coli* preprotein translocase is exposed to the periplasm. *Journal of Bacteriology*. [Online] 180 (21), 5776–5779. Available from: doi:10.1128/JB.180.21.5776-5779.1998/ASSET/18FAD21E-92E7-424F-A65D-765D6E59A675/ASSETS/GRAPHIC/JB2180763003.JPEG [Accessed: 29 April 2022].

Englesberg, E., Anderson, R.L., Weinberg, R., Lee, N., et al. (1962) L-Arabinose-sensitive, L-ribulose 5-phosphate 4-epimerase-deficient mutants of *Escherichia coli. Journal of Bacteriology*. 84 (1), 137–146.

Erlandson, K.J., Or, E., Osborne, A.R. & Rapoport, T.A. (2008) Analysis of polypeptide movement in the SecY channel during SecA-mediated protein translocation. *Journal of Biological Chemistry*. [Online] 283 (23), 15709–15715. Available from: doi:10.1074/jbc.M710356200.

Fagan, R.P. & Fairweather, N.F. (2011) *Clostridium difficile* Has Two Parallel and Essential Sec

Secretion Systems. *The Journal of Biological Chemistry*. [Online] 286 (31), 27483. Available from: doi:10.1074/JBC.M111.263889 [Accessed: 13 December 2022].

Fair, R.J. & Tor, Y. (2014) Antibiotics and bacterial resistance in the 21st century. *Perspectives in Medicinal Chemistry*. [Online] 6, 25–64. Available from: doi:10.4137/PMC.S14459.

Feltcher, M.E., Sullivan, J.T. & Braunstein, M. (2010) Protein export systems of *Mycobacterium tuberculosis*: novel targets for drug development? *Future Microbiology*. [Online] 5 (10), 1581. Available from: doi:10.2217/FMB.10.112 [Accessed: 26 April 2022].

Ferenci, T., Zhou, Z., Betteridge, T., Ren, Y., et al. (2009) Genomic sequencing reveals regulatory mutations and recombinational events in the widely used MC4100 lineage of *Escherichia coli* K-12. *Journal of Bacteriology*. [Online] 191 (12), 4025–4029. Available from: doi:10.1128/JB.00118-09.

Fernández-Castané, A., Vine, C.E., Caminal, G. & López-Santín, J. (2012) Evidencing the role of lactose permease in IPTG uptake by *Escherichia coli* in fed-batch high cell density cultures. *Journal of Biotechnology*. [Online] 157 (3), 391–398. Available from: doi:10.1016/J.JBIOTEC.2011.12.007.

Fessl, T., Watkins, D., Oatley, P., Allen, W.J., et al. (2018) Dynamic action of the Sec machinery during initiation, protein translocation and termination. *eLife*. [Online] 7, e35112. Available from: doi:10.7554/eLife.35112.

Fleming, A. (1929) On the Antibacterial Action of Cultures of a *Penicillium*, with Special Reference to their Use in the Isolation of *B. influenzæ*. *British Journal of Experimental Pathology*. 10 (3), 226–236.

Freymann, D.M., Keenan, R.J., Stroud, R.M. & Walter, P. (1997) Structure of the conserved GTPase domain of the signal recognition particle. *Nature*. [Online] 385 (6614), 361–364. Available from: doi:10.1038/385361a0.

Friedman, N.D., Temkin, E. & Carmeli, Y. (2016) The negative impact of antibiotic resistance. *Clinical Microbiology and Infection*. [Online] 22 (5), 416–422. Available from: doi:10.1016/J.CMI.2015.12.002 [Accessed: 29 July 2022].

Furniss, R.C.D., Kadeřábková, N., Barker, D., Bernal, P., et al. (2021) Breaking antimicrobial resistance by disrupting extracytoplasmic protein folding. *eLife*. [Online] 11, 2021.08.27.457985. Available from: doi:10.7554/ELIFE.57974 [Accessed: 14 January 2022].

Gan, K., Gupta, S.D., Sankaran, K., Schmid, M.B., et al. (1993) Isolation and characterization of a temperature-sensitive mutant of *Salmonella typhimurium* defective in prolipoprotein modification. *Journal of Biological Chemistry*. [Online] 268 (22), 16544–16550. Available from: doi:10.1016/S0021-9258(19)85453-4.

Garrison, J.L., Kunkel, E.J., Hegde, R.S. & Taunton, J. (2005) A substrate-specific inhibitor of protein translocation into the endoplasmic reticulum. *Nature*. [Online] 436 (7048), 285–289.

Available from: doi:10.1038/nature03821 [Accessed: 22 May 2020].

Gelis, I., Bonvin, A.M.J.J., Keramisanou, D., Koukaki, M., et al. (2007) Structural Basis for Signal-Sequence Recognition by the Translocase Motor SecA as Determined by NMR. *Cell*. [Online] 131 (4), 756–769. Available from: doi:10.1016/j.cell.2007.09.039.

de Gier, J.-W.L., Mansournia, P., Valent, Q.A., Phillips, G.J., et al. (1996) Assembly of a cytoplasmic membrane protein in *Escherichia coli* is dependent on the signal recognition particle. *FEBS Letters*. [Online] 399 (3), 307–309. Available from: doi:10.1016/S0014-5793(96)01354-3.

Gold, V.A.M., Robson, A., Bao, H., Romantsov, T., et al. (2010) The action of cardiolipin on the bacterial translocon. *Proceedings of the National Academy of Sciences of the United States of America*. [Online] 107 (22), 10044–10049. Available from: doi:10.1073/PNAS.0914680107/SUPPL_FILE/PNAS.0914680107_SI.PDF [Accessed: 31 October 2022].

Gold, V.A.M., Robson, A., Clarke, A.R. & Collinson, I. (2007) Allosteric regulation of SecA: Magnesium-mediated control of conformation and activity. *Journal of Biological Chemistry*. [Online] 282 (24), 17424–17432. Available from: doi:10.1074/jbc.M702066200.

Gold, V.A.M., Whitehouse, S., Robson, A. & Collinson, I. (2013) The dynamic action of SecA during the initiation of protein translocation. *Biochemical Journal*. [Online] 449 (3), 695–705. Available from: doi:10.1042/BJ20121314.

Goldstein, F.W., Gutmann, L., Williamson, R., Collatz, E., et al. (1983) In vivo and in vitro emergence of simultaneous resistance to both β-lactam and aminoglycoside antibiotics in a strain of *Serratia marcescens*. *Annales de l'Institut Pasteur / Microbiologie*. [Online] 134 (3), 329–337. Available from: doi:10.1016/S0769-2609(83)80058-1.

González-Bello, C. (2017) Antibiotic adjuvants – A strategy to unlock bacterial resistance to antibiotics. *Bioorganic & Medicinal Chemistry Letters*. [Online] 27 (18), 4221–4228. Available from: doi:10.1016/J.BMCL.2017.08.027 [Accessed: 26 November 2018].

González, L.J., Bahr, G., Nakashige, T.G., Nolan, E.M., et al. (2016) Membrane anchoring stabilizes and favors secretion of New Delhi metallo-β-lactamase. *Nature Chemical Biology*. [Online] 12 (7), 516–522. Available from: doi:10.1038/nchembio.2083.

Grady, L.M., Michtavy, J. & Oliver, D.B. (2012) Characterization of the *Escherichia coli* SecA signal peptide-binding site. *Journal of Bacteriology*. [Online] 194 (2), 307–316. Available from: doi:10.1128/JB.06150-11.

Gupta, S. & Wu, H. (1991) Identification and subcellular localization of apolipoprotein N-acyltransferase in *Escherichia coli*. *FEMS Microbiology Letters*. [Online] 78 (1), 37–41. Available from: doi:10.1016/0378-1097(91)90251-5 [Accessed: 14 November 2022].

Hall, B.S., Hill, K., McKenna, M., Ogbechi, J., et al. (2014) The Pathogenic Mechanism of the *Mycobacterium ulcerans* Virulence Factor, Mycolactone, Depends on Blockade of Protein

Translocation into the ER. *PLOS Pathogens*. [Online] 10 (4), e1004061. Available from: doi:10.1371/JOURNAL.PPAT.1004061 [Accessed: 10 October 2022].

Hamed, M.B., Burchacka, E., Angus, L., Marchand, A., et al. (2021) Effective Small Molecule Antibacterials from a Novel Anti-Protein Secretion Screen. *Microorganisms*. [Online] 9 (3), 592. Available from: doi:10.3390/microorganisms9030592 [Accessed: 14 April 2021].

Hamsanathan, S., Anthonymuthu, T.S., Bageshwar, U.K. & Musser, S.M. (2017) A Hinged Signal Peptide Hairpin Enables Tat-Dependent Protein Translocation. *Biophysical Journal*. [Online] 113 (12), 2650–2668. Available from: doi:10.1016/j.bpj.2017.09.036 [Accessed: 7 December 2022].

Hartl, F.-U., Lecker, S., Schiebel, E., Hendrick, J.P., et al. (1990) The binding cascade of SecB to SecA to SecY/E mediates preprotein targeting to the E. coli plasma membrane. *Cell*. [Online] 63 (2), 269–279. Available from: doi:10.1016/0092-8674(90)90160-G.

Hartman, B.J. & Tomasz, A. (1984) Low-affinity penicillin-binding protein associated with β-lactam resistance in *Staphylococcus aureus*. *Journal of Bacteriology*. [Online] 158 (2), 513–516. Available from: doi:10.1128/jb.158.2.513-516.1984.

Hartmann, E., Sommer, T., Prehn, S., Görlich, D., et al. (1994) Evolutionary conservation of components of the protein translocation complex. *Nature*. [Online] 367 (6464), 654–657. Available from: doi:10.1038/367654a0 [Accessed: 16 December 2022].

von Heijne, G. (1984) How signal sequences maintain cleavage specificity. *Journal of Molecular Biology*. [Online] 173 (2), 243–251. Available from: doi:10.1016/0022-2836(84)90192-X.

von Heijne, G. (1992) Membrane protein structure prediction. Hydrophobicity analysis and the positive-inside rule. *Journal of Molecular Biology*. [Online] 225 (2), 487–494. Available from: doi:10.1016/0022-2836(92)90934-C.

von Heijne, G. (1985) Signal sequences. The limits of variation. *Journal of Molecular Biology*. [Online] 184 (1), 99–105. Available from: doi:10.1016/0022-2836(85)90046-4.

von Heijne, G. (1989) The structure of signal peptides from bacterial lipoproteins. *Protein Engineering, Design and Selection*. [Online] 2 (7), 531–534. Available from: doi:10.1093/protein/2.7.531.

Hizlan, D., Robson, A., Whitehouse, S., Gold, V.A., et al. (2012) Structure of the SecY Complex Unlocked by a Preprotein Mimic. *Cell Reports*. [Online] 1 (1), 21–28. Available from: doi:10.1016/j.celrep.2011.11.003.

Holtkamp, W., Lee, S., Bornemann, T., Senyushkina, T., et al. (2012) Dynamic switch of the signal recognition particle from scanning to targeting. *Nature Structural and Molecular Biology*. [Online] 19 (12), 1332–1337. Available from: doi:10.1038/nsmb.2421.

Huang, C., Rossi, P., Saio, T. & Kalodimos, C.G. (2016) Structural basis for the antifolding activity of a molecular chaperone. *Nature*. [Online] 537 (7619), 202–206. Available from:

doi:10.1038/nature18965 [Accessed: 9 September 2022].

Huang, Q. & Palmer, T. (2017) Signal peptide hydrophobicity modulates interaction with the Twin-Arginine translocase. *mBio*. [Online] 8 (4), e00909-17. Available from: doi:10.1128/mBio.00909-17 [Accessed: 9 September 2019].

Huang, Y.-J., Wang, H., Gao, F.-B., Li, M., et al. (2012) Fluorescein analogs inhibit SecA ATPase: the first sub-μM inhibitor of bacterial protein translocation. *ChemMedChem*. [Online] 7 (4), 571–577. Available from: doi:10.1002/cmdc.201100594.

Huber, D., Boyd, D., Xia, Y., Olma, M.H., et al. (2005a) Use of thioredoxin as a reporter to identify a subset of *Escherichia coli* signal sequences that promote signal recognition particle-dependent translocation. *Journal of Bacteriology*. [Online] 187 (9), 2983–2991. Available from: doi:10.1128/JB.187.9.2983-2991.2005.

Huber, D., Cha, M., Debarbieux, L., Planson, A.-G., et al. (2005b) A selection for mutants that interfere with folding of *Escherichia coli* thioredoxin-1 in vivo. *Proceedings of the National Academy of Sciences of the United States of America*. [Online] 102 (52), 18872–7. Available from: doi:10.1073/pnas.0509583102.

Huber, D., Jamshad, M., Hanmer, R., Schibich, D., et al. (2017) SecA Cotranslationally Interacts with Nascent Substrate Proteins In Vivo. *Journal of Bacteriology*. [Online] 199 (2), e00622-16. Available from: doi:10.1128/JB.00622-16.

Huber, D., Rajagopalan, N., Preissler, S., Rocco, M.A., et al. (2011) SecA Interacts with Ribosomes in Order to Facilitate Posttranslational Translocation in Bacteria. *Molecular Cell*. [Online] 41 (3), 343–353. Available from: doi:10.1016/J.MOLCEL.2010.12.028 [Accessed: 19 December 2018].

Hunt, J.F., Weinkauf, S., Henry, L., Fak, J.J., et al. (2002) Nucleotide control of interdomain interactions in the conformational reaction cycle of SecA. *Science*. [Online] 297 (5589), 2018–2026. Available from: doi:10.1126/science.1074424 [Accessed: 4 May 2020].

Hussain, M., Ichihara, S. & Mizushima, S. (1980) Accumulation of glyceride-containing precursor of the outer membrane lipoprotein in the cytoplasmic membrane of *Escherichia coli* treated with globomycin. *Journal of Biological Chemistry*. [Online] 255 (8), 3707–3712. Available from: doi:10.1016/s0021-9258(19)85762-9.

Imada, A., Kitano, K., Kintaka, K., Muroi, M., et al. (1981) Sulfazecin and isosulfazecin, novel β-lactam antibiotics of bacterial origin. *Nature*. [Online] 289 (5798), 590–591. Available from: doi:10.1038/289590a0 [Accessed: 25 January 2022].

Izaki, K., Matsuhashi, M. & Strominger, J.L. (1966) Glycopeptide transpeptidase and D-alanine carboxypeptidase: penicillin-sensitive enzymatic reactions. *Proceedings of the National Academy of Sciences of the United States of America*. [Online] 55 (3), 656–663. Available from: doi:10.1073/pnas.55.3.656 [Accessed: 15 December 2022].

Janda, C.Y., Li, J., Oubridge, C., Hernández, H., et al. (2010) Recognition of a signal peptide by the signal recognition particle. *Nature*. [Online] 465 (7297), 507–510. Available from: doi:10.1038/nature08870.

Jaurin, B. & Grundström, T. (1981) ampC cephalosporinase of *Escherichia coli* K-12 has a different evolutionary origin from that of beta-lactamases of the penicillinase type. *Proceedings of the National Academy of Sciences of the United States of America*. 78 (8), 4897–4901.

Jiang, C., Wynne, M. & Huber, D. (2021) How Quality Control Systems AID Sec-Dependent Protein Translocation. *Frontiers in Molecular Biosciences*. [Online] 8, 227. Available from: doi:10.3389/FMOLB.2021.669376/BIBTEX.

Jilaveanu, L.B. & Oliver, D.B. (2007) In vivo membrane topology of Escherichia coli SecA ATPase reveals extensive periplasmic exposure of multiple functionally important domains clustering on one face of SecA. *The Journal of Biological Chemistry*. [Online] 282 (7), 4661–4668. Available from: doi:10.1074/JBC.M610828200 [Accessed: 14 December 2022].

Jin, J., Hsieh, Y.-H., Cui, J., Damera, K., et al. (2016) Using Chemical Probes to Assess the Feasibility of Targeting SecA for Developing Antimicrobial Agents against Gram-negative Bacteria. *ChemMedChem*. [Online] 11 (22), 2511–2521. Available from: doi:10.1002/cmdc.201600421.

Jomaa, A., Fu, Y.H.H., Boehringer, D., Leibundgut, M., et al. (2017) Structure of the quaternary complex between SRP, SR, and translocon bound to the translating ribosome. *Nature Communications*. [Online] 8. Available from: doi:10.1038/ncomms15470.

Josefsson, L.G. & Randall, L.L. (1981) Different exported proteins in *E. coli* show differences in the temporal mode of processing in vivo. *Cell*. [Online] 25 (1), 151–157. Available from: doi:10.1016/0092-8674(81)90239-7.

Jumper, J., Evans, R., Pritzel, A., Green, T., et al. (2021) Highly accurate protein structure prediction with AlphaFold. *Nature*. [Online] 596 (7873), 583–589. Available from: doi:10.1038/s41586-021-03819-2 [Accessed: 21 November 2022].

Junne, T., Wong, J., Studer, C., Aust, T., et al. (2015) Decatransin, a new natural product inhibiting protein translocation at the Sec61/SecYEG translocon. *Journal of Cell Science*. [Online] 128 (6), 1217–1229. Available from: doi:10.1242/jcs.165746.

Kaderabkova, N., Bharathwaj, M., Furniss, R.C.D., Gonzalez, D., et al. (2022) The biogenesis of β-lactamase enzymes. *Microbiology*. [Online] 168 (8), 001217. Available from: doi:10.1099/MIC.0.001217 [Accessed: 12 August 2022].

Käll, L., Krogh, A. & Sonnhammer, E.L.L. (2004) A combined transmembrane topology and signal peptide prediction method. *Journal of Molecular Biology*. [Online] 338 (5), 1027–1036. Available from: doi:10.1016/j.jmb.2004.03.016.

Karamanou, S., Vrontou, E., Sianidis, G., Baud, C., et al. (1999) A molecular switch in SecA protein

couples ATP hydrolysis to protein translocation. *Molecular Microbiology*. [Online] 34 (5), 1133–1145. Available from: doi:10.1046/J.1365-2958.1999.01686.X [Accessed: 13 December 2022].

Karim, A., Poirel, L., Nagarajan, S. & Nordmann, P. (2001) Plasmid-mediated extended-spectrum β-lactamase (CTX-M-3 like) from India and gene association with insertion sequence *ISEcp1*. *FEMS Microbiology Letters*. [Online] 201 (2), 237–241. Available from: doi:10.1111/J.1574-6968.2001.TB10762.X [Accessed: 29 September 2022].

Kaufmann, A., Manting, E.H., Veenendaal, A.K.J., Driessen, A.J.M., et al. (1999) Cysteine-directed cross-linking demonstrates that helix 3 of SecE is close to helix 2 of SecY and helix 3 of a neighboring SecE. *Biochemistry*. [Online] 38 (28), 9115–9125. Available from: doi:10.1021/BI990539D [Accessed: 10 November 2022].

Kavanaugh, J.S., Thoendel, M. & Horswill, A.R. (2007) A role for type I signal peptidase in *Staphylococcus aureus* quorum sensing. *Molecular Microbiology*. [Online] 65 (3), 780–798. Available from: doi:10.1111/J.1365-2958.2007.05830.X [Accessed: 17 June 2022].

Keenan, R.J., Freymann, D.M., Walter, P. & Stroud, R.M. (1998) Crystal structure of the signal sequence binding subunit of the signal recognition particle. *Cell*. [Online] 94 (2), 181–191. Available from: doi:10.1016/S0092-8674(00)81418-X.

Keller, R., de Keyzer, J., Driessen, A.J.M. & Palmer, T. (2012) Co-operation between different targeting pathways during integration of a membrane protein. *Journal of Cell Biology*. [Online] 199 (2), 303–315. Available from: doi:10.1083/JCB.201204149 [Accessed: 10 October 2022].

Kinch, M.S., Patridge, E., Plummer, M. & Hoyer, D. (2014) An analysis of FDA-approved drugs for infectious disease: antibacterial agents. *Drug Discovery Today*. [Online] 19 (9), 1283–1287. Available from: doi:10.1016/J.DRUDIS.2014.07.005.

King, D.T., Sobhanifar, S. & Strynadka, N.C.J. (2016) One ring to rule them all: Current trends in combating bacterial resistance to the β-lactams. *Protein Science*. [Online] 25 (4), 787–803. Available from: doi:10.1002/pro.2889.

Klein, E.Y., Van Boeckel, T.P., Martinez, E.M., Pant, S., et al. (2018a) Global increase and geographic convergence in antibiotic consumption between 2000 and 2015. *Proceedings of the National Academy of Sciences of the United States of America*. [Online] 115 (15), E3463–E3470. Available from: doi:10.1073/PNAS.1717295115/-/DCSUPPLEMENTAL [Accessed: 25 January 2022].

Klein, W., Rutz, C., Eckhard, J., Provinciael, B., et al. (2018b) Use of a sequential high throughput screening assay to identify novel inhibitors of the eukaryotic SRP-Sec61 targeting/ translocation pathway Alexander F. Palazzo (ed.). *PLoS ONE*. [Online] 13 (12), e0208641. Available from: doi:10.1371/journal.pone.0208641 [Accessed: 26 March 2020].

Klein, W., Westendorf, C., Schmidt, A., Conill-Cortés, M., et al. (2015) Defining a Conformational Consensus Motif in Cotransin-Sensitive Signal Sequences: A Proteomic and Site-Directed

Mutagenesis Study. *PLOS ONE*. [Online] 10 (3), e0120886. Available from: doi:10.1371/JOURNAL.PONE.0120886 [Accessed: 10 October 2022].

Knüpffer, L., Fehrenbach, C., Denks, K., Erichsen, V., et al. (2019) Molecular mimicry of SecA and signal recognition particle binding to the bacterial ribosome. *mBio*. [Online] 10 (4). Available from: doi:10.1128/mBio.01317-19.

Koshland, D. & Botstein, D. (1982) Evidence for posttranslational translocation of β-lactamase across the bacterial inner membrane. *Cell*. [Online] 30 (3), 893–902. Available from: doi:10.1016/0092-8674(82)90294-X [Accessed: 2 November 2022].

Kulanthaivel, P., Kreuzman, A.J., Strege, M.A., Belvo, M.D., et al. (2004) Novel Lipoglycopeptides as Inhibitors of Bacterial Signal Peptidase I. *Journal of Biological Chemistry*. [Online] 279 (35), 36250–36258. Available from: doi:10.1074/JBC.M405884200.

Kuo, D., Knight, W.B., Weidner, J., Griffin, P., et al. (1994) Determination of the Kinetic Parameters of *Escherichia coli* Leader Peptidase Activity Using a Continuous Assay: The pH Dependence and Time–Dependent Inhibition by β-Lactams Are Consistent with a Novel Serine Protease Mechanism. *Biochemistry*. [Online] 33 (27), 8347–8354. Available from: doi:10.1021/BI00193A023/ASSET/BI00193A023.FP.PNG_V03 [Accessed: 22 July 2022].

Kusakawa, N., Yura, T., Ueguchi, C., Akiyama, Y., et al. (1989) Effects of mutations in heat-shock genes *groES* and *groEL* on protein export in *Escherichia coli*. *The EMBO Journal*. [Online] 8 (11), 3517. Available from: doi:10.1002/J.1460-2075.1989.TB08517.X [Accessed: 2 November 2022].

Lam, V.Q., Akopian, D., Rome, M., Henningsen, D., et al. (2010) Lipid activation of the signal recognition particle receptor provides spatial coordination of protein targeting. *The Journal of Cell Biology*. [Online] 190 (4), 623. Available from: doi:10.1083/JCB.201004129 [Accessed: 13 December 2022].

Laminet, A.A., Kumamoto, C.A. & Plückthun, A. (1991) Folding in vitro and transport in vivo of pre-β-lactamase are SecB independent. *Molecular Microbiology*. [Online] 5 (1), 117–122. Available from: doi:10.1111/J.1365-2958.1991.TB01832.X [Accessed: 5 January 2022].

Laminet, A.A. & Pluckthun, A. (1989) The precursor of β-lactamase: Purification, properties and folding kinetics. *EMBO Journal*. [Online] 8 (5), 1469–1477. Available from: doi:10.1002/j.1460-2075.1989.tb03530.x [Accessed: 18 September 2020].

Laraki, N., Franceschini, N., Rossolini, G.M., Santucci, P., et al. (1999) Biochemical characterization of the *Pseudomonas aeruginosa* 101/1477 metallo-beta-lactamase IMP-1 produced by *Escherichia coli. Antimicrobial Agents and Chemotherapy*. [Online] 43 (4), 902–906. Available from: doi:10.1128/AAC.43.4.902.

Lauretti, L., Riccio, M.L., Mazzariol, A., Cornaglia, G., et al. (1999) Cloning and Characterization of *blaVIM*, a New Integron-Borne Metallo-β-Lactamase Gene from a *Pseudomonas aeruginosa* Clinical Isolate. *Antimicrobial Agents and Chemotherapy*. [Online] 43 (7), 1584. Available

from: doi:10.1128/AAC.43.7.1584 [Accessed: 29 July 2022].

Lee, C.W., Tseng, Y.H., Deng, F.S., Lin, J.W., et al. (2012) Contribution of Phe-7 to Tat-dependent export of β-lactamase in *Xanthomonas campestris. Antimicrobial Agents and Chemotherapy*. [Online] 56 (7), 3597–3602. Available from: doi:10.1128/AAC.06031-11/ASSET/EA2DAF28-8865-4492-ADDF-F9705E5CBCFB/ASSETS/GRAPHIC/ZAC9991009990001.JPEG [Accessed: 27 October 2022].

Lee, H.C. & Bernstein, H.D. (2001) The targeting pathway of *Escherichia coli* presecretory and integral membrane proteins is specified by the hydrophobicity of the targeting signal. *Proceedings of the National Academy of Sciences*. [Online] 98 (6), 3471–3476. Available from: doi:10.1073/pnas.051484198.

Lewis, K. (2013) Platforms for antibiotic discovery. *Nature Reviews Drug Discovery*. [Online]. 12 (5) pp.371–387. Available from: doi:10.1038/nrd3975 [Accessed: 15 October 2022].

Lewis, K. (2020) The Science of Antibiotic Discovery. *Cell*. [Online] 181 (1), 29–45. Available from: doi:10.1016/J.CELL.2020.02.056.

Li, L., Park, E., Ling, J.J., Ingram, J., et al. (2016) Crystal structure of a substrate-engaged SecY protein-translocation channel. *Nature*. [Online] 531 (7594), 395–399. Available from: doi:10.1038/nature17163.

Li, M., Huang, Y.J., Tai, P.C. & Wang, B. (2008) Discovery of the first SecA inhibitors using structure-based virtual screening. *Biochemical and Biophysical Research Communications*. [Online] 368 (4), 839–845. Available from: doi:10.1016/j.bbrc.2008.01.135.

Li, T., Wang, Q., Chen, F., Li, X., et al. (2013) Biochemical characteristics of New Delhi metallo-β-lactamase-1 show unexpected difference to other MBLs. *PLoS ONE*. [Online] 8 (4), e61914. Available from: doi:10.1371/journal.pone.0061914.

Li, X.Z. & Nikaido, H. (2004) Efflux-Mediated Drug Resistance in Bacteria. *Drugs*. [Online]. 64 (2) pp.159–204. Available from: doi:10.2165/00003495-200464020-00004 [Accessed: 13 December 2022].

Liang, F.-C., Bageshwar, U.K. & Musser, S.M. (2009) Bacterial Sec protein transport is rate-limited by precursor length: a single turnover study. *Molecular Biology of the Cell*. [Online] 20 (19), 4256–4266. Available from: doi:10.1091/mbc.e09-01-0075.

Liao, Y.-T., Kuo, S.-C., Chiang, M.-H., Lee, Y.-T., et al. (2015) *Acinetobacter baumannii* Extracellular OXA-58 Is Primarily and Selectively Released via Outer Membrane Vesicles after Sec-Dependent Periplasmic Translocation. *Antimicrobial Agents and Chemotherapy*. [Online] 59 (12), 7346–7354. Available from: doi:10.1128/AAC.01343-15.

Liu, Y., Law, B.K. & Luesch, H. (2009) Apratoxin A Reversibly Inhibits the Secretory Pathway by Preventing Cotranslational Translocation. *Molecular Pharmacology*. [Online] 76 (1), 91–104. Available from: doi:10.1124/MOL.109.056085 [Accessed: 10 October 2022].

Loos, M.S., Ramakrishnan, R., Vranken, W., Tsirigotaki, A., et al. (2019) Structural basis of the subcellular topology landscape of *Escherichia coli. Frontiers in Microbiology*. [Online] 10, 1–22. Available from: doi:10.3389/FMICB.2019.01670/FULL [Accessed: 29 April 2022].

López, C., Ayala, J.A., Bonomo, R.A., González, L.J., et al. (2019) Protein determinants of dissemination and host specificity of metallo-β-lactamases. *Nature Communications*. [Online] 10 (1). Available from: doi:10.1038/s41467-019-11615-w [Accessed: 2 November 2020].

López, C., Prunotto, A., Bahr, G., Bonomo, R.A., et al. (2021) Specific protein-membrane interactions promote packaging of metallo-β-lactamases into outer membrane vesicles. *Antimicrobial Agents and Chemotherapy*. [Online] 65 (10). Available from: doi:10.1128/AAC.00507-21/SUPPL_FILE/AAC.00507-21-S0001.PDF [Accessed: 9 December 2021].

Luirink, J., Ten Hagen-Jongman, C.M., Van Der Weijden, C.C., Oudega, B., et al. (1994) An alternative protein targeting pathway in Escherichia coli: studies on the role of FtsY. *The EMBO Journal*. [Online] 13 (10), 2289. Available from: doi:10.1002/J.1460-2075.1994.TB06511.X [Accessed: 13 December 2022].

Lyon, W.R., Gibson, C.M. & Caparon, M.G. (1998) A role for trigger factor and an rgg-like regulator in the transcription, secretion and processing of the cysteine proteinase of *Streptococcus pyogenes. The EMBO Journal*. [Online] 17 (21), 6263. Available from: doi:10.1093/EMBOJ/17.21.6263 [Accessed: 22 November 2022].

Ma, C., Wu, X., Sun, D., Park, E., et al. (2019) Structure of the substrate-engaged SecA-SecY protein translocation machine. *Nature Communications*. [Online] 10 (1), 1–9. Available from: doi:10.1038/s41467-019-10918-2.

Makarenkov, V., Zentilli, P., Kevorkov, D., Gagarin, A., et al. (2007) An efficient method for the detection and elimination of systematic error in high-throughput screening. In: *Bioinformatics*. [Online]. 1 July 2007 Bioinformatics. pp. 1648–1657. Available from: doi:10.1093/bioinformatics/btm145 [Accessed: 14 June 2021].

Marshall, C.G., Lessard, I.A.D., Park, I.S. & Wright, G.D. (1998) Glycopeptide antibiotic resistance genes in glycopeptide-producing organisms. *Antimicrobial Agents and Chemotherapy*. [Online] 42 (9), 2215–2220. Available from: doi:10.1128/AAC.42.9.2215 [Accessed: 13 December 2022].

Matsuhashi, M., Song, M.D., Ishino, F., Wachi, M., et al. (1986) Molecular cloning of the gene of a penicillin-binding protein supposed to cause high resistance to β-lactam antibiotics in *Staphylococcus aureus*. *Journal of Bacteriology*. [Online] 167 (3), 975–980. Available from: doi:10.1128/jb.167.3.975-980.1986.

McCann, J.R., McDonough, J.A., Pavelka, M.S. & Braunstein, M. (2007) β-lactamase can function as a reporter of bacterial protein export during *Mycobacterium tuberculosis* infection of host cells. *Microbiology (Reading, England)*. [Online] 153 (Pt 10), 3350. Available from:

doi:10.1099/MIC.0.2007/008516-0 [Accessed: 26 August 2022].

Mcdonough, J.A., Hacker, K.E., Flores, A.R., Pavelka, M.S., et al. (2005) The Twin-Arginine Translocation Pathway of *Mycobacterium smegmatis* Is Functional and Required for the Export of Mycobacterial-Lactamases. *Journal of Bacteriology*. [Online] 187 (22), 7667–7679. Available from: doi:10.1128/JB.187.22.7667-7679.2005.

Mercier, E., Holtkamp, W., Rodnina, M. V & Wintermeyer, W. (2017) Signal recognition particle binds to translating ribosomes before emergence of a signal anchor sequence. *Nucleic Acids Research*. [Online] 45 (20), 11858–11866. Available from: doi:10.1093/nar/gkx888 [Accessed: 17 March 2020].

Miller, J.D., Wilhelm, H., Gierasch, L., Gilmore, R., et al. (1993) GTP binding and hydrolysis by the signal recognition particle during initiation of protein translocation. *Nature*. [Online] 366 (6453), 351–354. Available from: doi:10.1038/366351a0.

Mitchell, C. & Oliver, D. (1993) Two distinct ATP-binding domains are needed to promote protein export by *Escherichia coli* SecA ATPase. *Molecular Microbiology*. [Online] 10 (3), 483–497. Available from: doi:10.1111/j.1365-2958.1993.tb00921.x [Accessed: 18 September 2020].

Mitra, K., Schaffitzel, C., Shaikh, T., Tama, F., et al. (2005) Structure of the *E. coli* protein-conducting channel bound to a translating ribosome. *Nature*. [Online] 438 (7066), 318–324. Available from: doi:10.1038/nature04133.

Moir, D.T., Di, M., Wong, E., Moore, R.A., et al. (2011) Development and application of a cellular, gain-of-signal, bioluminescent reporter screen for inhibitors of type II secretion in *Pseudomonas aeruginosa* and *Burkholderia pseudomallei*. *Journal of Biomolecular Screening*. [Online] 16 (7), 694–705. Available from: doi:10.1177/1087057111408605 [Accessed: 24 August 2020].

Moland, E.S., Seong, G.H., Thomson, K.S., Larone, D.H., et al. (2007) *Klebsiella pneumoniae* Isolate Producing at Least Eight Different β-Lactamases, Including AmpC and KPC β-Lactamases. *Antimicrobial Agents and Chemotherapy*. [Online] 51 (2), 800. Available from: doi:10.1128/AAC.01143-06 [Accessed: 15 December 2022].

Morán-Barrio, J., Limansky, A.S. & Viale, A.M. (2009) Secretion of GOB metallo-beta-lactamase in *Escherichia coli* depends strictly on the cooperation between the cytoplasmic DnaK chaperone system and the Sec machinery: completion of folding and Zn(II) ion acquisition occur in the bacterial periplasm. *Antimicrobial Agents and Chemotherapy*. [Online] 53 (7), 2908–2917. Available from: doi:10.1128/AAC.01637-08.

Morel, C. & Mossialos, E. (2010) Stoking the antibiotic pipeline. *BMJ*. [Online] 340 (7756), 1115–1118. Available from: doi:10.1136/BMJ.C2115 [Accessed: 9 November 2022].

Murphy, C.K. & Beckwith, J. (1994) Residues essential for the function of SecE, a membrane component of the *Escherichia coli* secretion apparatus, are located in a conserved cytoplasmic region. *Proceedings of the National Academy of Sciences of the United States of*

*America*. [Online] 91 (7), 2557–2561. Available from: doi:10.1073/PNAS.91.7.2557 [Accessed: 16 December 2022].

Murray, C.J., Shunji Ikuta, K., Sharara, F., Swetschinski, L., et al. (2022) Global burden of bacterial antimicrobial resistance in 2019: a systematic analysis. *The Lancet*. [Online] 0 (0). Available from: doi:10.1016/S0140-6736(21)02724-0 [Accessed: 31 January 2022].

Musial-Siwek, M., Rusch, S.L. & Kendall, D.A. (2007) Selective Photoaffinity Labeling Identifies the Signal Peptide Binding Domain on SecA. *Journal of Molecular Biology*. [Online] 365 (3), 637. Available from: doi:10.1016/J.JMB.2006.10.027 [Accessed: 14 December 2022].

Naas, T., Oueslati, S., Bonnin, R.A., Dabos, M.L., et al. (2017) Beta-lactamase database (BLDB) – structure and function. *Journal of Enzyme Inhibition and Medicinal Chemistry*. [Online] 32 (1), 917. Available from: doi:10.1080/14756366.2017.1344235 [Accessed: 28 July 2021].

Neumann-Haefelin, C., Schäfer, U., Müller, M. & Koch, H.-G. (2000) SRP-dependent co-translational targeting and SecA-dependent translocation analyzed as individual steps in the export of a bacterial protein. *The EMBO journal*. [Online] 19 (23), 6419–6426. Available from: doi:10.1093/emboj/19.23.6419.

Newton, G.G. & Abraham, E.P. (1954) Degradation, structure and some derivatives of cephalosporin N. *The Biochemical Journal*. [Online] 58 (1), 103–111. Available from: doi:10.1042/bj0580103 [Accessed: 25 January 2022].

Nikaido, H. (1976) Outer membrane of *Salmonella typhimurium*. Transmembrane diffusion of some hydrophobic substances. *Biochimica et biophysica acta*. [Online] 433 (1), 118–132. Available from: doi:10.1016/0005-2736(76)90182-6 [Accessed: 13 December 2022].

Nikaido, H. & Rosenberg, E.Y. (1981) Effect on solute size on diffusion rates through the transmembrane pores of the outer membrane of *Escherichia coli*. *Journal of General Physiology*. [Online] 77 (2), 121–135. Available from: doi:10.1085/JGP.77.2.121 [Accessed: 13 December 2022].

Novo, D., Perlmutter, N.G., Hunt, R.H. & Shapiro, H.M. (1999) Accurate Flow Cytometric Membrane Potential Measurement in Bacteria Using Diethyloxacarbocyanine and a Ratiometric Technique. *Cytometry*. [Online] 35, 55–63. Available from: doi:10.1002/(SICI)1097-0320(19990101)35:1 [Accessed: 20 October 2022].

Ochsner, U.A., Snyder, A., Vasil, A.I. & Vasil, M.L. (2002) Effects of the twin-arginine translocase on secretion of virulence factors, stress response, and pathogenesis. *Proceedings of the National Academy of Sciences of the United States of America*. [Online] 99 (12), 8312–8317. Available from: doi:10.1073/PNAS.082238299.

Oh, E., Becker, A.H., Sandikci, A., Huber, D., et al. (2011) Selective ribosome profiling reveals the cotranslational chaperone action of trigger factor in vivo. *Cell*. [Online] 147 (6), 1295–1308. Available from: doi:10.1016/j.cell.2011.10.044 [Accessed: 1 May 2020].

Oliver, D.B. & Beckwith, J. (1981) *E. coli* mutant pleiotropically defective in the export of secreted proteins. *Cell*. [Online] 25 (3), 765–772. Available from: doi:10.1016/0092-8674(81)90184-7.

Oliver, D.B. & Beckwith, J. (1982) Regulation of a membrane component required for protein secretion in *Escherichia coli*. *Cell*. [Online] 30 (1), 311–319. Available from: doi:10.1016/0092-8674(82)90037-X.

Oliver, D.B., Cabelli, R.J., Dolan, K.M. & Jarosik, G.P. (1990) Azide-resistant mutants of *Escherichia coli* alter the SecA protein, an azide-sensitive component of the protein export machinery. *Proceedings of the National Academy of Sciences of the United States of America*. 87, 8227–8231.

Orfanoudaki, G. & Economou, A. (2014) Proteome-wide subcellular topologies of *E. coli* polypeptides database (STEPdb). *Molecular and Cellular Proteomics*. [Online] 13 (12), 3674–3687. Available from: doi:10.1074/mcp.O114.041137.

Osano, E., Arakawa, Y., Wacharotayankun, R., Ohta, M., et al. (1994) Molecular characterization of an enterobacterial metallo beta-lactamase found in a clinical isolate of *Serratia marcescens* that shows imipenem resistance. *Antimicrobial Agents and Chemotherapy*. [Online] 38 (1), 71–78. Available from: doi:10.1128/AAC.38.1.71.

Osborne, A.R. & Rapoport, T.A. (2007) Protein Translocation Is Mediated by Oligomers of the SecY Complex with One SecY Copy Forming the Channel. *Cell*. [Online] 129 (1), 97–110. Available from: doi:10.1016/j.cell.2007.02.036 [Accessed: 10 November 2022].

Ouellette, M., Bissonnette, L. & Roy, P.H. (1987) Precise insertion of antibiotic resistance determinants into Tn21-like transposons: nucleotide sequence of the OXA-1 beta-lactamase gene. *Proceedings of the National Academy of Sciences of the United States of America*. 84 (21), 7378–7382.

Paetzel, M., Dalbey, R.E. & Strynadka, N.C.J. (1998) Crystal structure of a bacterial signal peptidase in complex with a β- lactam inhibitor. *Nature*. [Online] 396 (6707), 186–190. Available from: doi:10.1038/24196.

Paetzel, M., Goodall, J.J., Kania, M., Dalbey, R.E., et al. (2004) Crystallographic and Biophysical Analysis of a Bacterial Signal Peptidase in Complex with a Lipopeptide-based Inhibitor. *Journal of Biological Chemistry*. [Online] 279 (29), 30781–30790. Available from: doi:10.1074/JBC.M401686200.

Palmer, T. & Berks, B.C. (2012) The twin-arginine translocation (Tat) protein export pathway. *Nature Reviews Microbiology*. [Online]. 10 (7) pp.483–496. Available from: doi:10.1038/nrmicro2814.

Palmer, T. & Stansfeld, P.J. (2020) Targeting of proteins to the twin-arginine translocation pathway. *Molecular Microbiology*. [Online] 113 (5), 861–871. Available from: doi:10.1111/MMI.14461 [Accessed: 12 October 2021].

Parish, C.A., De La Cruz, M., Smith, S.K., Zink, D., et al. (2009) Antisense-guided isolation and structure elucidation of pannomycin, a substituted cis-decalin from *Geomyces pannorum*. *Journal of Natural Products*. [Online] 72 (1), 59–62. Available from: doi:10.1021/np800528a [Accessed: 30 January 2020].

Park, E. & Rapoport, T.A. (2012) Bacterial protein translocation requires only one copy of the SecY complex in vivo. *Journal of Cell Biology*. [Online] 198 (5), 881–893. Available from: doi:10.1083/JCB.201205140 [Accessed: 10 November 2022].

Parro, V., Schacht, S., Anné, J. & Mellado, R.P. (1999) Four genes encoding different type I signal peptidases are organized in a cluster in *Streptomyces lividans* TK21. *Microbiology*. [Online] 145 (9), 2255–2263. Available from: doi:10.1099/00221287-145-9-2255/CITE/REFWORKS [Accessed: 14 December 2022].

Patil, S.D., Sharma, R., Srivastava, S., Navani, N.K., et al. (2013) Downregulation of *yidC* in *Escherichia coli* by Antisense RNA Expression Results in Sensitization to Antibacterial Essential Oils Eugenol and Carvacrol Hendrik W. van Veen (ed.). *PLoS ONE*. [Online] 8 (3), e57370. Available from: doi:10.1371/journal.pone.0057370 [Accessed: 14 February 2020].

Payne, D.J., Gwynn, M.N., Holmes, D.J. & Pompliano, D.L. (2007) Drugs for bad bugs: confronting the challenges of antibacterial discovery. *Nature Reviews Drug Discovery*. [Online] 6 (1), 29–40. Available from: doi:10.1038/nrd2201.

Peng, S. Bin, Zheng, F., Angleton, E.L., Smiley, D., et al. (2001) Development of an Internally Quenched Fluorescent Substrate and a Continuous Fluorimetric Assay for *Streptococcus pneumoniae* Signal Peptidase I. *Analytical Biochemistry*. [Online] 293 (1), 88–95. Available from: doi:10.1006/ABIO.2001.5102.

Pereira, G.C., Allen, W.J., Watkins, D.W., Buddrus, L., et al. (2019) A High-Resolution Luminescent Assay for Rapid and Continuous Monitoring of Protein Translocation across Biological Membranes. *Journal of Molecular Biology*. [Online] 431 (8), 1689–1699. Available from: doi:10.1016/J.JMB.2019.03.007.

Perry, C.R., Ashby, M.J. & Elsmere, S.A. (1995) Penems as Research Tools to Investigate the Activity of *E. coli* Leader Peptidase. *Biochemical Society Transactions*. [Online] 23 (4), 548S-548S. Available from: doi:10.1042/BST023548S [Accessed: 22 July 2022].

Peters, J.E., Thate, T.E. & Craig, N.L. (2003) Definition of the *Escherichia coli* MC4100 Genome by Use of a DNA Array. *Journal of Bacteriology*. [Online] 185 (6), 2017. Available from: doi:10.1128/JB.185.6.2017-2021.2003 [Accessed: 18 November 2022].

Philippon, A., Jacquier, H., Ruppé, E. & Labia, R. (2019) Structure-based classification of class A beta-lactamases, an update. *Current Research in Translational Medicine*. [Online] 67 (4), 115–122. Available from: doi:10.1016/J.RETRAM.2019.05.003 [Accessed: 15 December 2022].

Phillips, G.J. & Silhavy, T.J. (1992) The *E. coli ffh* gene is necessary for viability and efficient protein

export. *Nature*. [Online] 359 (6397), 744–746. Available from: doi:10.1038/359744A0 [Accessed: 9 November 2022].

Plaxco, K.W., Simons, K.T. & Baker, D. (1998) Contact order, transition state placement and the refolding rates of single domain proteins. *Journal of Molecular Biology*. [Online] 277 (4), 985–994. Available from: doi:10.1006/JMBI.1998.1645 [Accessed: 21 November 2022].

Pogliano, J.A. & Beckwith, J. (1994a) SecD and SecF facilitate protein export in *Escherichia coli. EMBO Journal*. [Online] 13 (3), 554–561. Available from: doi:10.1002/j.1460-2075.1994.tb06293.x [Accessed: 2 June 2021].

Pogliano, K.J. & Beckwith, J. (1994b) Genetic and molecular characterization of the *Escherichia coli secD* operon and its products. *Journal of Bacteriology*. [Online] 176 (3), 804. Available from: doi:10.1128/JB.176.3.804-814.1994 [Accessed: 15 November 2022].

Poirel, L., Gniadkowski, M. & Nordmann, P. (2002) Biochemical analysis of the ceftazidime-hydrolysing extended-spectrum β-lactamase CTX-M-15 and of its structurally related β-lactamase CTX-M-3. *Journal of Antimicrobial Chemotherapy*. [Online] 50 (6), 1031–1034. Available from: doi:10.1093/JAC/DKF240 [Accessed: 29 September 2022].

Poirel, L., Naas, T., Nicolas, D., Collet, L., et al. (2000) Characterization of VIM-2, a carbapenem-hydrolyzing metallo-beta-lactamase and its plasmid- and integron-borne gene from a *Pseudomonas aeruginosa* clinical isolate in France. *Antimicrobial Agents and Chemotherapy*. [Online] 44 (4), 891–897. Available from: doi:10.1128/AAC.44.4.891-897.2000 [Accessed: 29 September 2022].

Pollitt, S. & Zalkin, H. (1983) Role of primary structure and disulfide bond formation in beta-lactamase secretion. *Journal of Bacteriology*. [Online] 153 (1), 27–32. Available from: doi:10.1128/JB.153.1.27-32.1983 [Accessed: 14 September 2022].

Poritz, M.A., Strub, K. & Walter, P. (1988) Human SRP RNA and *E. coli* 4.5S RNA contain a highly homologous structural domain. *Cell*. [Online] 55 (1), 4–6. Available from: doi:10.1016/0092-8674(88)90003-7.

Powers, T. & Walter, P. (1997) Co-translational protein targeting catalyzed by the *Escherichia coli* signal recognition particle and its receptor. *The EMBO Journal*. [Online] 16 (16), 4880. Available from: doi:10.1093/EMBOJ/16.16.4880 [Accessed: 13 December 2022].

Pradel, N., Delmas, J., Wu, L.F., Santini, C.L., et al. (2009) Sec- and Tat-dependent translocation of beta-lactamases across the *Escherichia coli* inner membrane. *Antimicrobial Agents and Chemotherapy*. [Online] 53 (1), 242–248. Available from: doi:10.1128/AAC.00642-08.

Van Puyenbroeck, V. & Vermeire, K. (2018) Inhibitors of protein translocation across membranes of the secretory pathway: novel antimicrobial and anticancer agents. *Cellular and Molecular Life Sciences*. [Online] 75 (9), 1541. Available from: doi:10.1007/S00018-017-2743-2 [Accessed: 13 September 2022].

Randall, L.B., Dobos, K., Papp-Wallace, K.M., Bonomo, R.A., et al. (2016) Membrane-bound PenA β-lactamase of *Burkholderia pseudomallei*. *Antimicrobial Agents and Chemotherapy*. [Online] 60 (3), 1509–1514. Available from: doi:10.1128/AAC.02444-15 [Accessed: 27 July 2021].

Rangama, S., Lidbury, I.D.E.A., Holden, J.M., Borsetto, C., et al. (2021) Mechanisms involved in the active secretion of CTX-M-15 β-lactamase by pathogenic *E. coli* ST131. *Antimicrobial Agents and Chemotherapy*. [Online] 65 (10), 2021.03.31.437630. Available from: doi:10.1101/2021.03.31.437630 [Accessed: 11 October 2021].

Rao, S., Bockstael, K., Nath, S., Engelborghs, Y., et al. (2009) Enzymatic investigation of the *Staphylococcus aureus* type i signal peptidase SpsB - Implications for the search for novel antibiotics. *FEBS Journal*. [Online] 276 (12), 3222–3234. Available from: doi:10.1111/J.1742-4658.2009.07037.X.

Rao, S., De Waelheyns, E., Economou, A. & Anné, J. (2014) Antibiotic targeting of the bacterial secretory pathway. *Biochimica et Biophysica Acta - Molecular Cell Research*. [Online]. 1843 (8) pp.1762–1783. Available from: doi:10.1016/j.bbamcr.2014.02.004.

Regalia, M., Rosenblad, M.A. & Samuelsson, T. (2002) Prediction of signal recognition particle RNA genes. *Nucleic Acids Research*. [Online] 30 (15), 3368. Available from: doi:10.1093/NAR/GKF468 [Accessed: 9 September 2022].

Review on Antimicrobial Resistance (2014) *Antimicrobial Resistance: Tackling a crisis for the health and wealth of nations.*

Reygaert, W. (2018) An overview of the antimicrobial resistance mechanisms of bacteria. *AIMS Microbiology*. [Online] 4 (3), 482–501. Available from: doi:10.3934/MICROBIOL.2018.3.482 [Accessed: 31 January 2022].

Rolinson, G.N. (1976) Naturally-occurring β-lactamase inhibitors with antibacterial activity. *Journal of Antibiotics*. [Online]. 29 (6) pp.668–669. Available from: doi:10.7164/antibiotics.29.668.

Romisch, K., Webb, J., Lingelbach, K., Gausepohl, H., et al. (1990) The 54-kD protein of signal recognition particle contains a methionine-rich RNA binding domain. *Journal of Cell Biology*. [Online] 111 (5), 1793–1802. Available from: doi:10.1083/JCB.111.5.1793 [Accessed: 14 December 2022].

Rose, R.W., Brüser, T., Kissinger, J.C. & Pohlschröder, M. (2002) Adaptation of protein secretion to extremely high-salt conditions by extensive use of the twin-arginine translocation pathway. *Molecular Microbiology*. [Online] 45 (4), 943–950. Available from: doi:10.1046/j.1365-2958.2002.03090.x [Accessed: 31 March 2020].

Ruiz, N., Falcone, B., Kahne, D. & Silhavy, T.J. (2005) Chemical conditionality: A genetic strategy to probe organelle assembly. *Cell*. [Online] 121 (2), 307–317. Available from: doi:10.1016/j.cell.2005.02.014.

Russel, M. & Model, P. (1981) A mutation downstream from the signal peptidase cleavage site

affects cleavage but not membrane insertion of phage coat protein. *Proceedings of the National Academy of Sciences of the United States of America*. [Online] 78 (3 I), 1717–1721. Available from: doi:10.1073/PNAS.78.3.1717 [Accessed: 14 December 2022].

Sachelaru, I., Petriman, N.A., Kudva, R., Kuhn, P., et al. (2013) YidC occupies the lateral gate of the SecYEG translocon and is sequentially displaced by a nascent membrane protein. *The Journal of Biological Chemistry*. [Online] 288 (23), 16295–16307. Available from: doi:10.1074/JBC.M112.446583 [Accessed: 10 November 2022].

Sadaie, Y. & Kada, T. (1985) *Bacillus subtilis* gene involved in cell division, sporulation, and exoenzyme secretion. *Journal of Bacteriology*. [Online] 163 (2), 648–653. Available from: doi:10.1128/JB.163.2.648-653.1985 [Accessed: 29 April 2022].

Saier, M.H., Tam, R., Reizer, A. & Reizer, J. (1994) Two novel families of bacterial membrane proteins concerned with nodulation, cell division and transport. *Molecular Microbiology*. [Online] 11 (5), 841–847. Available from: doi:10.1111/J.1365-2958.1994.TB00362.X [Accessed: 13 December 2022].

Sakharkar, K.R., Sakharkar, M.K. & Chow, V.T.K. (2004) A Novel Genomics Approach for the Identification of Drug Targets in Pathogens, with Special Reference to Pseudomonas Aeruginosa. *In Silico Biology*. 4, 355–360.

Samuelson, J.C., Chen, M., Jiang, F., Möller, I., et al. (2000) YidC mediates membrane protein insertion in bacteria. *Nature*. [Online] 406 (6796), 637–641. Available from: doi:10.1038/35020586 [Accessed: 2 June 2021].

Sander, P., Rezwan, M., Walker, B., Rampini, S.K., et al. (2004) Lipoprotein processing is required for virulence of *Mycobacterium tuberculosis. Molecular Microbiology*. [Online] 52 (6), 1543–1552. Available from: doi:10.1111/J.1365-2958.2004.04041.X.

Sankaran, K. & Wu, H.C. (1994) Lipid modification of bacterial prolipoprotein. Transfer of diacylglyceryl moiety from phosphatidylglycerol. *Journal of Biological Chemistry*. [Online] 269 (31), 19701–19706. Available from: doi:10.1016/s0021-9258(17)32077-x.

Santini, C.L., Ize, B., Chanal, A., Müller, M., et al. (1998) A novel sec-independent periplasmic protein translocation pathway in *Escherichia coli. The EMBO Journal*. [Online] 17 (1), 101. Available from: doi:10.1093/EMBOJ/17.1.101 [Accessed: 13 December 2022].

Sauvage, E., Kerff, F., Terrak, M., Ayala, J.A., et al. (2008) The penicillin-binding proteins: structure and role in peptidoglycan biosynthesis. *FEMS Microbiology Reviews*. [Online] 32 (2), 234–258. Available from: doi:10.1111/J.1574-6976.2008.00105.X [Accessed: 26 January 2022].

Schaffitzel, C., Oswald, M., Berger, I., Ishikawa, T., et al. (2006) Structure of the *E. coli* signal recognition particle bound to a translating ribosome. *Nature*. [Online] 444 (7118), 503–506. Available from: doi:10.1038/nature05182.

Schallenberger, M.A., Niessen, S., Shao, C., Fowler, B.J., et al. (2012) Type I signal peptidase and

protein secretion in *Staphylococcus aureus. Journal of Bacteriology*. [Online] 194 (10), 2677–2686. Available from: doi:10.1128/JB.00064-12.

Schatz, A., Bugie, E. & Waksman, S.A. (2005) Streptomycin, a substance exhibiting antibiotic activity against gram-positive and gram-negative bacteria. 1944. *Clinical Orthopaedics and Related Research*. [Online] 437, 3–6. Available from: doi:10.1097/01.blo.0000175887.98112.fe [Accessed: 8 November 2022].

Schibich, D., Gloge, F., Pöhner, I., Björkholm, P., et al. (2016) Global profiling of SRP interaction with nascent polypeptides. *Nature*. [Online] 536 (7615), 219–223. Available from: doi:10.1038/nature19070 [Accessed: 7 July 2020].

Schiebel, E., Driessen, A.J.M., Hartl, F.U. & Wickner, W. (1991) ΔμH+ and ATP function at different steps of the catalytic cycle of preprotein translocase. *Cell*. [Online] 64 (5), 927–939. Available from: doi:10.1016/0092-8674(91)90317-R [Accessed: 10 November 2022].

Schierle, C.F., Berkmen, M., Huber, D., Kumamoto, C., et al. (2003) The DsbA signal sequence directs efficient, cotranslational export of passenger proteins to the *Escherichia coli* periplasm via the signal recognition particle pathway. *Journal of Bacteriology*. [Online] 185 (19), 5706–5713. Available from: doi:10.1128/JB.185.19.5706-5713.2003.

Schimana, J., Gebhardt, K., Höltzel, A., Schmid, D.G., et al. (2002) Arylomycins A and B, New Biaryl-bridged Lipopeptide Antibiotics Produced by *Streptomyces sp.* Tü 6075 I. Taxonomy, Fermentation, Isolation and Biological Activities. *The Journal of Antibiotics*. [Online] 55 (6), 565–570. Available from: doi:10.7164/ANTIBIOTICS.55.565.

Schriefer, E.M., Hoffmann-Thoms, S., Schmid, F.X., Schmid, A., et al. (2013) *Yersinia enterocolitica* and *Photorhabdus asymbiotica* β-lactamases BlaA are exported by the twin-arginine translocation pathway. *International Journal of Medical Microbiology*. [Online] 303 (1), 16–24. Available from: doi:10.1016/J.IJMM.2012.11.002 [Accessed: 11 October 2021].

Schultz, S.C., Dalbadie-McFarland, G., Neitzel, J.J. & Richards, J.H. (1987) Stability of wild-type and mutant RTEM-1 β-lactamases: Effect of the disulfide bond. *Proteins: Structure, Function, and Bioinformatics*. [Online] 2 (4), 290–297. Available from: doi:10.1002/PROT.340020405 [Accessed: 14 September 2022].

Schulze, R.J., Komar, J., Botte, M., Allen, W.J., et al. (2014) Membrane protein insertion and proton-motive-force-dependent secretion through the bacterial holo-translocon SecYEG-SecDF-YajC-YidC. *Proceedings of the National Academy of Sciences of the United States of America*. [Online] 111 (13), 4844–4849. Available from: doi:10.1073/pnas.1315901111.

Scotti, P.A., Urbanus, M.L., Brunner, J., De Gier, J.W.L., et al. (2000) YidC, the *Escherichia coli* homologue of mitochondrial Oxa1p, is a component of the Sec translocase. *EMBO Journal*. [Online] 19 (4), 542–549. Available from: doi:10.1093/emboj/19.4.542 [Accessed: 2 June 2021].

Segers, K. & Anné, J. (2011) Traffic jam at the bacterial sec translocase: Targeting the SecA

nanomotor by small-molecule inhibitors. *Chemistry and Biology*. [Online]. 18 (6) pp.685–698. Available from: doi:10.1016/j.chembiol.2011.04.007.

Segers, K., Klaassen, H., Economou, A., Chaltin, P., et al. (2011) Development of a high-throughput screening assay for the discovery of small-molecule SecA inhibitors. *Analytical Biochemistry*. [Online] 413 (2), 90–96. Available from: doi:10.1016/j.ab.2011.02.012.

Serek, J., Bauer-Manz, G., Struhalla, G., Van Den Berg, L., et al. (2004) *Escherichia coli* YidC is a membrane insertase for Sec-independent proteins. *The EMBO Journal*. [Online] 23 (2), 294. Available from: doi:10.1038/SJ.EMBOJ.7600063 [Accessed: 10 November 2022].

Shan, S.O., Chandrasekar, S. & Walter, P. (2007) Conformational changes in the GTPase modules of the signal reception particle and its receptor drive initiation of protein translocation. *The Journal of Cell Biology*. [Online] 178 (4), 611. Available from: doi:10.1083/JCB.200702018 [Accessed: 13 December 2022].

Shiozuka, K., Tani, K., Mizushima, S. & Tokudas, H. (1990) The Proton Motive Force Lowers the Level of ATP Required for the in Vitro Translocation of a Secretory Protein in *Escherichia coli. Journal of Biological Chemistry*. [Online] 265 (31), 18843–18847. Available from: doi:10.1016/S0021-9258(17)30590-2.

Sianidis, G., Karamanou, S., Vrontou, E., Boulias, K., et al. (2001) Cross-talk between catalytic and regulatory elements in a DEAD motor domain is essential for SecA function. *The EMBO Journal*. [Online] 20 (5), 961. Available from: doi:10.1093/EMBOJ/20.5.961 [Accessed: 13 December 2022].

Siegel, V. & Walter, P. (1988) The affinity of signal recognition particle for presecretory proteins is dependent on nascent chain length. *The EMBO Journal*. [Online] 7 (6), 1769–1775. Available from: doi:10.1002/J.1460-2075.1988.TB03007.X [Accessed: 9 December 2021].

Simpkin, V.L., Renwick, M.J., Kelly, R. & Mossialos, E. (2017) Incentivising innovation in antibiotic drug discovery and development: progress, challenges and next steps. *The Journal of Antibiotics*. [Online] 70 (12), 1087. Available from: doi:10.1038/JA.2017.124 [Accessed: 9 November 2022].

Smith, P.A., Koehler, M.F.T., Girgis, H.S., Yan, D., et al. (2018) Optimized arylomycins are a new class of Gram-negative antibiotics. *Nature*. [Online] 561 (7722), 189–194. Available from: doi:10.1038/s41586-018-0483-6.

Smith, P.A. & Romesberg, F.E. (2012) Mechanism of action of the arylomycin antibiotics and effects of signal peptidase I inhibition. *Antimicrobial Agents and Chemotherapy*. [Online] 56 (10), 5054–5060. Available from: doi:10.1128/AAC.00785-12/SUPPL_FILE/ZAC999101225SO1.PDF [Accessed: 21 October 2022].

Smoyer, C.J., Katta, S.S., Gardner, J.M., Stoltz, L., et al. (2016) Analysis of membrane proteins localizing to the inner nuclear envelope in living cells. *The Journal of Cell Biology*. [Online] 215 (4), 575–590. Available from: doi:10.1083/jcb.201607043.

Socha, R.D., Chen, J. & Tokuriki, N. (2019) The Molecular Mechanisms Underlying Hidden Phenotypic Variation among Metallo-β-Lactamases. *Journal of Molecular Biology*. [Online] 431 (6), 1172–1185. Available from: doi:10.1016/j.jmb.2019.01.041.

Stanley, N.R., Palmer, T. & Berks, B.C. (2000) The twin arginine consensus motif of Tat signal peptides is involved in Sec-independent protein targeting in *Escherichia coli*. *The Journal of Biological Chemistry*. [Online] 275 (16), 11591–11596. Available from: doi:10.1074/JBC.275.16.11591 [Accessed: 1 November 2022].

Steenhuis, M., Koningstein, G.M., Oswald, J., Pick, T., et al. (2021) Eeyarestatin 24 impairs SecYEG-dependent protein trafficking and inhibits growth of clinically relevant pathogens. *Molecular Microbiology*. [Online] 115 (1), 28–40. Available from: doi:10.1111/MMI.14589 [Accessed: 10 August 2022].

Van Stelten, J., Silva, F., Belin, D. & Silhavy, T.J. (2009) Effects of antibiotics and a proto-oncogene homolog on destruction of protein translocator SecY. *Science*. [Online] 325 (5941), 753–756. Available from: doi:10.1126/science.1172221 [Accessed: 26 April 2022].

Stoll, H., Dengjel, J., Nerz, C. & Götz, F. (2005) *Staphylococcus aureus* deficient in lipidation of prelipoproteins is attenuated in growth and immune activation. *Infection and Immunity*. [Online] 73 (4), 2411–2423. Available from: doi:10.1128/IAI.73.4.2411-2423.2005/ASSET/789A215F-4C0B-4FCF-8E46-57721FF63E3D/ASSETS/GRAPHIC/ZII0040547800009.JPEG [Accessed: 14 December 2022].

Sugie, Y., Inagaki, S., Kato, Y., Nishida, H., et al. (2002) CJ-21,058, a new SecA inhibitor isolated from a fungus. *Journal of Antibiotics*. [Online] 55 (1), 25–29. Available from: doi:10.7164/antibiotics.55.25 [Accessed: 11 May 2020].

Sykes, R.B., Cimarusti, C.M., Bonner, D.P., Bush, K., et al. (1981) Monocyclic β-lactam antibiotics produced by bacteria. *Nature*. [Online] 291 (5815), 489–491. Available from: doi:10.1038/291489a0 [Accessed: 25 January 2022].

Tacconelli, E., Carrara, E., Savoldi, A., Harbarth, S., et al. (2018) Discovery, research, and development of new antibiotics: the WHO priority list of antibiotic-resistant bacteria and tuberculosis. *The Lancet Infectious Diseases*. [Online] 18 (3), 318–327. Available from: doi:10.1016/S1473-3099(17)30753-3 [Accessed: 13 September 2022].

Therien, A.G., Huber, J.L., Wilson, K.E., Beaulieu, P., et al. (2012) Broadening the spectrum of β-lactam antibiotics through inhibition of signal peptidase type I. *Antimicrobial Agents and Chemotherapy*. [Online] 56 (9), 4662–4670. Available from: doi:10.1128/AAC.00726-12.

Theuretzbacher, U., Outterson, K., Engel, A. & Karlén, A. (2020) The global preclinical antibacterial pipeline. *Nature Reviews Microbiology*. [Online]. 18 (5) pp.275–285. Available from: doi:10.1038/s41579-019-0288-0 [Accessed: 3 November 2022].

Tipper, D.J. & Strominger, J.L. (1965) Mechanism of action of penicillins: a proposal based on their

structural similarity to acyl-D-alanyl-D-alanine. *Proceedings of the National Academy of Sciences of the United States of America*. [Online] 54 (4). Available from: https://www.ncbi.nlm.nih.gov/pmc/articles/PMC219812/ [Accessed: 26 January 2022].

Tjalsma, H., Noback, M.A., Bron, S., Venema, G., et al. (1997) *Bacillus subtilis* contains four closely related type I signal peptidases with overlapping substrate specificities. Constitutive and temporally controlled expression of different sip genes. *The Journal of Biological Chemistry*. [Online] 272 (41), 25983–25992. Available from: doi:10.1074/JBC.272.41.25983 [Accessed: 14 December 2022].

Tjalsma, H., Zanen, G., Venema, G., Bron, S., et al. (1999) The Potential Active Site of the Lipoprotein-specific (Type II) Signal Peptidase of *Bacillus subtilis*. *Journal of Biological Chemistry*. [Online] 274 (40), 28191–28197. Available from: doi:10.1074/JBC.274.40.28191.

Toleman, M.A., Spencer, J., Jones, L. & Walsha, T.R. (2012) *blaNDM*-1 is a chimera likely constructed in *Acinetobacter baumannii*. *Antimicrobial Agents and Chemotherapy*. [Online] 56 (5), 2773–2776. Available from: doi:10.1128/AAC.06297-11 [Accessed: 26 October 2020].

Tooke, C.L., Hinchliffe, P., Bragginton, E.C., Colenso, C.K., et al. (2019) β-Lactamases and β-Lactamase Inhibitors in the 21st Century. *Journal of Molecular Biology*. [Online]. 431 (18) pp.3472–3500. Available from: doi:10.1016/j.jmb.2019.04.002.

Tschauder, S., Driessen, A.J.M. & Freudl, R. (1992) Cloning and molecular characterization of the secY genes from *Bacillus licheniformis* and *Staphylococcus carnosus*: comparative analysis of nine members of the SecY family. *Molecular & General Genetics*. [Online] 235 (1), 147–152. Available from: doi:10.1007/BF00286192 [Accessed: 16 December 2022].

Tsirigotaki, A., Chatzi, K.E., Koukaki, M., De Geyter, J., et al. (2018) Long-Lived Folding Intermediates Predominate the Targeting-Competent Secretome. *Structure*. [Online] 26 (5), 695-707.e5. Available from: doi:10.1016/j.str.2018.03.006.

Tsirigotaki, A., De Geyter, J., Šoštarić, N., Economou, A., et al. (2017) Protein export through the bacterial Sec pathway. *Nature Reviews Microbiology*. [Online] 15 (1), 21–36. Available from: doi:10.1038/nrmicro.2016.161.

Tsukazaki, T., Mori, H., Echizen, Y., Ishitani, R., et al. (2011) Structure and function of a membrane component SecDF that enhances protein export. *Nature*. [Online] 474 (7350), 235–238. Available from: doi:10.1038/nature09980 [Accessed: 15 November 2022].

Tullman-Ercek, D., DeLisa, M.P., Kawarasaki, Y., Iranpour, P., et al. (2007) Export Pathway Selectivity of *Escherichia coli* Twin Arginine Translocation Signal Peptides. *Journal of Biological Chemistry*. [Online] 282 (11), 8309–8316. Available from: doi:10.1074/JBC.M610507200 [Accessed: 12 October 2021].

Tuon, F.F., Rocha, J.L. & Formigoni-Pinto, M.R. (2018) Pharmacological aspects and spectrum of action of ceftazidime-avibactam: a systematic review. *Infection*. [Online] 46 (2), 165–181. Available from: doi:10.1007/S15010-017-1096-Y [Accessed: 15 December 2022].

Ulbrandt, N.D., Newitt, J.A. & Bernstein, H.D. (1997) The *E. coli* signal recognition particle is required for the insertion of a subset of inner membrane proteins. *Cell*. [Online] 88 (2), 187–196. Available from: doi:10.1016/S0092-8674(00)81839-5.

Vasil, M.L., Tomaras, A.P. & Pritchard, A.E. (2012) Identification and evaluation of twin-arginine translocase inhibitors. *Antimicrobial Agents and Chemotherapy*. [Online] 56 (12), 6223–6234. Available from: doi:10.1128/AAC.01575-12 [Accessed: 14 April 2021].

De Waelheyns, E., Segers, K., Sardis, M.F., Anné, J., et al. (2015) Identification of small-molecule inhibitors against SecA by structure-based virtual ligand screening. *Journal of Antibiotics*. [Online] 68 (11), 666–673. Available from: doi:10.1038/ja.2015.53 [Accessed: 14 April 2021].

Waite, R.D., Rose, R.S., Rangarajan, M., Aduse-Opoku, J., et al. (2012) *Pseudomonas aeruginosa* possesses two putative type i signal peptidases, LepB and PA1303, each with distinct roles in physiology and virulence. *Journal of Bacteriology*. [Online] 194 (17), 4521–4536. Available from: doi:10.1128/JB.06678-11.

Walker, J.E., Saraste, M., Runswick, M.J. & Gay, N.J. (1982) Distantly related sequences in the alpha- and beta-subunits of ATP synthase, myosin, kinases and other ATP-requiring enzymes and a common nucleotide binding fold. *The EMBO journal*. [Online] 1 (8), 945–951. Available from: doi:10.1002/J.1460-2075.1982.TB01276.X [Accessed: 13 December 2022].

Walter, P. & Blobel, G. (1981) Translocation of proteins across the endoplasmic reticulum III. Signal recognition protein (SRP) causes signal sequence-dependent and site-specific arrest of chain elongation that is released by microsomal membranes. *Journal of Cell Biology*. [Online] 91 (2), 557–561. Available from: doi:10.1083/JCB.91.2.557 [Accessed: 9 December 2021].

Wang, L., Miller, A., Rusch, S.L. & Kendall, D.A. (2004) Demonstration of a Specific *Escherichia coli* SecY–Signal Peptide Interaction. *Biochemistry*. [Online] 43 (41), 13185–13192. Available from: doi:10.1021/bi049485k.

Wehrman, T.S., Casipit, C.L., Gewertz, N.M. & Blau, H.M. (2005) Enzymatic detection of protein translocation. *Nature Methods*. [Online] 2 (7), 521–527. Available from: doi:10.1038/NMETH771.

Wild, J., Rossmeissl, P., Walter, W.A. & Gross, C.A. (1996) Involvement of the DnaK-DnaJ-GrpE chaperone team in protein secretion in *Escherichia coli. Journal of Bacteriology*. [Online] 178 (12), 3608. Available from: doi:10.1128/JB.178.12.3608-3613.1996 [Accessed: 2 November 2022].

Wimley, W.C. & White, S.H. (1996) Experimentally determined hydrophobicity scale for proteins at membrane interfaces. *Nature Structural Biology*. 3 (10), 842–848.

Woodford, N., Tierno, P.M., Young, K., Tysall, L., et al. (2004) Outbreak of *Klebsiella pneumoniae* producing a new carbapenem-hydrolyzing class A beta-lactamase, KPC-3, in a New York Medical Center. *Antimicrobial Agents and Chemotherapy*. [Online] 48 (12), 4793–4799. Available from: doi:10.1128/AAC.48.12.4793-4799.2004 [Accessed: 29 September 2022].

World Health Organisation (2017) *Antibacterial agents in clinical development: an analysis of the antibacterial clinical development pipeline, including tuberculosis*. [Online]. Available from: https://apps.who.int/iris/handle/10665/258965 [Accessed: 26 April 2022].

World Health Organization (2020) *A financial model for an impact investment fund for the development of antibacterial treatments and diagnostics*. [Online]. Available from: https://www.who.int/publications/i/item/a-financial-model-for-an-impact-investment-fund-for-the-development-of-antibacterial-treatments-and-diagnostics-a-user-guide [Accessed: 9 November 2022].

Yamada, K., Sanzen, I., Ohkura, T., Okamoto, A., et al. (2007) Analysis of twin-arginine translocation pathway homologue in *Staphylococcus aureus*. *Current Microbiology*. [Online] 55 (1), 14–19. Available from: doi:10.1007/S00284-006-0461-3/FIGURES/2 [Accessed: 5 December 2022].

Yamane, K., Ichihara, S. & Mizushima, S. (1987) In vitro translocation of protein across *Escherichia coli* membrane vesicles requires both the proton motive force and ATP. *The Journal of Biological Chemistry*. [Online] 262 (5), 2358–2362. Available from: doi:10.1016/s0021-9258(18)61662-x [Accessed: 16 December 2022].

Yigit, H., Queenan, A.M., Anderson, G.J., Domenech-Sanchez, A., et al. (2001) Novel carbapenem-hydrolyzing beta-lactamase, KPC-1, from a carbapenem-resistant strain of *Klebsiella pneumoniae*. *Antimicrobial Agents and Chemotherapy*. [Online] 45 (4), 1151–1161. Available from: doi:10.1128/AAC.45.4.1151-1161.2001 [Accessed: 29 July 2022].

Yong, D., Toleman, M.A., Giske, C.G., Cho, H.S., et al. (2009) Characterization of a new metallo-beta-lactamase gene, *bla(NDM-1)*, and a novel erythromycin esterase gene carried on a unique genetic structure in *Klebsiella pneumoniae* sequence type 14 from India. *Antimicrobial Agents and Chemotherapy*. [Online] 53 (12), 5046–5054. Available from: doi:10.1128/AAC.00774-09.

Yoshimura, F. & Nikaido, H. (1985) Diffusion of beta-lactam antibiotics through the porin channels of *Escherichia coli* K-12. *Antimicrobial Agents and Chemotherapy*. [Online] 27 (1), 84–92. Available from: doi:10.1128/AAC.27.1.84 [Accessed: 13 December 2022].

Zahn, R. & Plückthun, A. (1992) GroE prevents the accumulation of early folding intermediates of pre-beta-lactamase without changing the folding pathway. *Biochemistry*. [Online] 31 (12), 3249–3255. Available from: doi:10.1021/BI00127A029 [Accessed: 2 November 2022].

Zalucki, Y.M., Jen, F.E.C., Pegg, C.L., Nouwens, A.S., et al. (2020) Evolution for improved secretion and fitness may be the selective pressures leading to the emergence of two NDM alleles. *Biochemical and Biophysical Research Communications*. [Online] 524 (3), 555–560. Available from: doi:10.1016/j.bbrc.2020.01.135.

Zhang, J.H., Chung, T.D.Y. & Oldenburg, K.R. (1999) A simple statistical parameter for use in evaluation and validation of high throughput screening assays. *Journal of Biomolecular*

*Screening*. [Online] 4 (2), 67–73. Available from: doi:10.1177/108705719900400206.

Zhang, Y.B., Greenberg, B. & Lacks, S.A. (1997) Analysis of a *Streptococcus pneumoniae* gene encoding signal peptidase I and overproduction of the enzyme. *Gene*. [Online] 194 (2), 249–255. Available from: doi:10.1016/S0378-1119(97)00198-4 [Accessed: 14 December 2022].

Zhang, Y.J., Tian, H.F. & Wen, J.F. (2009) The evolution of YidC/Oxa/Alb3 family in the three domains of life: A phylogenomic analysis. *BMC Evolutionary Biology*. [Online] 9 (1), 1–11. Available from: doi:10.1186/1471-2148-9-137/FIGURES/4 [Accessed: 10 November 2022].

Zhou, J. & Xu, Z. (2003) Structural determinants of SecB recognition by SecA in bacterial protein translocation. *Nature Structural Biology*. [Online] 10 (11), 942–947. Available from: doi:10.1038/nsb980.

Zhou, Y., Ueda, T. & Müller, M. (2014) Signal Recognition Particle and SecA Cooperate during Export of Secretory Proteins with Highly Hydrophobic Signal Sequences. Eric Cascales (ed.). *PLoS ONE*. [Online] 9 (4), e92994. Available from: doi:10.1371/journal.pone.0092994.

Zhu, Z., Wang, S. & Shan, S. ou (2022) Ribosome profiling reveals multiple roles of SecA in cotranslational protein export. *Nature Communications*. [Online] 13 (1), 1–15. Available from: doi:10.1038/s41467-022-31061-5 [Accessed: 26 September 2022].

Zimmer, J., Nam, Y. & Rapoport, T.A. (2008) Structure of a complex of the ATPase SecA and the protein-translocation channel. *Nature*. [Online] 455 (7215), 936–943. Available from: doi:10.1038/nature07335.

Zopf, D., Bernstein, H.D. & Walter, P. (1993) GTPase domain of the 54-kD subunit of the mammalian signal recognition particle is required for protein translocation but not for signal sequence binding. *The Journal of Cell Biology*. [Online] 120 (5), 1113. Available from: doi:10.1083/JCB.120.5.1113 [Accessed: 14 December 2022].